Characterising the Notch-ligand binding interaction, and its modulation by glycosylation

A thesis submitted for the degree of Doctor of Philosophy at the University of Oxford



Paul B. Taylor

Department of Biochemistry and Lady Margaret Hall

Supervisor: Prof. Penny Handford

Trinity Term 2012

CHARACTERISING THE NOTCH-LIGAND BINDING INTERACTION, AND ITS REGULATION BY GLYCOSYLATION

Paul Taylor, Lady Margaret Hall and Department of Biochemistry, University of Oxford

A thesis submitted for the degree of Doctor of Philosophy, Trinity Term 2012

Abstract

The Notch signalling pathway is universally conserved in all metazoan species, and is involved in many aspects of cell fate determination and tissue homeostasis, during development and in adult organisms. Several developmental diseases are associated with defective Notch signalling, and the Notch pathway has been implicated in a growing number of cancers.

The Notch signalling pathway requires direct cell-cell contact for ligand binding and receptor activation to occur. Specific domains within the Notch receptors and ligands have been identified as necessary for the interaction to take place, and a series of enzymes are known to regulate Notch signalling via glycosylation. Other domains beyond the minimal ligand binding region of the Notch receptor are also known to influence binding.

The aim of this study was to characterise the molecular basis for ligand binding by the Notch receptor, and how this is regulated by glycosylation. The effects on ligand binding of specific amino acid substitutions and sugar modifications were tested using prokaryotically-expressed proteins, and a series of constructs containing additional domains N-terminal of the ligand binding region was produced prokaryotically and eukaryotically to test how additional domains might affect ligand binding.

Binding was assessed by a flow cytometry-based binding assay and by SPR in order to investigate how particular modifications affected ligand binding. These assays indicated that an evolutionarily-conserved hydrophobic site exists within the central β-sheet of EGF12 in the Notch receptor that is directly adjacent to the O-fucosylation site within this domain. The GlcNAc-fucose disaccharide modification at this position was found to increase binding of hNotch1 to both Jagged1 and DLL4. Additional EGF domains N-terminal to the ligand binding region showed opposite effects on binding to these two ligand classes, suggesting that the precise mode of binding may vary slightly between different Notch ligands.

Acknowledgements

I would like to thank my supervisor Professor Penny Handford for allowing me to work in her lab for the past three and a half years. I am grateful for the support and guidance she has given me during my time in her lab, and I appreciate for the helpful suggestions and comments she provided during the writing of this thesis.

I would like to thank Professor Christina Redfield for her assistance with setting up NMR experiments, and processing and analysing data. Thanks must also go to Professor Susan Lea and Dr Devon Shepperd for their roles in solving the crystal structures in this thesis, and for helping to finally get the SPR assay off the ground. Professor Robert Haltiwanger and Dr Hideyuki Takeuchi must also be thanked for performing the glycosylation modifications to the various Notch constructs.

I gratefully thank Pat for her time spent training me in the various techniques in the lab, Mouli for his assistance in setting up the eukaryotic protein expression system and discussing my results, and Sacha for his grumbles, Leffes and infectious enthusiasm throughout my time in the lab. Thanks also go to David and Ian for making every day interesting, and everyone else in the Handford lab – Philip, Shaoyan, Laurie, Sophie and all other members of the lab, past and present, for providing such an enjoyable atmosphere to work in.

Outside the lab, I would like to thank my parents and family for their support, and all of my friends who have helped keep me sane, in particular to Paddy, Sam, Beth, Nick, Helen and Seb for the Sunday night pub quizzes and good times. I also need to thank everyone who I've rowed with and coached over the past four years for providing a welcome distraction from the lab work: Peter and all of the old guard at LMHBC, and everyone at OULRC for teaching me the true value of cake.

Special thanks must also go to the Biotechnology and Biological Sciences Research Council (BBSRC) and Lady Margaret Hall for their financial support during my D.Phil.

Table of Contents

Table of contents.....**i**

List of abbreviations.....**vii**

Chapter 1 - Introduction

1.1 Introduction..... 2

1.2 The Notch Signalling Pathway..... 2

1.2.1 Discovery and function..... 2

1.2.2 The Notch signalling mechanism – *trans*-activation..... 6

1.2.3 *Cis*-inhibition..... 7

1.3 Notch signalling and disease..... 9

1.3.1 Alagille Syndrome..... 9

1.3.2 CADASIL disease..... 10

1.3.3 Notch in Cancer..... 12

1.3.4 Other developmental disorders associated with the Notch pathway..... 13

1.4 EGF domains – the major domain type within Notch receptors and their ligands..... 16

1.4.1 The EGF domain..... 16

1.4.2 The cbEGF domain..... 16

1.4.3 Class I vs Class II cbEGF domains..... 18

1.5 The Notch Receptors..... 19

1.5.1 The extracellular region..... 19

1.5.2 The EGF domains..... 19

1.5.3 The NRR of Notch..... 24

1.5.4 The Intracellular fragment..... 26

1.6 The Notch ligands..... 28

1.6.1 The ligand extracellular domains..... 29

1.6.2 Intracellular components required for signalling..... 32

1.6.3 The non-canonical Notch ligands..... 33

1.7 Post-translational modifications to the Notch extracellular domain..... 33

1.7.1 N-linked glycosylation..... 34

1.7.2 β-hydroxylation..... 34

1.7.3 O-linked glycosylation 35
1.8 Aims of this thesis 43

Chapter 2 - Materials and methods

2.1 DNA manipulation and cloning 45
2.1.1 Restriction digests 45
2.1.2 Ethanol precipitation 45
2.1.3 Gel electrophoresis 45
2.1.4 Measuring DNA concentration 46
2.1.5 Sticky end ligation 46
2.1.6 DNA sequencing 46
2.2 Amplification of DNA by the polymerase chain reaction (PCR) 46
2.2.1 Oligonucleotide primers 46
2.2.2 Amplification of DNA using *Pfu* polymerase 47
2.2.3 Colony screening using *Taq* polymerase 47
2.2.3 PCR mutagenesis using *Pfu* 47
2.2.4 PCR mutagenesis using Quikchange Lightning site-directed mutagenesis kit 48
2.3 Use of competent *E. coli* cells 48
2.3.1 Preparation of competent cells 48
2.3.2 Transforming competent cells 49
2.3.3 Bacterial glycerol stocks 49
2.3.4 Isolation of plasmid DNA 49
2.4 Bacterial protein expressing and purification 50
2.4.1 Expression of recombinant proteins 50
2.4.2 Extraction of proteins from bacterial cell pellet 50
2.4.3 Nickel affinity chromatography 51
2.4.4 Reverse-phase high performance liquid chromatography (HPLC) 51
2.4.5 *In vitro* refolding 51
2.4.6 His-RGS cleavage by Factor Xa 52
2.4.7 Purification by FPLC 52
2.5 Expression of ^{15}N enriched proteins 52
2.6 Site-specific biotinylation of BirA tagged proteins 53
2.7 Limited proteolysis of Notch fragments 54
2.8 Tissue culture 54

2.8.1 Maintaining cell lines 54
2.8.2 Sub-culturing of mammalian cells 55
2.8.3 Sub-culturing of insect cells 55
2.8.4 Freezing and thawing of mammalian cells 56
2.8.5 Freezing and thawing insect cells 56
2.9 Eukaryotic protein production and purification 57
2.9.1 Transient transfection of HEK 293T cells by PEI 57
2.9.2 Purification of recombinant protein from conditioned medium 57
2.9.3 purification of eukaryotic proteins using a Superdex 200 column 58
2.9.4 Transient transfection of *Drosophila* S2 cells using calcium phosphate 58
2.10 Measuring protein concentration 59
2.11 Identification of protein using ESI mass-spectroscopy 59
2.12 SDS-PAGE 59
2.13 Western blot and dot blot 60
2.14 Flow cytometry assay 61
2.14.1 Flow cytometry using mammalian cells 61
2.14.2 Flow cytometry using *Drosophila* S2 cells 62
2.14.3 Quantitative analysis of flow cytometry data 62
2.14.4 Statistical analysis of flow cytometry data 63
2.15 Surface Plasmon Resonance 64
2.16 Nuclear Magnetic Resonance Spectroscopy 64
2.16.1 1D and 2D NMR 64
2.16.2 Measuring calcium binding using NMR 65

Chapter 3 - Protein production and purification

3.1 Introduction 67
3.2 Production and purification of prokaryotically expressed proteins. 67
3.3 Production of $hN1_{11-13}$ WT 71
3.4 Production of mutant $hN1_{11-13}$ proteins 74
3.4.1 Site-directed mutagenesis 74
3.4.2 Expression and purification of Notch mutants 74
3.5 Production of $hN1_{9-13}$ and $hN1_{10-13}$ 79
3.6 Production of dN_{11-13} WT and mutant proteins 84
3.7 Production of eukaryotic proteins 87

3.7.1 Production of hNotch1 proteins 90
3.7.2 Production of hJagged1 MNNL-EGF3-Fc 92
3.8 Production of Serrate-GFP fusion protein 93

Chapter 4 - Identifying the ligand binding site in Notch1

4.1 Introduction 98
4.2 The target region for mutagenesis 99
4.3 Assaying $hN1_{11-13}$ mutant binding by flow cytometry 102
4.3.1 The flow cytometry assay 102
4.3.2 Mutant Notch constructs binding to B16 mJagged1 cells 104
4.3.3 Mutant Notch constructs binding to B16 mDLL4 cells 107
4.3.4 Mutant Notch constructs binding to HEK 293 Jagged1 cells 107
4.4 Binding of dN_{11-13} to Serrate 114
4.4.1 The dN_{11-13} – Serrate interaction 114
4.4.2 The dN_{11-13} – Serrate-GFP flow cytometry assay 115
4.4.3 Mutant dNotch constructs binding to S2 Serrate-GFP cells 120
4.5 Confirmation of folding and calcium binding to $hN1_{11-13}$ constructs 121
4.5.1 Limited proteolysis by Endoproteinase GluC 121
4.5.2 Assessment of calcium binding by 1D and 2D NMR spectroscopy 122
4.5.3 Assessment of fold of EGF12 by 2D NOESY NMR spectroscopy 128
4.6 Conclusions of binding experiments 130

Chapter 5 - The role of glycosylation in modulating ligand binding

5.1 Introduction 135
5.2 The effect on ligand binding of substituting the fucosylation site within EGF12 137
5.2.1 Assaying the effect on ligand binding of substituting T466 in $hN1_{11-13}$ 137
5.2.2 Assaying the effect of substituting S502 in dN_{11-13} on binding to Serrate 140
5.3 The effect of individual sugar modifications on ligand binding 141
5.3.1 Assaying the effect of sugar modifications on the mammalian interaction 141
5.3.2 The effect of sugar modifications on the *Drosophila* Notch/Serrate interaction 151
5.4 Surface Plasmon Resonance 152
5.4.1 The Surface Plasmon Resonance phenomenon 152
5.4.2 The BIAcore system 154
5.4.3 The BIAcore binding assay 157

5.4.4 Measuring the effect of the modifications at T466 on binding to hJagged1 157
5.4.5 Measuring effect of the modifications at T466 on binding to hDLL4 160
5.5 Structural effects of T466 substitutions 163
5.5.1 Crystallisation of $hN1_{11-13}$ with T466 substitutions 163
5.5.2 Substituting T466 does not significantly alter the structure of EGF12 163
5.6 Structures of sugar-modified $hN1_{11-13}$ 165
5.6.1 The requirement for structural data for EGF12 in its native context 165
5.6.2 Crystallisation of glycosylated $hN1_{11-13}$ 165
5.6.3 The effect of sugar-modifications on the structure of $hN1_{11-13}$ 167
5.6.4 The implications of the structures of modified $hN1_{11-13}$ 170

Chapter 6 - The effect of additional domains on ligand binding

6.1 Introduction 176
6.2 Assaying the effects of longer prokaryotically-expressed hNotch1 constructs on binding 177
6.2.1 Assaying binding of longer prokaryotically-expressed hNotch1 constructs to mJagged1 177
6.2.2 Assaying binding of longer prokaryotically-expressed hNotch1 constructs to mDLL4 179
6.3 Assaying the effects of longer eukaryotically-expressed hNotch1 constructs on binding 181
6.3.1 Assaying binding of longer eukaryotically-expressed hNotch1 constructs to mJagged1 . 182
6.3.2 Assaying binding of longer eukaryotically-expressed hNotch1 constructs to mDLL4 184
6.5 Blocking the interaction between $hN1_{11-13}$ and its ligands 186
6.5.1 Defining how the 39E mAb binds to glycosylated $hN1_{11-13}$ 187
6.5.2 Defining how the 39E mAb block binding of the longer prokaryotically-expressed hNotch1 constructs to Jagged1 189
6.5.3 Defining how the 39E mAb block binding of the longer eukaryotically-expressed hNotch1 constructs to Jagged1 190

Chapter 7 - Discussion and future work

7.1 Objectives of this thesis 194
7.2 The location of the ligand binding site within the Notch receptor 194
7.3 Regulation of Notch-ligand binding by O-glycosylation 195
7.4 Docking $hN1_{11-13}$ and hJagged1 DSL-EGF3 197
7.4.1 HADDOCK docking 199
7.4.2 Possible implications of the docking models 200
7.4.3 Towards the structure of a Notch-ligand complex 202

7.5 The effect of additional domains on ligand binding 202
7.6 Future work 203
7.7 Summary 203

References.....205

Appendix A.....219

Appendix B.....221

Appendix C.....223

List of Abbreviations

A	adenine
Å	Ångstrom
ADAM	a disintegrin and metalloprotease domain-containing protease
ANK	ankyrin domain
APS	ammonium persulphate
ATP	adenosine triphosphate
Ax	abruptex mutation
bp	base pairs
BSA	bovine serum albumin
cbEGF	calcium-binding epidermal growth factor
C	cytosine
CADASIL	cerebral autosomal dominant arteriopathy with subcortical infarcts and leukoencephalopathy
CHO	Chinese hamster ovarian
CSL	CBF1/RBP-Jκ/Suppressor of Hairless/LAG-1 transcription factor
d	*Drosophila*
dH_2O	distilled water
dNTPs	deoxynucleotide 5' triphosphates
Da	Dalton
DMEM	Dulbecco's modified Eagles medium
DMSO	dimethyl sulphoxide
DNA	deoxyribonucleic acid
DSL	Delta/Serrate/Lag-2 domain
DTT	dithiothreitol
ECD	1-Ethyl-3(3-dimethylamino-propyl)-carbodiimide hydrochloride
ECM	extra-cellular matrix
EDTA	ethylenediaminetetraacetic acid
EGF	epidermal growth factor
EGTA	ethylene glycol bis-(β-aminoethyl ether)-N,N'-tetraacetic acid
ER	endoplasmic reticulum
ESI-MS	electrospray ionisation mass spectroscopy
FCS	foetal calf serum
FPLC	fast protein liquid chromatography
G	guanine
GlcNAc	N-acetylglucosamine
GluC	endoproteinase Glu-C enzyme
h	human
hDLL1	human Delta-like ligand 1
hDLL4	human Delta-like ligand 4
hr	hour
HBSS	Hank's buffered saline solution
HD	heterodimerisation

HEPES	(4-(2-hydroxyethyl)-1-piperazineethanesulfonic acid
HES	hairy/enhancer of split
HPLC	high performance liquid chromatography
HSQC	hereronuclear single quantum correlation spectroscopy
Hz	hertz
I	ionic strength
IPTG	isopropyl-β-D-thiogalactopyranoside
LNR	Lin12/Notch repeat
K	Kelvin
Kb	kilobase
K_D	dissociation constant
kDa	kilodalton
m	mouse
mA	milliamp
mg	milligram
min	minute
ml	millilitre
µl	microlitre
MAML	mastermind-like protein
MNNL	module at the N-terminus of Notch ligands
N_{ECD}	Notch extracellular domain
N_{ICD}	Notch intracellular domain
NHS	N-hydroxysuccinimide
NMR	nuclear magnetic resonance
NOE	nuclear Overhauser effect
NOESY	nuclear Overhauser effect spectroscopy
NRR	negative regulatory region
Ofut1	O-fucosyltransferase-1
1D	one-dimensional
PAGE	polyacrylamide gel electrophoresis
PBS	phosphate buffered saline
PCR	polymerase chain reaction
PDB	protein data bank
PEG	polyethylene glycol
PEST	proline, glutamate, serine, threonine rich
ppm	parts per million
QH_2O	milliQ water
RAM	RBP-jk-associated molecule
RIP	regulated intramembrane proteolysis
RNA	ribonucleic acid
rpm	revolutions per minute
RU	response units
SDS	sodium docecyl sulphate
secs	seconds

spl	split phenotype
SPR	surface plasmon resonance
T	thymine
T-ALL	T-cell acute lymphoblastic lymphoma
TACE	TNF-α Converting Enzyme
TAE	tris/acetate/EDTA
TBE	tris/borate/EDTA
TE	tris/EDTA
TEMED	N,N,N',N'-tetramethylethylenediamine
TfB	transformation buffer
TFA	trifluoroacetic acid
T_m	melting temperature
TM	transmembrane
Tris	tris (hydroxymethyl) aminomethane
2D	two dimensional
UV	ultraviolet
V	volts
WT	wild type
YT	yeast tryptone medium

List of amino acid abbreviations used:

A	Ala	Alanine
C	Cys	Cysteine
D	Asp	Aspartic acid
E	Glu	Glutamic acid
F	Phe	Phenylalanine
G	Gly	Glycine
H	His	Histidine
I	Ile	Isoleucine
K	Lys	Lysine
L	Leu	Leucine
M	Met	Methionine
N	Asn	Asparagine
P	Pro	Proline
Q	Gln	Glutamine
R	Arg	Arginine
S	Ser	Serine
T	Thr	Threonine
V	Val	Valine
W	Trp	Tryptophan
Y	Tyr	Tyrosine

Standard symbols from the Periodic Table have been used to represent the chemical elements.

Chapter 1

Introduction

1.1 Introduction

The Notch signalling pathway is universally conserved in all metazoan species. It is involved in many aspects of cell fate determination during development, and also has roles in adult cell homeostasis and apoptosis. It has been implicated in a wide range of developmental and adult onset diseases, as well as many different cancers.

Canonical Notch signalling is activated through direct cell-to-cell contact. Ligand molecules from either the Jagged/Serrate or Delta families on the surface of a signal-sending cell can interact with Notch receptors on the signal-receiving cell. Following ligand binding, the ligand-receptor complex undergoes endocytosis, which induces a conformational change in the Notch receptor that exposes a proteolytic cleavage site in the protein near to the cell membrane. Two proteolytic cleavage events allows the intracellular portion of the Notch receptor to be released from the membrane, which then translocates to the nucleus and can relieve repression and activate certain effector genes, and alter patters of gene expression.

The extracellular portions of the Notch receptors and their ligands contain multiple tandem of Epidermal Growth Factor-like domain (EGF) repeats, many of which contain consensus sequences for binding calcium (cbEGF). Both ligands and receptors are extensively glycosylated with both N-linked and O-linked glycans, and these have been found to be essential for activation and regulation of the signalling pathway.

1.2 The Notch Signalling Pathway

1.2.1 Discovery and function

The Notch pathway was first identified in *Drosophila melanogaster*, when small notches were noticed in the wing tip (Morgan, 1917), (Mohr, 1919). Haploinsufficiency caused by only a single allele of the *Notch* gene resulted in reduced signalling in the developing wing, and was found to be sex-linked on the X chromosome (Welshons, 1965). A developmental abnormality that showed an

increased level of neural tissue in the brain at the expense of epidermal tissue (Poulson, 1937) was later found to be associated with mutations in the *Notch* locus (Wright, 1970), and mutations in this and several other genes became known as the neurogenic loci (Lehmann *et al.*, 1981), (Lehmann *et al.*, 1983). These were later found to other essential components of the Notch signalling pathway (Xu *et al.*, 1990). Together, these loci highlighted the importance of the pathway in development. Notch signalling has since been found to be important in the development of many adult structures in flies, such as the retina (Cagan and Ready, 1989), leg, wing and bristles (Shellenbarger and Mohler, 1978).

The Notch receptor is expressed as a single-pass membrane protein (Wharton *et al.*, 1985) at the cell surface (Johansen *et al.*, 1989), (Kidd *et al.*, 1989), which when coupled with the observation that S2 cells expressing Notch and its ligands aggregate (Fehon *et al.*, 1990) implies that direct cell-cell contact is required in order for signalling to occur. This was confirmed in a single-cell transplantation study, where a dorsal ectoderm cell was moved to a ventral position in *Drosophila* embryos, and adopted the abnormal neural fate (Technau and Campos-Ortega, 1986). Further evidence is provided by other work studying the development of model organisms; pattern formation in the *Drosophila* ommatidium requires Notch signalling (Shellenbarger and Mohler, 1978) and is driven by cell-cell contact (Tomlinson and Ready, 1987), and laser ablation experiments on the somatic gonad in C. elegans (Kimble, 1981) and on neurodermal cells in grasshopper embryos (Doe and Goodman, 1985) (both of which require Notch signalling to develop normally (Greenwald *et al.*, 1983), (Yochem *et al.*, 1988), (Wheeler *et al.*, 2008)) caused neighbouring cells to develop abnormally.

There are three main mechanisms by which Notch signalling can affect cell fate determination during development. These are: lateral inhibition, binary lineage decisions, and boundary formation (Figure 1-1) Lateral inhibition arises when stochastic differences between two otherwise similar cells become amplified through feedback loops (Greenwald, 1998) (Figure 1-1 A). This causes one cell to adopt a signal-sending state, and the other to receive a strong Notch signal. This is the mechanism

employed in neural development, to ensure the correct ratio of neural to epidermal cells arises (Heitzler and Simpson, 1991).

Lineage decisions are caused by asymmetrical distribution of regulatory factors between daughter cells after cell division. For example, the protein Numb is inherited unevenly in the division of the *Drosophila* sensory organ precursor cells (SOP) (Uemura *et al.*, 1989). The presence of Numb inhibits Notch signalling in one of the daughter cells causing it to adopt a signal-sending state, whilst the other cell adopts a Notch signalling state (Figure 1-1 B) (Frise *et al.*, 1996) (Portin, 2001).

Boundaries between two cell types can also be maintained by Notch signalling. For example in the *Drosophila* primordial wing, Notch is activated in two lines of cells at the dorsal-ventral boundary. In order to achieve this, cells on each side of the boundary need to signal to the other side of the boundary, but not to cells on the same side. The ligand Serrate and the glycosyltransferase Fringe (see section 1.7) are expressed on cells at the dorsal side of this boundary, whereas the ligand Delta is only expressed on cells at the ventral side. Fringe inhibits Notch binding to Serrate, but increases binding to Delta (Panin *et al.*, 1997a), leading to enhanced Notch signalling in both lines of cells, and formation of the boundary (Kim *et al.*, 1995) (Rauskolb *et al.*, 1999) (Figure 1-1 C).

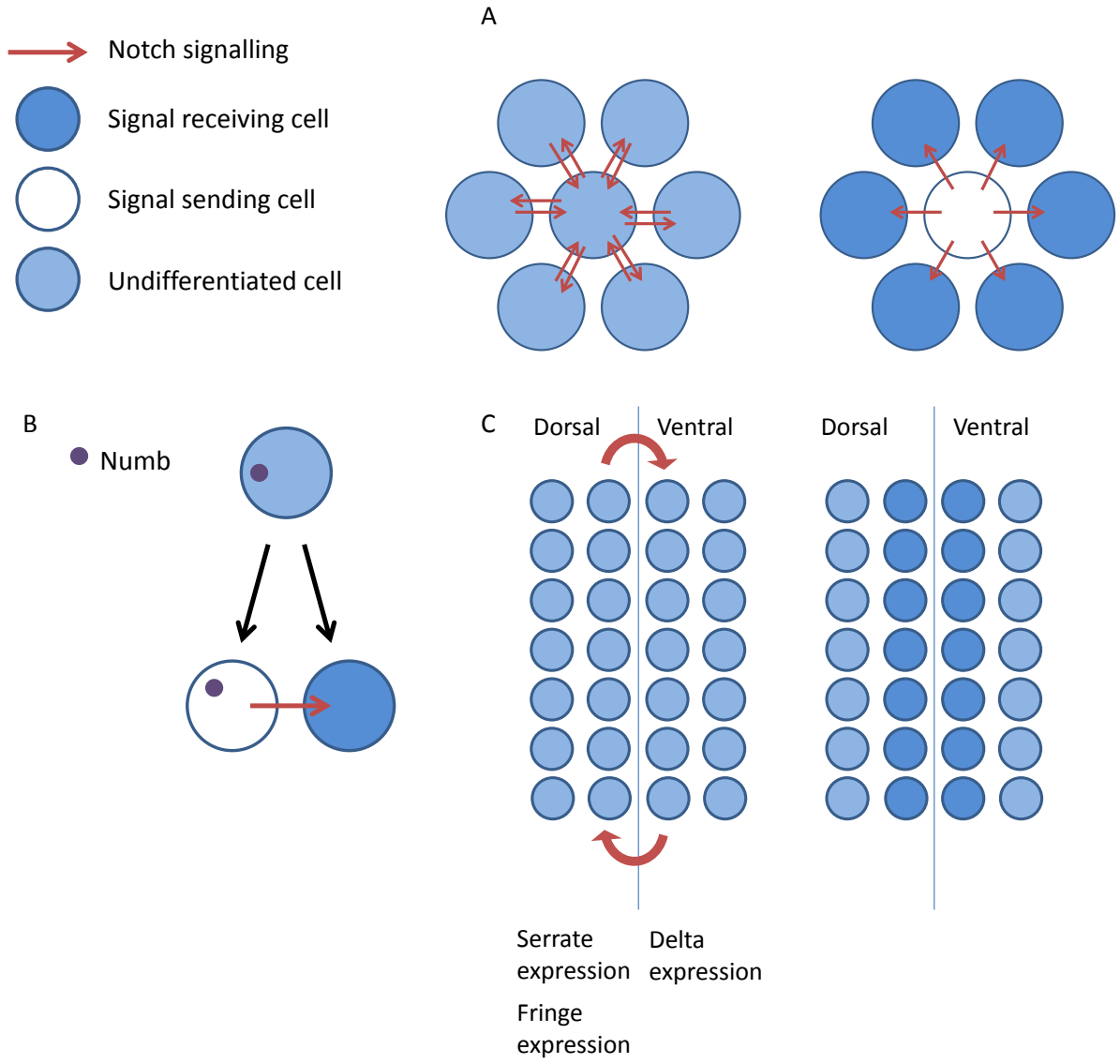


Figure 1-1 The three modes of action of Notch signalling in determining cell fate. A) Lateral inhibition can cause one cell within a tissue to adopt a particular fate. Notch signal sending and receiving cells can arise through feedback between otherwise undifferentiated cells. B) Asymmetrical inheritance of certain factors that promote or inhibit Notch signalling can cause one daughter cell to adopt a signal-sending state, and the other to undergo Notch signalling. C) In the developing Drosophila wing disc, a band of Notch signalling arises. Delta is expressed in the ventral portion of cells, and Serrate is expressed along with Fringe in the dorsal region. Fringe potentiates Delta-induced signalling, and reduces Serrate-induced signalling, so Delta signals to Notch-expressing cells in the dorsal compartment, and Serrate signals to cells in the ventral compartment. This results in a two cell wide band of Notch signalling in the developing disc. Cis-inhibition (see Section 1.2.3) is avoided because Fringe expression is limited to the dorsal cells – Notch on the dorsal cells binds Serrate weakly, whereas Notch on the ventral side binds Delta weakly.

1.2.2 The Notch signalling mechanism – *trans*-activation

The Notch signalling pathway contains three core components: a transmembrane receptor, transmembrane ligands on the signal-sending cell, and a transcription factor that effects gene expression patterns. Notch signalling relieves repression and activates transcription of the Hairy/Enhancer of Split (HES) genes (Jarriault *et al.*, 1995), (Lecourtois and Schweisguth, 1995), (Bailey and Posakony, 1995) (Figure 1-2), which encode a family of helix-loop-helix proteins that in turn repress transcription of other HLH genes (Kageyama and Nakanishi, 1997). The number of each of the components involved in signalling varies from species to species. The number of Notch receptors varies between species; *D. melanogaster* contains only one receptor, whereas in humans and other mammals there are four. Both flies and humans share two main classes of canonical ligand – Serrate (Jagged in mammals) and Delta. *Drosophila* contains one of each of these classes of ligands, whereas in mammals there are two Jagged ligands (Jagged1&2) and three Delta-like ligands (DLL1, 3 & 4). In *C. elegans* there are two Notch homologues (Lin-12 and Glp-1) and two canonical ligands (Apx-1 and Lag-1), as well as a large number of non-canonical ligands that have also been reported to affect Notch signalling, some of which are soluble (Komatsu *et al.*, 2008).

During biosynthesis the Notch receptor is glycosylated with N-linked and O-linked sugars in the endoplasmic reticulum, before undergoing further glycosylation in the Golgi. The Notch receptor also undergoes cleavage by the furin-like convertase at the S1 proteolysis site at this stage, and the receptor is presented as a heterodimer at the cell surface. Binding of the ligand to the receptor causes a conformational change in the NRR region of the Notch receptor (see Section 1.5.3) that allows regulated intramembrane proteolysis (RIP) to occur. This involves two proteolytic cleavage events at the cell membrane: the first proteolysis event occurs at the S2 cleavage site, by the metalloprotease ADAM10/Kuzbanian (van Tetering *et al.*, 2009), (Bozkulak and Weinmaster, 2009), approximately 100 residues N-terminal to the transmembrane region of Notch. S2 cleavage exposes a second proteolysis site that lies within the transmembrane region Notch (S3), that is cut by the γ-secretase complex, and releases the intracellular domain (N_{ICD}) from the membrane (De Strooper *et*

al., 1999). It can then translocate to the nucleus, where it displaces a protein co-repressor from the CBF1/Suppressor of Hairless/LAG-1 transcription factor (CSL). This allows the recruitment of the Mastermind-like protein (MAML) (Petcherski and Kimble, 2000), (Kovall, 2007) which forms the active transcription complex, and leads to the transcription of the *HES* family of genes.

1.2.3 *Cis*-inhibition

In addition to the *trans*-activation mechanism outlined above, Notch receptor molecules are able to interact with ligand molecules expressed in the same cell, in a process known as *cis*-inhibition. This process down-regulates the activity of Notch signalling in a cell-autonomous manner, and has been found to be involved in a number of processes including wing development (de Celis and Bray, 1997) and sensory bristle formation (Simpson, 1990) in flies, and somitogenesis (Ladi *et al.*, 2005) and stem cell homeostasis (Lowell *et al.*, 2000) in vertebrates.

The receptor and ligand co-localise at the cells surface and interact via their respective extracellular regions (Fehon *et al.*, 1990), and the same domains in Notch receptor and the Serrate class of ligands that are required for activation are also thought to be involved in *cis*-inhibition (Glittenberg *et al.*, 2006) (de Celis *et al.*, 1993) (Cordle *et al.*, 2008a) (Becam *et al.*, 2010). Increasing the concentration of Delta expressed in *trans* leads to a gradual linear increase in Notch activity, whereas there is a sharp threshold *cis* ligand concentration above which Notch signalling is completely inhibited (Sprinzak *et al.*, 2010). This suggests that cis-inhibition involves the formation of receptor-ligand complexes that are inactive for Notch signalling, and preclude the formation of the trans-activation complex. Ligand expressed in *cis* is able to prevent the ligand-independent activation of Notch by EDTA (Fiuza *et al.*, 2010). However, it is not yet clear if the molecular basis for both of these interactions is actually the same, or if these domains may interact in two different ways. A simulated docking interaction between the ligand-binding region of Notch and the receptor-binding region of hJagged1 has suggested that these molecules may in fact interact in both a parallel and antiparallel

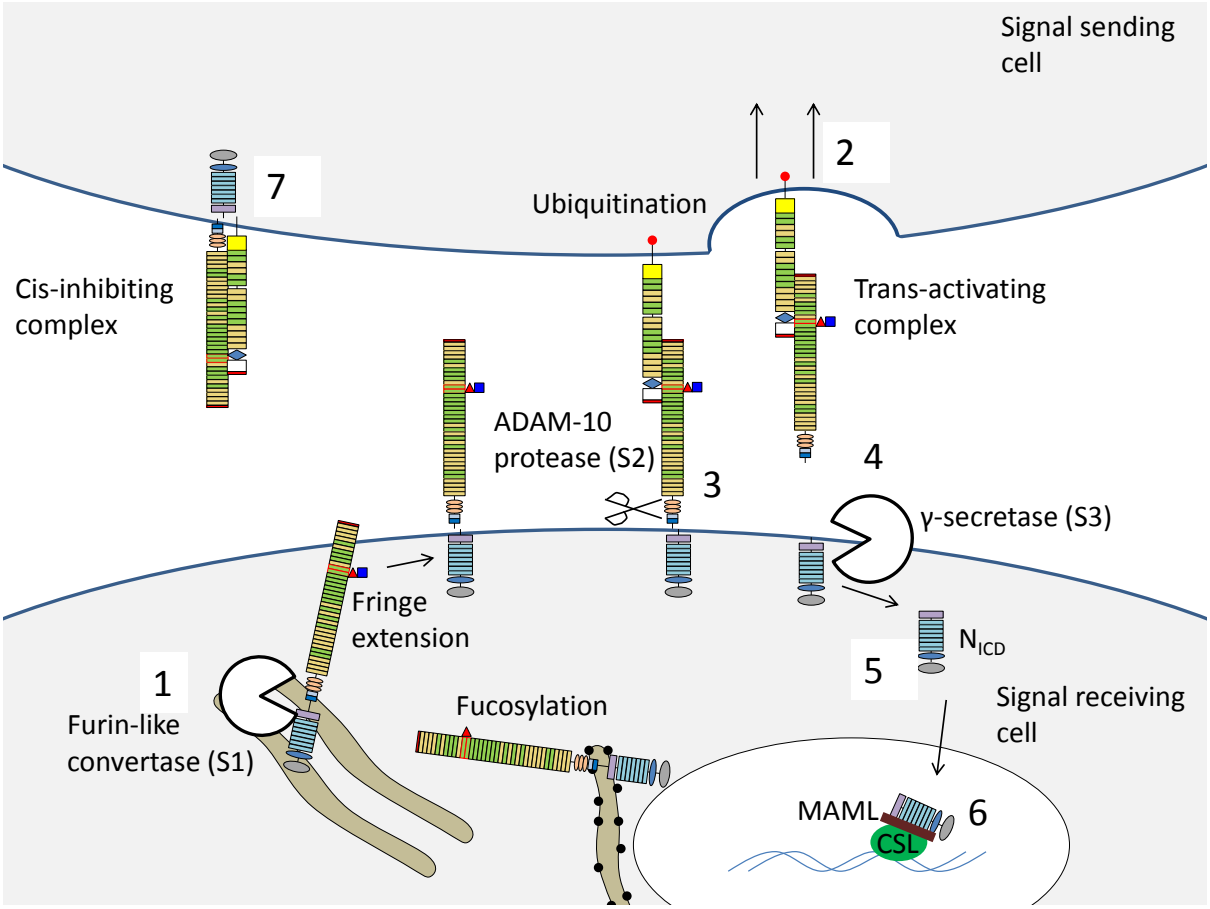


Figure 1-2 Outline of the canonical Notch activation pathway. The Notch polypeptide is synthesised in the ER, where it is fucosylated. This aids folding (see Section 1.7). 1) S1 furin cleavage occurs in the Golgi prior to presentation of the receptor at the cell surface. 2) Endocytosis by the ligand-presenting cell leads to a conformational change in the NRR of Notch (see Section 1.5.3). 3) This allows S2 cleavage by ADAM10, and exposes the S3 intramembrane cleavage site. 4) S3 cleavage by γ-secretase. 5) After S3 cleavage the N_{ICD} translocates to the nucleus 6) N_{ICD} relieves repression of Hes/Hey genes by forming the CSL-MAML complex (see Section 1.5.4). 7) Ligand expressed on the same cell is capable of inhibiting Notch signalling. For the purposes of this figure the receptors and ligands are shown as extended molecules, but the domain organisation and inter-molecular interactions are not known.

manner (Cordle *et al.*, 2008a) but it is not clear if these represent the cis and trans protein complexes.

In addition to Notch signalling being inhibited by ligand expressed on the same cell, the Notch receptor is also able to sequester ligand and decrease that cell's ability to activate Notch signalling in neighbouring cells (Becam *et al.*, 2010). This effect of gene dosage is demonstrated in a $Notch^{+/-}$

Delta$^{+/-}$ fly that shows neither the Notch nor the Delta phenotype in its developing wing, as the reduction in the level each protein presumably compensates for each other (de Celis and Bray, 2000).

1.3 Notch signalling and disease

Deregulation of the Notch signalling pathway is known to cause a wide-range of developmental or adult-onset diseases. It has also been implicated in a number of different types of cancer. For a brief summary, see Table 1-1.

1.3.1 Alagille Syndrome

Alagille syndrome is an autosomal dominant congenital disorder associated with mutations in the gene encoding Jagged1 (*JAG1*) (Li *et al.*, 1997). It is typically characterised by abnormal hepatic bile ducts, cardiac disease, skeletal defects and eye abnormalities, and normally has characteristic facial features. Patients with Alagille syndrome have been reported with a deletion of the *JAG1* gene (Krantz *et al.*, 1998), frameshift mutations that give rise to premature termination codons, splice site mutations, and missense mutations (Spinner *et al.*, 2001). Premature termination and splice-site mutations will produce transcripts that are rapidly degraded by nonsense-mediated decay, or will produce non-functional truncated proteins. Two point mutations in the MNNL of Jagged1 that are known to cause Alagille syndrome result in the production of Jagged1 protein that accumulates in intracellular compartments and is abnormally glycosylated, resulting in a functional haploinsufficiency (Morrissette *et al.*, 2001). A large number of other missense mutations have been mapped to the MNNL domain of Jagged1, but it is unclear why these mutations destabilise the protein (Röpke *et al.*, 2003). Several other mutations that result in the substitution of conserved cysteine residues within the EGF region of Jagged1 have also been reported to cause Alagille syndrome (Warthen *et al.*, 2006). All of these different classes of mutations will result in a reduction in the level of functional Jagged1 at the cell surface, and therefore it is likely that haploinsufficiency is the major mechanism of pathogenesis (Crosnier *et al.*, 1999).

Mutations in the gene encoding Notch2 have recently been found to cause Alagille syndrome, suggesting that the Notch2-Jagged1 interaction is physiologically important during development, and Jagged1 and Notch2 have previously been shown to interact in hepatic bile duct formation (Hofmann *et al.*, 2010). Missense, nonsense, frameshift, and splice-site mutations in the *NOTCH2* gene have been found to cause Alagille syndrome (Kamath *et al.*, 2012). As in the *JAG1* mutants outlined above, nonsense, frameshift and certain splice-site mutations are likely to result in degradation of the Notch2 mRNA. The missense mutations that have been found in the *NOTCH2* gene occur in the regions that code for both the extracellular and the intracellular region of Notch (Kamath *et al.*, 2012). The mutations affecting the intracellular region cluster in the ankyrin domains which suggests that they might disrupt the interaction between the N_{ICD} and the CSL protein (see Section 1.5.4). Six mutations have been found that cause amino acid substitutions in the N_{ECD}. Specifically these substitutions cluster around the ligand binding region of Notch2. Three of these are C→X substitutions, and two are P→X substitutions (where X is another amino acid). These are all are likely to cause misfolding in an EGF domain. The last of these mutations causes the I681N substitution in EGF18. This occurs N-terminal to the calcium binding consensus sequence in this domain, and hence may disrupt calcium binding in this domain, or inter-domain packing. There is some data that suggests a role for this region in regulating Notch signalling in *Drosophila* (Lawrence *et al.*, 2000), and hence loss of calcium binding here could disrupt this. All of these mutations that cause an amino acid substitution in the extracellular domain of Notch2 are likely result in a non-functional Notch receptor, and have been found to signal poorly *in vitro* (Kamath *et al.*, 2012).

1.3.2 CADASIL disease

Cerebral autosomal dominant arteriopathy with subcortical infacts and leukoencephalopathy (CADASIL) is an inherited disease associated with mutations in *Notch3* (Joutel *et al.*, 1996). The majority of mutations associated with CADASIL result in a mis-sense mutation that either removes or introduces a cysteine residue in an EGF in Notch3, leading to an EGF containing an odd number of cysteine residues (Joutel *et al.*, 1996). Based on studies of disease-causing mutations affecting EGF

domains in fibrillin1 (Suk *et al.*, 2004), these are likely to cause either local or more global misfolding of the protein. CADASIL is characterised by the accumulation of granular osmiophilic material within smooth muscle tissue, which leads to the degeneration of smooth muscle cells and thickening of the arterial wall in the brain. This material is found extracellularly, near to the cell wall within the muscle (Tikka *et al.*, 2009). This can lead to ischemic stroke; hence CADASIL is also known as hereditary stroke disorder. Notch3 expression is restricted to smooth muscle cells in adults (Joutel *et al.*, 2000), explaining the vascular phenotype.

Various mouse models for CADASIL have been studied, to try and understand the effects of particular mutations. Mice with the *Notch3-/-* genotype have impaired arterial growth, and structural defects in the vascular systems (Domenga *et al.*, 2004), but do not exhibit CADASIL symptoms, suggesting that the disease is not necessarily caused a lack of Notch3 signalling. A series of mutations in *Notch3* that are known to be associated with CADASIL and cause amino acid substitutions (R90C, C212S, R1006C, R133C, C183R) were found to have near wild-type ligand binding and Notch3 activity in co-culture assays (Peters *et al.*, 2004), (Joutel *et al.*, 2004). In addition to this, Notch3 containing the R90C substitution is able rescue *Notch3* mutant mice (Monet *et al.*, 2007), although some granular material is still deposited within smooth muscle in these mice. Two other mutations that affect the ligand binding region (EGF 10-11) of Notch3 produce protein that fails to either bind ligand or activate signalling in the same studies.

Overexpression of a human disease-causing mutant form of Notch3 (R169C) in mice leads to CADASIL symptoms (Joutel *et al.*, 2010), and two separate CADASIL-causing mutations cause spontaneous aggregation of a short construct containing EGF domains 1-5 of Notch 3 (R133C, C183R) *in vitro* (Duering *et al.*, 2011). This supports the hypothesis that it is the accumulation of misfolded protein within smooth muscle tissue that causes CADASIL, rather than defective Notch signalling caused by mutations in the *Notch3* gene (Opherk *et al.*, 2009).

1.3.3 Notch in Cancer

Notch signalling has been associated with a wide variety of cancers, and can act either as an oncogene or a tumour suppressor. Mutations affecting the NRR region, including deletions of the LNR domains (see Section 1.5.3), or mutations in the PEST degradation domain (see Section 1.5.4) can lead to a constitutively active form of Notch. Alternatively, mutations in the Anykyrin domain or in other components of the Notch signalling machinery such as MAML or the γ-secretase complex can prevent Notch activation.

T-cell Acute-Lymphoblastic Lymphoma (T-ALL) is associated with mutations in the Notch1 receptor (Ellisen *et al.*, 1991). A chromosome translocation that was found to cause T-ALL (Reynolds *et al.*, 1987) was later found to produce a version of the Notch receptor lacking the EGF and LNR regions (Ellisen *et al.*, 1991). A large number of point mutations associated with T- ALL have been mapped to the NRR (Weng *et al.*, 2004), (Gordon *et al.*, 2007) (see Section 1.5.3). These substitutions are thought to disrupt the packing between the HD and LNR domains, which could leave the S2 site exposed and susceptible to cleavage by ADAM10. Since this initial discovery, a second class of mutations that contains a 12-15 amino acid insertion has been identified that causes the S2 sequence to be exposed (Malecki *et al.*, 2006). This means the S2 site is not protected against TACE cleavage, so therefore is susceptible to proteolysis.

Inhibition of Notch activation in a T-ALL cell line using either presenillin inhibitors (part of the γ-secretase complex) or an artificial MAML peptide can inhibit cell growth, demonstrating that the mutations associated with T- ALL lead to a constitutively activate Notch receptor that can undergo RIP in the absence of ligand (Weng *et al.*, 2003). Antibodies that stabilise the interaction between LNH-A and the HD domain of Notch, and hence protect against S2 cleavage have been shown to be effective in reducing Notch activation in a Notch isoform-specific manner (Li *et al.*, 2008).

The N_{ICD} also has mutations and deletions associated with it, typically within the PEST domain. These disrupt the degradation of the intracellular fragment by altering its phosphorylation state. Several

cases of Chronic Lymphocytic Leukemia (CLL) and Mantle Cell lymphoma (MCL) have been linked to PEST mutations or deletions in Notch1 (Kridel *et al.*, 2011), and an increasing number of solid tumours are being found with mutations affecting the PEST domain of Notch (Westhoff *et al.*, 2009).

Several Notch loss of function mutations have been found in cancers, and chronic anti-DLL4 antibody treatment for certain cancers has ironically been found to lead to an increased risk of skin cancer (Yan *et al.*, 2010). A recent trial of semegacastat, a γ-secretase inhibitor, in Alzheimers patients lead to similar side- effects (Henley *et al.*, 2009) (Li *et al.*, 2007).

1.3.4 Other developmental disorders associated with the Notch pathway

Mutations in several components of the Notch signalling pathway have also been found to cause a variety of other genetic disorders. For a concise summary of each, see Table 1-1:

- Tetralogy of Fallot – characterised by a severe cardiac phenotype, and can be one of the range of symptoms associated with other developmental syndromes, such as Alagille Syndrome. However, it can present as an isolated disorder, and these individuals do not have other symptoms associated with Alagille Syndrome. Jagged1 is highly expressed in the developing heart (Loomes *et al.*, 1999), and symptoms typically include defects in the ventricular septum (hole in the heart) and defective pulmonary valve development (Eldadah *et al.*, 2001).
- Aortic valve disease – associated with calcification of the aortic valve. Notch1 normally represses the expression of *Runx2*, which causes cells to adopt an osteoblast fate. Mutations associated with aortic valve disease typically cause premature termination of Notch1, and result in nonsense-mediated decay so *Runx2* is no longer repressed, leading to calcification of the valve (Garg *et al.*, 2005).
- Spondylocostal/spondylothoracic dysostosis – associated with severe skeletal phenotypes, caused by defective somitogenesis (Sparrow *et al.*, 2007). Due to the complex spatial and temporal regulation Notch signalling during somitogenesis, mutations in genes encoding

several different components of the Notch signalling pathway have been found to cause improper somitogenesis, resulting in spondylocostal or spondylothoracic dysotosis. These include *Lunatic Fringe* (Sparrow *et al.*, 2006), *DLL3* (Bulman *et al.*, 2000), *HES7* (Sparrow *et al.*, 2008) and MESP2 (Whittock *et al.*, 2004) (a class of helix-turn-helix molecules associated with Notch activation).

- Hadju-Cheney syndrome – autosomal dominant bone disease. Severe osteoporosis and focal bone loss, some craniofacial abnormalities and renal cysts (CHENEY, 1965). Caused by mutations/truncations in Notch2 PEST domain, leading to hyperactivation of Notch signalling (Simpson *et al.*, 2011).

Table 1-1 A summary of the main diseases associated with the Notch pathway

Disease	Associated molecules	Mutations	Phenotypes
Alagille	Jagged1/Notch2	Mis-sense/frameshift/splice site, leading to nonsense mediated decay or retention of Jagged1 within cells	Skeletal, ocular, hepatic blle duct, cardiac, renal developmental abnormalities
CADASIL	Notch3	C→X / X→C substitutions*	Granular osmiophilic material accumulation, ischaemic stroke, loss of capillary smooth muscle
T-ALL	Notch1	N-terminal truncations, missense mutations in HD domain, duplication of S2 site	Hyperproliferation of T cells
Tetralogy of Fallot	Jagged1	Missense mutations clustered in N-terminal domain but occurring elsewhere too	Hole in septum of heart
Aortic valve disease	Notch1	Frameshift mutations, leading to nonsense mediated decay	Calcified aortic valve, bicuspid valve
Hadju-Cheney	Notch2	Mutations/truncations to PEST domain – typically in last exon n.b. protein is made but not degraded once activated	Osteoporosis, craniofacial defects, renal cysts
Spondylocostal/ Spondylothoracic dysostosis	Lunatic Fringe/DLL3, MESP2, HES7	DLL3: truncations/missense Lfng: missense mutation – inactive enzyme with incorrect subcellular localisation MESP2: frameshift insertion HES7:	Fused/deleted/ uneven vertebrae, severe curvature of the spine, truncal shortening

*X represents any amino acid

1.4 EGF domains – the major domain type within Notch receptors and their ligands

1.4.1 The EGF domain

The Epidermal Growth Factor-like (EGF) domain makes up the majority of the extracellular portion of both the Notch receptor and its ligands, as well as a wide variety of other proteins involved in blood clotting (factor IX and X), cholesterol uptake and many components of the extracellular matrix, including fibrillins, fibulins, LTBPs. Some EGF domains contain a consensus sequence in their N-terminus that allows them to bind calcium (cbEGF) and the Notch receptor and its ligands contain a mixture of EGF and cbEGF domains. Each EGF domain contains six cysteine residues that usually form three disulphide bridges in the pattern 1-3, 2-4, 5-6 (Figure 1-3 A). These domains do not have a well-defined hydrophobic core – instead they contain a central β-hairpin, and otherwise have largely unstructured loops between cysteine residues.

1.4.2 The cbEGF domain

A set of consensus residues in the N-terminus of some EGF domain that enables them to bind calcium (**D/N**-X-**D/N**-**E/Q**-X_m-**D/N**-X_n-**Y/F**, where m and n are variable) (Figure 1-3 B) was first identified in the first EGF domain of human Factor IX (Rees *et al.*, 1988) (Handford *et al.*, 1991) (Mayhew *et al.*, 1992). There are several different combinations of amino acids that are capable of binding calcium, which is usually coordinated by pentagonal bi-pyramidal binding geometry, with up to seven ligands contributing towards calcium binding. Anionic oxygen ligands are required, which typically come from the side chain residues of the third and fourth residues in the consensus. The first residue in the consensus donates a ligand to the calcium ion, and the second residue forms an AsX turn by forming a hydrogen bond with the amide group from following cysteine. Two backbone carbonyl oxygen ligands are donated from residues above and below the pentagonal arrangement of ligands, while Y/F aromatic residue in the consensus packs against other hydrophobic residues in the domain to stabilises the calcium-binding site (Rao *et al.*, 1995).

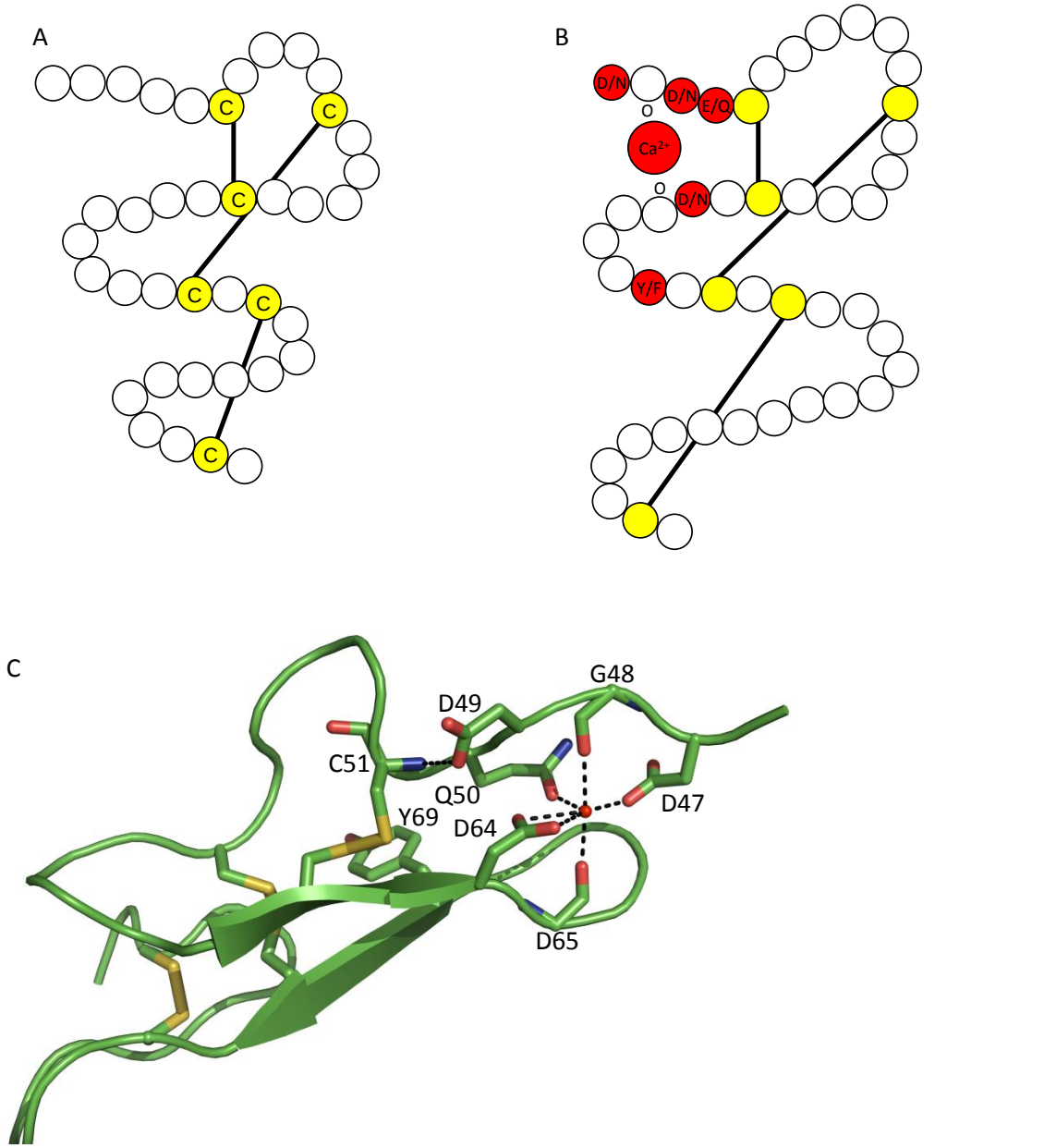


Figure 1-3 Schematic diagram of EGF and cbEGF domain, to highlight disulphide bonding pattern and position of calcium binding consensus residues, and the geometry of calcium binding within cbEGF from human Factor IX. An EGF (A) has the same overall structure as a cbEGF domain (B). The relative positions of the calcium binding consensus residues in the N-terminus of the cbEGF that confer the ability to bind calcium are indicated highlighted in red. C) The calcium binding residues from Factor IX (pdb 1EDM) are indicated – D47 donates an anionic oxygen ligand, D64 donates two ligands from a delocalised carboxylic acid group, Q50 donates a side-chain carbonyl oxygen ligand. G48 and D65 donate backbone carbonyl oxygen ligands. Y69 packs against other hydrophobic side-chains to stabilise calcium binding. D49 forms an AsX turn by hydrogen-binding with the backbone amide group in C51.

A cbEGF domain in isolation can behave differently when it is placed in its native context within a molecule. A C-terminal cbEGF domain with a domain N-terminal to it has a higher affinity for calcium than it would without the N-terminal domain present due to this inter-domain packing (Downing *et al.*, 1996). Tandem cbEGF repeats tend to pack in an extended conformation (Downing *et al.*, 1996), as the calcium ion together with a hydrophobic packing interaction creates a stable inter-domain packing interface. Both domains in a cbEGF pair tend to align well with each other along their long axes, and binding of calcium to the C-terminal domain in the pair stabilises the entire domain on a fast NMR timescale (Werner *et al.*, 2000).

1.4.3 Class I vs Class II cbEGF domains

cbEGF domains fall into two broad classes, based on the length of amino acid spacer between the final cysteine domain in the N-terminal domain, and the first calcium-binding consensus residue in the C-terminal domain. Class I cbEGF proteins have a single amino acid as a linker, and include the majority of the proteins involved in forming elastic fibres and connective tissue (fibrillins, LTBPs, fibulins etc) (Downing *et al.*, 1996). All of the proteins associated with the Notch pathway contain Class II cbEGF domains, which have a two amino acid linker between the domains. This additional amino acid in the linker changes the relative orientation of adjacent cbEGF: a twist angle of ~119 ±5° in Class II (Hambleton *et al.*, 2004) vs 159 ± 6° for Class I (Downing *et al.*, 1996) cbEGF domains. The tilt between the two domains is consistent, at around 17-18° for tandem repeats of both classes of cbEGF, and tandem repeats of both classes adopt a rod-shaped extended conformation with hydrophobic packing at the interface between the domains.

1.5 The Notch Receptors

The *D. melanogaster Notch* receptor was the first component of the pathway to have its gene sequenced (Wharton *et al.*, 1985). It encodes a 300 kDa single-pass transmembrane protein consisting of 2,703 amino acids. It has four homologues in humans (Notch1-4), and two homologues in *C. elegans* (Lin-12 and Glp-1) (Yochem and Greenwald, 1989), (Yochem *et al.*, 1988) (Figure 1-4). The Notch receptor is synthesised as a single polypeptide in all species, and can undergo proteolysis in the trans-Golgi network at the S1 site by a furin-like convertase (Blaumueller *et al.*, 1997). Cleavage here is essential for Notch activity (Lake *et al.*, 2009). The S1 site is located ~70 amino acids N-terminal to the transmembrane region, and the short extracellular portion of the intracellular domain interacts with the extracellular domain to form a heterodimer at the cell surface. The intracellular region of Notch is tethered to the cell membrane by the transmembrane region, and contains the domains required for DNA binding and activation of the *HES* genes.

1.5.1 The extracellular region

The extracellular domain of the Notch receptor (N_{ECD}) is made up of a variable number of EGF and cbEGF domains, and the Negative Regulatory Region (NRR) that keeps the receptor in an inactive state. This comprises three Lin-12/Notch repeats (LNRs) that interact with the heterodimerisation domain. The EGF domains are involved in ligand binding and receptor activation, and vary in number according to species: *Drosophila* Notch contains 36 EGF domains, human Notch4 contains 29, whereas the *C. elegans* homologues are much smaller and contain 14 (Lin-12) and 12 (Glp-1) (Figure 1-4).

1.5.2 The EGF domains

A series of deletion mutants identified EGF repeats 11-12 of *Drosophila* Notch (dNotch) as necessary and sufficient for ligand binding (Rebay *et al.*, 1991) in a cell-aggregation study. The same region of the Notch receptor has been implicated in *cis*-inhibition (Becam *et al.*, 2010). An *in vivo* mutagenesis

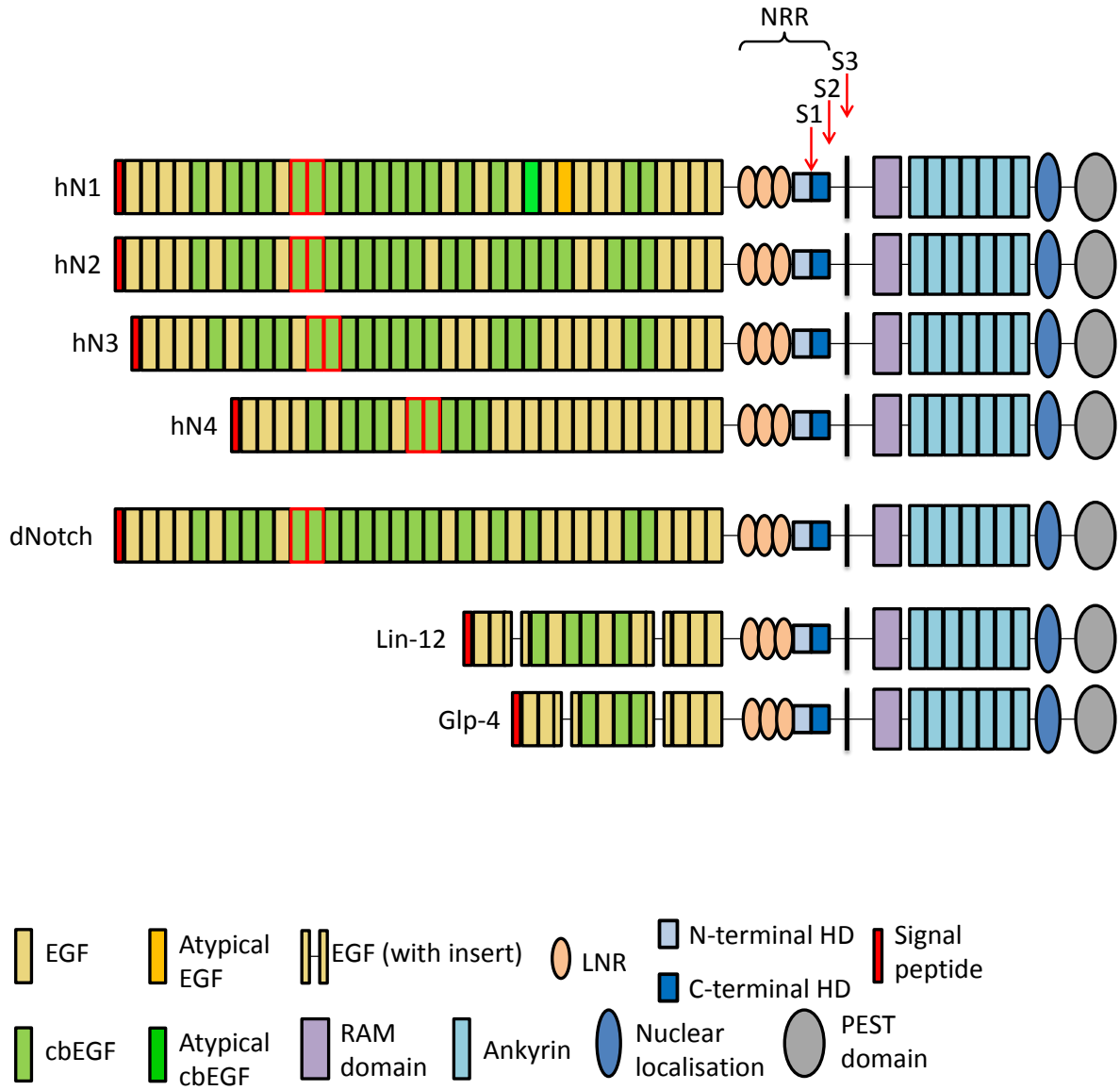


***Figure 1-4 Domain architecture of the Notch receptor from* Drosophila*, mammals, and* C. elegans.** The Drosophila Notch receptor and human Notch1-4, shown as single pass membrane proteins. The human proteins exist as heterodimers at the cell surface. dNotch and Notch1-2 contain 36 EGF domains, Notch3 contains 35, and Notch4 contains 29. The EGF domains implicated in ligand binding are outlined in red. C-terminal to the EGF domains are three LNR domains and the heterodimerisation (HD) domain, which together form the NRR. The orientation of the receptors relative to the membrane is shown, with the extracellular region on the left. The relative positions of the furin cleavage site (S1), ADAM-10 (S2) and γ-secretase (S3) sites are indicated.

screen in *Drosophila* has identified an E→V substitution within the calcium binding consensus sequence in EGF12 (N^{M1}), that acts as an antimorphic *Notch* allele (de Celis *et al.*, 1993). This suggests that not only does this substitution eliminate ligand binding and Notch signalling, but that the mutant protein can also interact with WT Notch and reduce its ability to signal. A series of

calcium binding mutants within Notch EGF repeats 11-14 have shown that only calcium binding in EGF12 is essential for binding to Delta, both in SPR and flow cytometry (Cordle *et al.*, 2008b), and the Notch 11-13 construct binds to cells expressing full length DLL1 in a calcium-dependent manner. The structure of this region of human Notch1 was first solved by NMR (Hambleton *et al.*, 2004). This shows that each individual domain resembles EGF domains from Factor IX and Fibrillin (Downing *et al.*, 1996), and that tandem cbEGF domains in Notch form an extended rod-like structure that is stabilised by calcium ions that promote inter-domain packing interactions. The crystal structure of this region (Figure 1.5) closely resembles this solution structure (Cordle *et al.*, 2008a). A conserved aromatic residue between C_5 and C_6 packs against the turn in the main β-sheet in the adjacent EGF domain (Downing *et al.*, 1996) (Cordle *et al.*, 2008a) (Figure 1-5) and this interaction stabilises the rod-like structure of the tandem pair.

Given the high number of predicted cbEGF domains within the Notch receptors, together with the conservation of residues involved in inter-domain packing, it is likely that overall they form an extended structure, as has been postulated for another cbEGF-containing protein fibrillin1 (Jensen *et al.*, 2005). It is possible however that the interface between an N-terminal cbEGF and C-terminal EGF domains (eg at EGF5-6, 9-10, 19-26) does not form a rod-like structure, and instead could introduce either regions of flexibility, or 'kinks' in the Notch receptor, though as yet there is no structural data for this configuration of domains. Interestingly, whilst the aromatic residue mentioned above is conserved in the majority of the Notch EGF domains, cbEGFs 9 and 31 do not contain aromatic residues in this location, suggesting that they could be areas of flexibility within the Notch receptor.

A cluster of mutations that causes a separate class of Notch wing vein phenotypes has been identified within the region spanning EGF domains 24-29. These are known as the *Abruptex* mutations, and cause interruptions in the wing vein (Welshons, 1971). They fall into three separate classes, based on their phenotype when either homozygous, or heterozygous with *Notch* or other *Abruptex* alleles (Foster, 1975), (Portin, 1975), (de Celis and Garcia-Bellido, 1994).

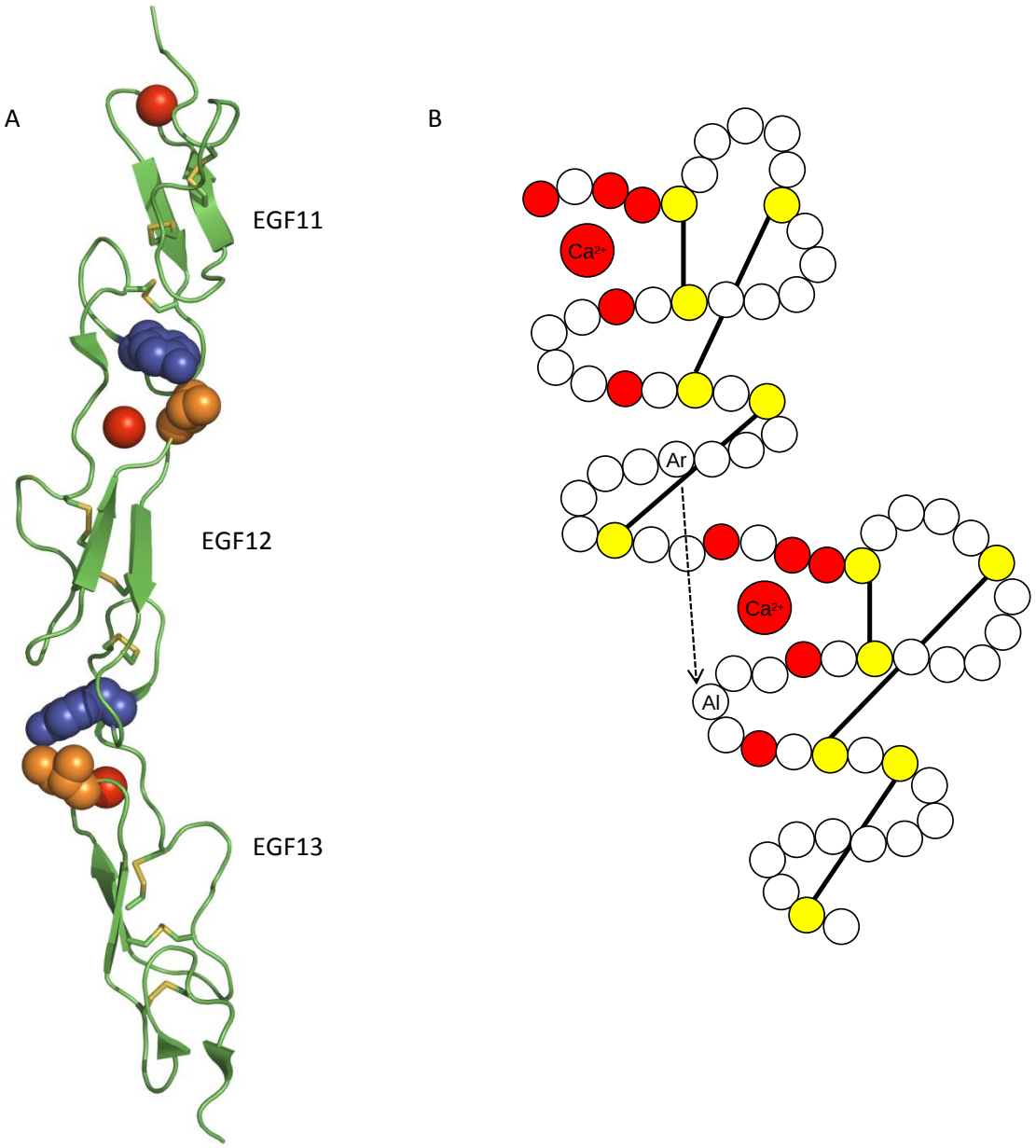


Figure 1-5 Crystal structure of hN1$_{11-13}$ with inter-domain packing indicated, and the position of the conserved aromatic residue within the EGF domain. (A) Notch1 EGF1$_{11-13}$ forms an extended structure (PDB 2VJ3), stabilised by packing between adjacent EGF domains. Conserved aromatic residues (blue) pack against aliphatic residues (orange) in the β-hairpin of the C-terminal domain. This is dependent on calcium binding - indicated as red spheres. (B) The positions of the aromatic (Ar) and aliphatic (Al) residues within a tandem EGF pair, and the packing interaction between them, are indicated. Amino acids highlighted in red form part of the calcium-binding consensus sequence, cysteine residues are highlighted in yellow.

The lethal alleles (Ax^{59d} and Ax^{59b}) are characterised by C → X mutations (Kelley *et al.*, 1987), and are likely to disrupt the fold of the EGF24 domain. They are not embryonic lethal however, as flies with these mutations are viable to the larval or pupal stage of development respectively. The enhancer alleles cause a more severe *Notch* phenotype (Ax^{E2} and Ax^{16172}) (Hartley *et al.*, 1987), and the suppressor alleles cause a WT phenotype when heterozygous with a *Notch* null allele (Ax^{28} and Ax^{9B2}) (Kelley *et al.*, 1987). Enhancer alleles crossed with suppressor alleles are lethal at the pupal stage of development (Foster, 1975).

It has been proposed that the Abruptex region of Notch might interact with either Notch ligands, or the ligand-binding portion of the Notch receptor, as a possible mechanism for the complementation seen in the genetic studies. A recent electron-microscopy study on the N_{ECD} from both humans and flies has suggested that the Notch may not be fully extended in solution, and that it might form a dimer (Kelly *et al.*, 2010). Several other studies have seen glimpses of Notch-Notch protein interactions (Sakamoto *et al.*, 2005), (Vooijs *et al.*, 2004), (Kidd *et al.*, 1989), and it is clear from the various crosses carried out in *Drosophila* that the protein products of the two alleles of Notch appear to interact. It would appear that this interaction is able to down-regulate Notch signalling, but the precise molecular mechanism of dimerisation is not known.

A construct containing the domains 21-30, which encompasses the Abruptex region of Notch, has been found to interact with Notch 11-20 (which includes the ligand binding region) (Pei and Baker, 2008), with an apparent K_d of the same order of magnitude as that of Delta for N11-20. There is some also some evidence that domains 17-26 might interact with Serrate and Delta, as Notch constructs lacking these domains show reduced signalling to both ligand classes (Lawrence *et al.*, 2000). Certain Ax mutations also show reduced sensitivity to *cis*-inhibition, and are less effective at sequestering ligand molecules at the cell surface (de Celis and Bray, 2000).

1.5.3 The NRR of Notch

Between the EGF repeats and the transmembrane region of the Notch receptor lies the Negative Regulatory Region (NRR) (Figure 1-4). This comprises three Lin-12/Notch repeats (LNR) domains, and both the N-terminal and C-terminal halves of the heterodimerisation domain. The two parts of the heterodimerisation domain are intertwined in a single fold, which ensures the two parts of the Notch receptor are held together after S1 cleavage.

A solution structure of a LNR domain from Notch1 has been obtained (Vardar *et al.*, 2003), and later confirmed in the crystal structure of the intact NRR from Notch2 (Gordon *et al.*, 2007) (Figure 1-6). LNR domains are mainly unstructured, with only two short regions of α-helix. These domains do not possess a hydrophobic core, but contain several surface-exposed hydrophobic amino acids that contribute to the packing against the HD domain. Each LNR contains six cysteine residues, which form three disulphide bonds in a 1-5, 2-4, 3-6 bonding pattern, and contains conserved acidic residues that confer the ability to bind calcium, which helps stabilise the domain The LNR repeats fold around the HD domain in such a way as to conceal the S2 cleavage site in the C-terminal heterodimerisation domain (Gordon *et al.*, 2007) (Figure 1-6).

Overall the surface area buried by the interaction between the LNR repeats and the HD domain is ~3000Å^2, and is stabilised by additional hydrogen bonds and salt bridges between the domains (Gordon *et al.*, 2007). The S2 cleavage site is directly shielded by the peptide linking LNR-A and LNR-B, whilst the rest of the LNRs pack against the HD domain. Ligand binding to the Notch receptor leads to endocytosis of the ligand-receptor complex by the ligand-expressing cell (Klueg and Muskavitch, 1999), (Meloty-Kapella *et al.*, 2012), which generates a pulling force (Shergill *et al.*, 2012) that causes a conformational change in the NRR (Parks *et al.*, 2000), exposing the S2 site and allowing proteolysis to occur. A recent single-molecule AFM study has managed to measure the forces required to unfold the NRR (Dey and Szoszkiewicz, 2012) and has found that ~100pN is required to remove a single LNR domain from the surface of the HD domain. Notch signalling can be

activated by EDTA in a ligand-independent manner, as removing the calcium ions from the LNR domains destabilises their fold and causes them to detach from the surface of the HD domain.

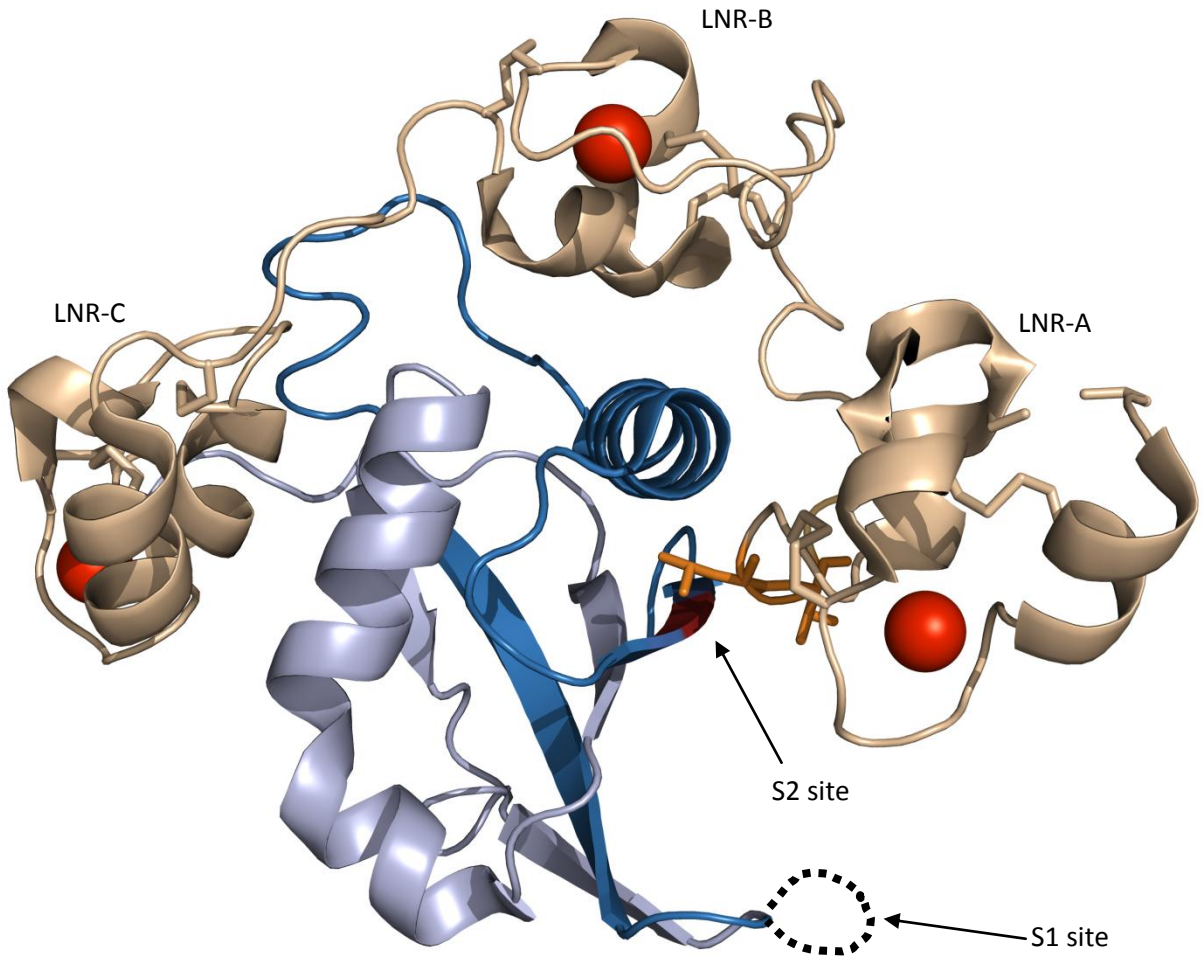


Figure 1-6 The NRR of Notch2. The structure of the NRR region of Notch2 (PDB 2OO4) The NRR region consists of three LNR repeats (A-C, brown), and the HD domain. Each LNR binds Ca^{2+} (red spheres). The LNR repeats are shown in light brown, the N-terminal HD domain is shown in grey, and the C-terminal HD domain is shown in blue. The S2 site is indicated in dark red (S1665, V1666), within the HD domain. The linker between LNR-A and LNR-B is indicated by residues shown as sticks (L1457, T1458), which are coloured dark orange. These residues are required to inhibit S2 cleavage. The loop removed by the furin at the S1 cleavage site is shown as the dashed line; the two halves of the HD domain are a single polypeptide chain in this model.

1.5.4 The Intracellular fragment

The Notch intracellular domain (N_{ICD}) contains a RAM domain, a series of Ankyrin domains, a PEST sequence and a nuclear localisation sequence. Together, the RAM and Ankyrin domains are able to relieve repression of the *HES* family of genes. The RAM domain forms a largely unstructured protein in solution that does not adopt any formal structure when expressed as the larger RAM-ankyrin protein. By contrast, the ankyrin domain consists of seven well-defined ankyrin repeats.

In the absence of Notch signalling, gene expression is repressed by a complex formed of a CSL transcription factor and SMRT/NcoR/HDAC1 (Kao *et al.*, 1998) or CIR/HDAC2/SAP30 (Hsieh *et al.*, 1999) binding to specific DNA sequences upstream of *HES* genes (Dou *et al.*, 1994). Once Notch signalling is activated, N_{ICD} translocates to the nucleus, where it can displace the co-repressor protein, and form a ternary complex with the CSL protein and MAML. This then allows the recruitment of several other activators of transcription, including p300 and PCAF (Kurooka and Honjo, 2000), (Fryer *et al.*, 2002), (Wallberg *et al.*, 2002).

Several structural and binding studies have revealed how the N_{ICD}-CSL complex assembles (Kovall, 2008), and recently a high resolution structure of the RAM-ANK/CSL/MAML complex was obtained (Figure 1-7) (Choi *et al.*, 2012). The isolated ankyrin region can bind CSL weakly (Nam *et al.*, 2003), but N_{ICD} interacts strongly through its RAM domain (Johnson *et al.*, 2010) to displace the co-repressor proteins (Tamura *et al.*, 1995) (Friedmann *et al.*, 2008). Formation of the N_{ICD}-CSL complex creates an extended groove at the interface between the ankyrin domain and CSL that binds the N-terminal (residues 13-74) of MAML. This peptide is unstructured in solution and undergoes a significant rearrangement to form a long α-helix upon binding (Nam *et al.*, 2006). Neither the CSL nor the ankyrin domain is able to bind MAML independently, highlighting the importance of the formation of the composite binding site. Some HES genes have tandem upstream CSL binding sites, and it is possible for two N_{ICD}-CSL complexes to form an antiparallel dimer bound to DNA, via salt-bridge contacts between the ankyrin domains (Figure 1-7 B) (Arnett *et al.*, 2010).

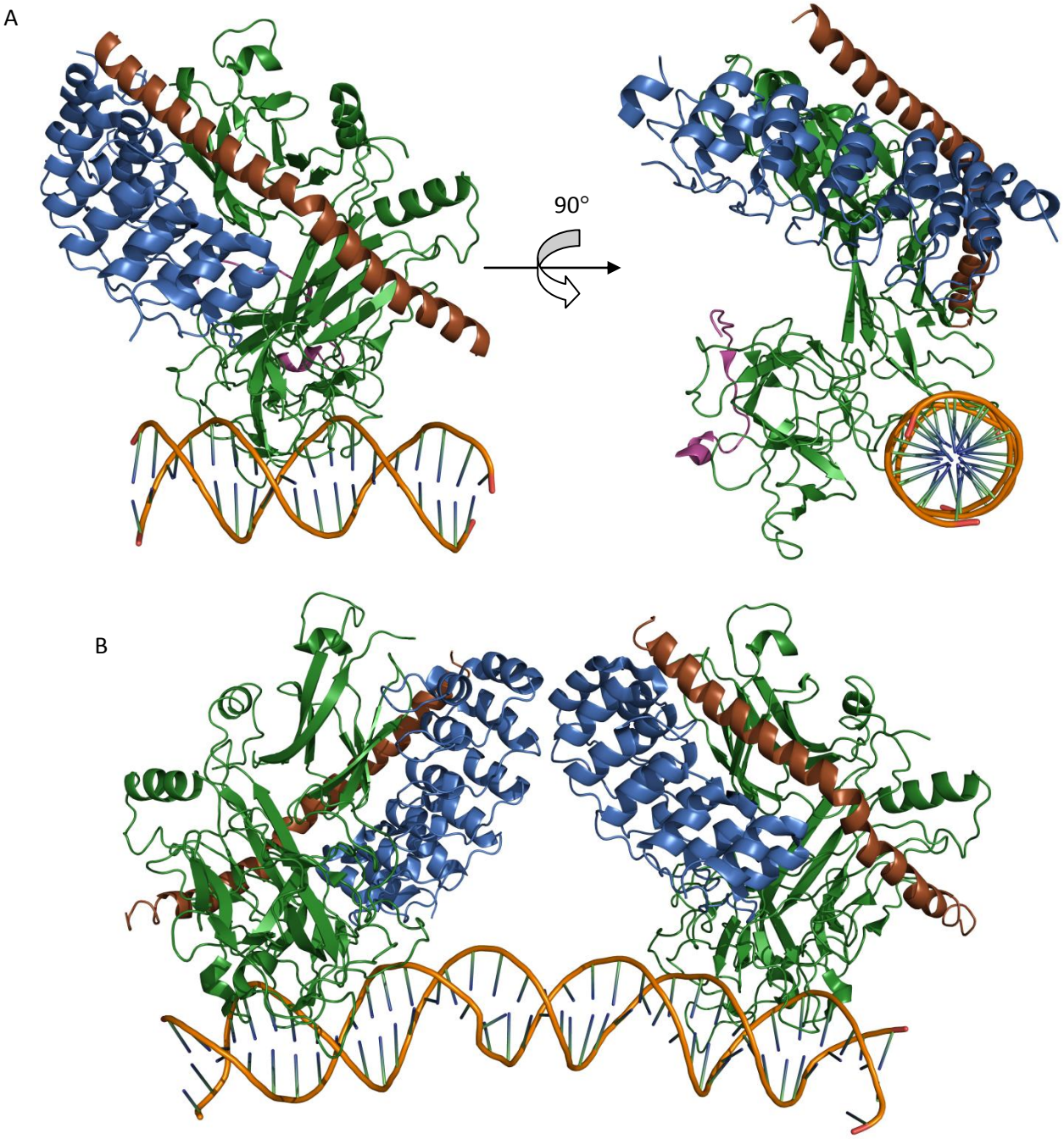


Figure 1-7 Structures of the N_{ICD}-CSL complex, and the N_{ICD}-CSL complex dimer bound to DNA containing two CSL binding sites. A) Binding of the N_{ICD} to CSL is driven by RAM (pink) binding to the rear face of CSL (green). The ankyrin domain (blue) and CSL protein then form an extended groove that allows MAML (brown) to bind (3V79). B) Two copies of the N_{ICD}-CSL complex can interact via their ankyrin domains, if there are two CSL DNA binding sequences present (PDB 3NBN).

The PEST domain is defined by a high incidence of Proline (P), Glutamate (E), Serine (S) or Threonine (T) residues (Rogers *et al.*, 1986). These sequences typically target proteins for ubiquitin-mediated proteolysis via the 26S proteasome (Oberg *et al.*, 2001), and mutations or deletions in this region are thought to increase the half-life of the N_{ICD} in the cell. An increasing number of cancers are being found with mutations in this region, including mantle cell lymphomas (Kridel *et al.*, 2012), which is associated with hyperactive Notch signalling.

1.6 The Notch ligands

The *Drosophila* Notch receptor was found to bind to two distinct ligands in cell-aggregation studies: Delta (Fehon *et al.*, 1990) and Serrate (Rebay *et al.*, 1991). *Delta* mutant flies exhibit the same *Notch* neurogenic phenotype as *Notch* null mutants (Lehmann *et al.*, 1981). Both ligands are expressed as single-pass trans-membrane proteins, with a large extracellular region containing many tandem EGF repeats (Figure 1-8). In mammals, there are two homologues of the Serrate class of ligands (Jagged1 and 2) and three homologues of the Delta ligand (DLL1, 3 and 4).

Jagged1 and 2, and DLL1 and DLL4 have all been found to interact with various Notch paralogues (Shimizu *et al.*, 1999), and activate Notch signalling. By contrast, there is no evidence that DLL3 is able to bind to Notch1 or Notch2, or induce Notch signalling (Ladi *et al.*, 2005). It is also unable to rescue a mouse DLL1 knockout during embryogenesis, even when inserted in the DLL1 locus (Geffers *et al.*, 2007), and unlike DLL1 and DLL4 is unable to rescue Delta signalling in *Drosophila*. Despite the apparent inability of DLL3 to interact with Notch in *trans*- or activate Notch signalling, it is able to repress Notch signalling in a cell-autonomous manner (Ladi *et al.*, 2005), in a similar manner to other Notch ligands (Sakamoto *et al.*, 2002). DLL3 has also been found to co-localise with unprocessed Notch1 peptide in intracellular compartments, targeting the protein in regulating Notch signalling. DLL3 inhibition of Notch is of particular importance during somitogenesis, where it is involved in switching off Notch signalling in the S-1 somite, which explains why a range of DLL3 mutations

(Bulman *et al.*, 2000) result in birth defects associated with abnormal somitogenesis (see section 1.3).

1.6.1 The ligand extracellular domains

The canonical Notch ligands consist of an N-terminal domain (Module at the N-terminus of Notch ligands – MNNL) a DSL domain (Delta, Serrate, Lag2) and a varying numbers of EGF and cbEGF domains (Figure 1-8). A large number of Alagille Syndrome mutations (see section 1.3.1) map to the MNNL domain (Röpke *et al.*, 2003) of hJagged1. This domain, in conjunction with the DSL and EGF1-2 domains, has been shown to be necessary and sufficient for Delta binding to dNotch (Parks *et al.*, 2006), but is unable to activate Notch signalling. The Serrate/Jagged class of ligands differs from the Delta class of ligands as the former contains a cysteine-rich (CR) domain at the C-terminus of the extracellular domain. EGFs 4, 6 and 10 in *Drosophila* Serrate contain large insertions of between 38 and 62 amino acids, though their function is unknown. Human Jagged 1 & 2 also contain inserts in domain 10. In both the human and the fly proteins, the insert in domain 10 coincides with an additional pair of cysteine residues; a feature that is also present in EGF2 of DLL3, and in two domains in each of the *C. elegans* Notch receptors. The DSL domain has been shown to be essential for ligand binding to Notch (Henderson *et al.*, 1997). Deletion experiments have shown that a Jagged1 construct containing the N-terminus-EGF2 domains can interact with the Notch2 receptor (Shimizu *et al.*, 1999), and more recent studies have shown that a Jagged1 construct containing only the DSL-EGF3 domains can interact with the $hN1_{11-13}$ fragment, albeit weakly (Cordle *et al.*, 2008a). The DSL domain is present in all canonical Notch ligands in both mammals and flies, but several *C. elegans* ligands lack it. It contains six cysteine residues that form a 1-2, 3-4, 5-6 disulphide bonding pattern. It forms a structure similar to an EGF domain, suggesting that it may have evolved from a pair of EGF domains in the past. The DSL domain is required for both activation and repression of Notch signalling, and the same binding face appears to be involved in both of these functions of the Notch ligands (Cordle *et al.*, 2008a). Sequence homology between the DSL domain from each of the ligands is remarkably low, with the exception of a highly conserved group of surface-exposed amino

acids that form a binding site for Notch (Cordle *et al.*, 2008a) (Figure 1-9). Like the structure of $hN1_{11-13}$, hJagged1 DSL-EGF3 forms an extended structure. Currently there is no published structural information about either the N-terminal domain (MMNL), or the other EGF domains of the Notch receptors, but work is ongoing in this area. However, it appears likely that the binding surface between Notch and its ligands may extend over several domains.

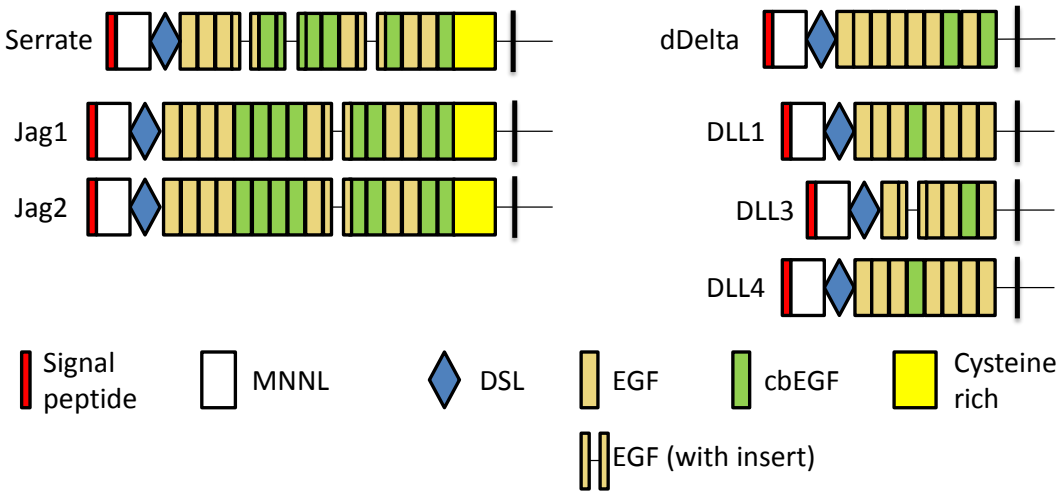


***Figure 1-8 Domain architecture of the canonical Notch ligands from humans and* Drosophila.** The canonical Notch ligands are expressed as single-pass membrane proteins, with short intracellular regions that contain the amino acid sequences required for endocytosis, such as lysine for ubiquitination. The Serrate/Jagged ligand class contains a cysteine-rich domain C-terminal to the EGF domains. Both ligand classes contain EGF domains with an extended loop within them, as indicated by the split EGF domains.

In *C. elegans*, there are two classes of ligands: one containing a DSL domain, and a second class that lacks a DSL domain and instead contains a DOS (Delta and OSM-11) motif (Komatsu *et al.*, 2008). The DOS motif is defined by the consensus C-X(3)-C-X-(3-8)-C-X-(2-5)-C-[K/V/E/R]-C-X(10-12)-C-X(1-3)-P-X(6-9)-C-X(1-4)-W-X(1-4)-C and could be viewed as an EGF domain followed by a pair of cysteine residues. Proteins containing this motif can interact with other *C. elegans* proteins containing a DSL domain in order to promote Notch signalling. It has been suggested that this motif can be found within EGF1-2 of the canonical Notch ligands, and hence that the DSL-DOS pairing in these ligands leads to a greater level of activation of Notch signalling than would be achieved by either of these

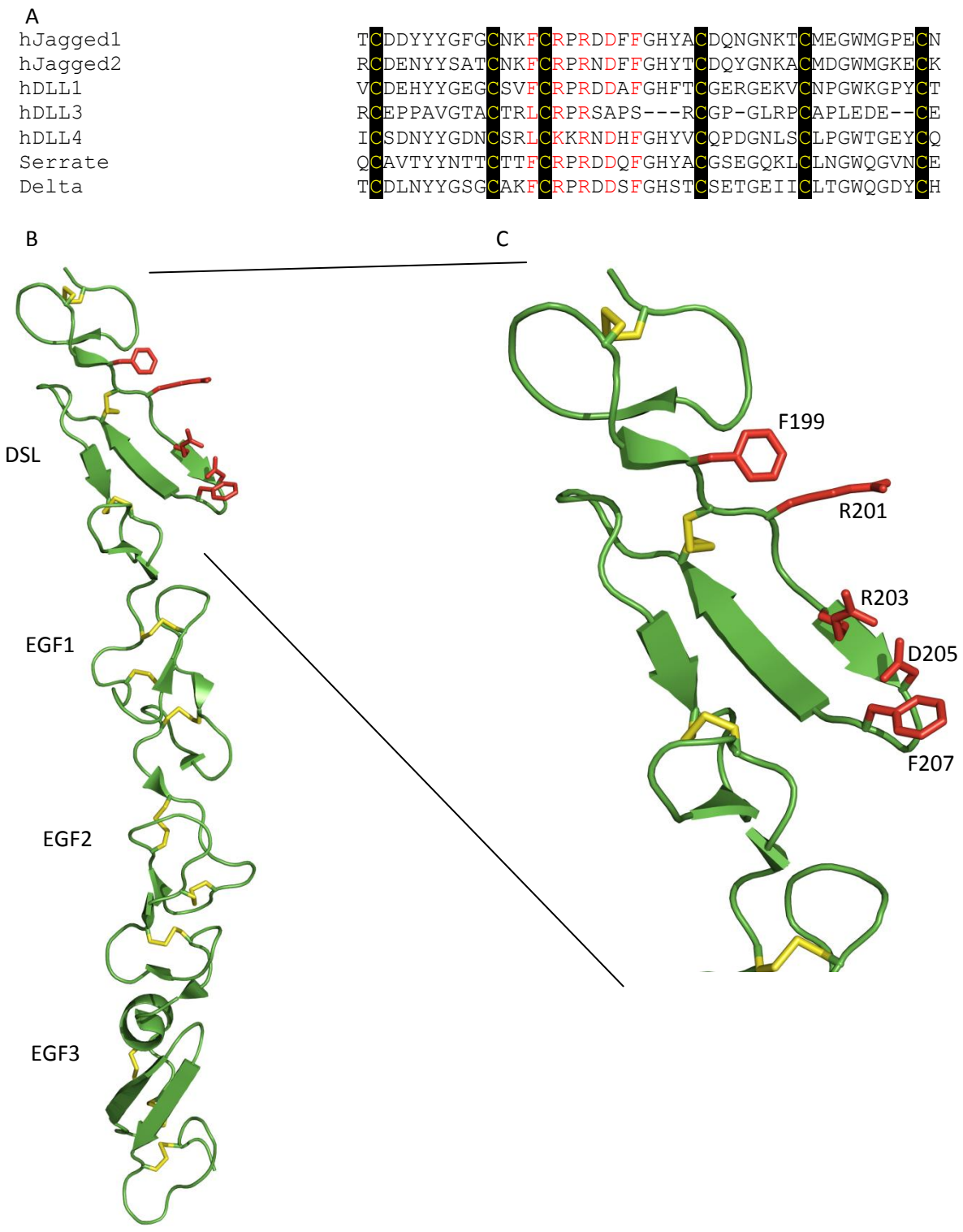


Figure 1-9 DSL-EGF3 of Jagged1, with a magnified view of the DSL domain. A) The DSL domain from different Notch ligands contains a series of highly conserved residues (indicated in red). These have been found to be essential for binding to Notch, and the same residues are involved in ligand binding both in trans-activation and cis-inhibition. B) The DSL-EGF3 domains form an extended rod-like structure (pdb 2VJ2). C) The residues involved in Notch binding map to a single face of the DSL domain (residue numbers from hJagged1).

domains alone (Komatsu *et al.*, 2008). Future structural studies on the DOS proteins could shed some light on the function of the DOS domain, and could potentially reveal similarities to the structure of EGF1-2 from other sources.

1.6.2 Intracellular components required for signalling

In order for a Notch receptor to be activated by a ligand on an adjacent cell, the signal-sending cell must be able to internalise the ligands on its surface and provide a pulling force (Fortini and Bilder, 2009). Constructs lacking the intracellular region of the Notch ligands causes an accumulation of neuronal tissue in developing *Xenopus* embryos (Chitnis *et al.*, 1995), and deletion of the intracellular region of the Delta ligands prevents ligand endocytosis (Itoh *et al.*, 2003), and renders cells unable to induce Notch signalling *in vitro* (Nichols *et al.*, 2007). This suggests that the intracellular region of the Notch ligands is recognised by components of the cells' endocytosis machinery, and that there must be several other intracellular proteins that are required in order for a cell to induce Notch signalling.

The intracellular domains of the DSL ligands contain multiple lysine residues (Glittenberg *et al.*, 2006) that can be ubiquitinated by the E3 ubiquitin ligases Mindbomb (Mib) (Itoh *et al.*, 2003) and Neuralized (Neu) (Deblandre *et al.*, 2001), (Lai *et al.*, 2001). $Mib1^{-/-}$ mice are not viable, due to reduced Notch signalling (Koo *et al.*, 2005), and *neutralized* was amongst the first neurogenic loci associated with defective Notch signalling (Lehmann *et al.*, 1983). Whilst there is a degree of redundancy between these various enzymes and across different species, there is an absolute requirement for the Notch ligands to be ubiquitinated in order for them to activate Notch signalling (Weinmaster and Fischer, 2011).

The Notch ligands also contain a PDZ binding domain that binds to components of the cytoskeleton (Pintar *et al.*, 2007). Ubiquitinated DSL ligands interact with epsin (Wang and Struhl, 2004), (Tian *et al.*, 2004), ubiquitination enhances ligand endocytosis (Hicke and Dunn, 2003). Clathrin, dynamin and auxilin are all also required for endocytosis-induced signalling (Parks *et al.*, 2000), and together,

with actin, these components of the cellular endocytosis machinery are thought to provide the mechanical force required for trans-endocytosis and receptor activation (Meloty-Kapella *et al.*, 2012). It is interesting to note that DLL3 lacks the PDZ domain and lysine residues, which could further explain why it is unable to activate Notch signalling (Geffers *et al.*, 2007).

1.6.3 The non-canonical Notch ligands

In addition to the ligands outlined above, there are several other proteins that can interact with the Notch receptors directly to regulate signalling including the ligands Delta-like 1 and 2 (Dlk1 and 2) (Sánchez-Solana *et al.*, 2011), and DNER (Eiraku *et al.*, 2002). Many of these ligands, including Dlk1 and 2, contain multiple tandem EGF repeats with high homology to known canonical ligands. These have generally been less well studied than the canonical ligands, but there have been several key findings into their function.

Dlk1 contains 6 EGF domains with high homology to DLL4, but unlike Delta, does not have a DSL domain. It has been found to interact with EGF domains in the ligand binding region of Notch1, and can decrease the level of Notch activation (Baladrón *et al.*, 2005). Despite the *in vitro* binding data, little is known about the degree to which Notch activity is regulated by Dlk1 *in vivo*. Dlk1 has been associated with the maturation of several different cell types in development (Nueda *et al.*, 2007), but although Dlk1 null mice show some marked developmental abnormalities, they are still viable (Moon *et al.*, 2002).

1.7 Post-translational modifications to the Notch extracellular domain

In addition to furin cleavage and disulphide bond formation within the folded EGF and LNR domains, there are several other classes of post-translational modifications that take place during the maturation of the Notch receptor, some of which significantly affect the function of the receptor in signalling. The following section focuses on the modifications made to the extracellular region of the Notch receptor.

1.7.1 N-linked glycosylation

N-linked glycosylation is a common post-translational modification in proteins that are synthesised in the endoplasmic reticulum (ER), and the N-linked glycans are involved in the protein folding and quality control mechanisms within the ER. Both the mammalian and *Drosophila* Notch receptors contain the N-glycosylation consensus sequence (N-X-S/T) within their EGF domains (Figure 1-10), though the N-glycosylation machinery differs between species (Aoki *et al.*, 2007) (Moloney *et al.*, 2000b). *Drosophila* Notch binds to a lentil lectin affinity column (Johansen *et al.*, 1989), confirming the presence of N-linked glycans. Mouse models that lack all N-glycosylation machinery are embryonically lethal, but do not show the typical Notch phenotype (Marek *et al.*, 1999). As mentioned in section 1.3, hyperglycosylation of Jagged1 is associated with various Alagille syndrome mutations, confirming the role of N-linked modifications in quality control in the folding of Jagged1 (Morrissette *et al.*, 2001). However no specific role for N-glycosylation in regulating the Notch pathway has been found.

1.7.2 β-hydroxylation

A specific aspartic acid or asparagine residue within the calcium binding consensus of EGF domains (C^3-X-**D/N**-X-X-X-X-Y/F-X-C^4) (Stenflo *et al.*, 1988) can be post-translationally hydroxylated to give β-hydroxyaspartate or β-hydroxyasparagine (Fernlund and Stenflo, 1983) by the enzyme asparatyl β-hydroxylase (BAH) (Stenflo *et al.*, 1989). This modification has been documented in a number of different proteins containing EGF domains including coagulation factors VIII and IX (Rees *et al.*, 1988), and the LDL receptor. 10 of the 16 EGF domains in hJagged1, and 24 of the 36 EGF domains in hNotch1 contain this consensus. The modification has not been found to have an effect on calcium binding affinity (Sunnerhagen *et al.*, 1993).

BAH is widely evolutionarily conserved (Dinchuk *et al.*, 2000). Mice with a catalytically inactive form of the enzyme show developmental defects similar to Jagged-2 mutants, including syndactyly (Sidow *et al.*, 1997), and also show an increase in intestinal polyps compared to WT mice (Dinchuk *et al.*,

2002). BAH has also been found to be upregulated in several cancers (Lavaissiere *et al.*, 1996), suggesting that that β-hydroxylation may have a role in regulating Notch signalling, and that excessive hydroxylation may cause Notch to act as an oncogene, though no direct evidence of β-hydroxylation of the Notch receptor *in vivo* has been found.

1.7.3 O-linked glycosylation

The Notch receptor contains consensus sequences for multiple O-glucosylation and O-fucosylation sites (Figure 1-10). Fly and mouse knockout models for various glycosyltransferase enzymes involved in O-glycosylation have been linked to several Notch phenotypes. Recently a third class of modification has been identified – GlcNAc can be added to a conserved Ser/Thr residue between C_5 and C_6 (Sakaidani *et al.*, 2010) by the enzyme Eogt1 (Sakaidani *et al.*, 2012), though the role of this modification in Notch signalling is not known. Although the core glycosylation machinery varies slightly between species, the importance of glycosylation in modulating Notch signalling cannot be overstated, and is described below.

1.7.3.a O-linked glucosylation

Glucose can be added to EGF domains with the consensus sequence C^1-X-**S**-X-P-C^2 by the enzyme Rumi in *Drosophila* (Acar *et al.*, 2008). The glucose sugar is extended with two xylose sugars via an α1,3 linkage, to form a trisaccharide (Xylose-α1,3-Xylose-α1,3-glucose-β-O-Ser). There are two enzymes that can catalyse the first extension (GXYLT1 and GXYLT2) (Sethi *et al.*, 2010), and the human xylosyltransferase XXYlT1 has recently been identified (Sethi *et al.*, 2012). The glucosyltransferase GXYLT1 has also been found to be able to add a xylose sugar onto the consensus sequence if the amino acid immediately following it is a serine, but the biological significance of this has not yet been established (Takeuchi *et al.*, 2011).

Loss of glucosylation leads to a temperature-sensitive Notch phenotype in *Drosophila* that shows reduced Notch activation at temperatures above 25°C (Acar *et al.*, 2008). However, Notch-Delta binding was found to be unaffected in the same study. It is possible that the loss of O-glucosylation

may cause Notch to fold incorrectly, and therefore that Rumi is essential for the Notch receptor to adopt a stable conformation that is able to signal at higher temperatures. A protein with high homology to *Drosophila* Rumi has also been found in mice (Fernandez-Valdivia *et al.*, 2011), and *Rumi* knockout mice are embryonically lethal. Mouse models with reduced *Rumi* expression also show reduced Notch activation (Fernandez-Valdivia *et al.*, 2011). As in *Drosophila*, ligand binding to the receptor is unaffected. A recent study looking at the effect of removing individual glucosylation sites across the entire Notch molecule by site-directed mutagenesis has found that removing any one individual glucosylation site does not seem to have any deleterious effect on Notch activation. Rather, the molecule has to be considered as a whole (Leonardi *et al.*, 2011).

1.7.3.b O-linked fucosylation

The glycosyltransferase Ofut-1 (Pofut-1 in mammals) (Wang *et al.*, 2001) attaches an L-fucose sugar to EGF domains with the consensus sequence C^2-X-X-X-X-**S/T**-C^3 through an α-1 O linkage (Harris *et al.*, 1993), (Shao *et al.*, 2003) in the endoplasmic reticulum (Luo and Haltiwanger, 2005). Knockout of this enzyme is embryonically lethal in both flies and mice (Sasamura *et al.*, 2003), (Shi and Stanley, 2003). Ofut1 has been found to have chaperone activity in flies as well as glycosyltansferase activity (Okajima *et al.*, 2005), (Stahl *et al.*, 2008), and a mutant that can no longer bind to the fucose donor molecule GDP-fucose ($OFUT1^{R245A}$) has no catalytic activity but retains its chaperone activity can rescue embryonically lethal Notch phenotypes lacking $Ofut1^{WT}$ in flies (Okajima *et al.*, 2008). Knockout of *Ofut1* by RNAi has also been found to eliminate cell aggregation of S2 cells expressing Notch and Delta (Ahimou *et al.*, 2004), and abolishes binding of a soluble Notch-AP fusion protein to both Serrate and Delta expressing cells (Okajima *et al.*, 2003). By contrast overexpression of *Ofut1* has been found to impair the ability of Notch to bind Delta, and increased the binding to Serrate-expressing cells *in vitro* (Okajima *et al.*, 2003). In a separate study overexpression has also been found to cause a reduction in Notch signalling *in vivo*, and a loss of lateral inhibition (Okajima and Irvine, 2002), which is a process normally associated with Delta-induced Notch signalling (see Section 1.2.1, Figure 1-2).

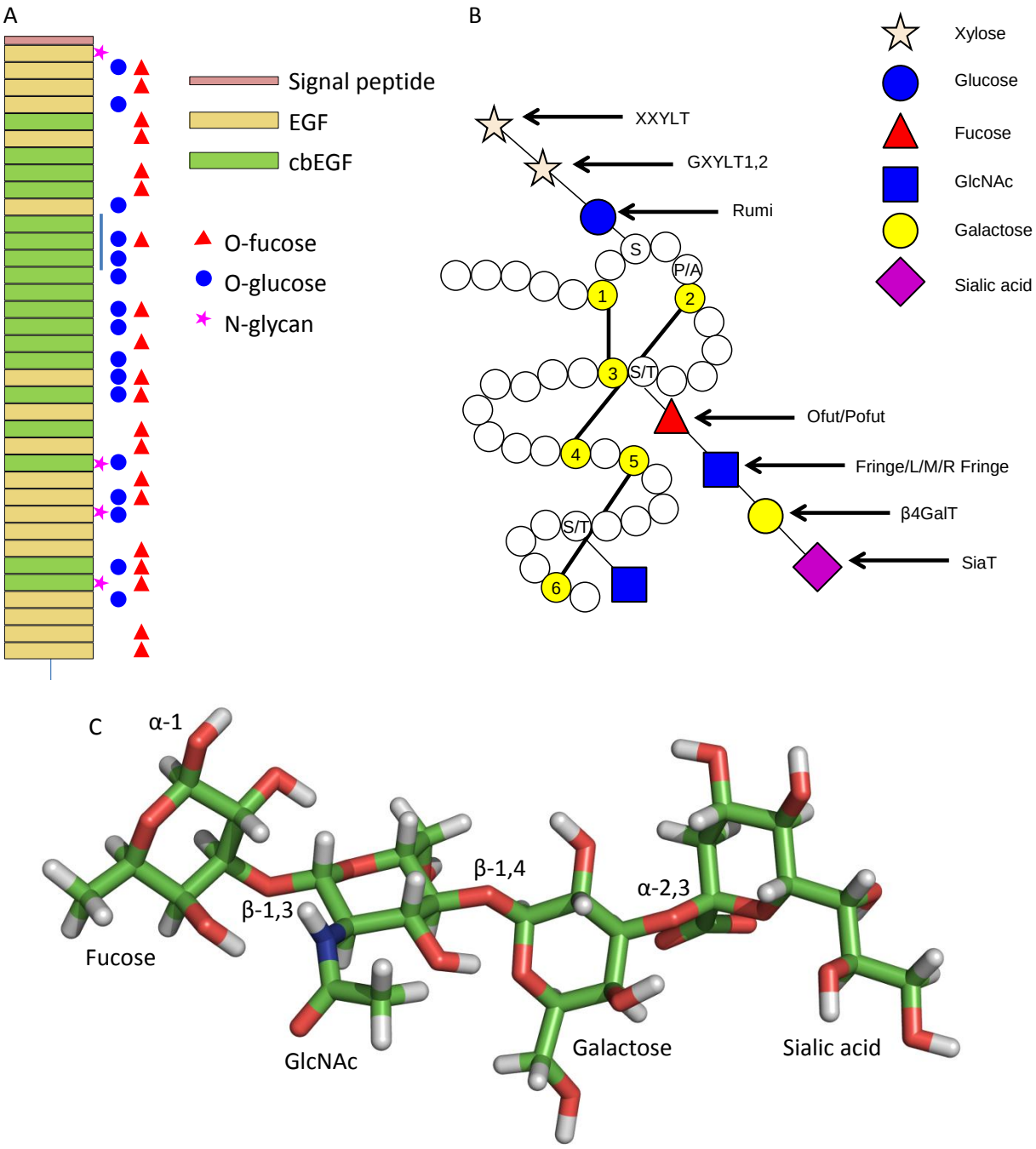


Figure 1-10 The human Notch1 receptor contains multiple EGF domains with predicted glycosylation consensus sequences. A) Domains containing the consensus sequences required for glycosylation of EGFs are indicated. B) Rumi can add glucose between C^1 and C^2 with the consensus C^1-X-**S**-X-P/A-C^2, and can be extended with two xylose sugars in mammals by GXYLT1 and 2, and XXYLT1. Fucose can be added to the consensus C^2-X-X-X-X-**S/T**-C^3 by the enzyme Ofut (Pofut in mammals), and can be extended by the Fringe family of enzymes (Fringe in Drosophila, Lunatic/Manic/Radical Fringe in mammals.) This can then be further extended with a galactose sugar by β4GalT and sialic acid by SiaT in mammals. A recently-discovered site for GlcNAc addition lies between C^5 and C^6. C) The linkages of the sugars are indicated, and it is likely that they form an extended structure (bond angles are representative only). (Sugars are labelled according to Consortium for Functional Glycomics guidelines.)

There is a requirement for Notch to be fucosylated in mammals in order for signalling to occur (Moloney *et al.*, 2000a), (Chen *et al.*, 2001), although low levels of ligand binding to Notch1-expressing Lec13 cells grown in the absence of fucose is seen for both Delta1 and Jagged1 (Stahl *et al.*, 2008). These cells are unable to manufacture GDP-fucose from GDP mannose, and hence are unable to attach fucose to proteins (Ripka *et al.*, 1986). Some activation of Notch by both ligand classes is seen in these cells too, suggesting that fucosylation isn't essential for Notch signalling in mammals, but is required for optimal functioning of the Notch receptor (Stahl *et al.*, 2008). The chaperone activity of mammalian Pofut1 has not yet been fully established, although cells lacking Pofut1 show a small decrease in cell-surface Notch, and mild intracellular Notch accumulation.

The fucose sugar can be extended via the attachment of a β-1,3 N-acetylglucosamine sugar by the glycosyltransferase Fringe (Moloney *et al.*, 2000a), (Haltiwanger and Stanley, 2002), (Chen *et al.*, 2001), (Wang *et al.*, 2001) in the Golgi apparatus (Munro and Freeman, 2000) (Figure 1-10). The role of Fringe was first implicated in the *Drosophila* wing disc dorsal-ventral boundary formation (Figure 1-1) (Irvine and Wieschaus, 1994). *Fringe* is expressed alongside *Serrate* in dorsal cells under the control of the homeobox gene *apterous* (Kim et al., 1995). The presence of Fringe in the dorsal Notch-expressing cell reduces the ability of cells expressing Serrate in the same compartment to induce Notch signalling in the dorsal cells, but potentiates the ability of these cells to signal ventrally, whilst in the ventral compartment cells expressing Delta are able signal dorsally (Panin *et al.*, 1997b). This creates a positive feedback loop that helps maintains the D-V boundary in the developing wing (see Section 1.2.1, Figure 1-1). The effect of the Fringe modification on the binding of the full-length Notch extracellular fragment to both ligand classes has also been characterised *in vitro*. When cells are co-transfected with Notch and Fringe, soluble Delta binds to Notch with a higher affinity, and soluble Serrate binds to Notch with a lower affinity than for cells transfected with Notch alone (Xu *et al.*, 2007). Note that the effect of Fringe is refractory to the effect of *Ofut1* overexpression (Okajima *et al.*, 2003), which suggests that the effects seen in the *Ofut1* overexpression experiments are due to Fringe activity being limited in these studies.

Fringe has three mammalian homologues – Lunatic Fringe (Lfng), Radical Fringe (Rfng) and Manic Fringe (Mfng) (Johnston *et al.*, 1997), (Rampal *et al.*, 2005), and a summary of previous work on understanding the effects of each of the Fringe enzymes is shown below in Table 1-2. These enzymes can differentially modulate binding of the various Notch receptors to each of the four canonical ligands by the addition of GlcNAc (Figure 1-10). For example in the case of Jagged1, only Lfng has been found to significantly increase binding to Notch1, but binding is not affected by Rfng or Mfng (Hicks *et al.*, 2000). All three Fringe enzymes have been found to increase the binding of DLL1 to cells expressing Notch1 and increase signalling by DLL1 (Yang *et al.*, 2005). However, unlike in *Drosophila*, altering ligand binding does not always directly correlate to changes in receptor activation. For example, Lfng and Mfng have been found to decrease Notch1 signalling by Jagged1 and Rfng has been found to increase signalling by Jagged1 in a co-culture assay (Yang *et al.*, 2005), despite the finding that neither Mfng nor Rfng alter Jagged1 binding to Notch1, and Lfng actually increases the affinity of this interaction! The situation is further complicated when different Notch receptors are studied – Lfng has been found to increase activation of Notch2 by both DLL1 and Jagged1 (Hicks *et al.*, 2000), though a separate study has also found that Notch2 signalling by Jagged1 can be decreased by Lfng (Shimizu *et al.*, 2001). What is apparent from these studies is that the different mammalian Fringe enzymes can have very different roles in regulating Notch signalling, and that more work is required to establish the precise effect of each enzyme as the data are at times contradictory.

In mammals, the disaccharide added by the Fringe enzymes can be extended first with galactose and then with sialic acid, to give a tetrasaccharide (Figure 1-10 C). The final tetrasaccharide has the same sugar linkage as found in a factor IX EGF domain: Sia-α2,3-Gal-β1,4-GlcNAc-β1,3-Fuc-α1-O-Ser/Thr (Moloney *et al.*, 2000b). Galactose is added by β4galactosyltransferase-1 in mammalian cells (Chen *et al.*, 2001), and forms the minimal glycan required to modulate Notch signalling (Chen *et al.*, 2001). *Drosophila* has two proteins with high homology to the mammalian galactosyltransferase enzymes,

Table 1-2 The effect of the Fringe enzymes on ligand binding and Notch activation

	Ligand	Jagged1/Serrate		Jagged2		DLL1/Delta	
Receptor	Enzyme	Signalling	Binding	Signalling	Binding	Signalling	Binding
Notch1	LFng	-	++/=[1]			++	++
	MFng	--	=			+	+
	RFng	+/=[2]	=			+	+
Notch2	LFng	+/-[3]	-	+		+/=[4]	+
	MFng	--	--	=		=	+
	RFng						
dNotch	Fringe	---	---	NA		+++	+++

[1]Large increase in binding of Jagged1-Fc to HEK293 cells expressing Notch1 (Hicks *et al.*, 2000), very mild/no increase in binding of Jagged-1Fc to 3T3 cells expressing Notch1 (Yang *et al.*, 2005).

[2]CSL-Luciferase reporter assay shows 2-fold increase in Notch1 activation by Jagged1 expressed in the surface of 3T3 cells, but no increase in activation by pre-clustered ligands (Yang *et al.*, 2005).

[3]In a CBF1 reporter assay Notch2 activation in C2C12 cells co-transfected with LFng is increased in co-culture with L cells expressing Jagged1 (Hicks *et al.*, 2000), but activation was reduced in a co-culture luciferase reporter assay (Shimizu *et al.*, 2001).

[4]DLL1 induced ligand activation of Notch2 was slightly increased by LFng in a co-culture luciferase reporter assay (Shimizu *et al.*, 2001), and significantly increased by LFng in a CBF1 reporter assay (Hicks *et al.*, 2000).

but these transfer GalNAc rather than Gal. Flies defective for these enzymes have no visible Notch phenotype (Haines and Irvine, 2005), and the addition of artificially elongated glycans to *Drosophila* Notch receptors using mammalian glycosyltransferase enzymes does not seem to affect binding to either ligand class (Xu *et al.*, 2007).

A recent comparative NMR study of the solution structure of the human Notch1 EGF12 domain compared its unmodified and glycosylated structures. This study suggests that the elongation of the fucose sugar with GlcNAc could potentially cause a conformational change in the central β-hairpin in this domain (Hiruma-Shimizu *et al.*, 2010) (Figure 1-11 A, i-iii). These experiments were performed on an isolated EGF domain in the absence of calcium at pH 5.3, so it is possible that these findings may not truly represent the structural changes that occur upon glycosylation within the context of

the intact Notch receptor under physiological extracellular calcium concentrations. However, it is interesting to note that the orientation of the fucose sugar and the structure of the protein backbone within the disaccharide-modified EGF are both very similar to the NMR structure of fucosylated cbEGF domain from Factor VII (Kao *et al.*, 1999) (Figure 1-11 A, iii-iv), collected in the presence of 100mM calcium at pH 5.5. In both of these solution structures, the C_6 methyl group of the fucose packs between two hydrophobic amino acid side chains at the C-terminal end of the central β-sheet in the EGF. This could play a role in stabilising the structure of the isolated EGF12 domain (Figure 1-12 B) in this context, and could therefore explain the conformational changes seen in this study.

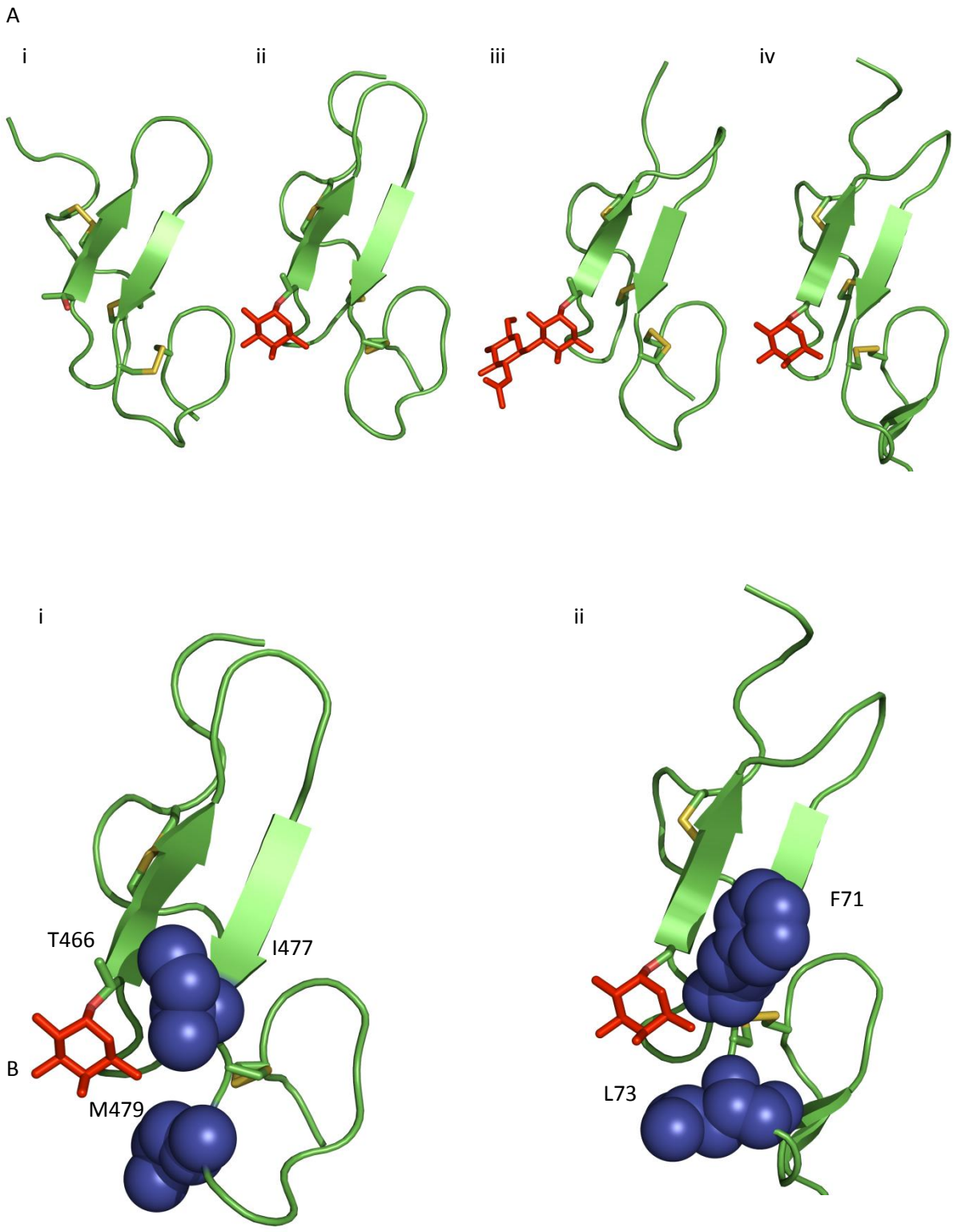


Figure 1-11 Previous structural studies on the effect of glycosylation on the structure of EGF domains. A) i) Notch1 cbEGF12 (PDB 2RR0), ii) + fucose (PDB 2RR2), iii) + GlcNAc-fucose (PDB 2RRZ), iv) factor VII + fucose (PDB 1FFM). B) i) EGF12 + fucose vs ii) Factor VII EGF + fucose, to illustrate conserved packing of fucose against hydrophobic amino acids in the C-terminal region of the EGF domain (shown in blue).

1.8 Aims of this thesis

Binding of the Notch receptor to its ligands can lead to RIP and activation of Notch signalling. Whilst a great deal of work has established the role of the downstream effectors of Notch signalling, the molecular basis of the interaction of the receptor with its ligands, and its regulation by glycosylation is not known. How ligand binding leads to proteolysis at the S2 and S3 sites is also not known. This thesis aims to investigate the Notch ligand recognition, and its modulation by O-glycosylation, specifically focussing on the EGF11-13 region of hNotch1 and its interaction with Jagged1 and DLL4.

The aims of the individual chapters in this thesis can be summarised as follows:

Chapter 3: Production, purification and characterisation of both prokaryotically and eukaryotically expressed Notch constructs used in this study.

Chapter 4: Identifying the ligand binding site within the human Notch1 EGF11-13 fragment using site-directed mutagenesis, via a flow cytometry assay.

Chapter 5: Modulation of the receptor-ligand binding interaction by O-glycosylation.

Chapter 6: How longer constructs, beyond the minimal-binding fragment affect binding to different ligand classes.

Chapter 7: Summary, conclusions and future work.

Chapter 2

Materials and methods

2.1 DNA manipulation and cloning

2.1.1 Restriction digests

Digests were performed with 1 unit (U) of restriction enzyme per 100 ng DNA, at a final concentration of 100 ng/µl. The appropriate DNA restriction buffer (New England Biosciences - NEB) was added in ratio of 1:10 of the final volume, and the reaction was incubated at 37°C for 1 hour. For double digests with incompatible buffer requirements, single digests were carried out sequentially, with the DNA precipitated (see Section 2.1.2) between each digestion step to allow the buffer to be changed. Cutting by each enzyme was confirmed by carrying out a small-scale test reaction with a single restriction enzyme, and visualizing the DNA on an agarose gel.

2.1.2 Ethanol precipitation

DNA in solution was precipitated by adding 1/10 volume of 3 M Sodium Acetate, and 2.5 volumes of 100% EtOH. The mixture was stored at -20°C for 30 minutes, prior to the precipitated DNA being centrifuged at 13,000 rpm for 30 minutes at room temperature. The supernatant was removed, and the DNA pellet was washed with 500 µl 70% EtOH and allowed to air-dry, before being dissolved in a suitable volume of buffer. DNA stocks were resuspended in TE buffer (10 mM Tris-HCl pH 8.0, 1 mM EDTA).

2.1.3 Gel electrophoresis

Agarose gels ranging from 0.7% – 2.0% w/v were with TAE or TBE buffer, depending on the size of the DNA fragments being analysed. 0.05% v/v Ethidium Bromide was added to the mixture. DNA samples were mixed with 1/6 volume 6x DNA loading buffer (NEB) and resolved using either 1 kb or 100 bp DNA marker ladders (NEB). Electrophoresis was performed at 80mA for 30 minutes in a Mini-Sub DNA Cell (Bio-Rad) electrophoresis tank. For analytical gels, bands were visualized on a UV transilluminator (Uvitec) and photographed (Uvitec). For preparative gels, bands were visualized under a hand-held UV lamp to minimize DNA damage and excised from

the gel with a sharp scalpel, and the DNA was extracted from the agarose gel slice using a Gel Extraction kit (Qiagen) before being eluted in MilliQ water.

2.1.4 Measuring DNA concentration

DNA samples were diluted 1:50 to a final volume of 100 µl, and absorbance was measured at 260nm (A_{260}) using a Shimizu spectrophotometer. The concentration of DNA was calculated based on the assumption that a 50 µg/ml dsDNA solution has an A_{260} of 1.0.

2.1.5 Sticky end ligation

DNA ligation was performed using Rapid DNA Ligation Kit (Roche). 50ng vector DNA was added to varying amounts of insert DNA, ranging from 1:3 to 3:1. The total volume of the reaction was 20 µl. 10 µl 2 x ligase buffer and 1 µl Rapid DNA ligase was added to the mixture. The volume was adjusted using DNA dilution buffer and the reaction was left at room temperature for 5 minutes, before 10 µl was transformed into NM554 cells.

2.1.6 DNA sequencing

Samples for DNA sequencing were diluted to a final concentration of 100 ng/µl in a final volume of 15 µl in MilliQ H_2O. Samples were sent to the DNA sequencing facility in Oxford (Source Bioscience). Sequencing was performed on an Illumina automated sequencing machine, and results traces were read using FinchTV software.

2.2 Amplification of DNA by the polymerase chain reaction (PCR)

2.2.1 Oligonucleotide primers

Oligonucleotide primers for amplification of DNA or mutagenesis in PCR were ordered from Invitrogen Life Sciences. On arrival the lyophilized oligonucleotides were dissolved in dH_2O. A list of primers used is listed in Appendix A. Primer annealing temperatures were calculated by the following formula:

$$T_m\ (°C) = 4° \times (G + C) + 2° \times (A + T)$$

2.2.2 Amplification of DNA using *Pfu* polymerase

PCR was performed in a final reaction volume of 50 µl unless otherwise indicated. 1-2 ng template DNA was added to a reaction mixture containing A thermal cycler was used in order to amplify the DNA, using the following programme:

Temperature	Duration		
95°C	1 minute	Initial melt	
95	1 minute	Melt	Repeat x 30
XX*	1 minute	Anneal	
72°C	1 minute/1 kb	Elongation	
72°C	10 minutes	Terminal elongation	
4°C	Pause		

*Annealing temperature depended on the T_m of the primers – T_m - 5°C

2.2.3 Colony screening using *Taq* polymerase

After transformation, bacterial colonies were screened for the presence of specific DNA sequence. Individual colonies were picked into 50 µl MilliQ H_2O and re-suspended by pipetting. PCR was performed by adding 5 µl of the bacterial suspension to 25 µl reaction mixture containing a final concentration of 0.2 mM dNTPs, 0.2 µM forward and reverse primers, 1 x *Taq* reaction buffer (Roche), 0.5 U *Taq* polymerase (Roche). The same amplification programme was used as for the *Pfu* amplification, but with an elongation temperature of 68°C.

2.2.3 PCR mutagenesis using *Pfu*

Some of the mutant Notch proteins were generated using a back-to-back PCR mutagenesis method. A forward primer was designed containing the required DNA bases changes towards the middle of the primer. A reverse primer was designed against the reverse complement DNA strand, starting immediately 5' to the forward primer annealing site (see Section 3.4). PCR was performed as above, following which a 10 µl sample of the reaction mixture was visualised on an agarose gel. The remainder the mixture had the DNA precipitated by ethanol precipitation, following which the DNA was run on an agarose gel and purified as above. Blunt end ligation

was performed to circularise the DNA, and the reaction was left at room temperature for 16 hours, before transformation into NM554-pREP4 cells.

MilliQ H_2O	3.5 μl
5 x ligation buffer*	2 μl
DNA (from gel elute)	3 μl
Polynucleotide kinase	0.5 μl
T4 ligase	1 μl

*5 x ligation buffer contains: 5 mM ATP, 250 mM Tris-HCl pH 7.5, 50 mM $MgCl_2$, 70 mM DTT

2.2.4 PCR mutagenesis using Quikchange Lightning site-directed mutagenesis kit

Complementary forward and reverse primers of between 30-33 bp were designed with the required mutation towards the middle of the primer, flanked by stretches of unmodified nucleotide sequence. Mutagenesis using the Lightning Quikchange site-directed mutagenesis kit (Stratagene) was performed according to manufacturer's instructions (see Section 3.4).

2.3 Use of competent *E. coli* cells

2.3.1 Preparation of competent cells

An aliquot of a glycerol stock of the cells required was streaked out onto an agar plate containing the appropriate selection reagent. After overnight growth on the plate, a single colony was picked and inoculated into 2.5 ml 2 x YT medium (16 g Tryptone-B, 10g Yeast Extract-B, 5 g NaCl per L) containing either 25 μg/ml kanamycin (for cells containing the pREP4 plasmid) or no selection marker, for overnight growth at 37°C. A 1 ml aliquot was used to inoculate 100 ml 2 x YT medium, and was grown at 37°C until A_{600} reached 0.4. At this point the cells were harvested by centrifuging at 5,000 rpm at 4°C for 10 minutes, using pre-cooled centrifuge bottles. The cells were gently re-suspended in 50 ml sterile ice-cold Tfb buffer, incubated on ice for 30 minutes and centrifuged as above. Cell were then re-suspended in 5ml of Tfb buffer and aliquoted into individual 100 μl samples for flash-freezing using liquid N_2.

2.3.2 Transforming competent cells

DNA plasmids for amplification were transformed into NM554 cells, and prokaryotic expression vectors for protein expression were transformed into BL21 cells. Prokaryotic expression vectors were transformed into cells containing the pREP4 plasmid, whereas vectors for eukaryotic expression were transformed into NM554 cells for amplification.

Cells were gently thawed on ice, and a 50 μl aliquot was incubated with DNA on ice for 30 minutes, prior to heat-shock at 42°C. BL21 and NM554 cells were heat-shocked for 90 seconds, XL-10 Gold cells were heat-shocked for 45 seconds. The amount of DNA added varied according to the *E. coli* strain being transformed – BL21 cells required ~100 ng of DNA, NM554 cells required ~1 ng. After heat shock, the cells were mixed with equal volume of 2 x YT medium and incubated at 37°C to allow recovery and were plated out onto a 2 x YT agar plate containing a suitable antibiotic selection marker; cells containing the pREP4 plasmid were plated onto agar plates containing 100 μg/ml ampicillin and 25 μg/ml kanamycin, cells lacking the pREP4 plasmid were plated into agar plates containing ampicillin alone. The plate was allowed to dry, and was incubated overnight at 37°C.

2.3.3 Bacterial glycerol stocks

After overnight growth of the starter cultures for protein growth, a small amount of the bacterial suspension was retained to make stocks for freezing. 325μl bacterial suspension was mixed with 75μl 80% glycerol, and quickly frozen to -80°C. To use an aliquot of cells, the glycerol stock was thawed gently on ice before being streaked out onto an agar plate containing the appropriate antibiotic selection marker with a sterile metal loop.

2.3.4 Isolation of plasmid DNA

Plasmid DNA was extracted using the range of Qiagen plasmid extraction kits. These use a modified alkaline lysis protocol to extract large quantities of DNA (Birnboim and Doly, 1979). Depending on the scale of DNA preparation required, cells were grown in an appropriate

volume of 2 x YT medium containing 100 μg/ml ampicillin and 25 μg/ml kanamycin (10, 100 or 500 ml medium), and extracted using a Miniprep, Midiprep or Megaprep kit respectively (Qiagen) according to the manufacturer's instructions.

2.4 Bacterial protein expressing and purification

2.4.1 Expression of recombinant proteins

A pQE30 expression vector containing the gene of interest was transformed into BL21 cells containing the pREP4 plasmid as outlined above. The following day a streak of cells was inoculated into 200 ml 2 x YT medium containing 100 μg/ml ampicillin and 25 μg/ml kanamycin and incubated overnight at 37°C with vigorous shaking. The following day 25 ml of starter culture was added to each flask containing 500ml 2 x YT medium supplemented with 100 μg/ml ampicillin and 25 μg/ml kanamycin, and incubated at 37°C until the A_{600} reached 0.8-1, when IPTG (isopropyl β-D-thiogalactopyranoside) was added to a final concentration of 2mM. After induction, the cells were grown for 3hr before harvesting by centrifuging the medium at 5000 rpm for 10 minutes at 4°C (Beckman J-2, JLA-10.500 rotor). The pelleted cells were collected in a falcon tube and left overnight at -20°C to aid lysis.

2.4.2 Extraction of proteins from bacterial cell pellet

The pellet was allowed to thaw and was re-suspended in a total of 60ml lysis buffer (6 M guanidine-HCl, 25 mM sodium phosphate pH 7.4, 5 mM β-mercaproethanol). An additional 10 g guanidine-HCl was added to the cell suspension, which was left stirring for 1hr until lysis was complete. This was then sonicated (Jencons Ultrasonic processor) for 3 x 30s at 20W to shear genomic DNA and ensure the cells were fully lysed. The bacterial lysate was then centrifuged in an ultracentrifuge (Beckman L7-55 Ultracentrifuge, 60Ti rotor) at 40,000 rpm for 30 minutes at 25°C, and the supernatant was decanted and run on a Nickel affinity column.

2.4.3 Nickel affinity chromatography

2-3 ml FastFlow Chelating Sepharose was packed in a pre-cast plastic column. 10 ml 1M nickel was passed through the Sepharose beads, which were then washed with 20ml MilliQ H_2O, and equilibrated with 10 ml guanidine buffer. The bacterial cell lysate supernatant was allowed to flow down the column under gravity. The column was then washed with 2 x 10ml guanidine buffer to remove any unbound protein. Protein was eluted from the column by 30ml guanidine buffer containing 25mM EDTA. 0.4g DTT and 3 ml Tris-HCl pH 8.3 was added to the eluted protein to ensure complete reduction of the cysteine residues, and left for 1hr at room temperature. After an hour the pH was lowered to <2 using HCl, and the eluted protein was dialysed against 0.1% TFA overnight at room temperature to remove the guanidine from the solution, before being purified by reverse-phase high performance liquid chromatography (HPLC).

2.4.4 Reverse-phase high performance liquid chromatography (HPLC)

Protein solutions were adjusted to pH <2, and centrifuged at 13,000 rpm for 5 minutes to remove any precipitated protein from solution. The supernatant was injected onto a semi-preparative reverse phase C8 column (Rainin). A gradient from 20% - 80% gradient of HPLC Buffer B (80 % Acetonitrile, 0.1 % TFA) was run over 50 minutes (Buffer A contained 0.1 % TFA alone). Protein elution was monitored using A_{280}, and protein was collected manually. Fractions containing protein were lyophilised by freezing using liquid Nitrogen and were placed under vacuum overnight to remove any water and Acetonitrile.

2.4.5 *In vitro* refolding

Lyophilised protein was dissolved in MilliQ H_2O and the concentration was measured by spectrophotometry at 280nm. The protein was refolded using an *in-vitro* oxido-shuffling system, containing 300 uM L-Cysteine and 30 uM L-Cystine. In addition to this, $CaCl_2$ was added to refold proteins containing cbEGF domains. The pH was adjusted to 8.3 using 100 mM Tris.

Protein refolds were left at 4°C for at least 36 hours. After refolding, the solution was acidified, and the protein was purified using reverse-phase HPLC.

2.4.6 His-RGS cleavage by Factor Xa

Lyophilised protein was dissolved in MilliQ H_2O, and the concentration was measured by spectrophotometry at 280 nm. The final protein concentration was diluted to 2-3 mg/ml in buffer containing 50 mM Tris-HCl pH 8.3, 0.1 M NaCl, 1 mM $CaCl_2$. Recombinant FactorXa (Greiner) was added at a concentration of 1 U enzyme/1 mg protein. Following removal of the His-tag using Factor Xa the protein solution was desalted using reverse-phase HPLC.

2.4.7 Purification by FPLC

Lyophilised protein was dissolved in a suitable volume of MonoQ Buffer A (50 mM Tris-HCl pH 7.5, 2 mM $CaCl_2$, and centrifuged at 13,000 rpm for 5 minutes at room temperature to remove any precipitated material. The supernatant was injected onto a MonoQ column (Pharmacia) and a gradient from 0% to 50% MonoQ BufferB (1 M NaCl, 50 mM Tris-HCl pH 7.5, 2 mM $CaCl_2$) was run over 20 minutes. Protein elution was monitored using A_{280} and protein was collected manually. Following this purification stage the protein was purified by a final reverse-phase HPLC purification.

2.5 Expression of ^{15}N enriched proteins

BL21 pRep4 cells were transformed as above, and the following day a streak was inoculated into 100ml minimal medium and incubated overnight at 37°C with vigorous shaking. The following day, 25 ml of the starter culture was added to each flask containing 500ml minimal medium, and incubated at 37°C until the A_{600} reached 0.8-1. The flasks were transferred to an incubator at 28°C and IPTG (Isopropyl β-D-1-thigalactopyranoside) was added to a final concentration of 2mM. After induction, the cells were left for 3 hours before harvesting by centrifuging the medium at 5000 rpm for 10 minutes at 4°C. ^{15}N enriched proteins were purified using the same protocol as above.

Minimal medium components:

Component	Volume added (ml)	Final concentration
10x Salts*	50	-
1M $MgSO_4$	0.5	1mM
0.1M $CaCl_2$	0.5	100uM
1M Thiamine	0.5	1mM
20% (w/v) Glucose	12.5	0.5% (w/v)
10x YNB (Yeast Nitrogen Base)	50	1x
Trace elements†	5	-
0.2mg/ml $^{15}NH_4Cl$	2.5	1µg/ml
MilliQ H_2O	378.5	-

*10x Salts: 60g Na_2HPO_4, 30g KH_2PO_4, 5g NaCl dissolved in 1L MilliQ H_2O
†Trace elements: 5g EDTA, 0.5g $FeCl_2$, 0.05g $ZnCl_2$, 0.01g $CuCl_2$, 0.01 $CoCl_2.6H_2O$, 0.01g H_3BO_3 dissolved in 1L MilliQ H_2O. pH was adjusted to 7.0 before addition of salts, and after each addition

10x Salts, Trace elements and MilliQ H_2O were autoclaved prior to use. All other components were filter-sterilised with a .22uM syringe-driven filter prior to use.

2.6 Site-specific biotinylation of BirA tagged proteins

Prokaryotic protein solutions were made up to a final concentration of 40uM. 10x Biomix A (0.5 M Bicine pH 8.3) and Biomix B (100 mM ATP, 100 mM MgOAc, 500 µM Biotin) (Avidity) were each added at a ratio of 1/10, and 1U BirA enzyme was added per 1 mg protein. The mixture was incubated overnight at room temperature, before purification by HPLC. After injecting the samples onto the HPLC column, the column was allowed to equilibrate for 20 minutes to wash away any unbound ATP and biotin. A normal elution programme was then run, and hte biotinylated protein was collected and freeze-dried. Successful biotinylation was confirmed by ESI-MS and Western Blot using a Streptavidin-HRP fusion protein. Eukaryotic proteins were concentrated after purification by S200 column, and 25 µl Biomix A and Biomix, and 1 µl BirA enzyme B were added, to a reaction final volume of 250 µl. After biotinylation the entire reaction was purified on a S200 column and the proteins concentrated to 1 mg/ml. Successful biotinylation was confirmed with Streptavidin-HRP using a dot-blot.

2.7 Limited proteolysis of Notch fragments

Endoprotease GluC was added in a ratio of 1:1000 to 50 µl protein solution, at 1 mg/ml. The reactions were buffered by 50 mM Tris-HCl pH 7.5. Digests were performed in the presence of 10 mM $CaCl_2$ or 10 mM EGTA, and the ionic strength was adjusted to 0.15 with NaCl using the following formula:

$$I = \frac{1}{2}\Sigma(cZ^2)$$

(*I* = ionic strength, c = concentration, Z = charge)

Samples were incubated at 37°C and 10 µl aliquots were taken after 5, 15, 30, and 60 minutes. Samples were boiled for 5 minutes at 95°C with 10 µl 2x Laemmli's buffer (including β-ME) to stop the reaction. After 5 minutes the samples were removed from the block and stored at room temperature before being loaded onto a 16% SDS-PAGE gel.

2.8 Tissue culture

2.8.1 Maintaining cell lines

HEK293T cells were maintained in Dulbecco's modified Eagle's Medium (DMEM), supplemented with 10% FCS, 50 U/ml penicillin, 50U/ml Streptomycin and 2 mM glutamine (complete medium). For transient transfection and protein production the medium was changed to DMEM without additives (incomplete). HEK 293 cells stably transfected with human Jagged1 were maintained in complete DMEM containing 0.5 mg/ml geneticin. B16 mouse melanoma cells were maintained in RPMI 1640 medium supplemented with 10% FCS, 50 U/ml penicillin, 50 U/ml streptomycin and 2 mM glutamine (complete medium). *Drosophila* S2 cells were maintained in Schneider's *Drosophila* medium supplemented with 2 mM L-glutamine, 10% FCS, and 50 U/ml penicillin, 50 U/ml streptomycin.

All mammalian cell lines were grown in a 37°C humidified incubator in an atmosphere of 5% CO_2. All *Drosophila* S2 cells were grown in a non-humidified incubator at 28°C under normal atmospheric conditions. Cell lines were grown in 25 cm^2, 75 cm^2 175 cm^2 tissue culture flasks (Greiner). *Drosophila* S2 cells for transfection were grown in 6-well plates (Greiner). All media and reagents were supplied by Gibco, and all tissue culture work was performed in a laminar flow sterile hood.

2.8.2 Sub-culturing of mammalian cells

Cells were grown to ~90 % confluence in complete medium. The medium was removed, and the cells were washed briefly with 2ml phosphate buffered saline (PBS) containing 10 mM EDTA. This was then removed and the cells were incubated with 5 ml PBS containing 10 mM EDTA at 37°C for 5 minutes. The cells were dislodged from the flask using gentle tapping. 5 ml complete medium was added to the flask and the cells were gently re-suspended to disperse clumps of cells. The cell suspension was then centrifuged at 1000 rpm for 3 minutes to pellet the cells. The supernatant was siphoned off, and the cells were re-suspended in an appropriate volume of fresh complete medium. Cells were then added to a fresh 75cm^2 flask containing 12 ml complete medium at a level to ensure the correct split ratio, and gently mixed before being replaced in the incubator. For large-scale protein expression HEK 293T cells were split into 175 cm^2 flasks containing 20 ml complete medium. HEK 293 and HEK 293T cells were split at a 1:10 ratio, B16 cells were split to a 1:15 level.

2.8.3 Sub-culturing of insect cells

Cells were grown to a density of 5-10 x 10^6 cells/ml. Cells were dislodged from the flask using gentle tapping and the flask was washed down using a 5 ml pipette to remove any adherent cells and disperse clumps of cells. Cells were counted before sub-culturing using a haemocytometer, and were seeded into fresh medium at a density of 2 x 10^6 cells/ml in a fresh 75 cm^2 flask containing 10 ml complete medium.

2.8.4 Freezing and thawing of mammalian cells

For freezing, cells were grown to ~90% confluence in complete medium. Cells were prepared as for sub-culturing, but were re-suspended in FCS containing 10% DMSO (to act as a cryoprotectant). 1ml aliquots were pipetted into a cryotube (Nunc). Cells were cooled to -80°C overnight using a cryofreezer (Stratacool), before being transferred to liquid nitrogen for longer term storage.

To thaw cells, a cryotube was removed from cold storage and placed immediately into a beaker of water at 37°C. 9 ml complete medium was added to the cells with gentle shaking over the course of a minute to reduce the risk of osmotic shock. The cell suspension was then centrifuged at 1000 rpm for 3 minutes at room temperature to pellet the cells. The supernatant was siphoned off, and the cells were re-suspended in 12 ml complete medium before being placed in a 75cm^2 flask and left to attach to the flask overnight. The following day the medium was replaced with 12ml complete medium, to remove any trace of DMSO.

2.8.5 Freezing and thawing insect cells

For freezing, cells were grown in a 75 cm^2 flask to a density of 1-2 x 10^7 cells/ml. Cells were counted at this step using a haemocytometer, before being centrifuged at 1000 rpm for 3 minutes at 4°C. The conditioned medium was siphoned off and reserved. The cells were re-suspended in 10ml PBS and centrifuged at 1000 rpm for 3 minutes at 4°C. The cells were re-suspended in freezing medium (45 % conditioned medium, 45 % fresh complete Schneider's *Drosophila* medium, 10 % DMSO) to a final density of 1.1 x 10^7 cells/ml, and placed into cryotubes (Nunc) in 1 ml aliquots. Cells were cooled to -80°C overnight using a cryofreezer (Stratacool), before being transferred liquid nitrogen for longer term storage.

To thaw cells, a cryotube was removed from cold storage and immediately placed into a beaker of water at 30°C. Once the vial had thawed, the cells were placed into 5 ml room temperature complete Schneider's *Drosophila* medium in a 25 cm^2 flask, and left at room temperature for 30

minutes. After this time, the cells were dislodged from the flask using gentle tapping and the flask was washed down using a 5 ml pipette in order to remove any adherent cells and disperse clumps of cells. Cells were centrifuged at 1000 rpm for 3 minutes at 4°C. The supernatant was removed, and the cells were re-suspended in 5 ml complete Schneider's *Drosophila* medium, and replaced in the 25 cm^2 flask for 3-4 days to allow the cell density to reach 6-10 x 10^6 cells/ml.

2.9 Eukaryotic protein production and purification

2.9.1 Transient transfection of HEK 293T cells by PEI

DNA and PEI were added sequentially in a 1:2 ratio to incomplete DMEM. For each 175 cm^2 flask, 50 µg DNA and 100 µg PEI were added to 2 ml DMEM. This mixture was incubated at room temperature for 30 minutes to allow complex formation.

Cells were grown to ~90% confluence in 175cm^2 flasks. This medium was carefully siphoned off the cells to remove all traces of serum. 20 ml DMEM without additives was then added to each flask, along with 2 ml of DMEM containing the PEI/DNA complexes.

2.9.2 Purification of recombinant protein from conditioned medium

Conditioned medium was collected from cells 3-4 days post-transfection, and filtered using a .45um filter to remove any cell debris. The medium was added to 2x volume of buffer containing 50 mM Tris-HCl pH 9.0, 200 mM NaCl, to aid binding of His-tagged proteins to Nickel. 2-3ml of FastFlow Chelating Sepharose beads were bound to 1M $NiSO_4$ and washed with the same buffer. A suspension of the beads was incubated with the medium at 25°C for 1hr with shaking.

After 1 hour the mixture was removed from the shaker and the beads were allowed to settle. Excess medium was siphoned off using a vacuum pump, leaving <50ml medium. This was then poured into a pre-cast column with a porous base to separate the beads from the medium. The

beads were washed with 2 x 10 ml buffer containing 50 mM Tris-HCl pH 9.0, 200 mM NaCl, before eluting the protein with the same buffer containing 300 mM Imidazole.

2.9.3 purification of eukaryotic proteins using a Superdex 200 column

The eluted protein from the nickel column was concentrated to <500 µl using a Vivaspin 20 concentrator, and then added to 20ml buffer containing 50 mM Tris-HCl pH 7.5, 200 mM NaCl, 1 mM $CaCl_2$ (for Notch constructs) or 50 mM Tris-HCl pH 9.0, 200 mM NaCl (for Jagged constructs).. This was then concentrated to <500 µl in order to remove the imidazole, andthe sample was injected onto the S200 column.

A Superdex 200 column (GE Healthcare Ltd) was equilibrated with the appropriate buffer (see above) and the sample was injected onto the column at 0.6ml/min flow rate. The presence of protein in the flow-through was recorded at 280nM. Peaks were collected manually, and fractions were assayed by Western Blot using an anti-6xHis pAb to confirm the elution time of the protein of interest.

2.9.4 Transient transfection of *Drosophila* S2 cells using calcium phosphate

Drosophila S2 cells were sub-cultured into 6-well plates as described above, and were seeded at a density of 1 x 10^6 cells/ml in 3 ml complete medium per well. The following day, 10 µg pUAST plasmid and 10 µg pMTGal4 plasmid were mixed with $CaCl_2$ (final concentration 240uM) and tissue culture sterile water, to a final volume of 300 µl. This was added dropwise to 300 µl 2x HEPES-buffered saline solution (50 mM HEPES, 1.5mM Na_2HPO_4, 280 mM NaCl, pH 7.1), and mixed continuously to ensure that a fine calcium phosphate precipitate forms. This was incubated at room temperature for 30 minutes, before being added slowly to cells.

The next day, the cells were dislodged from the flask using gentle tapping and the well was washed down using a 5 ml pipette to remove any adherent cells and disperse clumps of cells. The cells were removed from the well and centrifuged at 1000 rpm for 3 minutes at 4°C, and

were washed with 3ml complete Schneider's *Drosophila* medium. This was repeated, and the cells were returned to the same well in the 6-well plate. 500 μM $CuSO_4$ was added to the cells to induce expression in the pUAST plasmid, via the pMTGal4 plasmid.

2.10 Measuring protein concentration

Protein concentrations were measured using a Shimadzu UV mini 1240 spectrophotometer. Absorbance was recorded at 280 nm (A_{280}), and protein concentrations were calculated using the following formula:

$$Protein\ concentration\ (mM) = \frac{Dilution\ factor\ x\ A_{280}}{\varepsilon}$$

The theoretical extinction coefficient for each protein was calculated according the ExPASy bioinformatics server, using ProtParam (Gasteiger *et al.*, 2001).

2.11 Identification of protein using ESI mass-spectroscopy

Prokaryotically expressed proteins were analysed by ESI mass-spectroscopy in order to confirm the correct mass. Proteins were dissolved to a final concentration of 10uM in 50% Acetonitrile, 0.1% Formic acid. Protein samples were manually loaded onto sample injector (kd Scientificc) and analysed my ESI-MS (Micromass). The final mass of the protein was calculated using the Maximum Entropy deconvolution process using MassyLynx.

2.12 SDS-PAGE

Gels were poured in two stages in a 1.5mm gel casting stand (Bio-Rad). The separating gel (8-16% 19:1 acrylamide:bisacrylamide depending on the sample, 0.1% SDS, 0.38 M Tris-HCl pH 8.8, 0.1% APS, 0.1% TEMED) was poured first and allowed to set under layer of isopropanol. After the gel had set, the isopropanol was removed, and the stacking layer (6% 19:1 acrylamide:bisacrylamide, 0.25 M Tris-HCl pH 6.8, 0.1% SDS, 0.1% APS, 0.1% TEMED) was poured, and a gel comb was inserted to create lanes.

Protein samples for analysis by SDS-PAGE were mixed in a suitable volume of 2x Laemmli's buffer (Laemmli, 1970), either with or without 5% β-Mercaptoethanol, and boiled at 100°C for 5 minutes. Gels were run at 180V for 50 minutes in Tris-glycine electrophoresis buffer (0.1% SDS, 30 mM Tris-HCl pH 8.3, 250 mM glycine). Gels were stained in protein stain solution (10% Acetic acid, 10% Methanol, 0.25% (w/v) R250 Coomassie Brilliant Blue) for an hour. After the gel was stained, it was placed into destain solution (10% Acetic acid, 10% methanol) overnight. Gel images were taken using a scanner attached to a computer (Canon LiDE).

2.13 Western blot and dot blot

Samples for analysis by Western Blot were run on an appropriate SDS-PAGE gel (see above) under non-reducing conditions. After completion, the proteins were transferred by immunoblotting to a nitrocellulose membrane in ice-cold blotting buffer (3.03g Tris, 14.4g Glycine, 20% MeOH, 0.05% SDS) at 100V for 120 minutes by the immunoblotting method (Towbin *et al.*, 1979) using Mini Trans-Blot Cell blotting electrodes (Bio-Rad). For analysis by dot blot, protein solution was directly pipetted onto a nitrocellulose membrane and allowed to dry.

After blotting, the nitrocellulose membrane was transferred to blocking buffer (PBS containing 5% Skimmed Milk powder, 0.01% Triton X-100) to block for at least 1hr at 25°C. Where primary antibody was used, it was added to fresh blocking buffer at an appropriate dilution and incubated for 1hr. The membrane was then washed 3 x 10 minutes with fresh blocking buffer to remove any primary antibody. Secondary antibody peroxidise conjugates (GE Healthcare Ltd) were then added in fresh blocking buffer at an appropriate dilution, and incubated for 1 hour at 25°C.

Detection of certain proteins used antibodies directly conjugated to peroxidise, and hence did not require a secondary antibody. For detection of these proteins, the nitrocellulose membrane was blocked as above, and then washed 3 x 10 minutes using PBST (PBS, 0.01 % Triton X-100).

The peroxidise conjugate was then added at the appropriate dilution in PBST and incubated for 1 hour at 25 °C. For detection of 6xHis tagged proteins, an anti-His pAb peroxidise conjugate (Acbam) was added to 10ml PBST at a 1:5,000 dilution. For detection of biotinylated proteins, a Streptavidin peroxidase conjugate (Sigma) was added to 10ml PBS/Tween at a dilution of 1:50,000.

After incubation with the peroxidise conjugate, the membrane was washed 3 x 10 minutes with fresh PBST, and 3 x 10 minutes with PBS. Excess buffer was removed, ECL Plus Western blotting detection reagent (Amersham Biosciences) was added to nitrocellulose membrane, and left to develop for 1 minute. This was then removed and the membrane was gently dried, before exposing with chemiluminescence film (Amersham Biosciences) in a dark room. The film was then developed using a Compact-X4 automated developer (Xenograph Imaging Systems).

2.14 Flow cytometry assay

2.14.1 Flow cytometry using mammalian cells

Cells were grown to ~90% confluence in 75cm^2 flasks. The cells were prepared as for sub-culturing, and were re-suspended in 2ml ice-cold Hank's Buffered Saline Solution (HBSS) containing 10% FCS and centrifuged at 1000 rpm for 3 minutes. This was repeated, before the cells were finally re-suspended in 1ml ice-cold HBSS/FCS. The cells were then incubated on ice in the dark for 1hr.

Avidin-coated 0.7-0.9 μm purple fluorescent beads (Spherotech) (10 μl per reaction) were suspended in HBSS containing 1% BSA (100 μl per reaction). The beads were spun at 13,000 rpm for 5 minutes, and the supernatant was removed. The beads were re-suspended in 50 μl HBSS/BSA per reaction, and added to 1μg biotinylated protein (at 1 mg/ml). Beads were incubated with protein overnight in the dark at 4°C to avoid bleaching the beads. A protein fragment encompassing cbEGF domains 12-14 from human fibrillin1 was immobilized on the

beads for use as a negative control in each experiment. After incubation, the beads were spun at 13,000 rpm for 5 minutes, and the supernatant was removed. The beads were re-suspended in 100 µl HBSS/BSA per reaction to wash off any unbound protein and spun at 13,000. The supernatant was removed, and the beads were re-suspended in 50 µl ice-cold HBSS containing 10% FCS per reaction. A 5µl aliquot of beads was taken to check protein loading by Western Blot.

Once the cells were ready, they were placed into pre-chilled FACS tubes (BD) in 50 µl aliquots, and mixed with 45µl beads. This was incubated on ice for 1 hour in the dark. After 1hr the mixture was suspended in 500 µl ice-cold FBSS, and placed on a FACSCalibur flow cytometry machine (Beckton Dickinson), with a flow rate <2,500 cells/min. Fluorescence was measured with no gate in the FL1-H and FL3-H channels at 530 and >670 nm respectively, with excitation at 488 nm.

2.14.2 Flow cytometry using *Drosophila* S2 cells

Cells were collected 2 days post induction by $CuSO_4$ for use in a flow cytometry assay. Cells were dislodged from the flask using gentle tapping and the flask was washed down using a 5 ml pipette to remove any adherent cells and disperse clumps of cells. The cells and beads were prepared as for the mammalian cells, and incubated with fluorescent beads for 1 hour.

Gating in the FL1-H channel was used in order to detect the cells that had been successfully transfected with the GFP fusion protein. A gate was applied for cells with fluorescence > 99% of untransfected cells. Fluorescence in the FL3-H channel was recorded as for mammalian cells.

2.14.3 Quantitative analysis of flow cytometry data

In order to produce a quantitative analysis of the binding data obtained by flow cytometry, the following analysis was performed.

- A marker was placed to the right of 99% cells for the negative control (fibrillin cbEGF 12-14) fluorescence profile in the FL3 (λ > 670 nm) channel (Figure 2-1 A).
- The number of cells to the right of this marker was recorded for the positive control interaction (Figure 2-1 B).
- The number of cells to the right of this marker was recorded for each mutant in turn (Figure 2-1 C).
- The ratio of the values obtained for the mutant and positive interactions was calculated (relative binding) for each repeat of the experiment, and an average and standard deviation of this value were calculated.

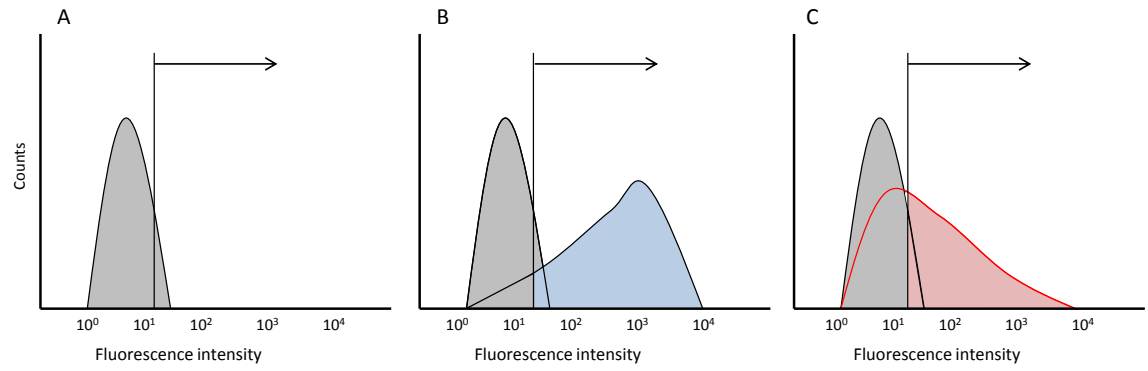


Figure 2-1 Quantitative analysis of flow cytometry data. A marker was placed to the right of 99% of the cells in the FL3 channel for the fluorescence profile of the negative control interaction (A). The areas under the WT (B - blue) and mutant (C - red) fluorescence profiles were measured, and the mutant:WT ratio was calculated.

2.14.4 Statistical analysis of flow cytometry data

Once the ratio of the values had been obtained (see above), a mean value and standard deviation was calculated for each of the sets of binding data. Using these values, 95% confidence limits were calculated using a 2-tailed t-distribution. The calculated upper and lower limits were inspected to see whether the WT binding interaction (defined as 1) lay within these limits, in order to determine whether or not binding had been affected.

2.15 Surface Plasmon Resonance

The interaction between Notch1 and its ligands was studied using a BIAcore3000 machine (GE Healthcare Ltd). Running buffer containing 150 mM NaCl, 0.005 % Tween P20, 1 mM $CaCl_2$, 10 mM HEPES pH 7.4 was used for all experiments, at a flow rate of 25µl/min. Approximately 3,000 RU of Jagged1 or DLL4 was immobilised on flow cells using amine coupling. 1-Ethyl-3-[3-dimethylaminopropyl]carbodiimide hydrochloride (ECD) and N-hydroxysuccinimide (NHS) were mixed in a 1:1 ratio and flowed over all four flow cells on a standard BIAcore CM5 chip at 10 µl/min to activate the surface. Proteins were injected at a concentration of 1 µg/ml in Acetate pH 4.5 at 10 µl/min. After the protein was immobilised to the chip, 70 µl ethanolamine was flowed over all four channels in order to quench any unreacted carbonyl groups from the dextran matrix.

Equilibrium binding analysis was carried out at a protein concentration of 10uM. Notch fragments were flown over the chip at 25µl/min for 36 seconds, using the KINJECT injection command. Background binding to the empty flow channel was subtracted from each channel to calculate the actual binding response seen. Calcium dependence of binding was confirmed by an addition injection a final injection of wild-type Notch protein performed with 10 mM EGTA added to the running buffer.

2.16 Nuclear Magnetic Resonance Spectroscopy

2.16.1 1D and 2D NMR

Proteins for analysis by NMR spectroscopy were dissolved in matrix buffer (150 mM NaCl, 5 mM Tris-HCl pH 7.5 in 100% D_2O) to a concentration of 300 µM, and adjusted to pH 7.5 using DCl or NaOD. Samples were analysed in either a 5 mm emperor grade NMR tube (600 µl), or a Shigemi tube (300 µl).

All NMR experiments were performed with the assistance of Prof Christina Redfield. Data was collected at 25°C on home-build MNR spectrometers, operating at between 500 MHz. 1D NMR experiments were performed with a spectral width of 5494.5 MHz and a block size of 4 K, and 512 spectra were acquired for each sample. 2D NOESY spectra were collected with a mixing time of 150 ms. A spectral width of 5494.5 Hz was used in each dimension, and water suppression was achieved using field pre-saturation. A minimum of 96 scans were performed for each spectrum, and 1024 complex points were acquired in the F_2 dimension. 256 complex points were collected in the F_1 dimension. NMR data were analysed using Analysis (CCPN).

2.16.2 Measuring calcium binding using NMR

Lyophilised protein was dissolved in 300 µl matrix buffer and the pH was adjusted to 7.5 as above. Small aliquots (1-5 µl) of $CaCl_2$ solutions dissolved in D_2O were added incrementally, and the pH adjusted following each addition. 1D spectra were recorded at each calcium concentration, up to 15 mM $CaCl_2$, and 2D spectra was recorded at the 0 mM and 15 mM $CaCl_2$ points. The chemical shift of the Hε proton from Y444 was used as an indicator for calcium binding to EGF12 in $hN1_{11\text{-}13}$, and the position of this chemical shift was recorded at each calcium concentration, in order to calculate an apparent K_d for calcium binding to EGF12. The same procedure was carried out for $hN1_{11\text{-}13}$ WT, as well as protein containing the T466A and I477A substitutions.

Chapter 3

Protein production and purification

3.1 Introduction

A construct containing EGF domains 11-13 of hNotch1 ($hN1_{11-13}$) has previously been found to bind to various Notch ligands (Cordle *et al.*, 2008). A good deal of work has been done to characterise this construct, and both a solution structure and a crystal structure of this protein have been obtained (Hambleton *et al.*, 2004) (Cordle *et al.*, 2008). The constructs used to obtain these structures differ as the latter contains a 15 residue C-terminal BirA tag that allows for site-specific biotinylation. This tag appears to increase the calcium-binding affinity of EGF13 (Dr Jemima Cordle, unpublished data) and stabilises the EGF12-EGF13 packing interface. This causes the protein to adopt a rigid rod-like structure in the presence of calcium.

The construct containing the BirA tag is used to test the effect on binding of a series of mutants in order to define the ligand binding site in EGF12 in Chapter 4, and as a substrate for glycosylation in order to test the effect of specific sugar modifications in Chapter 5. A series of longer proteins with EGF domains N-terminal to this region were produced using either a prokaryotic or a eukaryotic expression system in order to see whether these additional domains affect binding to different Notch ligands in Chapter 6. In addition to these human proteins, the minimal binding region of the *Drosophila* Notch molecule was made, along with several mutants. All proteins made using a prokaryotic expression system were expressed using the pQE30 prokaryotic expression vector (Qiagen) in BL21 *E. coli* cells containing the pREP4 plasmid, and all proteins made using a eukaryotic expression system were expressed using a modified pHLSec eukaryotic expression vector in HEK 293T cells (courtesy of Dr Chandramouli Chillakuri). The cloning, production and purification of these proteins is described here in this chapter.

3.2 Production and purification of prokaryotically expressed proteins.

A flow diagram to describe the production of prokaryotically expressed Notch proteins is shown below (Figure 3-1), and the details of how each step was performed are outlined in this chapter and in Chapter 2. This purification strategy has been used in multiple previous studies to generate large

quantities of correctly-folded protein in order to investigate the molecular properties of proteins containing multiple tandem cbEGF repeats, including of the Notch receptor (Hambleton *et al.*, 2004) and fibrillin1 (Jensen *et al.*, 2005). This protocol relies on *E. coli* cells producing large amounts of recombinant protein which the cells are incapable of folding correctly. Cell lysis using denaturing and reducing guanidine buffer solubilises the misfolded protein, and allows the protein to be purified by nickel column before being refolded using an *in vitro* oxido-shuffling refolding protocol and purified by HPLC and FPLC.

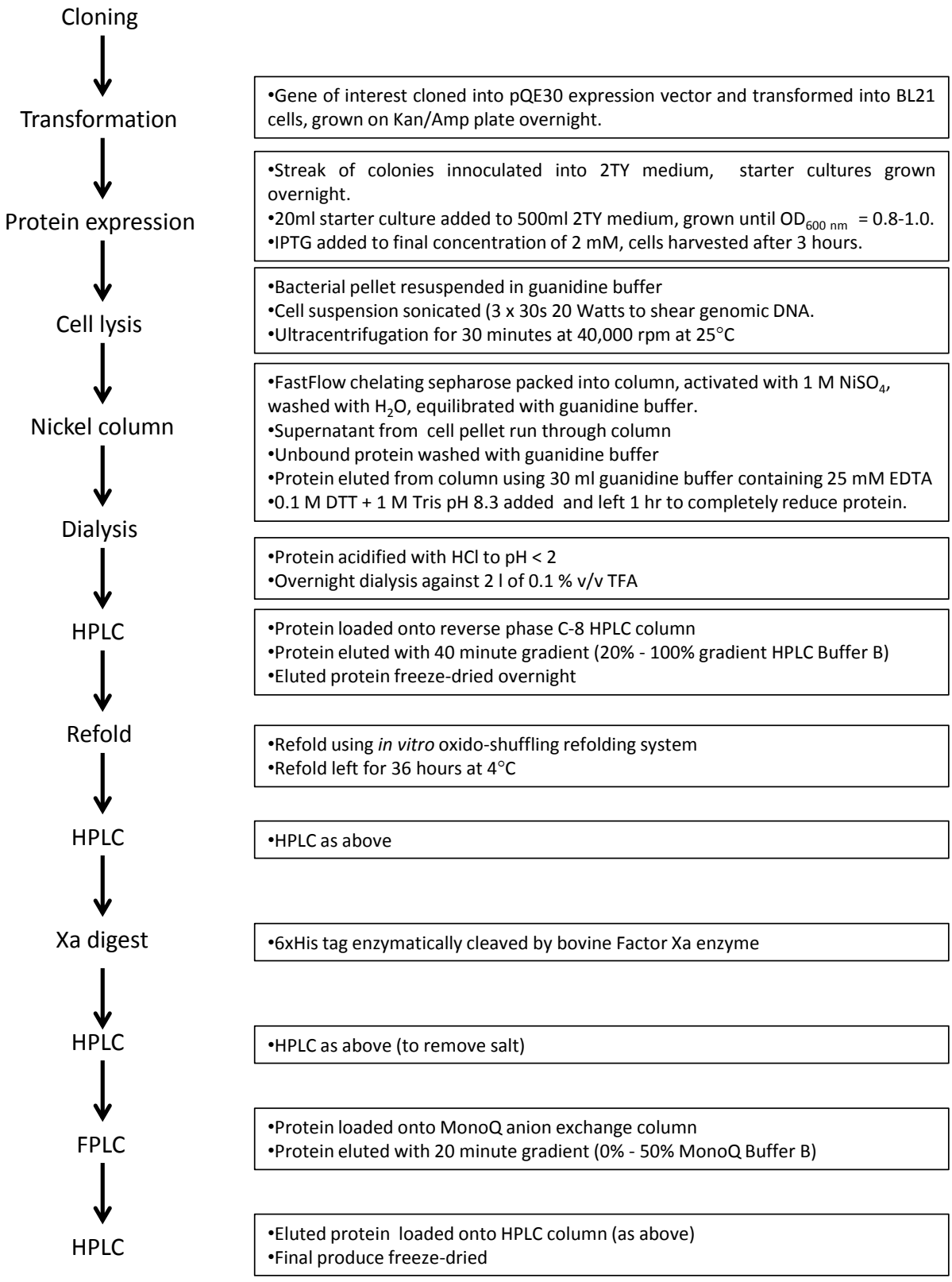


Figure 3-1 A flow diagram for the production and purification of prokaryotically expressed Notch proteins. Details of each step are outlined below, and in Chapter 2.

All of these constructs were inserted into the pQE30 plasmid (Figure 3-2). This plasmid encodes an N-terminal 6 x His tag that can be cleaved using recombinant Factor Xa, and uses a T5 promoter sequence for a high level of gene expression. Gene expression is also controlled by a pair of *lac* operator sites, which causes protein expression to be tightly repressed, until induction by the lactose mimic IPTG. Repression of gene expression is achieved in *trans* by using *E. coli* cells containing the pREP4 plasmid, which expressed the *lac* repressor protein. This is essential in order to prevent unwanted gene expression, as the cysteine-rich proteins produced in this way are toxic to the bacterial cells as they grow.

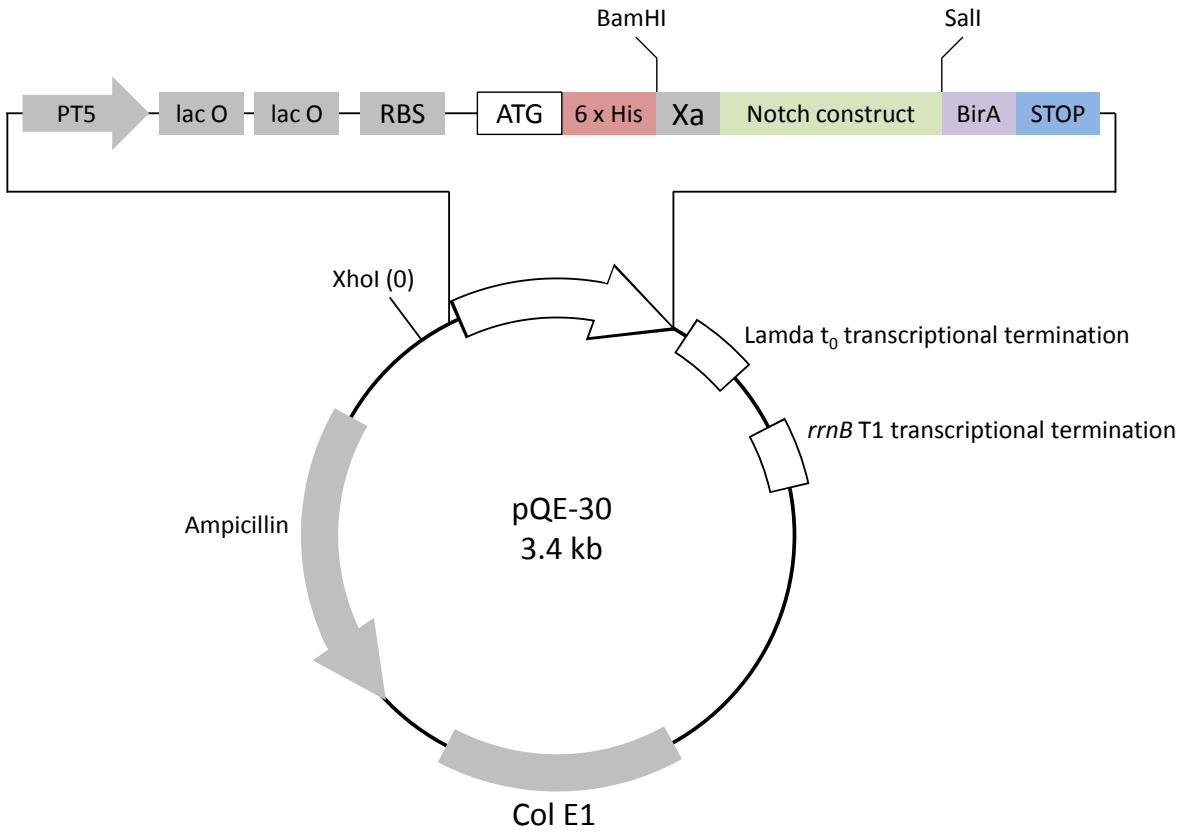


Figure 3-2 Plasmid map of the pQE-30 prokaryotic expression vector. The major components of the vector are indicated. T5 phage promoter and two *lac* operator sequences control protein expression. RBS – ribosome binding sequence. The plasmid encodes an N-terminal 6 x His tag with a Factor Xa protease site. The Notch construct is inserted into the plasmid via 5' BamHI and 3' SalI restriction sites. The t_0 and T1 termination sequences prevent read-through and ensure the stability of the transcript (adapted from www.qiagen.com).

3.3 Production of $hN1_{11-13}$ WT

$hN1_{11-13}$ contains three tandem cbEGF domains (Figure 3-3). After protein expression, cell lysis and an initial purification by nickel column, the reduced protein was purified by HPLC. The reduced protein elutes over a broad range of the elution gradient, and can form several overlapping peaks. However, the entire range is collected for further purification (Figure 3-4 A).

After the initial purification, the protein was refolded using an *in vitro* oxido-shuffling system. The $hN1_{11-13}$ fragment has been extensively studied in the past, and the refolding conditions for this protein are well-established. The following components were added to the protein solution in order, with the protein diluted to a final concentration of 0.2 mg/ml with MilliQ H_2O: 3 mM L-cysteine, 10 mM $CaCl_2$, 50 mM Tris-HCl pH 8.3, 300 µM L-cystine. The refold mixture was left at 4°C for 48 hours, and purified by HPLC. In contrast to the broad elution profile seen for the reduced material, the refolded protein eluted as a single peak, and at an earlier point in the elution gradient (Figure 3-4 B). This is evidence of refolding, as the folded protein is more homogeneous, and presents a less hydrophobic surface to the matrix of the column and hence requires a lower level of acetonitrile in order to be displaced from the column than the unfolded protein does.

Recombinant bovine factor Xa was used to remove the N-terminal 6 x His tag from the protein. It was found that $hN1_{11-13}$ elutes from a MonoQ anion exchange column at a low salt concentration, and fails to bind to the column properly at the salt concentrations used for the factor Xa cleavage (not shown). Therefore after the overnight incubation the protein was purified by HPLC in order to desalt the protein sample (not shown). Cleavage of the N-terminal 6 x His tag was confirmed by comparing the migration of the protein on a 16% SDS-PAGE gel before and after proteolytic cleavage. Purification of $hN1_{11-13}$ by FPLC on a MonoQ anion exchange column produced a single sharp peak during the elution gradient (Figure 3-4 C). At the end of the gradient, washing the column with 100% MonoQ Buffer B caused a large amount of protein to elute from the column. This was found to be misfolded protein. Once the protein was eluted from the MonoQ column a final

purification by HPLC was performed. Samples from each of the four HPLC purification steps were taken for analysis on a 16% SDS-PAGE gel (Figure 3-4 E).

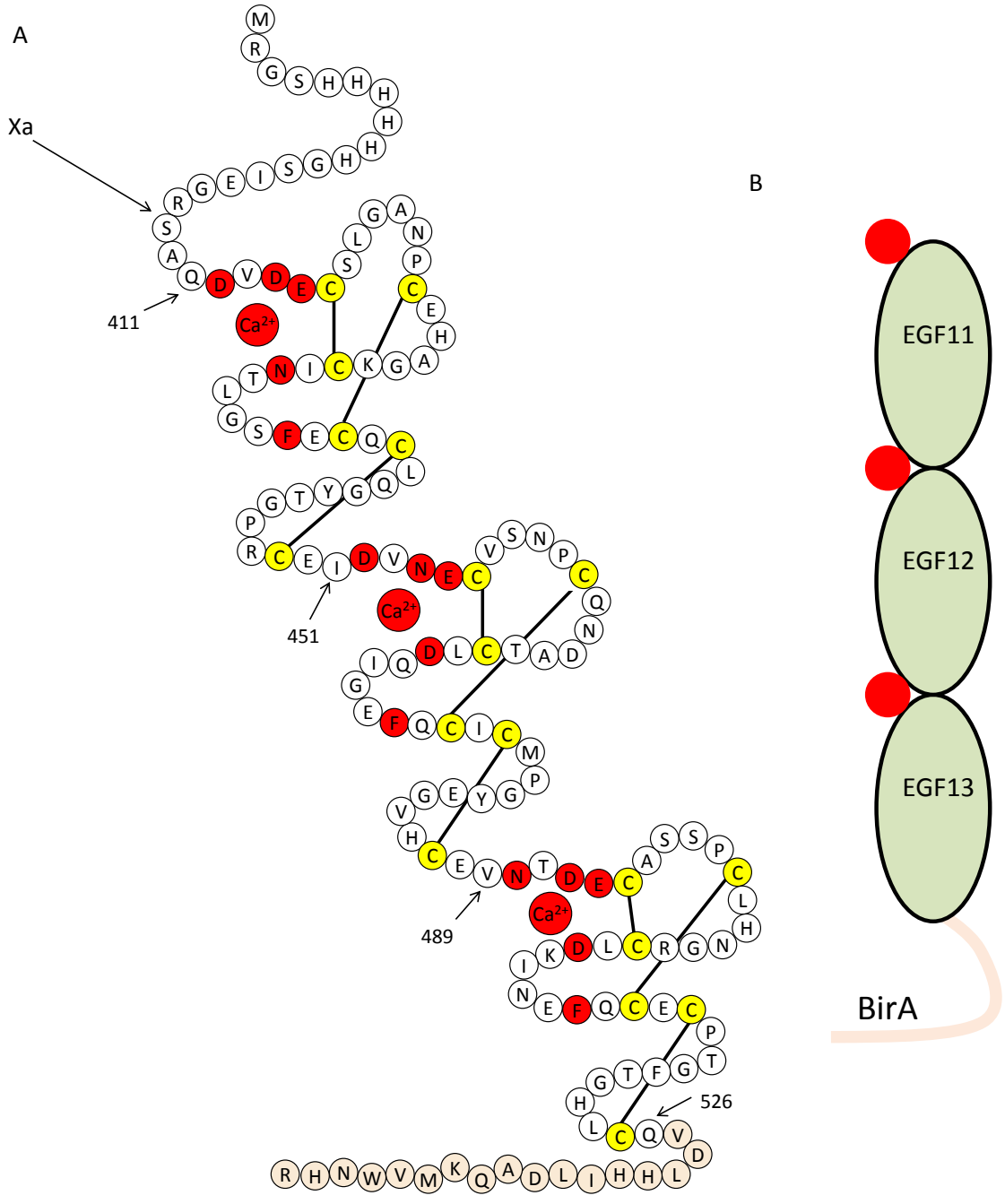


Figure 3-3 Diagram to show the amino acid sequence and domain organisation of hN1$_{11-13}$. A) The three EGF domains from hN1$_{11-13}$ all contain the calcium binding consensus, and the C-terminal BirA tag helps stabilise calcium binding in EGF13. B) The domain organisation of hN1$_{11-13}$, indicating that all of the domains bind calcium. Residue numbers indicating the start of each domain are shown.

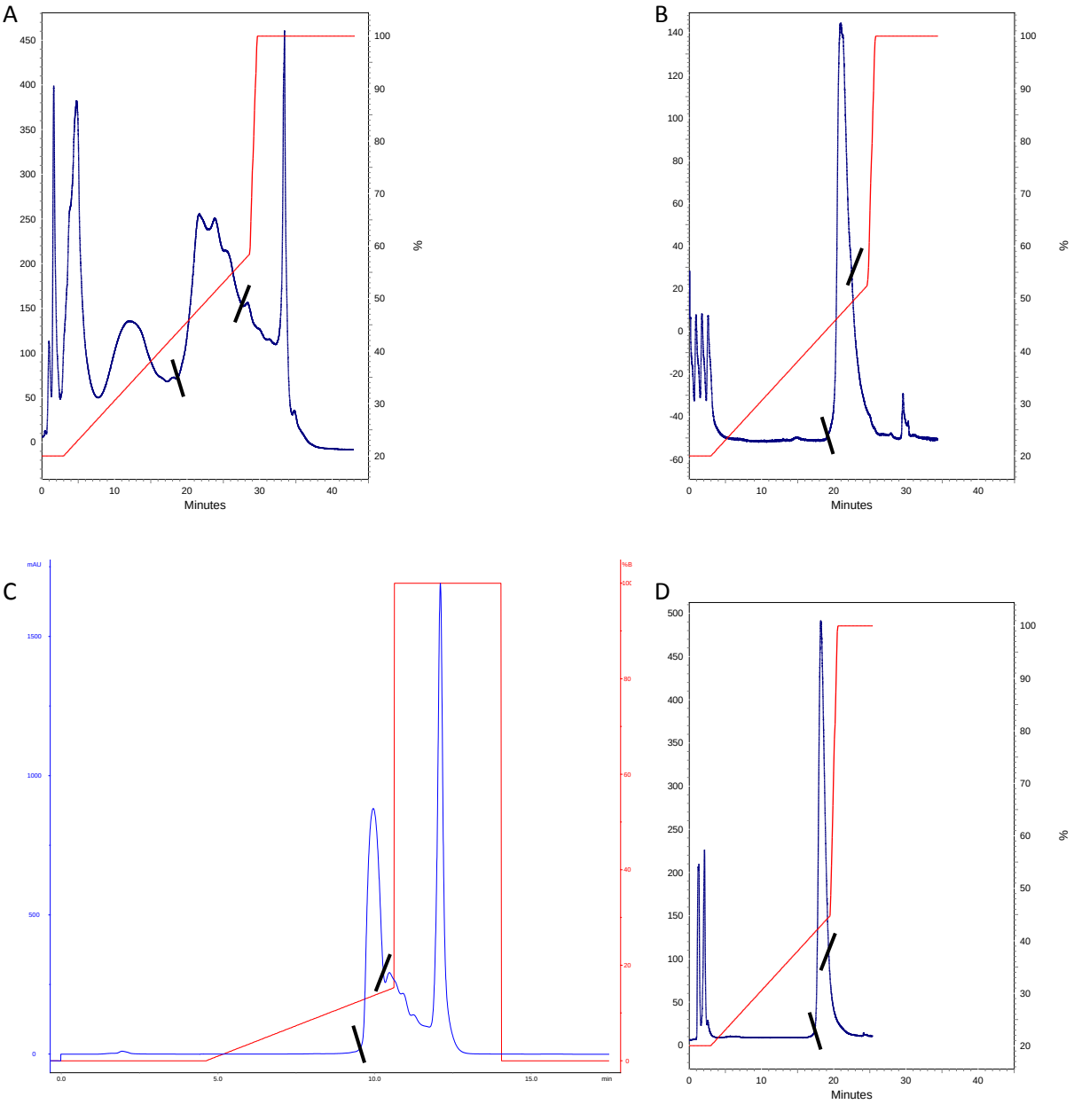


Figure 3-4 Purification of hN1$_{11-13}$ BirA WT. A) HPLC of reduced hN1$_{11-13}$. B) HPLC of hN1$_{11-13}$ after refold. C) MonoQ FPLC purification. D) Final HPLC pufication. The fractions collected are indicated by the black lines. E) Gel to follow purification of hN1$_{11-13}$.

3.4 Production of mutant $hN1_{11-13}$ proteins

A series of single amino acid substitutions were made in $hN1_{11-13}$ in order to identify the location of the ligand binding site within EGF12 (see Chapter 4). Amino acid substitutions were introduced into $hN1_{11-13}$ by designing primers to mutate specific DNA bases, before the mutant constructs were expressed and the proteins purified in a similar way to $hN1_{11-13}$ WT (see Appendix A for a list of primers).

3.4.1 Site-directed mutagenesis

Two separate PCR mutagenesis methods were employed in order to produce the desired mutations in $hN1_{11-13}$: a 'back-to-back PCR' reaction or the Lightning Mutagenesis kit (Stratagene). Back-to-back PCR mutagenesis requires two non-overlapping primers, with the mutation of interest only being present within the forward primer, with the reverse primer complementary to the WT DNA (Figure 3-5 A). Primers for use with the Lightning Mutagenesis kit are complementary to each other, and both the forward and reverse primers contain the mutation of interest (Figure 3-5 B). The back-to-back amplification produces linear DNA which needs to be circularised by blunt-end ligation before transformation into NM554 (pRep4) cells, whereas DNA produced via the Lightning method was transformed directly into XL10 gold ultracompetent cells after the template DNA is digested by the endonuclease DpnI. The DNA for each mutant was sequenced by automated sequencing (Source Bioscience) to confirm that the desired DNA sequence had been obtained.

3.4.2 Expression and purification of Notch mutants

Mutant $hN1_{11-13}$ constructs were expressed in the same way as $hN1_{11-13}$ WT. After cell lysis and purification by nickel column and HPLC, refolding conditions were tested for each mutant. The same oxido-shuffling *in vitro* refolding system was used as for $N1_{11-13}$ WT, and initially a variety of calcium concentrations ranging from 2 mM to 50 mM were tested, along with a further refold condition containing 10 mM EDTA, in order to test whether the amino acid substitutions introduced in EGF12 affected the ability of the proteins refold in a calcium-dependent manner.

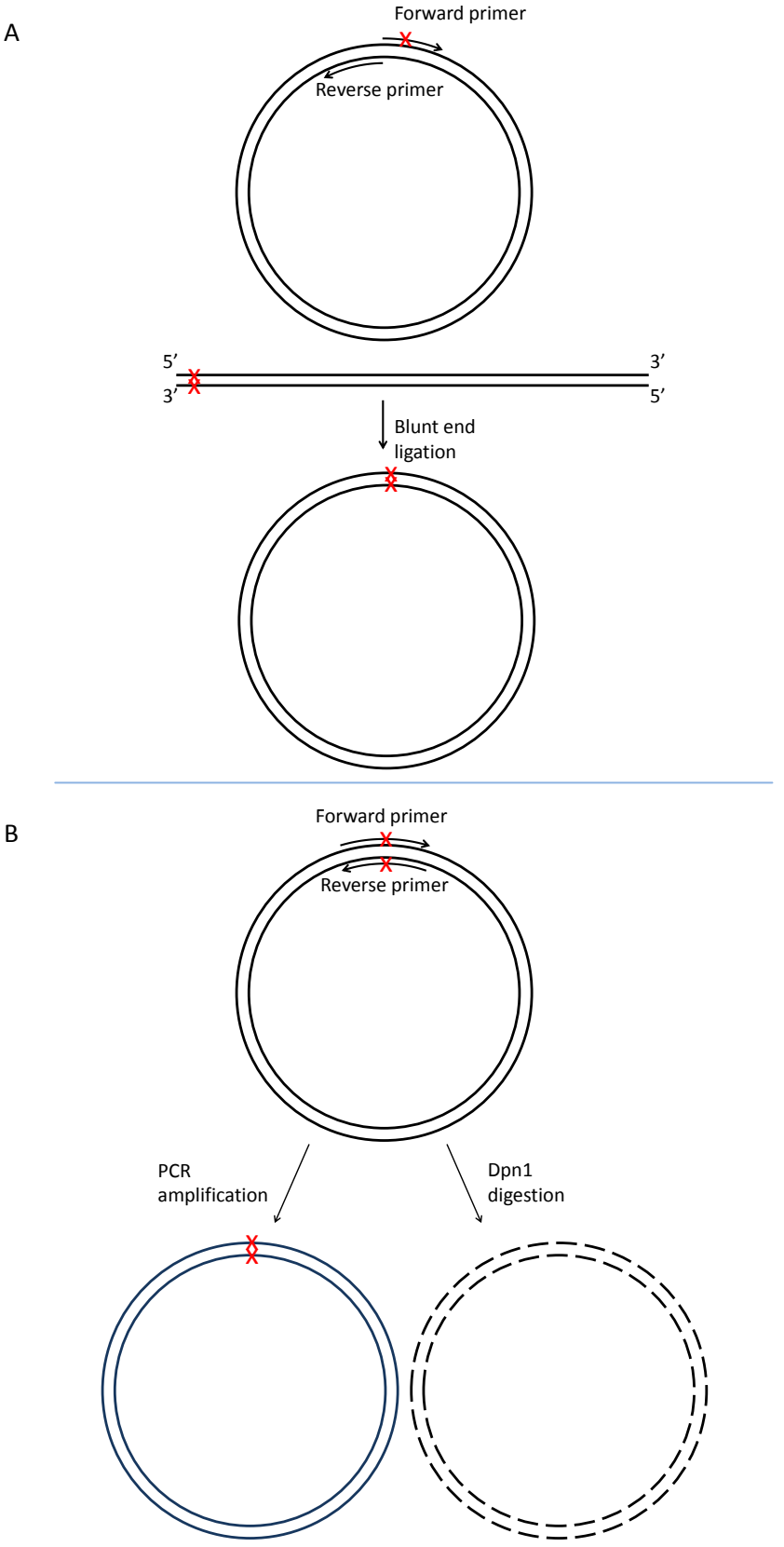


Figure 3-5 Schematic diagram to explain PCR mutagenesis. The required mutation is indicated with a red cross. A) Back-to-back PCR mutagenesis produces a DNA that needs to be circularised. B) Lightning mutagenesis produces non-methylated DNA (blue) containing the required mutation, and template DNA containing methyl-cytosine (black) is digested by the endonuclease Dpn1.

Each of the mutant proteins was found to refold in a calcium-dependent manner (Figure 3-6). Each of the refold conditions containing $CaCl_2$ eluted as sharp single peaks when the refold products were purified by HPLC, and the purified protein ran as a single sharp band under both reducing and non-reducing conditions when visualised on a 16% SDS-PAGE gel. Altering the concentration of calcium added to the refold mixture within the range of 2-50mM, had no significant effect on the refolding of any of the mutants suggesting that the affinity of calcium binding in EGF12 is not significantly altered by any of the substitutions introduced into EGF12. By contrast, when the refold conditions contained 10 mM EDTA, the protein eluted as a broader peak when the products were purified by HPLC. The products of this trial refold ran as a sharp band on a 16% SDS-PAGE gel under reducing conditions, but under non-reducing conditions ran as a broad band, indicating that the protein may not be natively-folded (Figure 3-6). This suggests that calcium is required for the formation of the correct disulphide bonding pattern in each of the mutants produced in this study, and that the products of refold conditions lacking calcium are likely to contain EGF domains with the incorrect disulphide bond pattern.

All of the mutant proteins were refolded and purified to homogeneity by HPLC and FPLC using the same protocol as for $hN1_{11\text{-}13}$. The final product for each mutant was collected and visualised on a 16% SDS-PAGE gel, and they were indistinguishable from the WT protein (Figure 3-7). This suggests that all of the mutants retain the ability to bind calcium, and that they are correctly folded. Each protein was analysed by mass spectroscopy to confirm the correct amino acid substitution was present, and that the 6 x His tag had been successfully removed, and were found to differ by only a few Daltons from the expected molecular weight (Table 3-1).

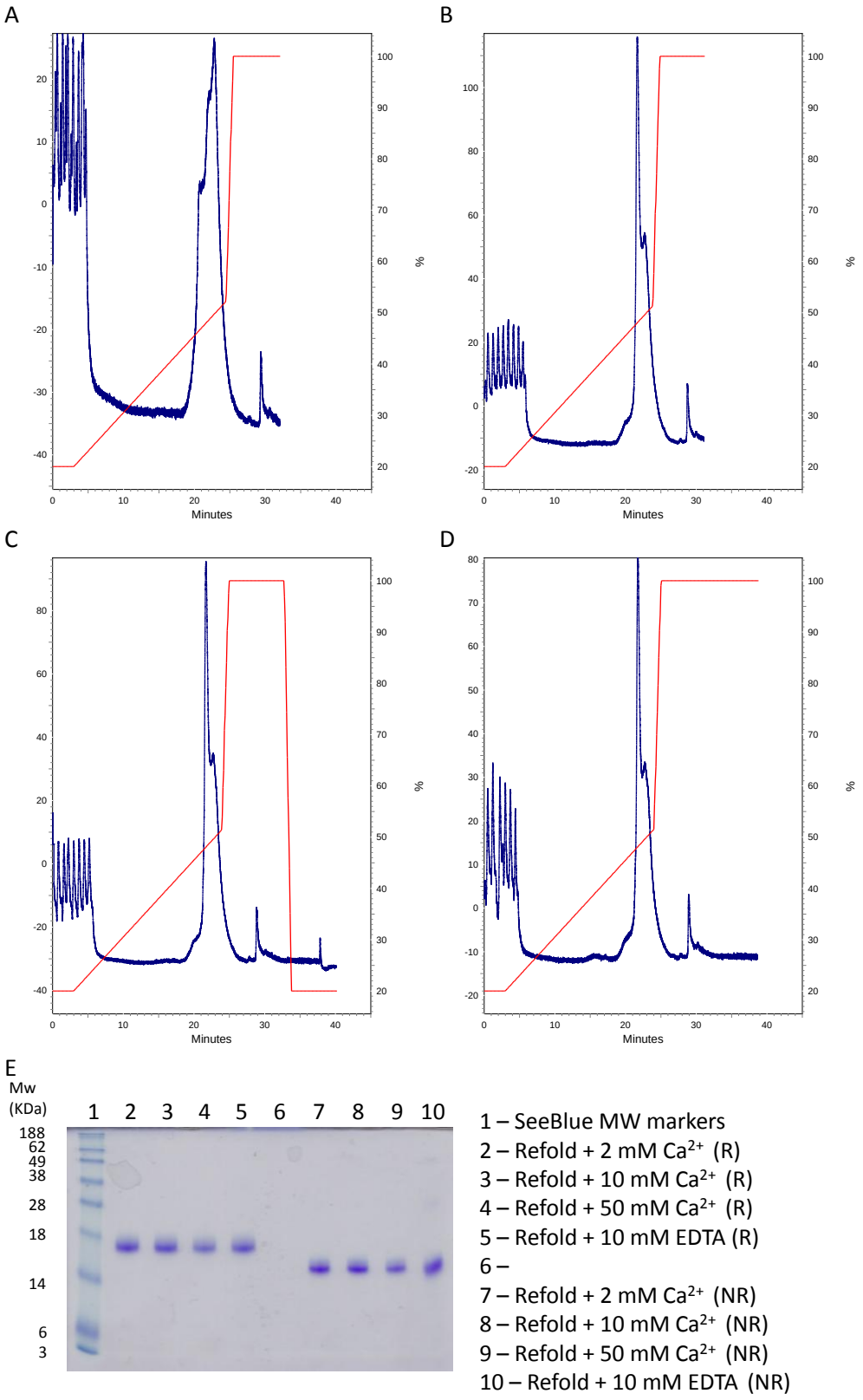


Figure 3-6 Refold trial for hN1$_{11-13}$ BirA E473A to confirm calcium dependence of refolding. Refold conditions as outlined above were set up containing 10 mM EDTA (A), 2 mM $CaCl_2$ (B), 10 mM $CaCl_2$ (C) or 50 mM $CaCl_2$ (D) in order to test whether the E473A substitution refolded in a calcium dependent manner. E) These fractions were visualised on a 16% SDS-PAGE gel to establish whether the sharpness of the peak correlated with protein folding.

Table 3-1

Protein	Predicted mass (Da)	Actual mass – ESI-MS (Da)
$hN1_{11-13}$ WT	14,826.58	14,826
$hN1_{11-13}$ T466A	14,796.56	14,798
$hN1_{11-13}$ T466V	14,824.61	14,832
$hN1_{11-13}$ T466S	14,812.56	14,818
$hN1_{11-13}$ L468A	14,784.50	14,785*
$hN1_{11-13}$ Q470A	14,769.53	14,768
$hN1_{11-13}$ E473A	14,768.55	14,771
$hN1_{11-13}$ Q475A	14,769.53	14,768
$hN1_{11-13}$ I477A	14,784.50	14,784
$hN1_{11-13}$ M479A	14,766.47	14,769*

*Denotes that ESI-MS analysis was performed by Fiona Taylor

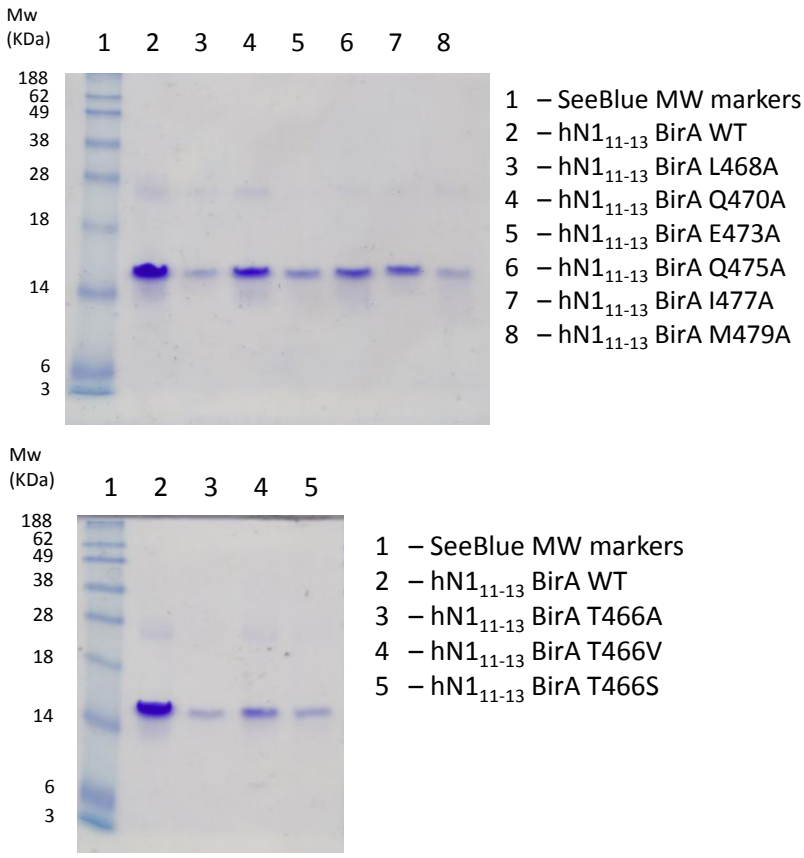


Figure 3-7 Gel showing each of the $hN1_{11-13}$ mutants. The final purification products for each of the mutants used in Chapters 4 and 5 is shown here. Each protein was loaded in non-reducing buffer.

3.5 Production of $hN1_{9-13}$ and $hN1_{10-13}$

Extended hNotch1 constructs spanning EGF domains 9-13 ($hN1_{9-13}$) and 10-13 ($hN1_{10-13}$) were produced using the prokaryotic expression system in order to investigate the effects of further EGF domains N-terminal to the ligand binding region. The $hN1_{10-13}$ construct was purified in a similar manner to $hN1_{11-13}$ as the refolded protein eluted from the HPLC as a single peak (Figure 3-8). This is despite EGF10 not containing the consensus residues for binding calcium (Figure 3-9).

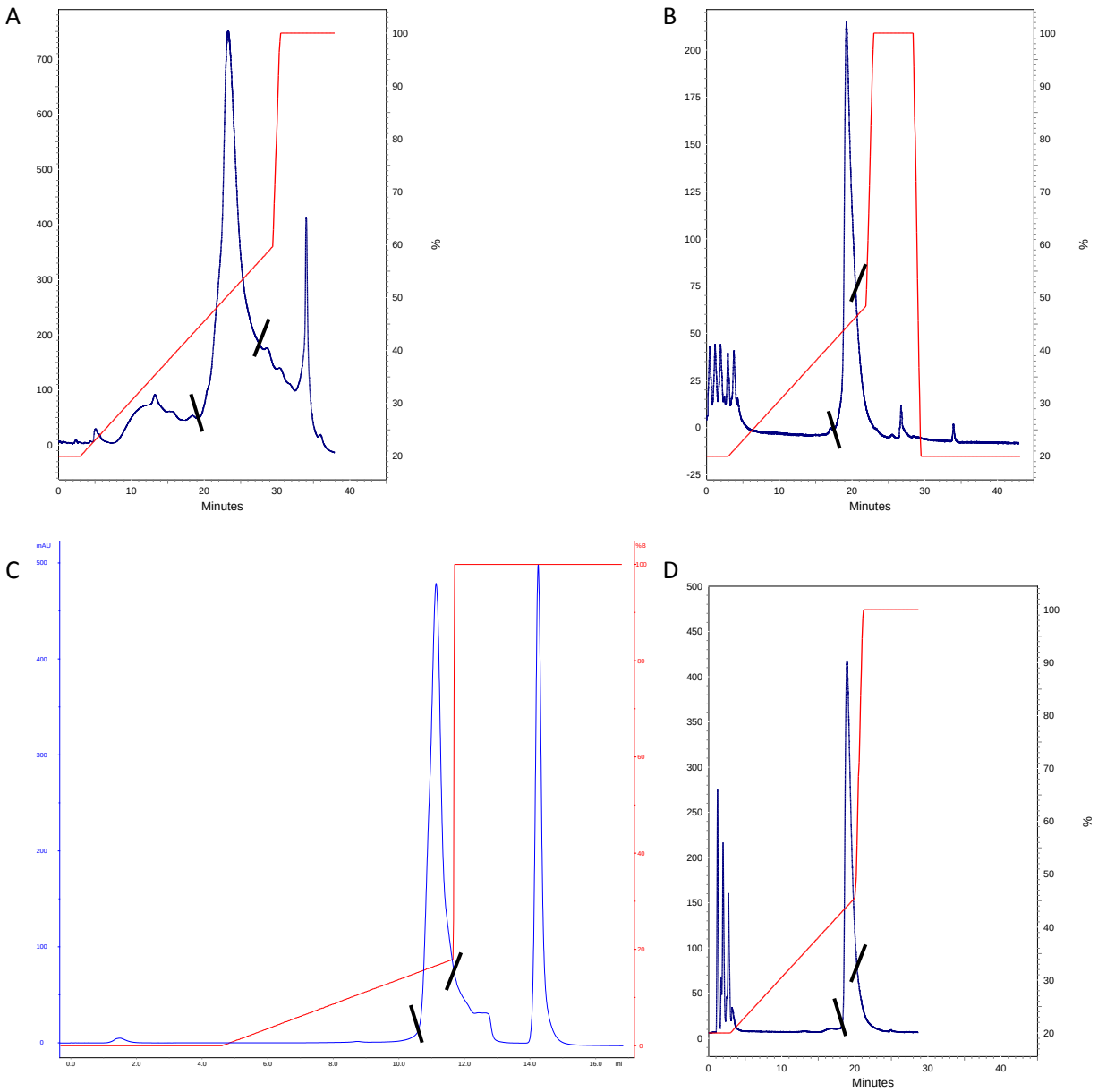


Figure 3-8 Purification of $hN1_{10-13}$ BirA WT. A) HPLC of reduced $hN1_{10-13}$. B) HPLC of $hN1_{10-13}$ after refold. C) MonoQ FPLC purification. D) Final HPLC pufication. The fractions collected are indicated by the black lines.

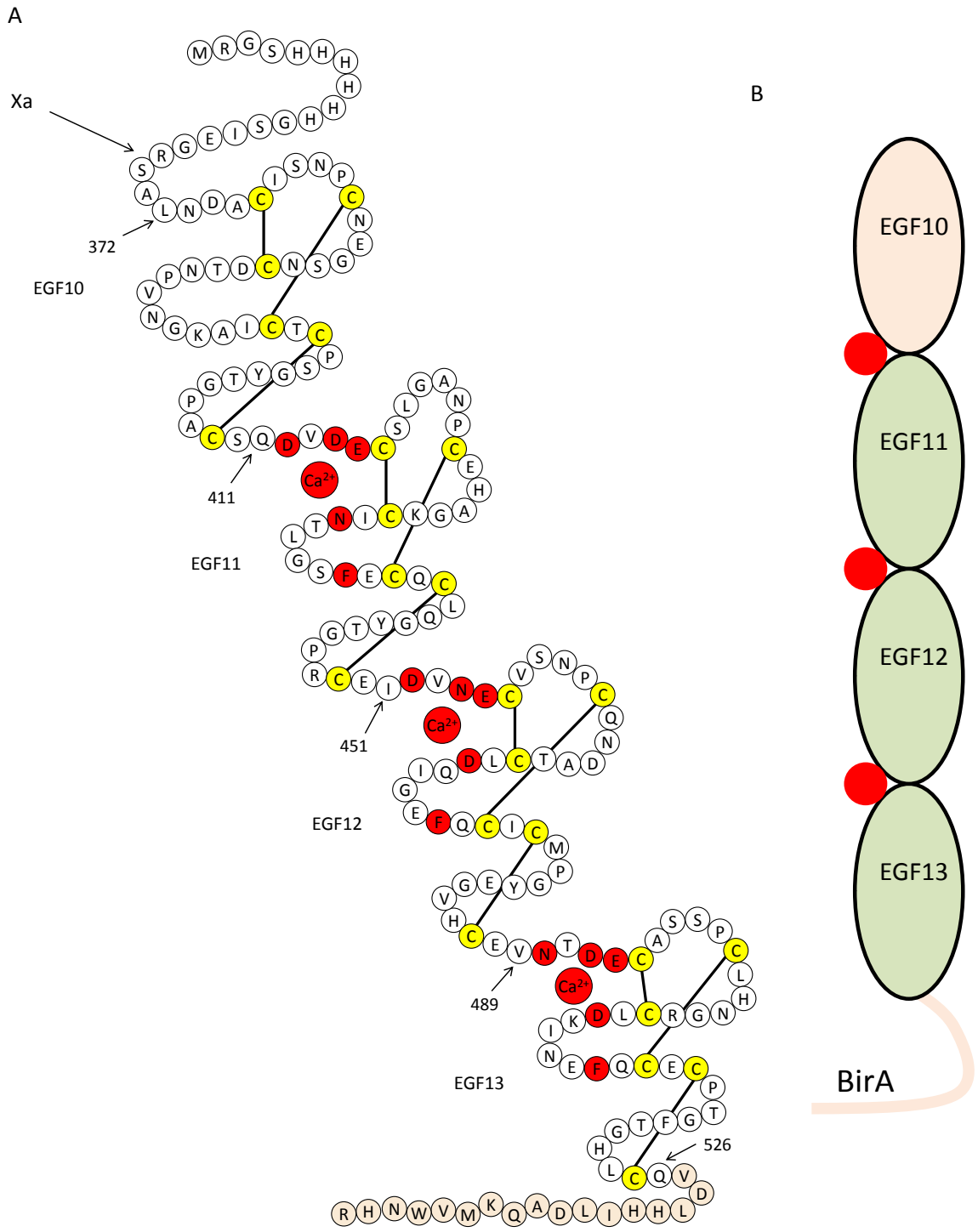


Figure 3-9 Diagram to show the amino acid sequence and domain organisation of hN1$_{10-13}$. A) Three of the EGF domains from hN1$_{10-13}$ contain the calcium binding consensus, whereas EGF10 does not. The same C-terminal BirA as in hN1$_{11-13}$ tag helps stabilise calcium binding in EGF13. B) The domain organisation of hN1$_{10-13}$. Residue numbers indicating the start of each domain are shown.

The $hN1_{9-13}$ construct was produced with an N-terminal 6 x His tag that contained an enterokinase cleavage site, as the C-terminal region of EGF9 contain a cryptic Xa cleavage site. However, this protein was also found to contain a cryptic enterokinase cleavage site (not shown), so it was not possible to remove the 6 x His tag during the purification of this protein.

The refold of $hN1_{9-13}$ eluted as a broad peak from the HPLC, that could be separated into two separate fractions. These fractions were visualised on a 16% SDS-PAGE gel under both reducing and non-reducing conditions in order to see which contained the correctly folded protein (Figure 3-10). A sharp band was observed for both fractions under reducing conditions, but under non-reducing conditions only the right hand fraction contained a sharp band at the correct size. Therefore this fraction was collected and purified by FPLC and HPLC (Figure 3-11). EGF9 is predicted to bind calcium, as it contains each of the residues that form the calcium binding consensus sequence (Figure 3-12).

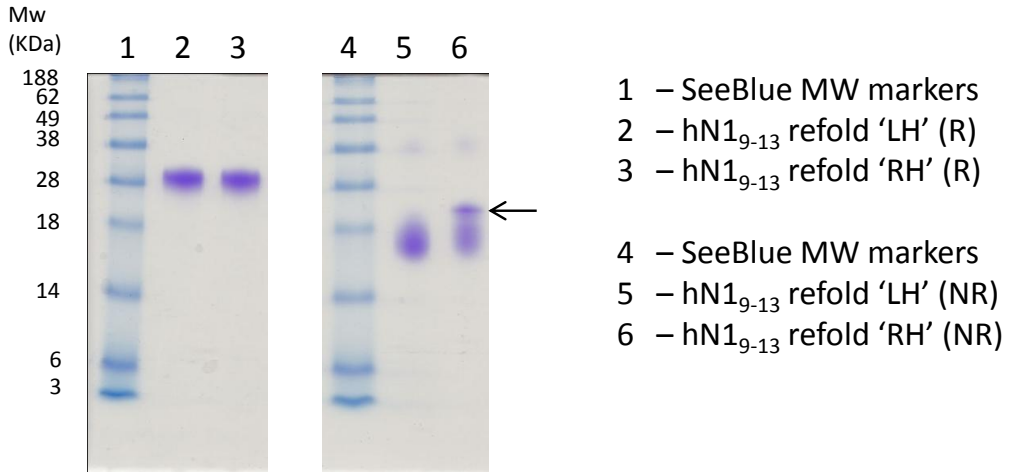


Figure 3-10 Analysis of the refold products of $hN1_{9-13}$. Both fractions from the refold of $hN1_{9-13}$ run as a single band under reducing conditions (lanes 2-3). Under non-reducing conditions (lanes 5-6) the protein from left hand peak ran as a broad band, but a portion of the protein from the right hand peak ran as a sharp band (indicated with an arrow).

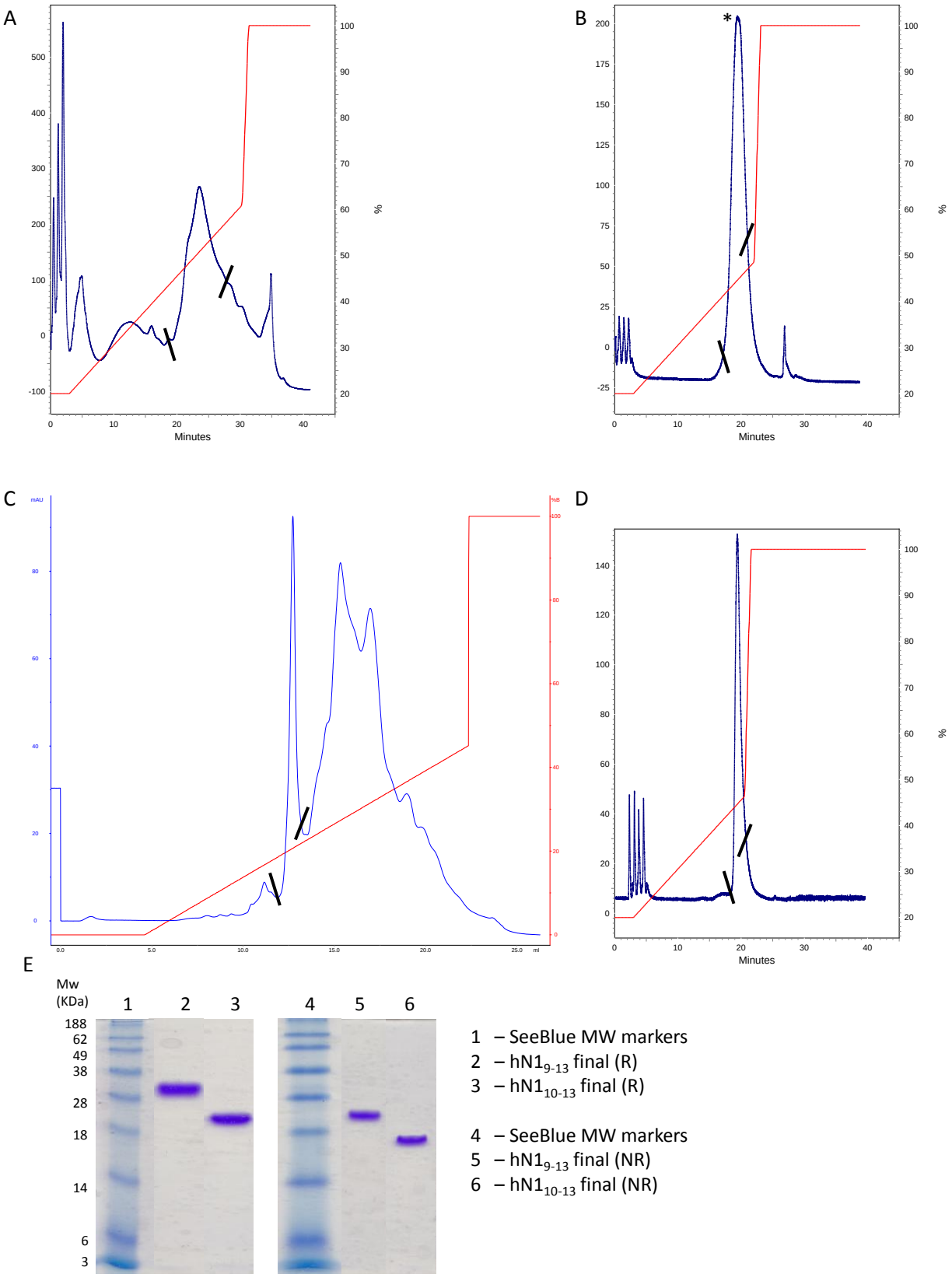


Figure 3-11 Purification of hN1$_{9-13}$ BirA WT. A) HPLC of reduced hN1$_{9-13}$. B) HPLC of hN1$_{9-13}$ after refold. The asterisk indicates a particularly broad peak, which was separated into two separate fractions. C) MonoQ FPLC purification. D) Final HPLC pufication. The fractions collected are indicated by the black lines. E) Gel to show final products for hN1$_{9-13}$ and hN1$_{10-13}$.

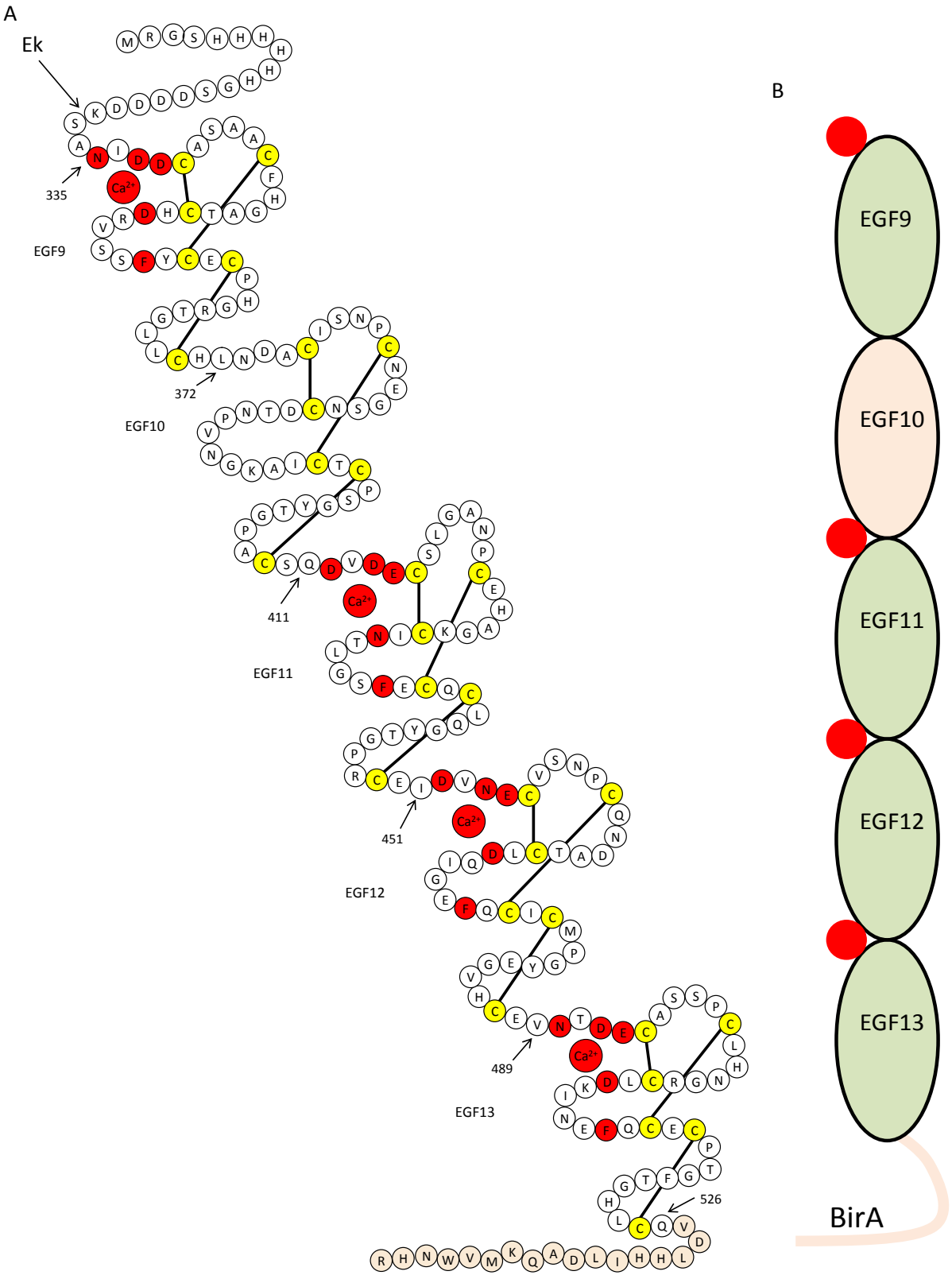


Figure 3-12 Diagram to show the amino acid sequence and domain organisation of hN1$_{9-13}$. A) EGF9 contains the calcium binding consensus. B) The domain organisation of hN1$_{9-13}$. Residue numbers indicating the start of each domain are indicated.

3.6 Production of dN_{11-13} WT and mutant proteins

The region of the *Drosophila* Notch protein spanning EGF domains 11-13 and containing a C-terminal BirA tag (dN_{11-13}) was made in order to investigate whether this protein was able to bind to Serrate in the absence of sugars. This construct was initially cloned and characterised by Shaoyan Liang. This protein contains three EGF domains that contain the calcium binding consensus, and each domain has been found to bind calcium. A schematic diagram to indicate the domain organisation and amino acid sequence of dN_{11-13} is shown below (Figure 3-13). The *Drosophila* protein refolded well using the same refold conditions as its human counterpart, and was purified by HPLC and FPLC following the same protocol as for $hN1_{11-13}$ (Figure 3-14). The products of the purification were visualised on a 16% SDS-PAGE gel.

Several amino acid substitutions were made in the central β-sheet in EGF12 of dNotch, in order to replicate the binding experiments performed with the equivalent human proteins. These mutations were produced using the Lightning Mutagenesis kit, and after transformation into XL10 gold ultracompetent cells the DNA was sequenced by automated sequencing. Each of these mutants were expressed and purified using the same protocol as for dN_{11-13} WT. The final products were visualised on a 16% SDS-PAGE gel, and were found to be indistinguishable from the WT protein. Each protein was analysed by mass spectroscopy to confirm that the correct amino acid substitution was present and that the 6 x His tag had been successfully removed, and were found to differ by only a few Daltons from the expected molecular weight (Table 3-2).

Table 3-2

Protein	Predicted mass (Da)	Actual mass – ESI-MS (Da)
$dN1_{11-13}$ WT	14,737	14738
$dN1_{11-13}$ S502A	14,721	14,724
$dN1_{11-13}$ L504A*	14,877	14,878
$dN1_{11-13}$ D506A*	14,875	14,876

*Denotes proteins were enriched with ^{15}N

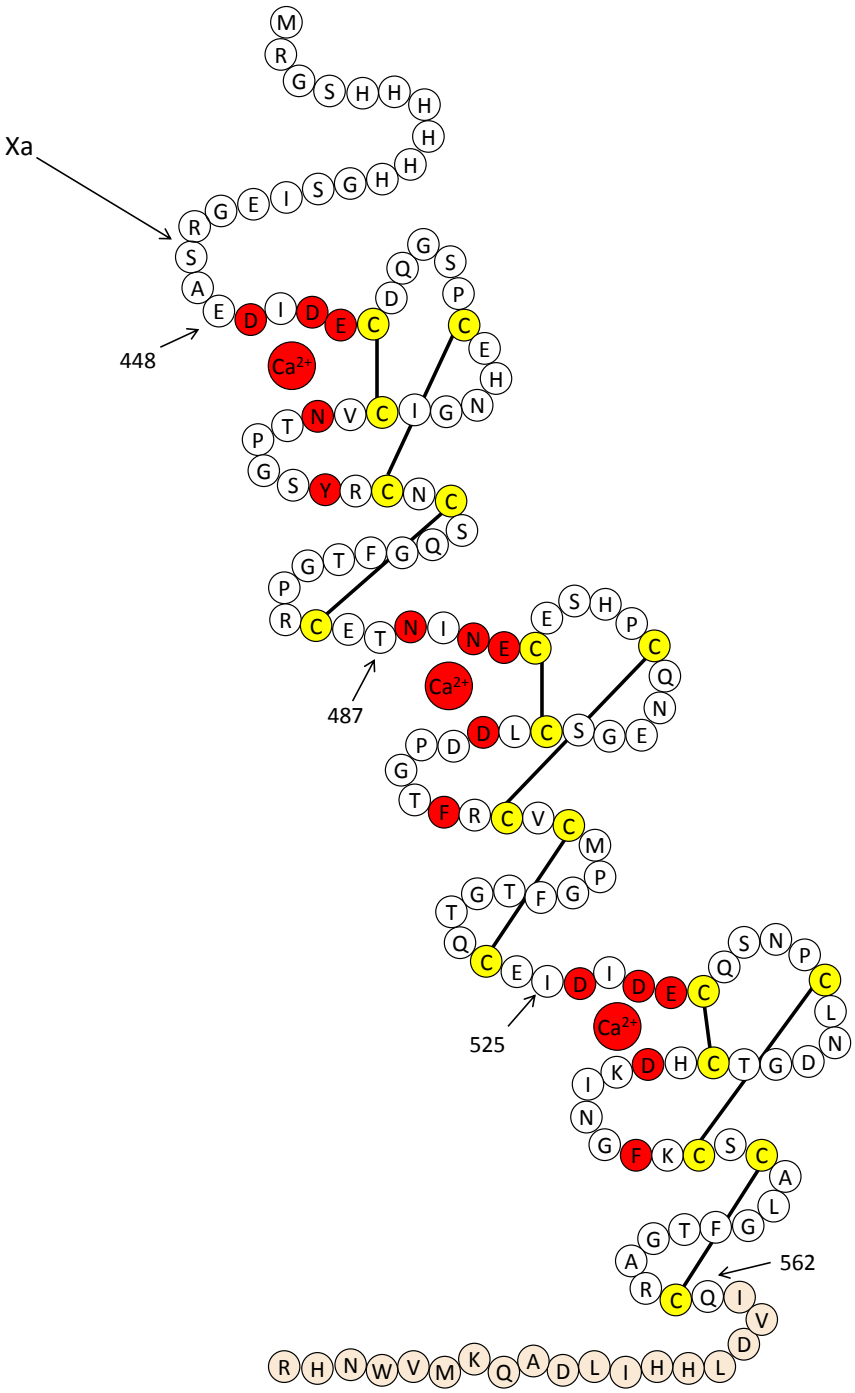


Figure 3-13 Diagram to show the amino acid sequence and domain organisation of dN1$_{11-13}$. The three EGF domains from dN1$_{11-13}$ all contain the calcium binding consensus. The C-terminal BirA tag allows for site-specific biotinylation.

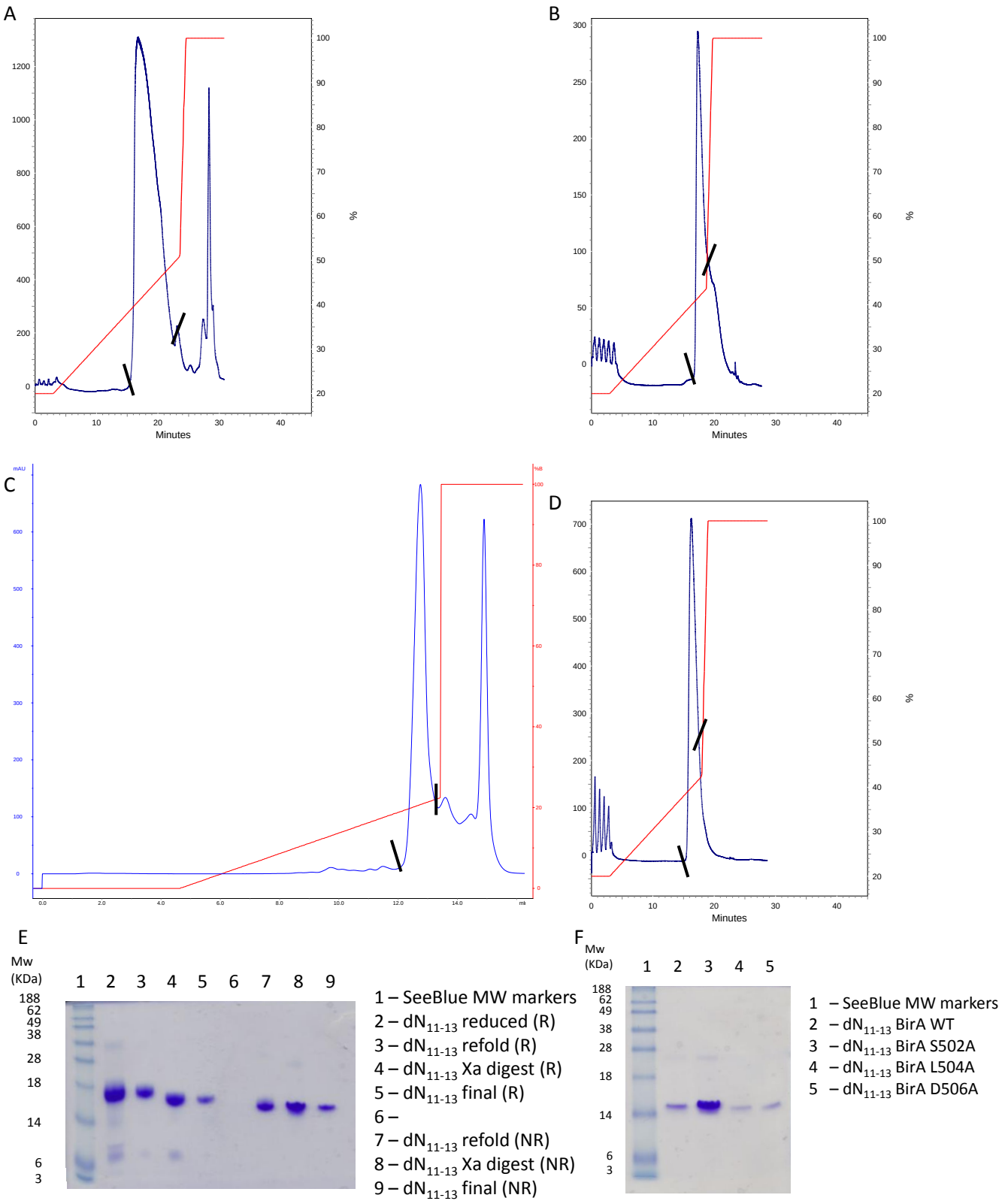


Figure 3-14 Purification of dN_{11-13} BirA proteins. A) HPLC of reduced dN_{11-13}. B) HPLC of dN_{11-13} after refold. C) MonoQ FPLC purification. D) Final HPLC pufication. The fractions collected are indicated by the black lines. E) Gel to follow purification of dN_{11-13}. F) Gel to show the final purification products for each of the mutants used in Chapters 4 and 5. Each protein was loaded in non-reducing buffer.

3.7 Production of eukaryotic proteins

A hJagged1-Fc fusion protein containing the MNNL domain N-terminal the DSL domain (hJagged1 MNNL-EGF3 Fc), and a series of longer hNotch1 proteins ranging from $hN1_{11-14}$ to $hN1_{3-14}$ containing a C-terminal AVI tag were produced to investigate how these domains might contribute to the Notch-ligand binding interaction (Figure 3-15).

The expression plasmids used for eukaryotic protein expression were based on the modified pLEXm eukaryotic expression plasmid (Aricescu *et al.*, 2006) (Figure 3-18) but were modified to contain the Ig κ-chain leader sequence from the pSecTag eukaryotic expression vector (Invitrogen) for secretion:

```
        M  E  T  D  T  L  L  L  W  V  L  L  L  W  V  P  G  S  T  G  D  E  F
GCCACCATGGAGACAGACACACTCCTGCTATGGGTACTGCTGCTCTGGGTTCCAGGTTCCACTGGTGACGAATTCGACGCC
Kozak                                                                 EcoRI
```

The hJagged1 protein was produced for immobilisation in an SPR assay, and each of the hNotch1 proteins was biotinylated so that they could be immobilised on avidin coated beads and their binding to the various Notch ligands could be investigated in a flow cytometry assay. HEK 293T cells were used for all eukaryotic protein production. These cells are HEK 293 cells that have been modified to contain the SV40 T-antigen that allows for plasmids containing a SV40 origin of replication to be replicated episomally, thereby increasing the life-span of the plasmid within the cells. It was necessary to use a eukaryotic expression system to produce these proteins as it is unlikely that either the Fc tag or the MNNL domain in the hJagged1 protein would fold correctly via *in vitro* refolding The *in vitro* refolding method outlined above also has an upper limit on the size of protein that can successfully be refolded, beyond which the yield from the refold decreases and the difficulty in separating and analysing the correctly folded protein increases. There is some evidence of this limit being approached in the production of $hN1_{9-13}$, which only contains 5 EGF domains, so it would not be feasible to use this method to produce the longer hNotch1 proteins containing up to 12 domains.

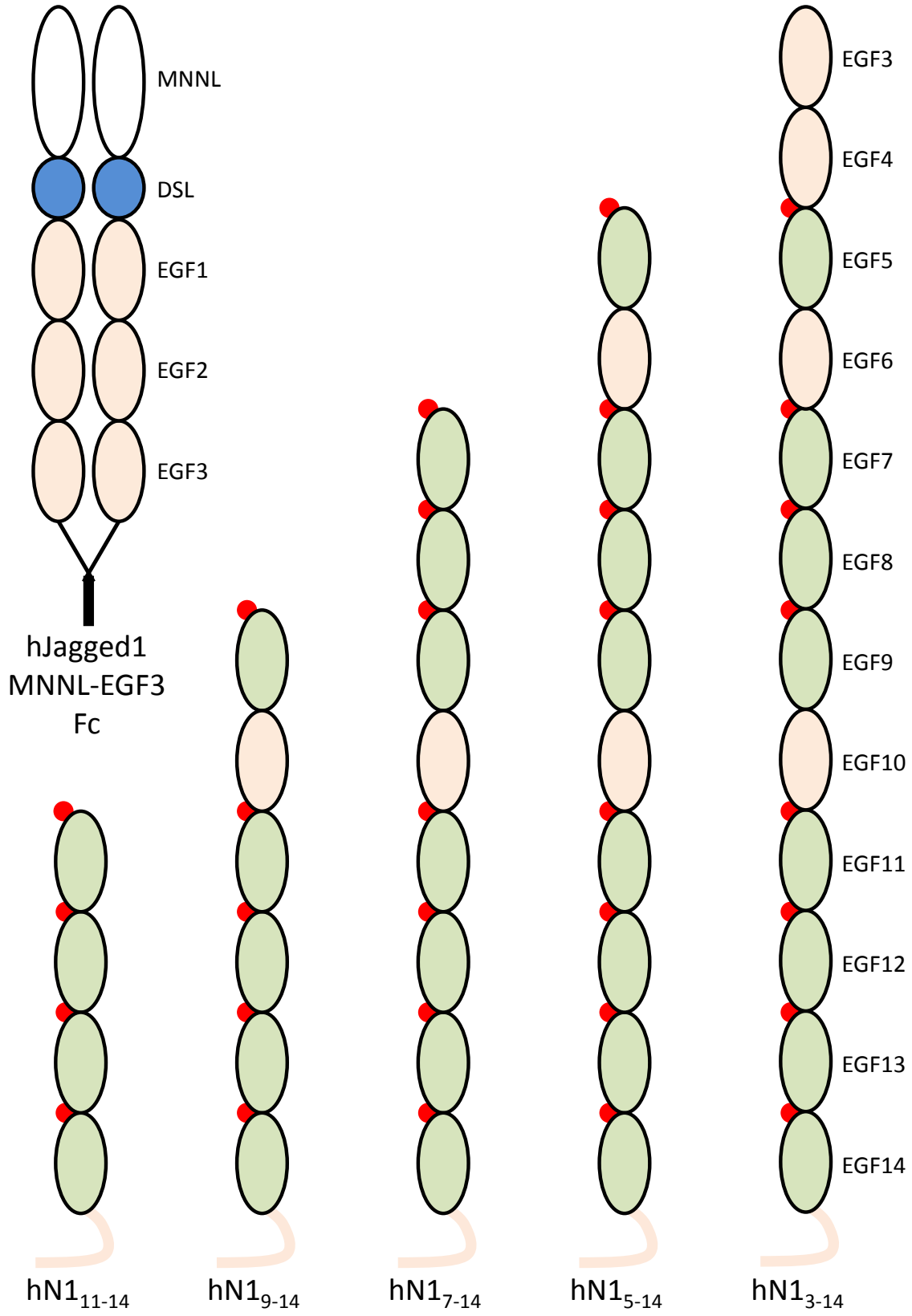


Figure 3-15 Domain organisation of eukaryotic constructs. cbEGF domains are shown in green, EGF domains are shown in beige. Calcium ions are shown as red circles. Each Notch protein contains a C-terminal AVI tag to allow site-specific biotinylation. The MNNL from hJagged1 is shown in white, the DSL domain in blue, and the Fc tag in black.

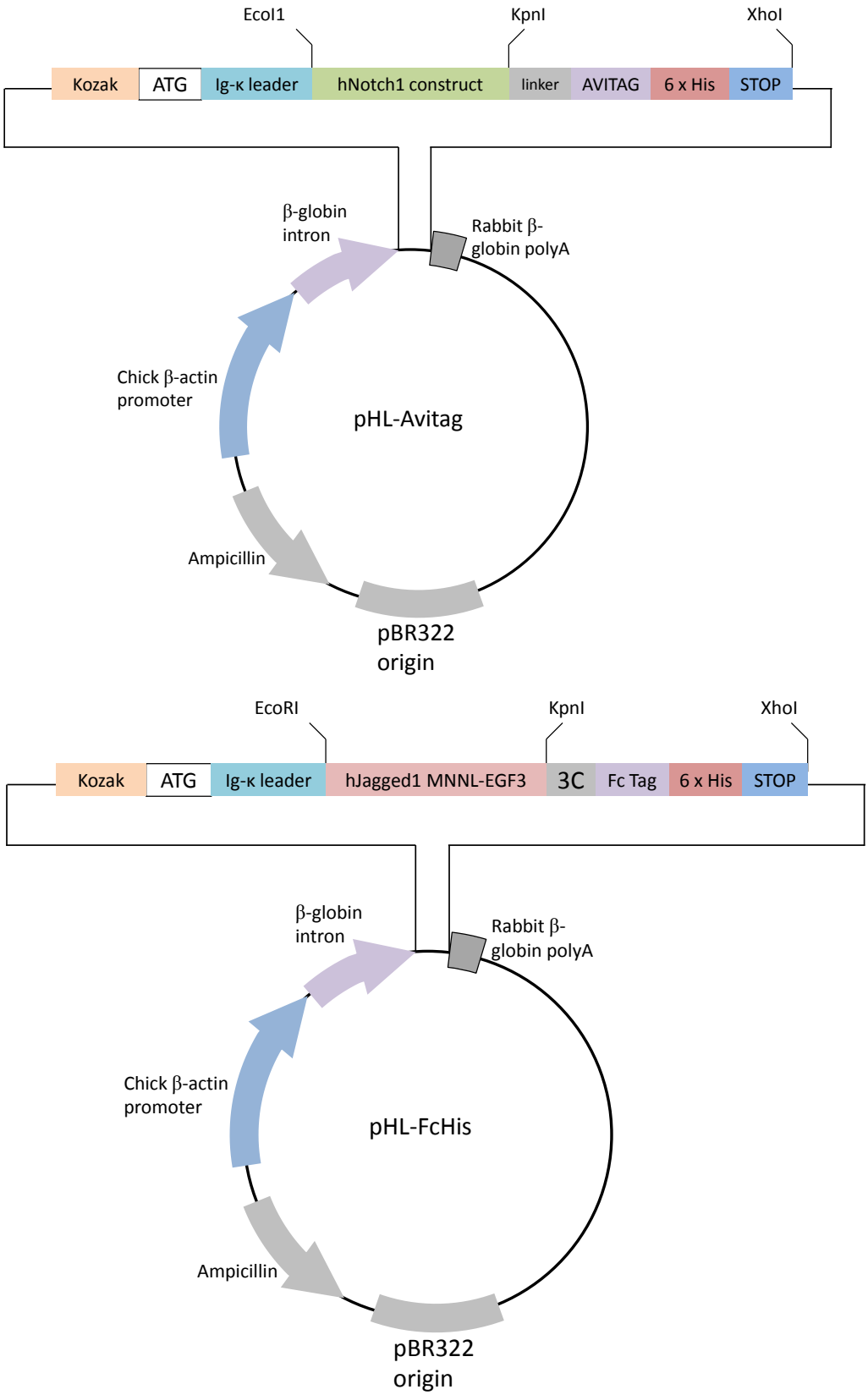


Figure 3-16 Plasmid maps of the pHL-Avitag and pHL-FcHis eukaryotic expression vectors. Eukaryotic expression was performed using these plasmids, which are modified versions of the pLEXm vector.

3.7.1 Production of hNotch1 proteins

The Notch1 constructs had previously been cloned into the pHL-FcHis vector by Dr Chandramouli Chillakuri. In order to replace the C-terminal Fc tag with a peptide sequence suitable to biotinylation, a pair of complementary primers were designed containing the Avitag-His oligo sequence:

```
  G  T  G  G  S  G  G  L  N  D  I  F  E  A  Q  K  I  E  W  H  E  G  K
5'    CGGAGGTTCCGGTGGTCTGAATGATATCTTTGAAGCTCAGAAGATTGAATGGCATGAAGGAAAG
3'CATGGCCTCCAAGGCCACCAGACTTACTATAGAAACTTCGAGTCTTCTAACTTACCGTACTTCCTTTC
   KpnI

 H  H  H  H  H  H  X  X
CACCACCATCACCATCACTAATGAC    3'
GTGGTGGTAGTGGTAGTGATTACTGAGCT5'
      6 x His        STOP  XhoI
```

These primers were dissolved to a final concentration of 200 nM, mixed together and heated to 95°C, before being allowed to cool slowly. This produces double-stranded DNA, with appropriate overhanging 5' and 3' sequences for insertion into a vector containing complementary sequences. The Fc tag was excised from the pHL-FcHis plasmids containing the Notch constructs by digestion with the KpnI and XhoI restriction enzymes, and the Avitag-His oligo sequence was inserted using the Rapid Ligation technique (see Section 2.1.5) to produce the modified pHL-Avitag vector.

Conditioned medium was collected three days after transfection, and filtered with a 0.22 μm filter in order to remove cell debris from the medium. The protein was first purified by nickel column using a batch purification method, before concentration to <500 μl and purification on a S200 Superdex column using buffer containing 200 mM NaCl, 1 mM $CaCl_2$, 50 mM Tris-HCl pH 7.5. Fractions from each of the peaks were collected and analysed on a SDS-PAGE gel. As multiple peaks were collected for each protein, it was necessary to establish which peak contained the hNotch1 protein of interest. This was performed by Western Blot for a small sample of each peak for each protein, using a polyclonal 6 x His peroxidase conjugate to detect the His-tagged proteins (not shown). The hNotch1 proteins were found to elute according to size – $hN1_{11-14}$ elutes significantly later than $hN1_{3-14}$, due to its much smaller size (Figure 3-18).

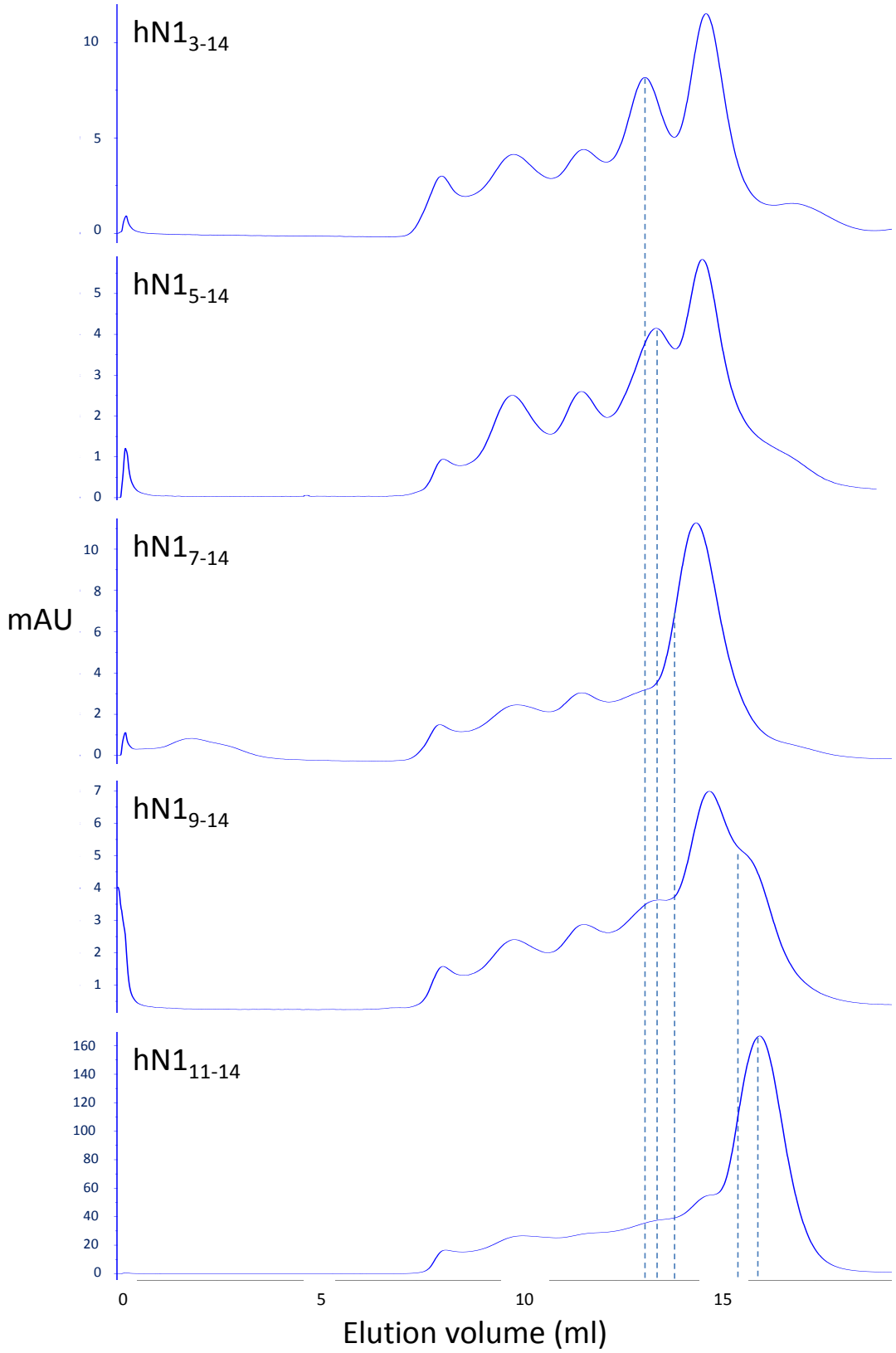


Figure 3-18 S200 Superdex elution profiles for the eukaryotic hNotch1 constructs. The indicated peaks represent the respective hNotch1 proteins, as determined by Western Blot.

3.7.2 Production of hJagged1 MNNL-EGF3-Fc

Conditioned medium was prepared in a similar manner to the hNotch1 constructs. Protein was purified by nickel column and S200 column in buffer containing 200 mM NaCl, 50 mM Tris-HCl pH 9.0.

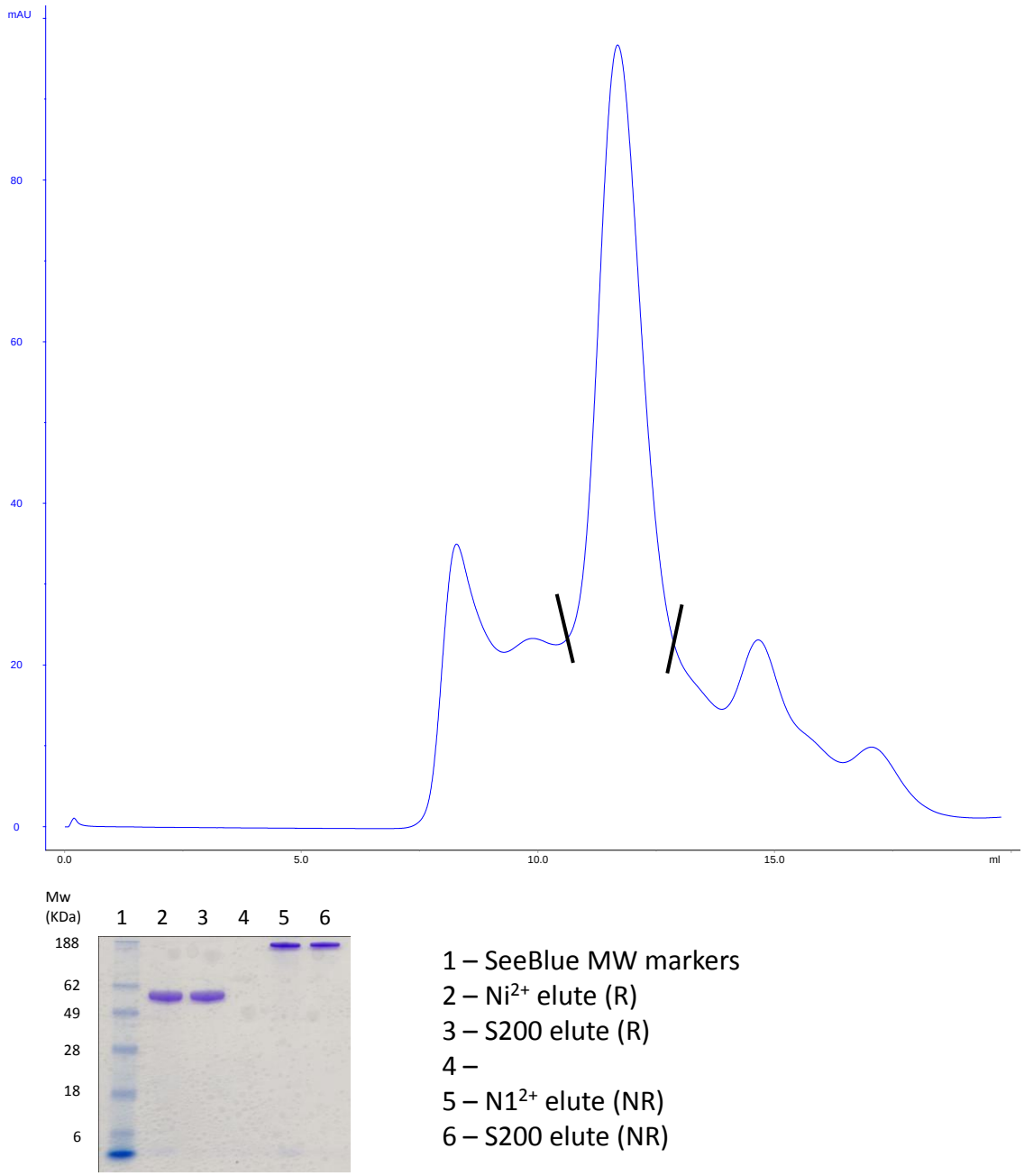


Figure 3-19 S200 purification of hJagged1 MNNL-EGF3 Fc. A) Elution of protein from S200 Superdex column. The fraction collected is indicated by the black lines. B) 12 % SDS-PAGE gel to confirm purification of the protein. Samples run under reducing conditions (lanes 2-3, marked 'R') run as monomers, whereas samples run under non-reducing conditions (lanes 5-6, marked 'NR') run as monomers, due to the Fc tag.

3.8 Production of Serrate-GFP fusion protein

In order to study the interaction between Serrate and dNotch, it was necessary to create a Serrate-GFP fusion protein so that transfected cells could be distinguished from untransfected cells. In order to do this, a triple-overlap PCR method was employed to insert the gene for GFP at the 3' end of the *Drosophila Serrate* gene within the pUAST plasmid. The desired sequence containing the GFP insert was achieved through 2 separate rounds of PCR.

The DNA sequence of the *Serrate* gene within the pUAST plasmid was already known, and unique restriction sites approximately 2 kb apart were identified so that the DNA template generated by PCR could be re-inserted into the plasmid. A SfiI site towards the 3' end of the *Serrate* gene, and a XhoI site from within the polylinker sequence of the pUAST plasmid were selected, and primers were designed that were complementary to these regions. Further primers were designed that contained regions complementary to *Serrate* and *eGFP* in order to generate three separate DNA fragments (see Appendix A). These fragments were combined in a further PCR reaction in order to generate the final DNA sequence (Figure 3-22) that was then digested with the appropriate restriction enzymes and ligated into the pUAST plasmid containing complementary sticky ends.

- Reaction 1 uses primers 1 & 6 to generate the DNA sequence from the 3' end of *Serrate*, with a 5' SfiI restriction site and a short (approximately 20 bases) 3' region that is complementary to the DNA from eGFP.
- Reaction 2 uses primers 3 & 4 to generate the DNA sequence from pUAST, with a 3' XhoI restriction site and a 5' region complementary to eGFP.
- Reaction 3 uses primers 2 & 5 to generate the DNA for eGFP, with 5' and 3' regions complementary to the products of reactions 1 and 3 respectively.
- Reaction 4 combines the fragments from reactions 1-3 along with the forward primer from reaction 1 and the reverse primer from reaction 3, in order to generate the Serrate-GFP fusion with the appropriate restriction sites.

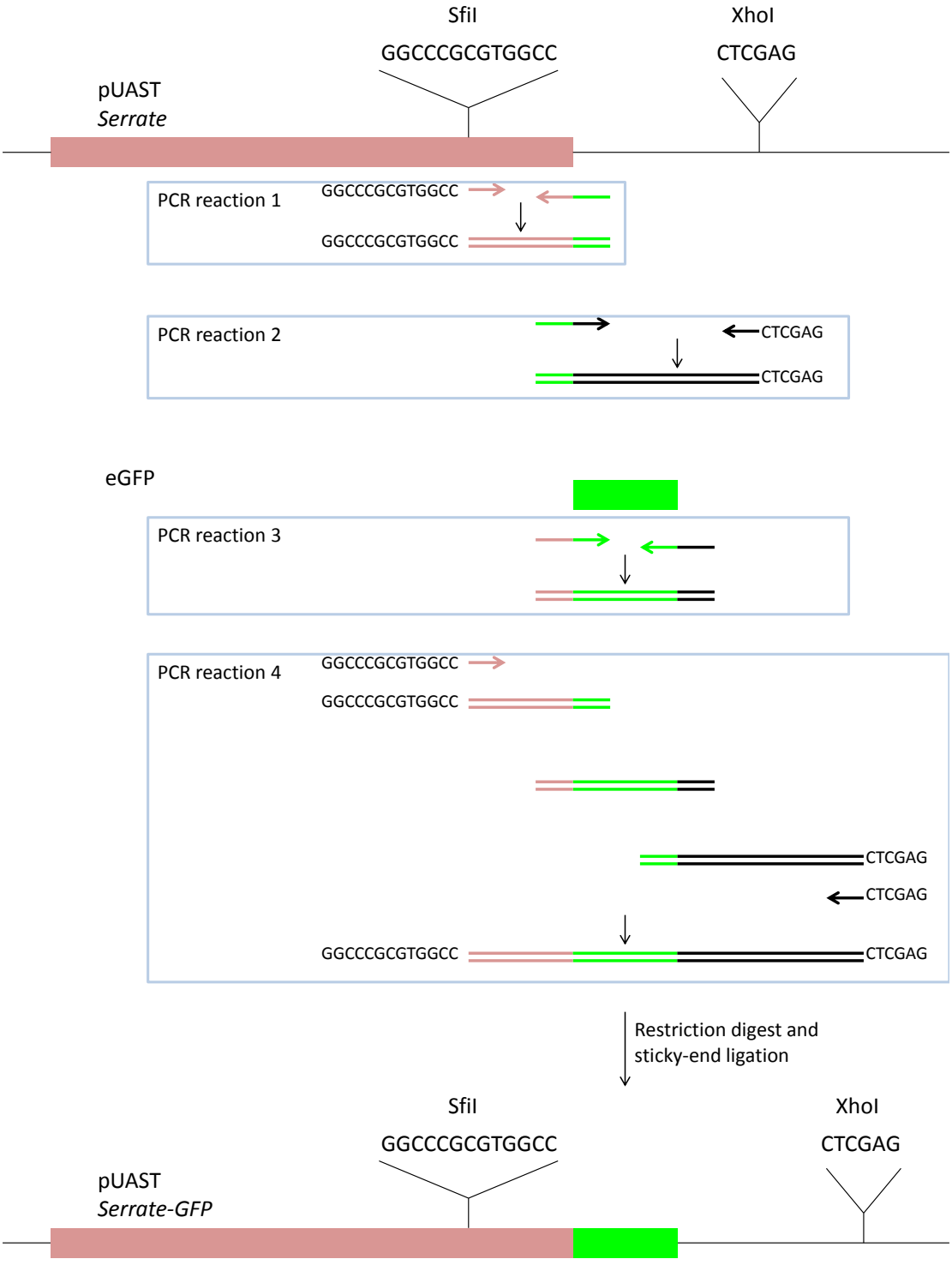


Figure 3-20 Cloning the* Serrate-GFP *construct for use in flow cytometry experiments. Serrate-GFP was produced using a triple overlap PCR method. The *Serrate* gene is shown in brown, the *eGFP* gene is shown in green. DNA from the plasmid is shown in black. Two rounds of PCR generated the DNA template, which was then cut and re-ligated into the pUAST plasmid.

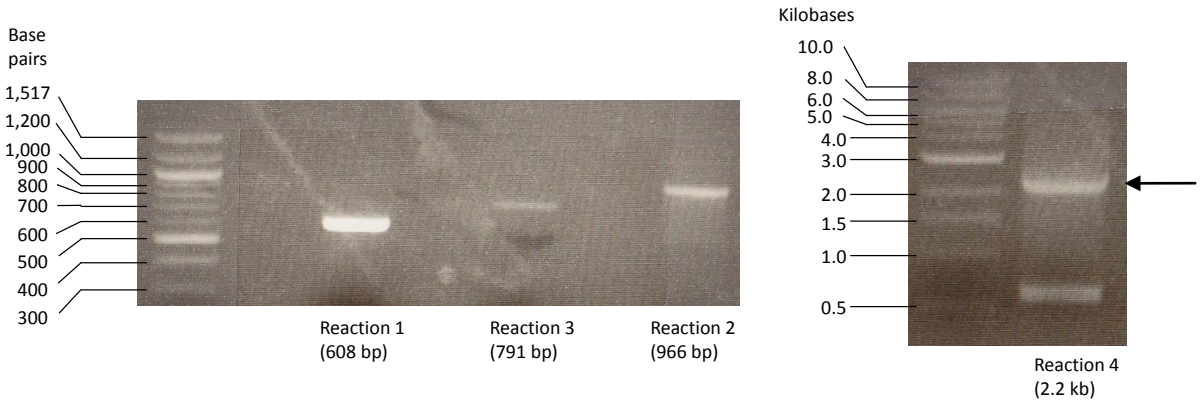


Figure 3-21 Agarose gels to visualise products from triple overlap PCR reactions. A) A small sample of each of the products from the first round of PCR reactions was run on a 1.2% TBE agarose gel to visualise the size of the products. B) The product of PCR reaction 4 was visualised on a 0.7% TBE agarose gel to confirm the correct size DNA fragment had been produced.

A small portion of the products from each of the individual PCR reactions was visualised on an agarose gel to confirm that the correct size fragments had been produced (Figure 3-23). The remainder of the PCR reaction run on a 1.2% TAE agarose gel, and bands were excised with a sharp scalpel and purified using the Qiagen Gel Extraction kit. The products were pooled, and the appropriate primers were added for the second round PCR reaction. Once the longer fragment was generated, sticky ends were generated by cutting with SfiI and XhoI. The vector containing the *Serrate* gene was also cut with the same enzymes in order to remove the equivalent portion of DNA. The insert was ligated into the vector and the sequence was confirmed by automated sequencing.

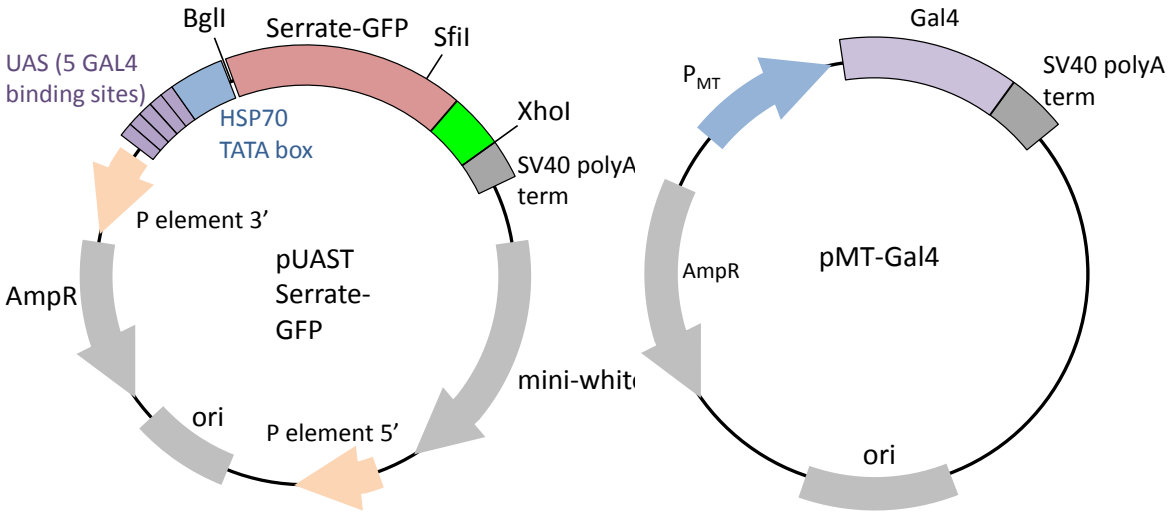


Figure 3-22 Plasmid maps for pUAST Serrate-GFP and pMT-Gal4. The pMT plasmid contains the metallothionein promoter that is inducible by Cu^{2+} ions. This leads to the expression of the Gal4 protein, which is able to bind to the UAS regions upstream of the Serrate-GFP gene in the pUAST plasmid and induce gene expression.

Chapter 4

Identifying the ligand binding site in Notch1

4.1 Introduction

EGF domains 11-12 of the *Drosophila* Notch receptor (dNotch) have been shown to be necessary and sufficient for ligand binding in a cell aggregation study (see Section 1.5.2). A series of single amino acid substitutions that eliminated calcium binding to individual domains of the human Notch receptor further defined the location of the main ligand binding site. A D469G substitution in the calcium binding consensus sequence of EGF12 of human Notch1 (hNotch1) within the context of a construct containing EGFs 11-14 completely eliminated binding to CHO cells expressing the full length ligand Delta-like ligand 1 (DLL1) in a flow cytometry assay whereas eliminating calcium binding in domains 11 or 13 had a negligible effect on ligand binding (Cordle *et al.*, 2008b). The previously described N^{M1} mutation in dNotch which causes a hypomorphic Notch allele (E491V substitution in EGF12) is likely to have a similar effect on ligand binding as this residue, equivalent to E455 in hNotch1 is predicted to be involved in calcium binding.

Initial attempts to identify the structural basis of the Notch1-ligand interaction hinted that two residues (V453 and G472) within EGF12 might be involved in ligand binding (Cordle *et al.*, 2008a). In an HSQC titration series, these residues showed the largest reduction in signal intensity upon the addition of a human Jagged1 construct containing the domains DSL-EGF3 to a ^{15}N-labelled hNotch1 construct containing EGFs 11-13 ($hN1_{11-13}$). As these residues lie on the same face of the $hN1_{11-13}$ structure, it was initially thought that they might form part of a ligand binding site, and the $hN1_{11-13}$ – hJagged1 DSL-EGF3 complex was subsequently modelled using these residues as input parameters.

This docking simulation suggested that these two molecules might be able to interact via the same residues in EGF12 of hN1 and the DSL domain of hJagged1 but in two different orientations – parallel and anti-parallel. It is not clear whether or not both orientations may exist *in vivo*, and might represent the *cis*-inhibition and *trans*-activating complexes. However, it is possible that the same orientation may be able to fulfil both roles *in vivo*. As there are little direct biochemical binding data for which residues within $hN1_{11-13}$ are involved in binding, these docking simulations may be

premature in attempting to model this interaction. For instance, the Q442A substitution was made in order to attempt to validate this docking model, but was found to have no effect on binding (Dr Joyce Tay unpublished data). Further attempts to model the Notch-ligand interaction have been carried out (Majumder *et al.*, 2012), but these have relied on using the same amino acids as the input parameters for docking, and therefore are subject to the same limitations as the original docking model.

The aim of this chapter is to identify the region on the surface of the Notch receptor that is involved in ligand binding. This was performed using site-directed mutagenesis, with a view to building a new model for how the minimal binding regions of Notch and its ligands might interact at a molecular level. The effect of the different amino acid substitutions on binding was tested in a flow-cytometry assay using cells expressing different full length ligands. Each substitution that led to a reduction in ligand binding was subsequently confirmed to act directly and not affect protein folding, or affect the ability of EGF12 to bind calcium.

4.2 The target region for mutagenesis

Mutagenesis was performed within the context of a construct containing domains 11-13 of the human Notch1 receptor, with a 15 amino acid BirA peptide at its C-terminus that allows for site-specific biotinylation. This construct has previously been shown to interact specifically with CHO cells expressing full length DLL1 when it is multimerised on the surface of avidin-coated beads (Cordle *et al.*, 2008b).

A series of amino acids in EGF12 were targeted for mutagenesis on the basis of sequence homology, as it is reasonable to expect that the residues within the Notch receptor that are essential for ligand binding would be highly conserved, as is the case for the Notch binding residues within the DSL domain of the ligands (Cordle *et al.*, 2008a). The amino acid sequences of the ligand binding domain from the Notch1 receptor from several different species were aligned, together with the four human isoforms of the Notch receptor (Figure 4-1). When selecting mutagenesis targets, it was important to

exclude residues that are required for a cbEGF to fold properly, and those involved in calcium binding (see Section 1.4.2).

The six cysteine residues that are required to ensure the correct 1-3, 2-4, 5-6 disulphide binding pattern within an EGF domain must be maintained, as C→X substitutions are known to cause EGF domains to fold incorrectly, as demonstrated by a number of reported mutations in hNotch3 and fibrillin1 that are associated with CADASIL and Marfan Syndrome (a hereditary disease associated with improper incorporation of fibrillin into microfibrils) respectively. In addition to this, a number of residues that are essential for inter-domain packing interactions between tandem EGF repeats were avoided. In EGF 12 these are I471 (which packs against Y444 in EGF11), and Y482 (which packs against I509 in EGF13) (see Section 1.5.2).

The residues L468 and M479 were initially targeted for mutagenesis in an earlier study (Handford lab, unpublished data). These residues are very highly conserved across species and across human Notch isoforms (Figure 4-1). The L468A substitution was found to knock out binding to CHO cells expressing full-length DLL1, whereas the M479A substitution bound cells as well as WT (Handford lab, unpublished data).

Based on these initial experiments, a second set of residues was selected for mutagenesis. As the L468 residue is located on the central β-hairpin within EGF12 (Cordle *et al.*, 2008a), the other resides that lie on the same face of the β-hairpin were selected for mutagenesis. The residues T466, Q470, E473, Q475 and I477 were all substituted with alanine, and the effects of these substitutions was tested for binding to different ligands in a similar flow cytometry assay.

A

```
                                          *  *  *   *  *  *  *
D. melanogaster   487 TNINECESHPCQNEGSCLDDPGTFRCVCMPGFTGTQCE 524

hNotch1           451 IDVNECVSNPCQNDATCLDQIGEFQCICMPGYEGVHCE 488
Pan troglodytes   451 IDVNECVSNPCQNDATCLDQIGEFQCICMPGYEGVHCE 488
Bos taurus        365 IDVNECVSNPCQNDATCLDQIGEFQCICMPGYEGLHCE 402
Canis familiaris  438 IDVNECISNPCQNDATCLDQIGEFQCICMPGYEGVHCE 475
Mus musculus      451 IDVNECISNPCQNDATCLDQIGEFQCICMPGYEGVYCE 488
Gallus gallus     447 IDVNECLSNPCQNDATCLDQIGEFQCICMPGYEGVYCE 484
Xenopus laevis    450 IDVNECLSNPCQNDSTCLDQIGEFQCICMPGYEGLYCE 487
Danio rerio       471 LDINECLSTPCQNDATCLDQIGGFHCICMPGYEGVFCQ 508

hNotch2           455 MDINECHSDPCQNDATCLDKIGGFTCLCMPGFKGVHCE 492
hNotch3           430 TDVNECLSGPCRNQATCLDRIGQFTCICMAGFTGTYCE 467
hNotch4           474 ADHNECLSQPCHPGSTCLDLLATFHCLCPPGLEGQLCE 511
```

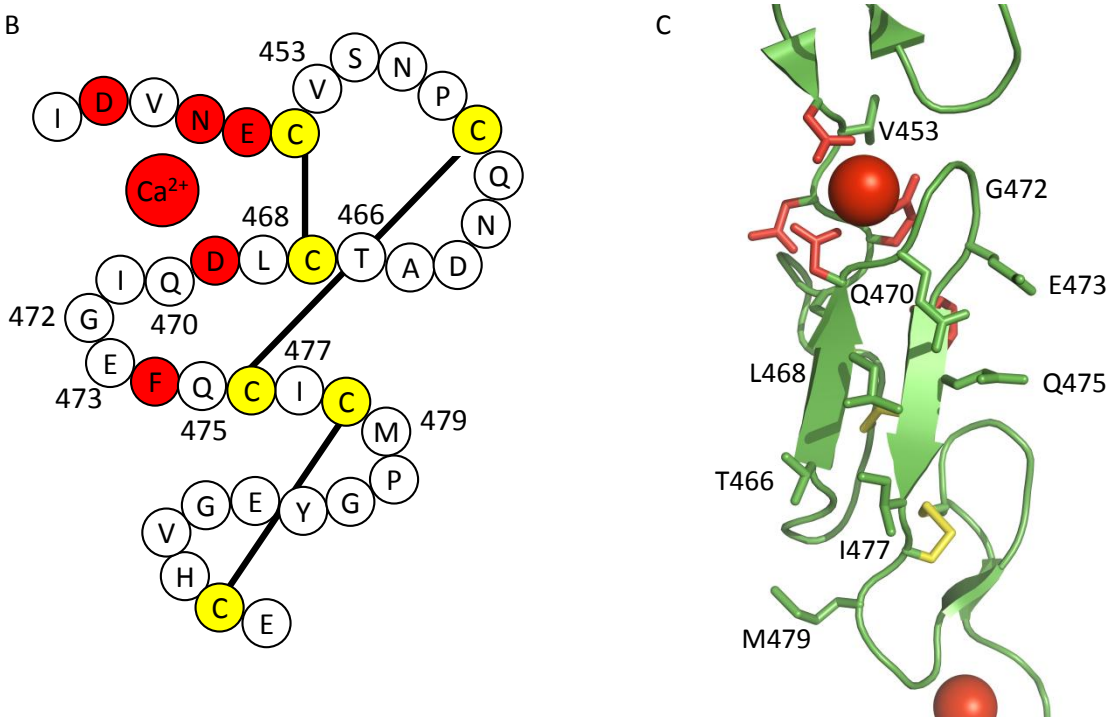


Figure 4-1 The region of the Notch receptor selected for mutagenesis. A) Sequence alignment of EGF12 from dNotch and Notch1 from various species shows that a number of residues are highly conserved. Calcium binding residues are highlighted in grey, cysteine residues are highlighted in black. Residues initially selected for mutagenesis are indicated by a black asterisk and other residues selected for mutagenesis are indicated with a red asterisk. B) Schematic diagram of EGF12 from hNotch1, indicating the positions of the residues selected for mutagenesis. C) The residues selected in this study are all located on the same face of the β-hairpin, whereas the residues V453 and G472 are located on a separate face of the EGF. Residues required to bind calcium are indicated in red.

4.3 Assaying $hN1_{11-13}$ mutant binding by flow cytometry

4.3.1 The flow cytometry assay

Following purification (see Chapter 3) each $hN1_{11-13}$ mutant protein was biotinylated via its C-terminal BirA tag, which enabled the protein to be immobilised and multimerised on the surface of purple fluorescent beads coated with avidin (Figure 4-2). Clustering the protein on the surface of beads allows multiple individual Notch-ligand binding interactions to take place between the immobilised proteins and the ligand on the cell surface. This increases the avidity of the interaction, leading to an apparent increase in the affinity, and allows the beads to bind to the cells. As the beads are fluorescent (λ_{ex} 488 nm, λ_{em} 680 nm), binding of the beads to the cells can be detected by flow cytometry in the FL3 (λ > 670 nm) channel. Presenting the Notch fragments in this fashion is a reasonable model for how Notch might bind to its ligands at the cell surface, as the interaction takes place in solution, but the orientation of the fragments is fixed relative to each other (the N-termini of both the molecules are distal to the surface on which they are presented).

B16 mouse melanoma cells expressing either full-length mouse Jagged1 (mJagged1) or mouse Delta-like ligand 4 (mDLL4) (courtesy of Prof. Adrian Harris, University of Oxford), or HEK239 cells expressing full length human Jagged1 (hJagged1) (courtesy of Dr Massimo Masiero) were used to investigate how these substitutions affected the ability of $hN1_{11-13}$ to bind to its ligands.

In order to establish the binding assay, a series of controls were put in place. Beads coated with $hN1_{11-13}$ were found not to bind to untransfected cells (Figure 4-2 B), confirming that ligand expression on the cells is required for binding. To check that ligand expressed at the cell surface does not bind the beads in a non-specific manner, beads coated with cbEGFs 12-14 from human fibrillin1 (courtesy of Vroni Knott) that had been purified using a similar protocol as $hN1_{11-13}$ were tested for binding to B16 cells mJagged1 cells (Figure 4-2 C). Fibrillin1 is functionally unrelated to hNotch1, but this fragment has similar overall domain architecture to $hN1_{11-13}$. The fluorescence profile for this interaction is similar to that seen for untransfected cells and $hN1_{11-13}$, indicating no binding.

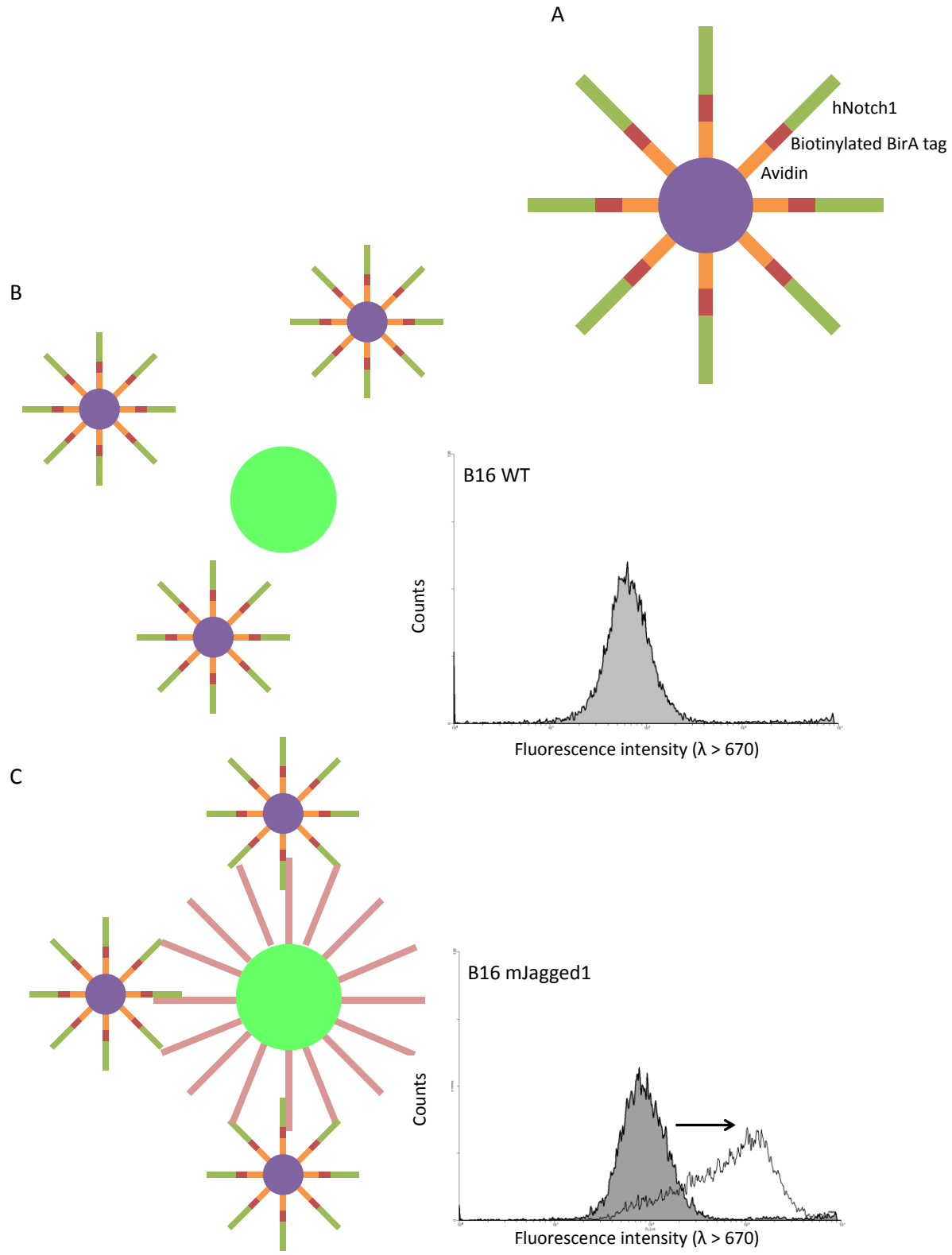


Figure 4-2 Establishing the flow cytometry assay using B16 melanoma cells. A) Notch constructs can be immobilised on the surface of avidin-coated purple fluorescent beads via the C-terminal BirA tag. B) $hN1_{11-13}$ shows no interaction with untransfected cells (green), as indicated by the low fluorescence intensity of the cells (shaded grey). C) Beads coated with $hN1_{11-13}$ bind to B16 cells transfected with mJagged1, as there is a clear rightwards shift which is not seen for the negative control protein fibrillin1 cbEGF12-14 (shaded grey) which corresponds to an increase in fluorescence intensity caused by beads binding to the cells.

$hN1_{11-13}$ WT was used as the positive control for testing the effects of each substitution on binding. Binding of $hN1_{11-13}$ WT to B16 cells transfected with mJagged1 leads to a rightwards shift in the fluorescence profile of the cells (Figure 4-2 C). The fluorescence profiles for the positive and negative control proteins indicate the changes in fluorescence intensity that are associated with binding, and mean that this assay can confidently be used to test the effect that the substitutions introduced into EGF12 have on binding. Each mutant protein was tested for binding in the flow cytometry assay against several different cell lines. The binding of each of the mutant proteins was initially qualitatively compared to both the $hN1_{11-13}$ WT and fibrillin1 cbEGF12-14 control binding profiles, and the relative binding of each of each of the mutant proteins was later compared in a more quantitative analysis (see Section 2.14.3).

In order to be certain that any changes seen in binding are not due to different amounts of protein being loaded onto the beads, a small sample of the resuspended beads was taken before they were incubated with the cells, and the amount of biotinylated protein immobilised on the beads was confirmed by Western blot. This ensures that if no binding is seen for a particular protein, that the protein had been correctly immobilised on the beads, and that any increase in binding was not due to an increase in the amount of protein present. In preliminary experiments, varying the amount of protein mixed with the beads indicated that the beads were saturated with protein for the protocol outlined in Chapter 2, and that for all of the binding experiments the amount of mutant protein was the same as for the WT protein.

4.3.2 Mutant Notch constructs binding to B16 mJagged1 cells

B16 m Jagged1 cells were used initially to assess the effect of the $hN1_{11-13}$ substitutions on binding to Jagged. Mouse Jagged1 has very high homology to human Jagged1, and in particular the face of the DSL domain associated with binding to Notch is entirely conserved between the two species. Therefore any changes in binding seen for the mutants are likely to be representative of the human interaction.

When the panel of mutants was tested for binding against B16 cells expressing mJagged1, several of the substitutions were found to cause a decrease in binding (Figure 4-3). Both the L468A and I477A substitutions reduced binding to a level comparable to the negative control interaction. The T466A substitution led to a significant reduction in binding, but did not completely eliminate it. Both the E473A and Q475A substitutions partially reduced binding, whilst the M479A substitution had no measurable effect on binding. Interestingly, the Q470A caused a small increase in binding. The data shown are representative of the binding interaction – several repeats of the experiment were performed with separate batches of cells and preparations of fluorescent beads.

The differences seen in the binding of each mutant can more clearly be seen when the relative binding of each of the mutant proteins is calculated relative to the binding of $hN1_{11\text{-}13}$ WT (see Section 2.14.3). It was possible to calculate 95% confidence limits for the level of binding observed for each of the mutants (see Section 2.14.4), and directly compare these with the level of binding for the WT interaction, which was defined as 1.

The data show that the T466A, L468A, Q470A, E473A, Q475A and I477A substitutions all altered binding to mJagged1 (Figure 4-3 C). This supports the initial observations made by comparing the flow cytometry profiles for each of the mutant proteins by eye, relative to the positive and negative controls, and suggests that these residues all contribute to binding. It is also important to note that the M479A substitution was indistinguishable to WT when the data was analysed in this way too.

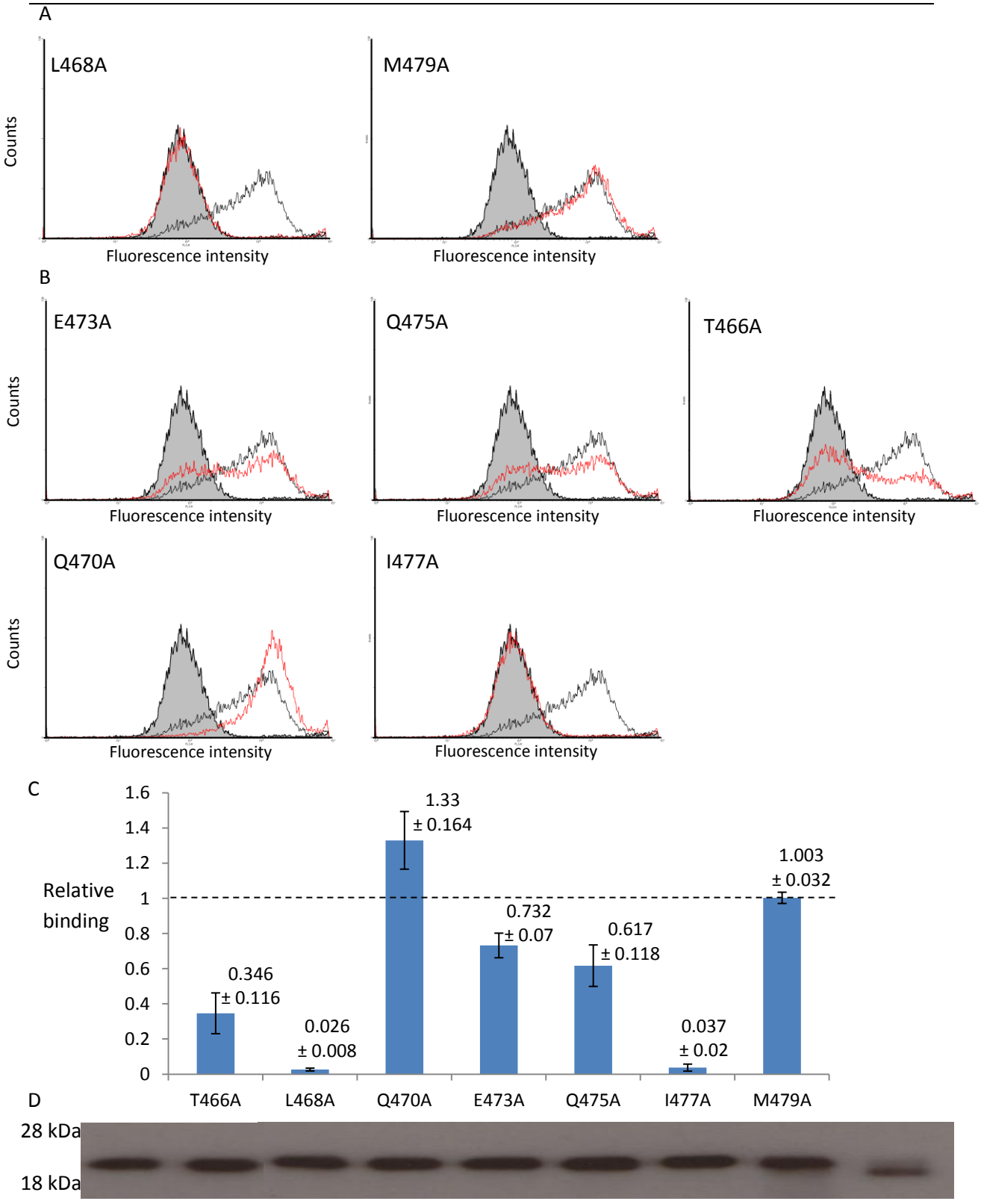


Figure 4-3 Binding of Notch EGF12 mutants to B16 mJagged1 cells. Binding to fibrillin1 cbEGF12-14 is shown in grey, WT in black and each mutant in red. A) The initial binding experiments showed that L468A abrogated binding completely, whereas M497A binds similarly to WT. B) Substituting several other residues with alanine also affected binding, with I477A having a similar effect to L468A. C) Quantitative analysis of the effect of each of these substitutions on binding (n≥3 for each mutant), with mean and 95% confidence limits indicated. D) Western blot to check protein loading – WT (left hand lane), mutant $hN1_{11\text{-}13}$, and fibrillin1 cbEGF 12-14 (right hand lane).

4.3.3 Mutant Notch constructs binding to B16 mDLL4 cells

The effect of each of the substitutions in EGF12 on binding to mDLL4 was tested using a similar assay (Figure 4-4). Binding to B16 mDLL4 cells was measured for each protein, and the same statistical analysis was performed. The results of this show some similarity to the experiments using mJagged1 but the effects of the substitutions are not the same, as only the L468A and I477A substitutions were found to cause a slight by significant reduction in binding. Although there was some variation in the level of binding seen for some of the other mutants, this was not statistically significant.

4.3.4 Mutant Notch constructs binding to HEK 293 Jagged1 cells

In order to confirm that the effects seen in the binding experiments using mJagged1 do not arise from using Jagged1 from a different species, the experiments were repeated using HEK 293 cells hJagged1 cells. Whilst the human and mouse sequences for Jagged1 show a very high degree of sequence conservation (Figure 4-5), there are several amino acids that are not conserved between the two species. It is possible that the changes in binding caused by certain substitutions in section 4.3.2 may have been due to these differences.

When $hN1_{11\text{-}13}$ WT binding to HEK 293 hJagged1 cells was studied via flow cytometry, two populations of cells were visible in the 2-D dot plot for forward scatter (FSC) vs side scatter (SSC) (Figure 4-6 A). The FL3 histogram also showed two distinct populations in the positive control experiment (Figure 4-6 B). It was possible to separate the two populations of cells in the 2-D dot plot into two regions – R1 and R2 – and place a gate around each one. The R1 population of cells corresponds to a low fluorescence peak in the FL3 channel, and the R2 population has a higher level of fluorescence for the positive control interaction (Figure 4.6 C-D). The cause of this is likely to be variation in hJagged1 expression levels, and the cells in the R2 region are likely to be the cells with a higher level of protein on their surface than the R1 cells. SSC is typically a measure of the internal complexity/granularity of cells, so it is possible that the cells in the R2 region might be coated with more beads and hence have a higher SSC value.

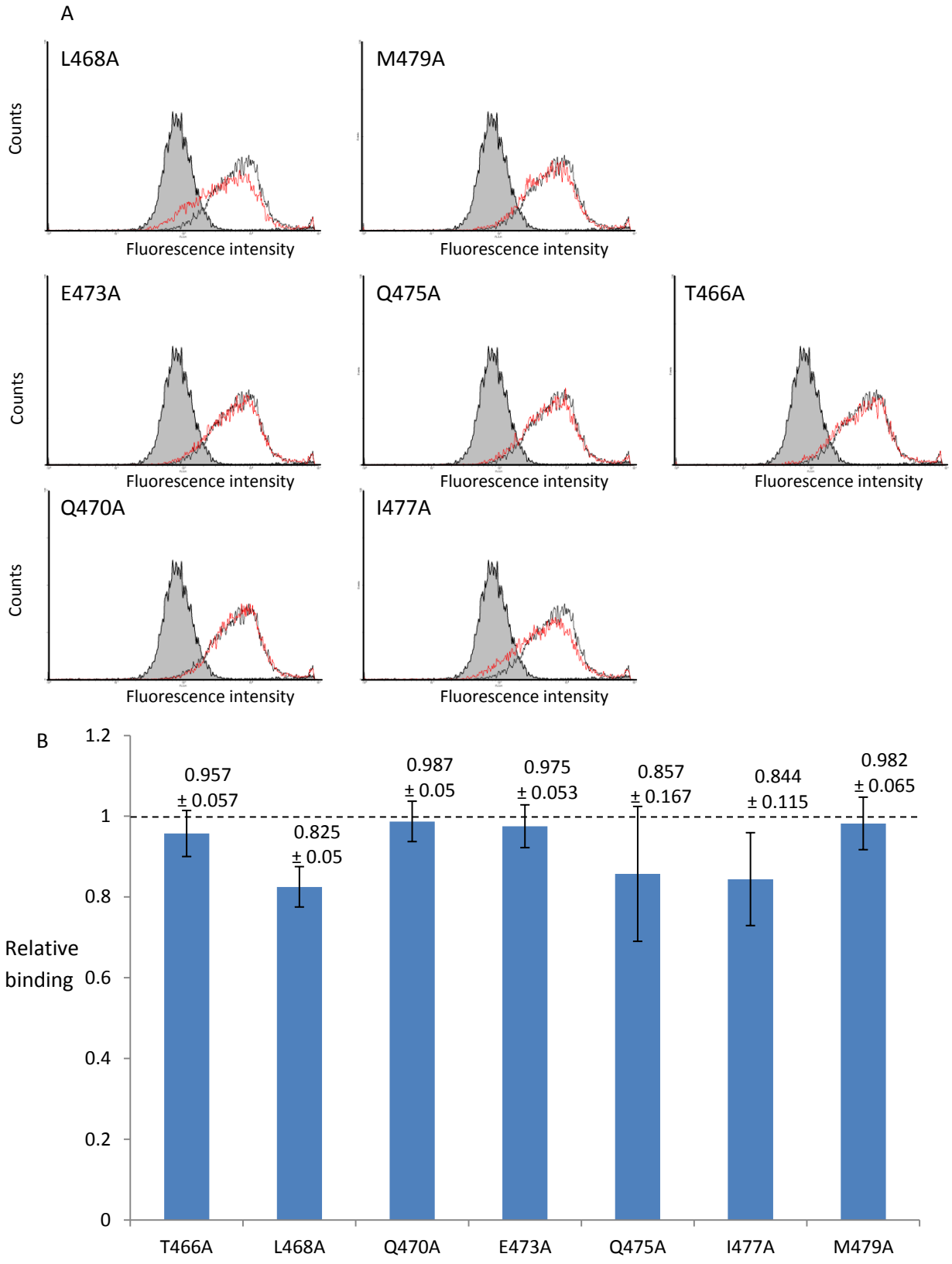


Figure 4-4 Binding of Notch EGF12 mutants to B16 mDLL4 cells. Binding to fibrillin1 cbEGF12-14 is shown in grey, WT in black and mutant in red. A) Mutagenesis in EGF12 shows less marked effects on binding to mDLL4 than mJagged1. B) Quantitative analysis of the effect of each of these substitutions on binding ($n \geq 3$ for each mutant), with mean and 95% confidence limits indicated. There is still some reduction seen in binding to mDLL4 for both the L468A and L477A substitutions.

```
hJagged1        MRSPRTRGRSGRPLSLLLALLCALRAKVCGASGQFELEILSMQNVNGELQNGNCCGGARN 60
mJagged1        MRSPRTRGRPGRPLSLLLALLCALRAKVCGASGQFELEILSMQNVNGELQNGNCCGGVRN 60

hJagged1        PGDRKCTRDECDTYFKVCLKEYQSRVTAGGPCSFGSGSTPVIGGNTFNLKASRGNDRNRI 120
mJagged1        PGDRKCTRDECDTYFKVCLKEYQSRVTAGGPCSFGSGSTPVIGGNTFNLKASRGNDRNRI 120

hJagged1        VLPFSFAWPRSYTLLVEAWDSSNDTVQPDSIIEKASHSGMINPSRQWQTLKQNTGVAHFE 180
mJagged1        VLPFSFAWPRSYTLLVEAWDSSNDTIQPDSIIEKASHSGMINPSRQWQTLKQNTGIAHFE 180

hJagged1        YQIRVTCDDYYYGFGCNKFCRPRDDFFGHYACDQNGNKTCMEGWMGPECNRAICRQGCSP 240
mJagged1        YQIRVTCDDHYYGFGCNKFCRPRDDFFGHYACDQNGNKTCMEGWMGPDCNKAICRQGCSP 240

hJagged1        KHGSCKLPGDCRCQYGWQGLYCDKCIPHPGCVHGICNEPWQCLCETNWGGQLCDKDLNYC 300
mJagged1        KHGSCKLPGDCRCQYGWQGLYCDKCIPHPGCVHGTCNEPWQCLCETNWGGQLCDKDLNYC 300

hJagged1        GTHQPCLNGGTCSNTGPDKYQCSCPEGYSGPNCEIAEHACLSDPCHNRGSCKETSLGFEC 360
mJagged1        GTHQPCLNRGTCSNTGPDKYQCSCPEGYSGPNCEIAEHACLSDPCHNRGSCKETSSGFEC 360

hJagged1        ECSPGWTGPTCSTNIDDCSPNNCSHGGTCQDLVNGFKCVCPPQWTGKTCQLDANECEAKP 420
mJagged1        ECSPGWTGPTCSTNIDDCSPNNCSHGGTCQDLVNGFKCVCPPQWTGKTCQLDANECEAKP 420

hJagged1        CVNAKSCKNLIASYYCDCLPGWMGQNCDININDCLGQCQNDASCRDLVNGYRCICPPGYA 480
mJagged1        CVNARSCKNLIASYYCDCLPGWMGQNCDININDCLGQCQNDASCRDLVNGYRCICPPGYA 480

hJagged1        GDHCERDIDECASNPCLNGGHCQNEINRFQCLCPTGFSGNLCQLDIDYCEPNPCQNGAQC 540
mJagged1        GDHCERDIDECASNPCLNGGHCQNEINRFQCLCPTGFSGNLCQLDIDYCEPNPCQNGAQC 540

hJagged1        YNRASDYFCKCPEDYEGKNCSHLKDHCRTTPCEVIDSCTVAMASNDTPEGVRYISSNVCG 600
mJagged1        YNRASDYFCKCPEDYEGKNCSHLKDHCRTTTCEVIDSCTVAMASNDTPEGVRYISSNVCG 600

hJagged1        PHGKCKSQSGGKFTCDCNKGFTGTYCHENINDCESNPCRNGGTCIDGVNSYKCICSDGWE 660
mJagged1        PHGKCKSQSGGKFTCDCNKGFTGTYCHENINDCESNPCKNGGTCIDGVNSYKCICSDGWE 660

hJagged1        GAYCETNINDCSQNPCHNGGTCRDLVNDFYCDCKNGWKGKTCHSRDSQCDEATCNNGGTC 720
mJagged1        GAHCENNINDCSQNPCHYGGTCRDLVNDFYCDCKNGWKGKTCHSRDSQCDEATCNNGGTC 720

hJagged1        YDEGDAFKCMCPGGWEGTTCNIARNSSCLPNPCHNGGTCVVNGESFTCVCKEGWEGPICA 780
mJagged1        YDEVDTFKCMCPGGWEGTTCNIARNSSCLPNPCHNGGTCVVNGDSFTCVCKEGWEGPICT 780

hJagged1        QNTNDCSPHPCYNSGTCVDGDNWYRCECAPGFAGPDCRININECQSSPCAFGATCVDEIN 840
mJagged1        QNTNDCSPHPCYNSGTCVDGDNWYRCECAPGFAGPDCRININECQSSPCAFGATCVDEIN 840

hJagged1        GYRCVCPPGHSGAKCQE
mJagged1        GYQCICPPGHSGAKCHE
```

Figure 4-5 Sequence alignment of the EGF regions of hJagged1 vs mJagged1. Sequence alignment of the EGF region from hJagged1 and mJagged1 shows that these two proteins have very high sequence homology. There are a handful of relatively conservative differences between these two proteins (highlighted in yellow), but the region in the DSL domain that has previously found to be essential for Notch binding and activation is conserved between the two species (indicated in red).

Binding was monitored for the whole cell population and for each of the two populations (R1, R2) of cells separately. The effect of each substitution was compared to the binding of $hN1_{11\text{-}13}$ WT (Figure 4-7). Each of the two populations of cells shows similar overall trends for binding to each of these proteins. The results seen for the R2 population of cells showed either full binding or no binding. The T466A, L468A and I477A substitutions completely eliminated the signal seen in the R2 region, whilst the other mutant proteins had no effect. The binding of the cells in the R1 region more closely resembled the results of the previous experiments using the B16 mJagged1 cells. Both the L468A and I477A substitutions completely abrogated binding, and the T466A substitution significantly reduced binding to hJagged1. The Q470A substitution caused the peak in the R1 region to shift to the right, indicating an increase in binding, but no change was seen for the E473A, Q475A and M479A substitutions.

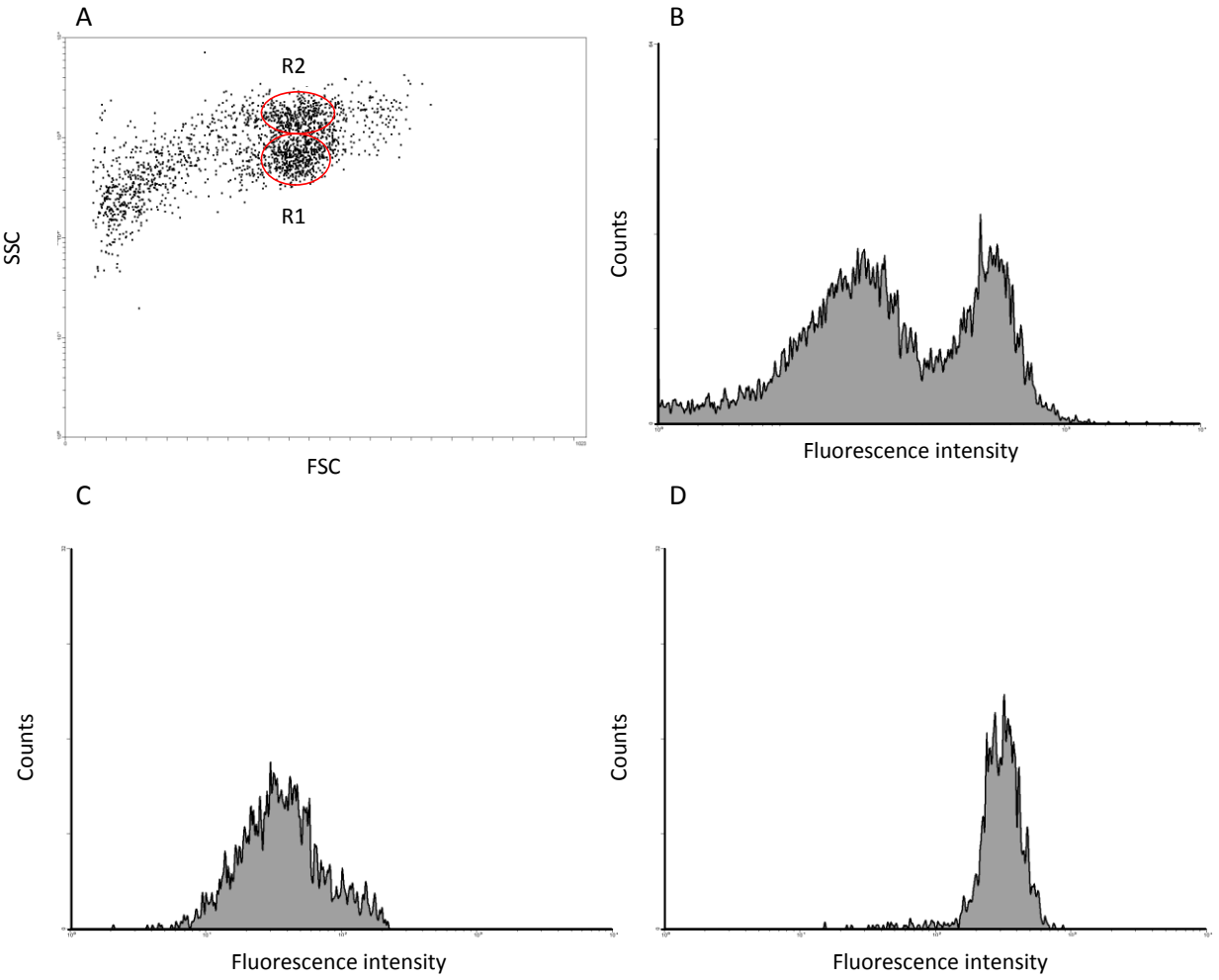


Figure 4-6 The effect of gating around different populations of HEK 293 hJagged1 cells. When beads coated with $hN1_{11-13}$ are incubated with HEK 293 hJagged1 cells, two distinct populations of cells can be seen, either in the FSC/SSC dot plot (A), or in the FL3 flow channel (B). When each of the regions in the dot-plot has a gate placed around it, they each correspond to a different to a different population of cells in the FL3 channel. C) The G1=R1 gate selects for the lower fluorescence intensity peak. D) The G2=R2 gate selects for the higher intensity peak.

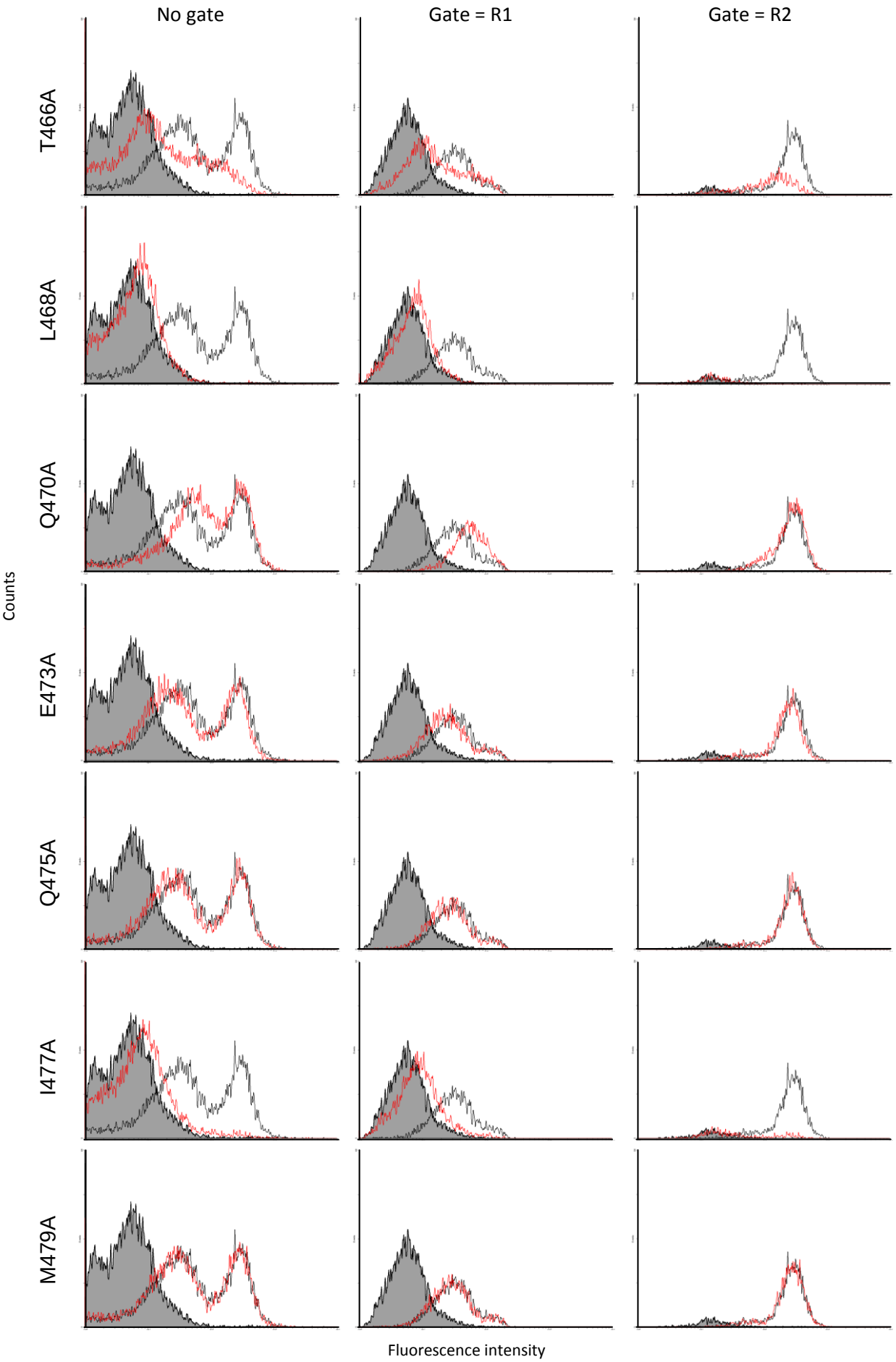

No gate
Gate = R1
Gate = R2
T466A
L468A
Q470A
E473A
Q475A
I477A
M479A
Counts
Fluorescence intensity

Figure 4-7 Binding of Notch EGF12 mutants to HEK 293 hJagged1 cells. Binding to fibrillin1 cbEGF12-14 is shown in grey, WT in black and mutant in red. In the R1 region both the L468A and I477A substitutions showed no binding to hJagged1, and the T466A substitution caused a large reduction in binding. The Q470A substitution caused an increase in binding. Both the E473A and Q475A substitutions caused a very minor decrease, whilst M479A binds similarly to WT. The lack of binding of the T466A, L468A and I477A substitutions to hJagged1 meant that only a very small proportion of cells were found in the R2 region for $hN1_{11\text{-}13}$ containing these substitutions.

4.4 Binding of dN_{11-13} to Serrate

In order to see if a similar ligand binding site to that found in EGF12 of hNotch1 exists in *Drosophila* Notch, a series of mutants was generated in a fragment containing EGF domains 11-13 of *Drosophila* Notch (dN_{11-13}) (initially cloned, expressed and characterised by Shaoyan Liang), and tested for binding to S2 cells transfected with Serrate. A pUAST plasmid containing Serrate (courtesy of Prof. Martin Barron) was used for transient transfection, and was co-transfected into S2 cells with the pMT-Gal4 copper-inducible plasmid (see Section 2.9.4). Only a small (but detectable) proportion of the cells was found to bind to beads coated with dN_{11-13} by fluorescence microscopy. This is due to the low efficiency of the method of transient transfection used in this assay. Therefore in order to study the Notch-Serrate interaction by flow cytometry it was necessary to produce a Serrate-GFP fusion protein (see Section 3.8) so that it was possible to gate the transfected cells.

4.4.1 The dN_{11-13} – Serrate interaction

Before it was possible to test the binding of any of the Notch mutant constructs by flow cytometry, it was first necessary to demonstrate that the minimal binding fragment of *Drosophila* Notch that had been expressed prokaryotically and purified via the *in vitro* oxido-shuffling protocol was able to bind to S2 cells expressing Serrate, and that the addition of the C-terminal GFP fusion protein to Serrate had no effect on binding. Cells were co-transfected with pMTGal4 and a pUAST plasmid containing either Serrate or Serrate-GFP. A third cell line was transfected with pMTGal4 alone. As in the flow cytometry experiments used to study the interaction for the mammalian proteins, either dN_{11-13} or fibrillin1 cbEGF12-14 was immobilised on purple fluorescent beads, to test for specific binding of the Notch protein to its ligand. Each of the cell lines was incubated with each of the proteins, and were visualised by fluorescence microscopy. Neither the beads coated with fibrillin1 cb12-14 nor the uncoated beads showed any form of interaction with cells (Figure 4-8 A). A third sample of cells was visualised in the absence of beads. The results of this show that a small proportion (~5%) of both the Serrate and Serrate-GFP cells are able to bind to beads coated with dN_{11-13} (Figure 4-8 B). A small

fraction of the cells transfected with Serrate-GFP cells were also visible in the GFP channel, and all of these cells also showed binding to Notch coated beads in the rhodamine channel. These data indicate that cells transfected with Serrate-GFP bind to dN_{11-13} in a specific manner, and that it ought to be feasible to gate the cells expressing Serrate-GFP in a flow cytometry experiment.

4.4.2 The dN_{11-13} – Serrate-GFP flow cytometry assay

The same trial experimental controls as were used to observe binding by fluorescence microscopy were repeated and tested for binding in a flow cytometry assay. Initially, cells transfected with Serrate were tested for binding to beads coated with dN_{11-13} WT. When this fluorescence profile in the FL3 (λ > 670 nm) channel was compared with the fluorescence profile for the negative control fibrillin1 cbEGF12-14 protein, a small peak emerges (Figure 4-9 A). This peak represents the small proportion of cells that had been successfully transfected with Serrate binding to the beads coated with dN_{11-13}. The same result was achieved for cells transfected with Serrate-GFP, again confirming that the fusion protein binds to dN_{11-13} in a similar manner to Serrate (Figure 4-9 B).

The fluorescence profile in the FL1 channel (λ = 530 nm) of untransfected cells was found to differ from the cells transfected with Serrate-GFP, as a small number of cells transfected with Serrate-GFP have a high level of fluorescence at this wavelength of light. This represents GFP fluorescence in cells that were successfully transfected, and accounts for approximately 5% of the entire population. These cells appear as a long tail in the FL1 channel that extends beyond the peak seen for the untransfected cells (Figure 4-10 A).

In order to select the cells that were transfected with Serrate-GFP, a marker was placed to the right of 99% of the events in the fluorescence profile of the untransfected cells in the FL1 channel. When a gate is applied to the right of this region, it is possible to record data only for these cells and discard the signal arising from the untransfected cells. This effectively increases the signal arising from the positive control interaction in the FL3 (λ > 670 nm) channel. As a result, a fluorescence profile for the dN_{11-13} positive control interaction in this channel shows the same rightwards shift as

seen in the experiments using the stably-transfected mammalian cells (Figure 4-10 B). This represents the positive control for this assay, and the combination of a clear positive and negative control allows us to use this assay to monitor the effect of amino acid substitutions in dN_{11-13} on binding to Serrate.

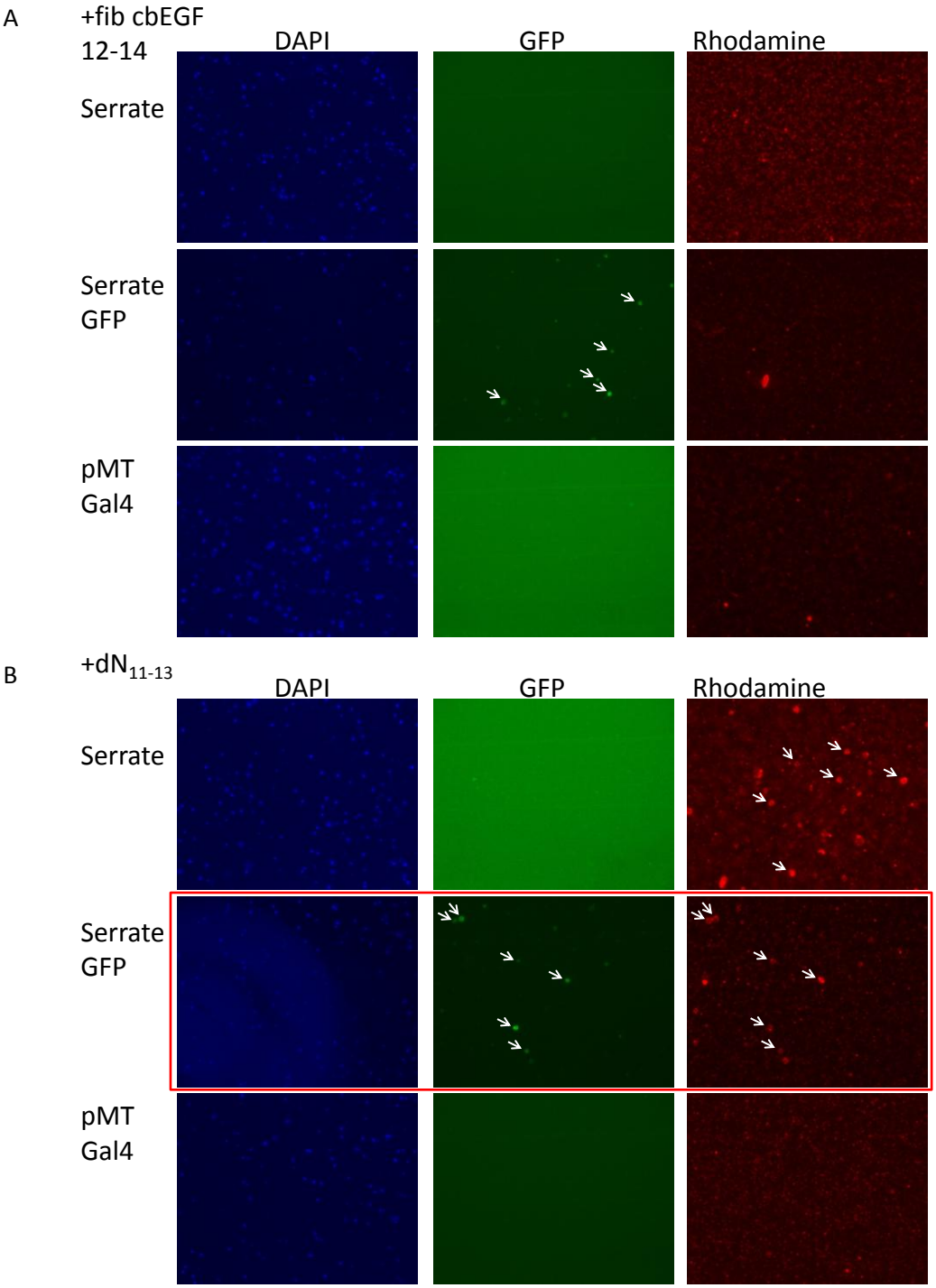


Figure 4-8 Fluorescence microscopy images of S2 cells binding to beads coated with dN_{11-13}. S2 cells were transfected with pMTGAl4 and a pUAST containing either Serrate, or the Serrate-GFP fusion gene, or pMTGal4 alone. Fluorescence is shown in the DAPI, GFP and Rhodamine channels. Cells transfected with Serrate-GFP are clearly visible in the GFP channel. A) Beads coated with fibrillin1 cbEGF12-14 show no specific interactions with S2 cells transfected with either Serrate or Serrate-GFP. B) Beads coated with dN_{11-13} interact with cells transfected with either Serrate or Serrate-GFP, and cells transfected with Serrate-GFP show co-localisation with the beads in the Rhodamine channel.

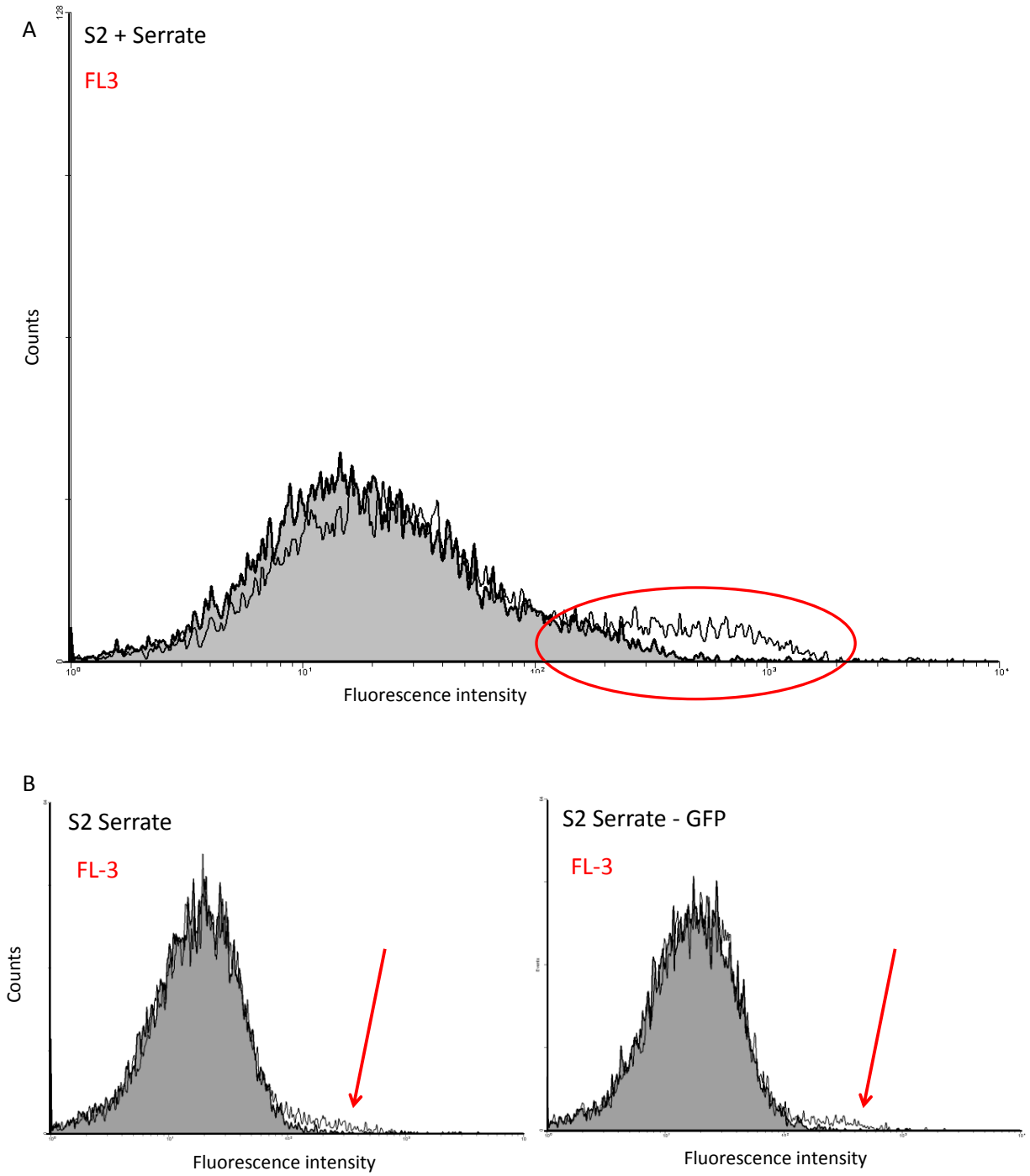


Figure 4-9 Binding of beads coated with dN_{11-13} to S2 cells transfected with Serrate can be detected by flow cytometry. The fluorescence profile for binding to fibrillin1 cbEGF12-14 is indicated by the grey shaded area, and the binding to dN_{11-13} is indicated by the hollow black line. A) A small sub-population of cells (circled) shows an increase in fluorescence in the FL3 channel. This indicates that there is binding of the beads to the cells, but that only a small proportion of the cells have been transfected and express Serrate at their surface. B) The proportion of cells that show binding to the beads is approximately the same for both Serrate and Serrate-GFP (indicated by the red arrows), indicating that the Serrate-GFP fusion binds to dN_{11-13} in a similar manner to Serrate.

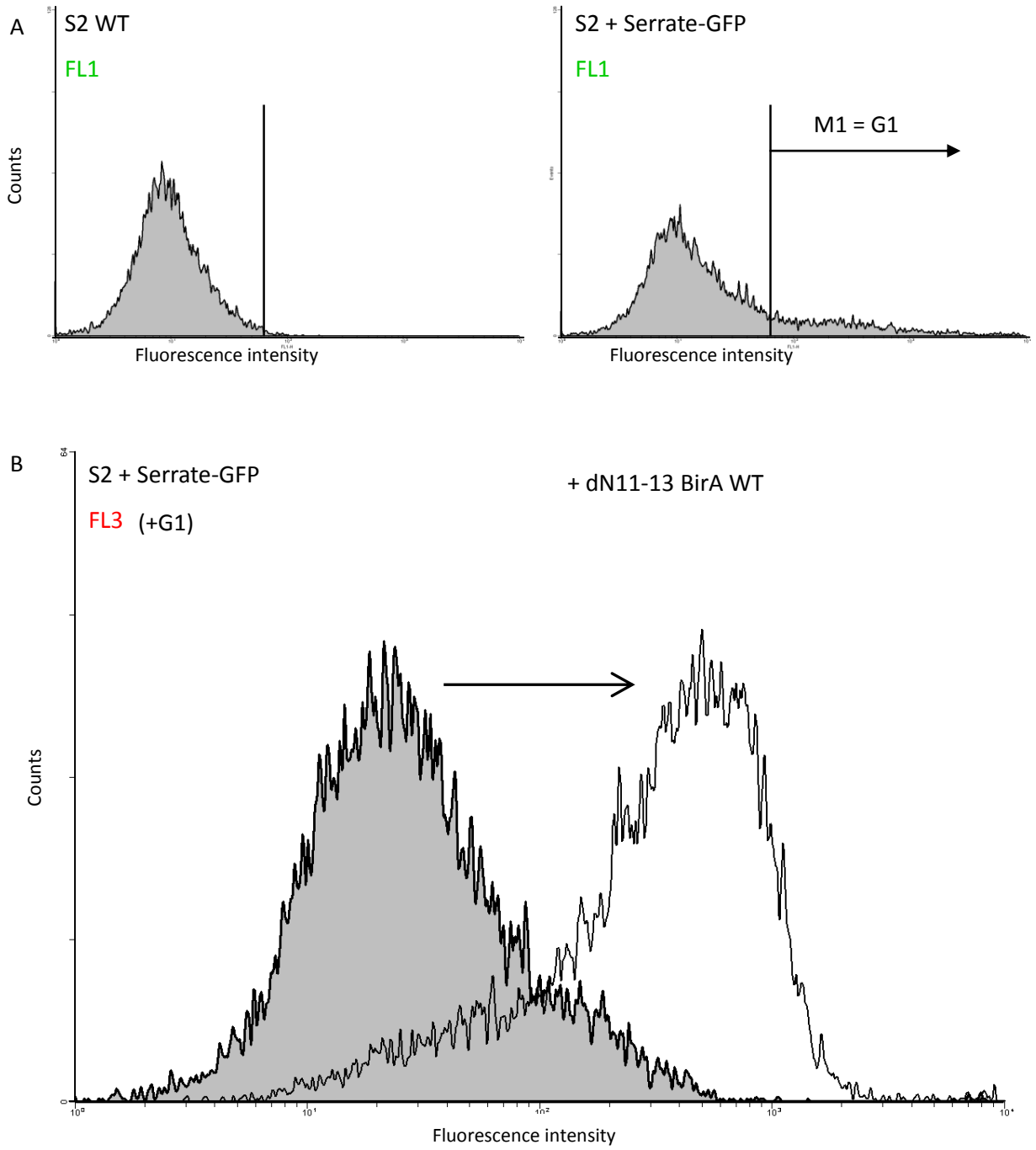


Figure 4-10 Gating can select the cells that have been transfected, and increase the signal for the binding interaction. In order to get a better signal from the positive control interaction, it is necessary to gate only for transfected cells. A) Untransfected S2 cells show a different fluorescence profile in the FL1 (λ = 530 nm) channel to cells transfected with Serrate-GFP. A marker (M1) is placed to the right of 99% of the untransfected cells in this channel (indicated by the black vertical line), and a gate (G1) was applied to only select for these cells. B) When this gate is applied in the FL1 channel, and the cells are examined for binding to beads coated with either $dN_{11\text{-}13}$ (black line) or fibrillin1 cbEGF12-14 (shaded grey area) in the FL3 channel, there is a significant rightwards shift of the fluorescence profile for the positive control protein, indicating binding of the beads to the cells.

4.4.3 Mutant dNotch constructs binding to S2 Serrate-GFP cells

The residues in dNotch that were substituted and tested for binding to Serrate were L504 and D506, which correspond to the residues L468 and Q470 in hNotch1 (Figure 4-1). The L504A substitution in $dN_{11\text{-}13}$ caused the complete elimination of binding to Serrate, which is the same effect as seen for the L468A substitution in $hN1_{11\text{-}13}$, and showed a complete elimination of binding to Serrate (Figure 4-11 A). The D506A substitution also completely eliminated binding to Serrate, which is the opposite result to that seen for the Q470A substitution in $hN1_{11\text{-}13}$ (Figure 4-11 B) (see Section 4.3.2). This suggests that the same region of EGF12 in dNotch is involved in ligand binding as in hNotch1, despite the differences in the residues that contribute to the binding interaction. A Western blot was performed in order to confirm protein loading (Figure 4-11 C). Each of these proteins had been analysed by ^{15}N HSQC NMR by Dr Devon Shepperd as part of an attempt to assign $dN_{11\text{-}13}$, and were found to be correctly folded and retained the ability to bind calcium (not shown).

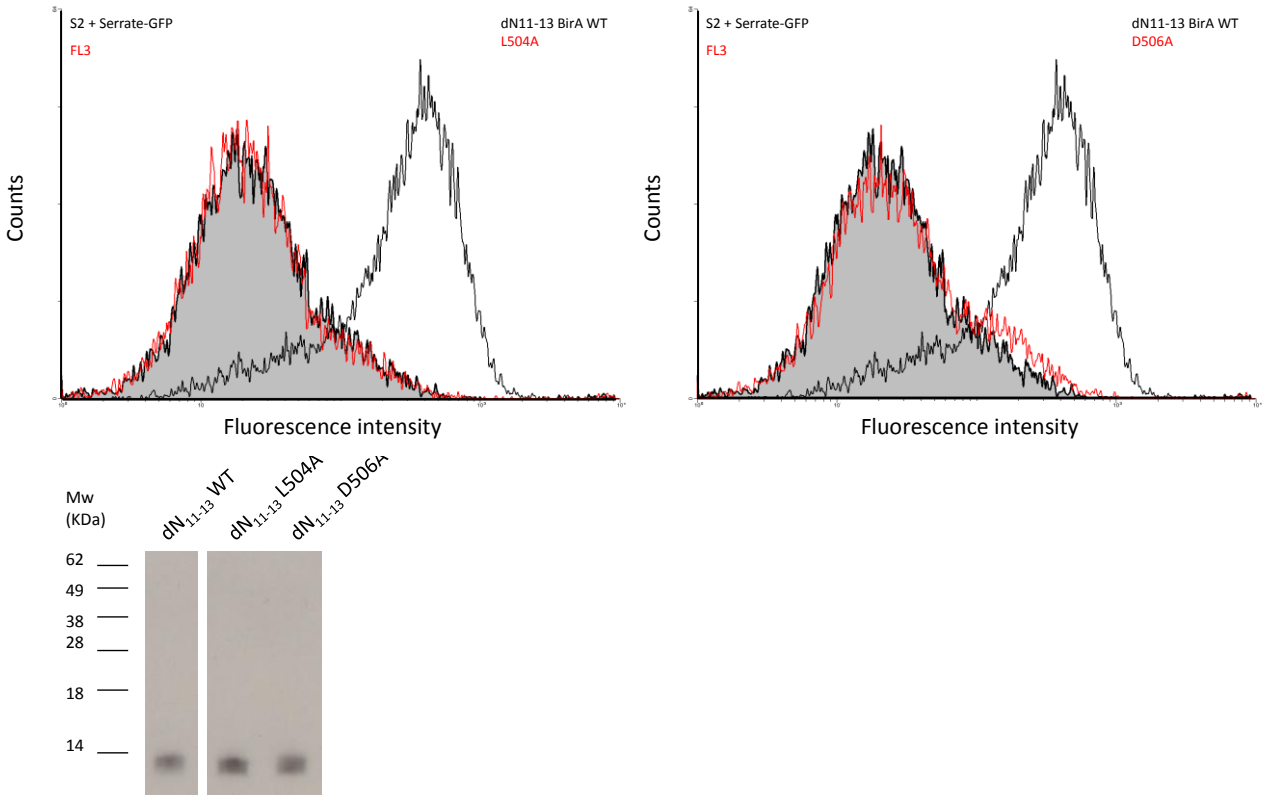


Figure 4-11 Binding of mutant $dN_{11\text{-}13}$ constructs to S2 cells transfected with Serrate-GFP. Binding to fibrillin1 cbEGF12-14 is shown in grey, WT in black and each mutant in red. Both the L504A (A) and D506A (B) substitutions knock out binding to Serrate. C) Western blot to indicate protein loading.

4.5 Confirmation of folding and calcium binding to $hN1_{11-13}$ constructs

It has already been shown that the loss of calcium binding caused by a single amino acid substitution in EGF12 results in $hN1_{11-13}$ being unable to bind to its ligands, due to conformational changes in this domain (Cordle *et al.*, 2008b). Therefore it was essential to check that the loss of ligand binding caused by certain amino acid substitutions was not due to either the loss of calcium binding, or protein misfolding. This was done in two ways by assessing the protection offered by calcium against proteolytic digestion, and by analysing the proteins that showed reduced binding to ligand by 1D and 2D NMR spectroscopy. The assessment of the calcium binding of $hN1_{11-13}$ L468A was performed by Natnee Vitticheep.

4.5.1 Limited proteolysis by Endoproteinase GluC

Calcium-dependent protection from proteolysis has been used in a number of previous studies to assess calcium binding by proteins containing cbEGF domains (Reinhardt *et al.*, 1997) (McGettrick *et al.*, 2000). When calcium is bound to an EGF domain, the protein becomes considerably less flexible, and the peptide backbone becomes less accessible to the active site of proteases. For the proteins used in this study, calcium-dependent protection from proteolysis by Endoproteinase GluC was used as an initial assay to confirm that the substitutions introduced into EGF12 had no effect on calcium binding. Each of the mutants that showed reduced binding to Jagged1 was tested for calcium binding in this way.

The WT protein, shows a high degree of protection from proteolysis in the presence of 10 mM $CaCl_2$. After 60 minutes there is no observable change in the mass of the protein, indicating that the protein is not degraded by the protease. By contrast, the samples containing 10 mM EGTA showed a proportion of the protein had been degraded after 5 minutes, and after 60' the majority of the protein had been degraded to products < 5 kDa, indicating that the protein is sensitive to proteolytic digestion (Figure 4-12 A). The same trends are observable for $hN1_{11-13}$ I477A: there is no observable change in the size of the protein in the presence of 10 mM $CaCl_2$, but the protein is completely

degraded after 60 minutes in the presence of 10 mM EGTA. This suggests that this substitution does not significantly abrogate calcium binding in EGF12, and therefore this is unlikely to be the cause of the loss of binding seen above. This was repeated for the T466A substitution, which was found to bind calcium in a similar manner to both $hN1_{11-13}$ WT and I477A (not shown), which suggests that none of the substitutions introduced into EGF12 reduce calcium binding in this domain.

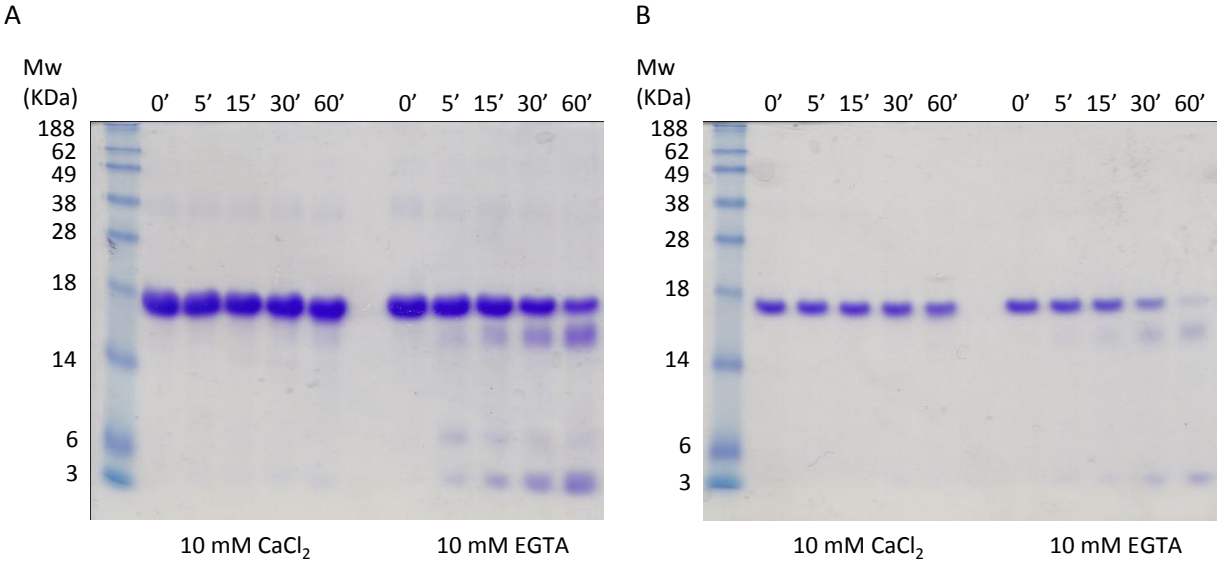


Figure 4-12 Calcium protection from proteolysis by Endoproteinase GluC. Both $hN1_{11-13}$ WT (A) and $hN1_{11-13}$ I477A (B) are protected from proteolysis by Endoproteinase GluC in the presence of 10 mM $CaCl_2$. In the presence of 10 mM EGTA, both proteins are degraded by the protease. These data confirm the presence of native calcium binding sites in the mutant protein, and suggest that the I477A substitution does not alter calcium binding.

4.5.2 Assessment of calcium binding by 1D and 2D NMR spectroscopy

Calcium binding was measured for each of the substitutions that caused a reduction or loss of ligand binding by both 1D and 2D NMR spectroscopy. These techniques have been used in the past to measure domain-specific calcium binding in a number of different proteins (Knott *et al.*, 1996) (Suk *et al.*, 2004) (Jensen *et al.*, 2005; Suk *et al.*, 2004)). The chemical shifts of atoms in residues close to the calcium binding site, as well as those involved in the formation of calcium-dependent inter domain packing interfaces change in response to an increase in the concentration of calcium in the sample buffer. These changes in chemical shift can be plotted as a function of calcium concentration

in order to calculate the affinity of individual calcium binding sites for calcium (Handford *et al.*, 1990). Resonances from an aromatic residue are usually selected as markers for calcium binding to a particular domain, as the peaks in the aromatic region of a ^{1}H 1D or 2D NOESY NMR spectrum are typically well dispersed, and resonances from aromatic residues involved in inter-domain packing interactions shift in a calcium dependent manner (Suk *et al.*, 2004).

Lyophilised protein was dissolved to a final concentration of 300 μM in Matrix buffer, and a series of 1D ^{1}H spectra were recorded at a range of calcium concentrations from 0 mM to 15 mM for T466A and I477A (Figure 4-13). The chemical shift of the ^{1}Hε from residue Y444 was used as a marker for calcium binding to EGF12. This residue is the conserved aromatic residue at the C-terminus of EGF11 that packs against I471 in the main β-hairpin of EGF12 (see Chapter 1). Due to the proximity of Y444 to the calcium binding site in EGF12, and the calcium dependence of the formation of this packing interface, the resonance for this proton shifts in response to calcium binding to EGF12.

The chemical shift for this resonance was measured at each calcium concentration. In order to compare calcium binding of the mutant proteins with the WT protein, it was necessary to calculate a $K_{D\ (apparent)}$ for each protein. To do this, it was first necessary to calculate the fractional change in chemical shift (Δ/Δ_0) of this resonance at each titration point. This value was calculated by calculating the total change in chemical shift for this resonance over the course of the titration (Δ_0), and dividing the relative change in chemical shift at each calcium concentration (Δ) by the total change in chemical shift. Δ/Δ_0 was then plotted against total calcium concentration for WT and each of T466A, L468A and I477A. To correct for any residual calcium that might be present in the sample, a further spectrum was recorded after the addition of 20 mM EGTA in order to obtain a true reference value for this resonance in the absence of calcium (Figure 4-14).

From this plot it was possible to calculate a $K_{D\ (apparent)}$ for EGF12 in each of these proteins. There was only a very slight variation in the ability of each of the proteins to bind calcium, and the $K_{D\ (apparent)}$ for each protein was well below 500 μM for each. It is important to note that this value is not a true K_D

value for calcium binding to EGF12, as it was calculated without correcting for free Ca^{2+}. However, as the experiments were performed under identical conditions for the same protein construct, it is an adequate means to compare how each substitution affects calcium binding in EGF12. As the flow cytometry binding experiments were performed in HBSS buffer containing 1.26 mM $CaCl_2$, the substitutions that cause the complete loss of ligand binding retain the ability to binding calcium in EGF12 under these experimental conditions, and therefore the loss of ligand binding cannot be attributed to the loss of calcium in EGF 12 for any of these proteins (Table 4-1).

Table 4-1

Substitution	EGF12 $K_{D\ (apparent)}$ (μM)
WT	251
T466A	397
L468A	380
I477A	233

The calcium binding ability of the proteins that showed a reduction in binding to mJagged1 was also confirmed by 2D NMR spectroscopy (Figure 4-15). A ^{1}H-^{1}H 2D NOESY spectrum was recorded for each protein at 0 mM and 15 mM $CaCl_2$, and the change in the position of the Hδ-Hε NOESY cross-peak from the same residue was used as a marker for calcium binding in EGF12. These spectra were compared with the equivalent spectra taken for the WT protein, and the cross-peak was found to move in the same calcium-dependent manner for each mutant as for the WT. This is a further demonstration that calcium binding is retained in each of the mutants generated in this study.

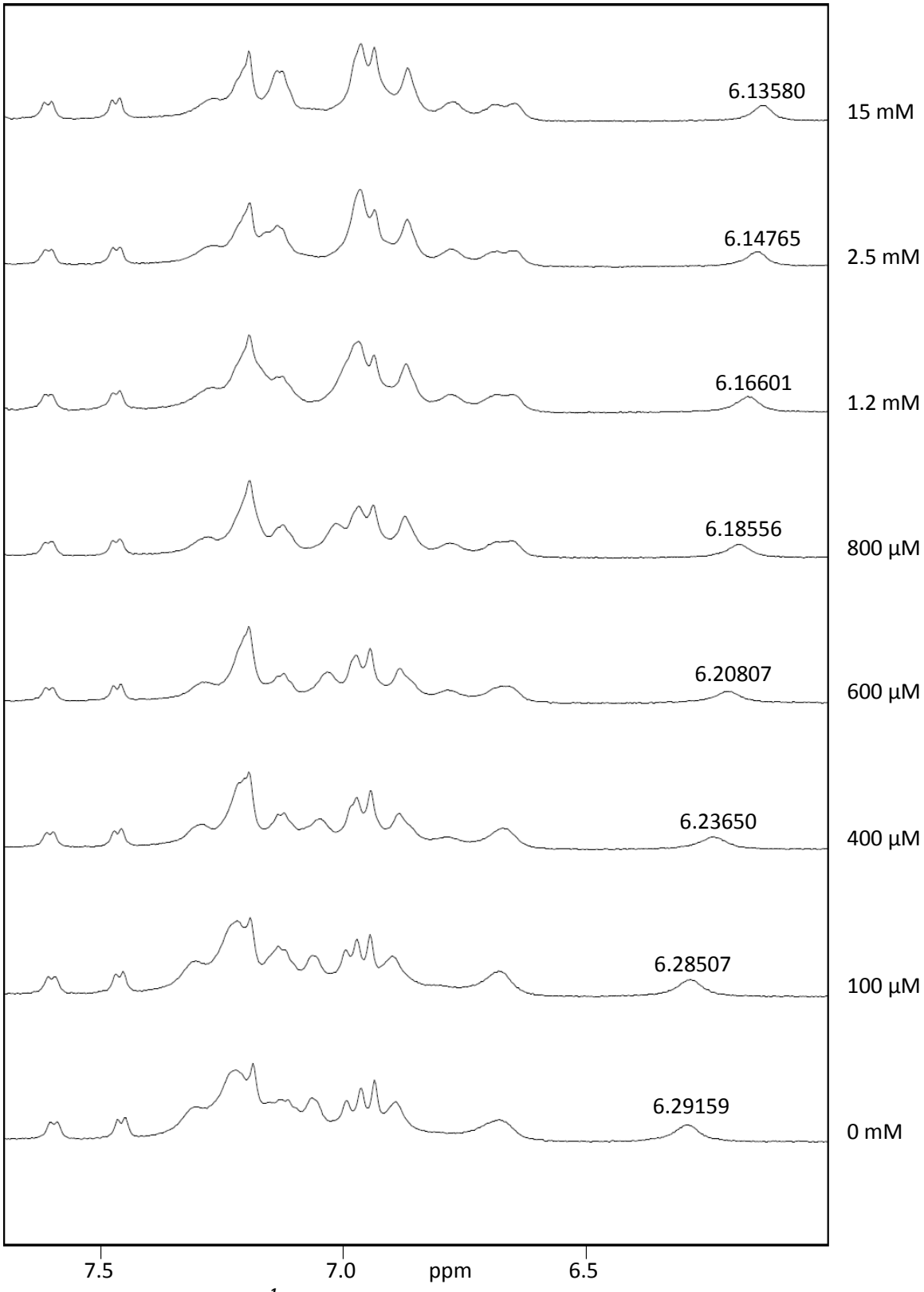


Figure 4-13 Position of the $^{1}H\varepsilon$ peak from Y444 from the T466A mutant in response to increasing calcium. This resonance moves in response to calcium, and becomes saturated at higher concentrations. This is representative of the shift seen in each of the substitutions that significantly reduce binding to hJagged1 and mJagged1.

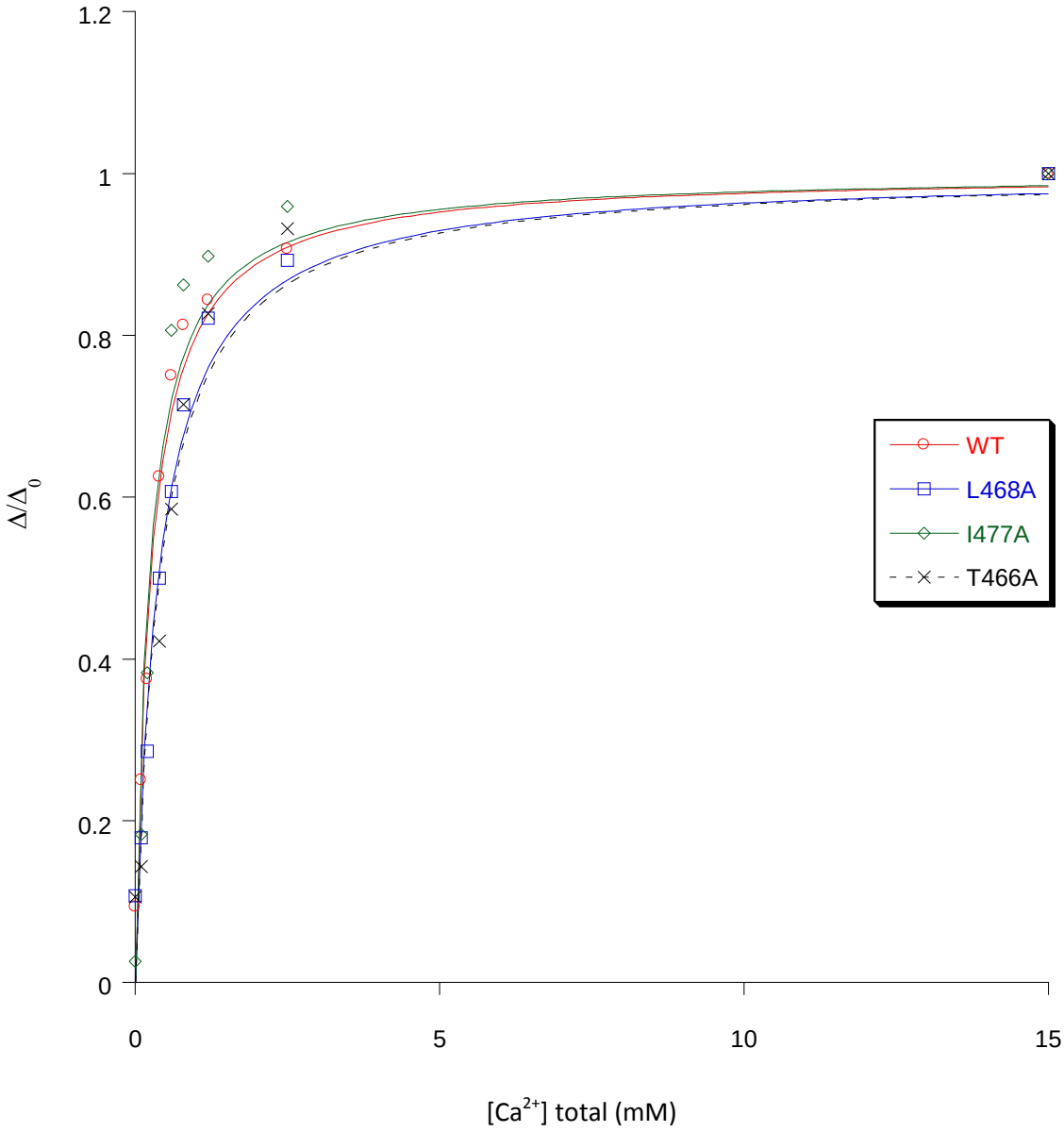


Figure 4-14 Calcium binding to EGF12 for WT, T466A, L468A and I477A proteins. Relative shift of the position of the ^{1}Hε peak from Y444 in response to increasing calcium concentration for each of the three mutant proteins that showed the largest reduction in binding to mJagged1 and hJagged1. This shows that calcium binding is retained for each substitution, and that calcium binding in EGF12 ought to be saturated in the conditions used for the FACS assay.

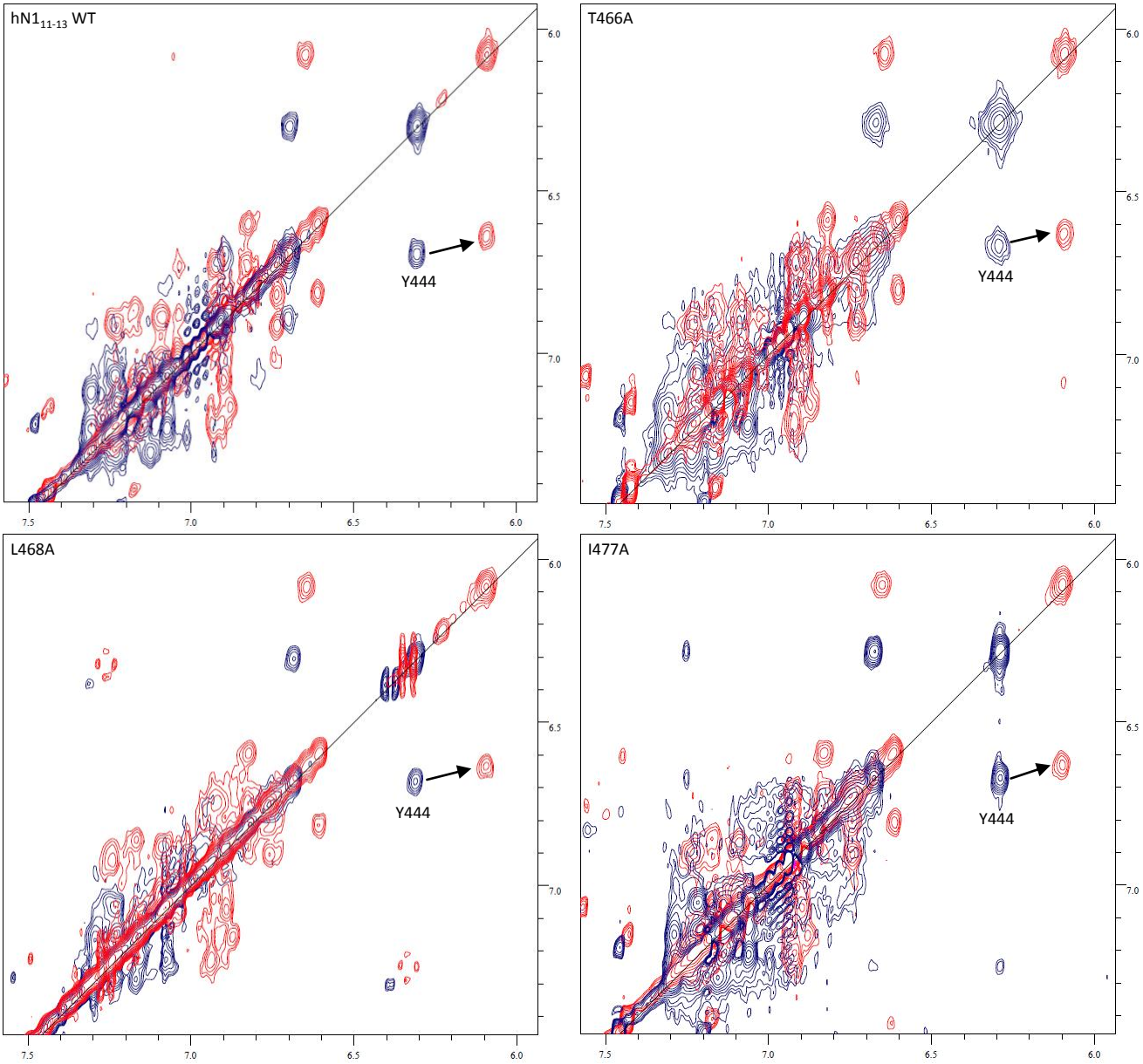


Figure 4-15 Aromatic region of the NOESY spectrum of hN1$_{11-13}$ showing the Y444 Hδ-Hε NOE in WT and mutant proteins. Calcium binding was assessed for each of the substitutions that led to the biggest decrease in binding to Jagged1. The Y444 Hδ-Hε NOE was measured in the absence (blue) and presence (red) of 15 mM $CaCl_2$. The calcium dependence of the change in the position of this resonance confirms that EGF12 in each mutant protein retains the ability to bind calcium. The Y444 assignment was made in a previous study (Hambleton *et al.*, 2004).

4.5.3 Assessment of fold of EGF12 by 2D NOESY NMR spectroscopy

In addition to confirming that calcium binding to EGF12 for T466A, L468A and I77A is similar to WT $hN1_{11-13}$ by NMR and confirming that all of the mutants that showed a reduction in binding to the Notch ligands still retained the ability to bind calcium by limited proteolysis, it was possible to confirm that the central β-sheet in this domain is still present for each of the substitutions in the presence of calcium. Cross-strand NOEs between the $^{1}H\alpha$ from D469 and F474, and C467 and C476 (Figure 4-16 A) indicative of β-sheet formation were visible for all of the mutants that significantly reduced binding to Jagged1 in this study. These were first identified in spectra for $hN1_{11-13}$ WT (Hambleton *et al.*, 2004), confirming that as expected EGF12 was correctly folded for each mutant protein, and that protein misfolding was not the cause of the loss of binding (Figure 4-16 B-C). These NOEs are not present in the spectra recorded in the absence of calcium (not shown).

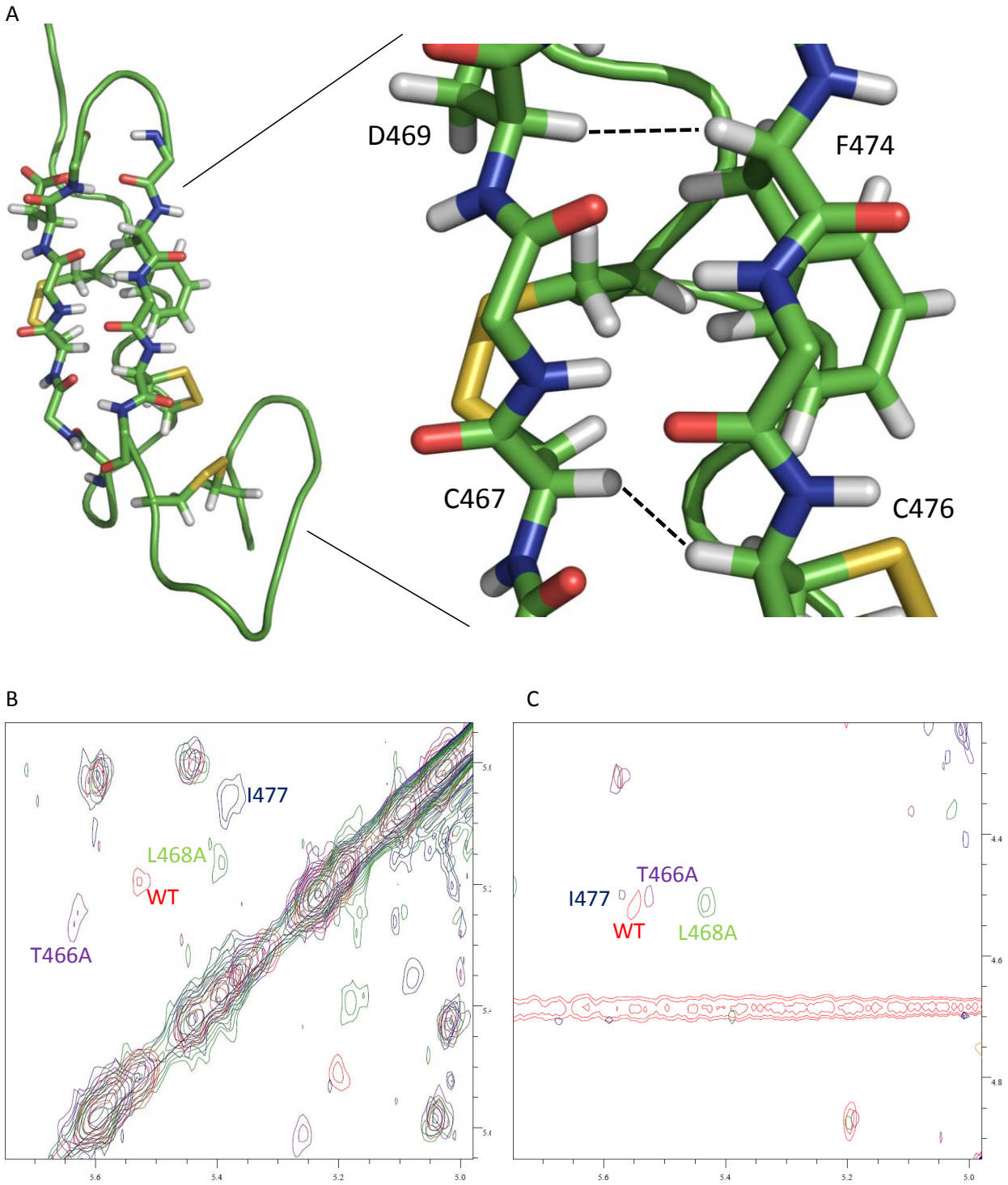


Figure 4-16 Cross-strand Hα-Hα NOEs can be seen between opposite strands of the central β-sheet in EGF12 for each of the mutant proteins. NOEs between the Hα from C467 and C476, and D469 and F474 (first identified in $hN1_{11-13}$ WT) can be seen for the mutants that reduce binding to Jagged1. The peak corresponding to each mutant is indicated on the spectrum, and although the chemical shifts of the NOEs vary slightly between the different mutants, the presence of the cross-peak indicates that the β-sheet within the EGF domain is properly formed. A) The positions of the amino acids within EGF12, and the interactions between the Hα protons on each strand of the β-sheet are indicated. B) The C467 Hα-C476 Hα NOE. C) The D469 Hα-F474 Hα NOE.

4.6 Conclusions of binding experiments

The substitutions that led to a reduction in binding to mJagged1 form a contiguous patch when mapped onto the surface of $hN1_{11-13}$ (Figure 4-17). Three of these substitutions led to a near-complete abrogation in binding – L468A, I477A and T466A, and the side chains from these amino acids pack against each other in the crystal structure of $hN1_{11-13}$. Substituting other residues in the central β-sheet of EGF12 reduced binding to Jagged1 to a lesser extent (E473A and Q475A), and the Q470A substitution led to an increase in binding.

Overall the experiments using cells expressing hJagged1 agreed well with the mJagged1 data. However, the E473A and Q475A substitutions cause a partial reduction in binding to B16 mJagged1 cells, but have no measurable effect on binding to HEK hJagged1 cells. These differences are surprising, given the high degree of sequence homology between mJagged1 and hJagged1 (Figure 4-6), and are particularly surprising considering that EGF12 of mNotch contains the same residues at these positions (Figure 4-1). Therefore it is possible that small variations in the level of Jagged1 expressed at the cell surface of each cell line could account for these differences, and that the same residues form part of the binding surface for mJagged1 and hJagged1.

It is clear that the substitutions that affect binding to Jagged1 do not appear to reduce binding to mDLL4 in the same way (Figure 4-4), as the L468A and I477A substitutions that completely abrogated binding to Jagged1 only caused a small but nevertheless significant decrease in binding to DLL4. The sequence of the MNNL, DSL and EGF regions of the mammalian Delta-like ligands shows a relatively high degree of divergence from the two Jagged1 proteins used in this study, and the SPR binding experiments in Chapter 5 appear to suggest that the affinity of $hN1_{11-13}$ for DLL4 is a good deal higher than for Jagged1. It is possible that this increased affinity could mask any small reduction in binding caused by some of the substitutions in EGF12 used in this study, and could explain why only the L468A and I477A substitutions had any visible effect on binding to DLL4. It is also possible that the B16 DLL4 cells express a higher level of ligand than either of the Jagged1 cell lines, which

could also act to mask any subtle changes caused in binding. A more quantitative technique, such as SPR, would be required in order to confirm whether the other residues within EGF12 are involved in binding to DLL4, but it is likely that a similar, if not identical, region of EGF12 is required to initiate binding to the two classes of mammalian Notch ligands.

The equivalent substitution to L468A in dNotch – L504A – completely abrogated binding to Serrate. Substituting the D506 residue to alanine also completely abrogated binding to Serrate, in contrast to the equivalent substitution in $hN1_{11\text{-}13}$ (Q470A) that appeared to increase binding to both Jagged1 cell lines. Together, these data indicate that residues within the central β-hairpin in EGF12 from both hNotch1 and dNotch are involved in binding to the various Notch ligands, and that certain residues (e.g. L468/L504) in this region that are highly conserved throughout evolution are essential for ligand binding. Work done in Prof. Martin Baron's laboratory in collaboration with this study substituted a number of residues in EGF12 in the full length dNotch molecule to alanine, and found that substituting L504, T509, R511 and V513 (corresponding to L468, E473, Q475 and L477 in hNotch1) reduced or eliminated binding to cells expressing Serrate in a cell aggregation assay, confirming that this region of EGF12 in hNotch1 and dNotch is the binding site for Notch ligands (Whiteman *et al.*, 2013).

Substituting the residues within the central β-hairpin of EGF12 had various effects on binding to the different Notch ligands used in this study. Three of the substitutions within EGF12 of hNotch1 (T466A, L468A and I477A) caused a complete reduction in binding to mJagged1 and hJagged1, and two of these (L468A and I477A) also led to a reduction in binding to DLL4. Substituting the corresponding residue to L468 in dNotch (L504A) also completely abrogated binding to Serrate. These amino acids are positioned at one end of EGF12 and their side chains pack against each other. They show a high degree of sequence conservation throughout evolution (see Figure 4-1), and are likely to form a hydrophobic platform that acts as the core of the ligand binding site in Notch. The variable effects of substituting the other residues in EGF12 on binding to the various Notch ligands

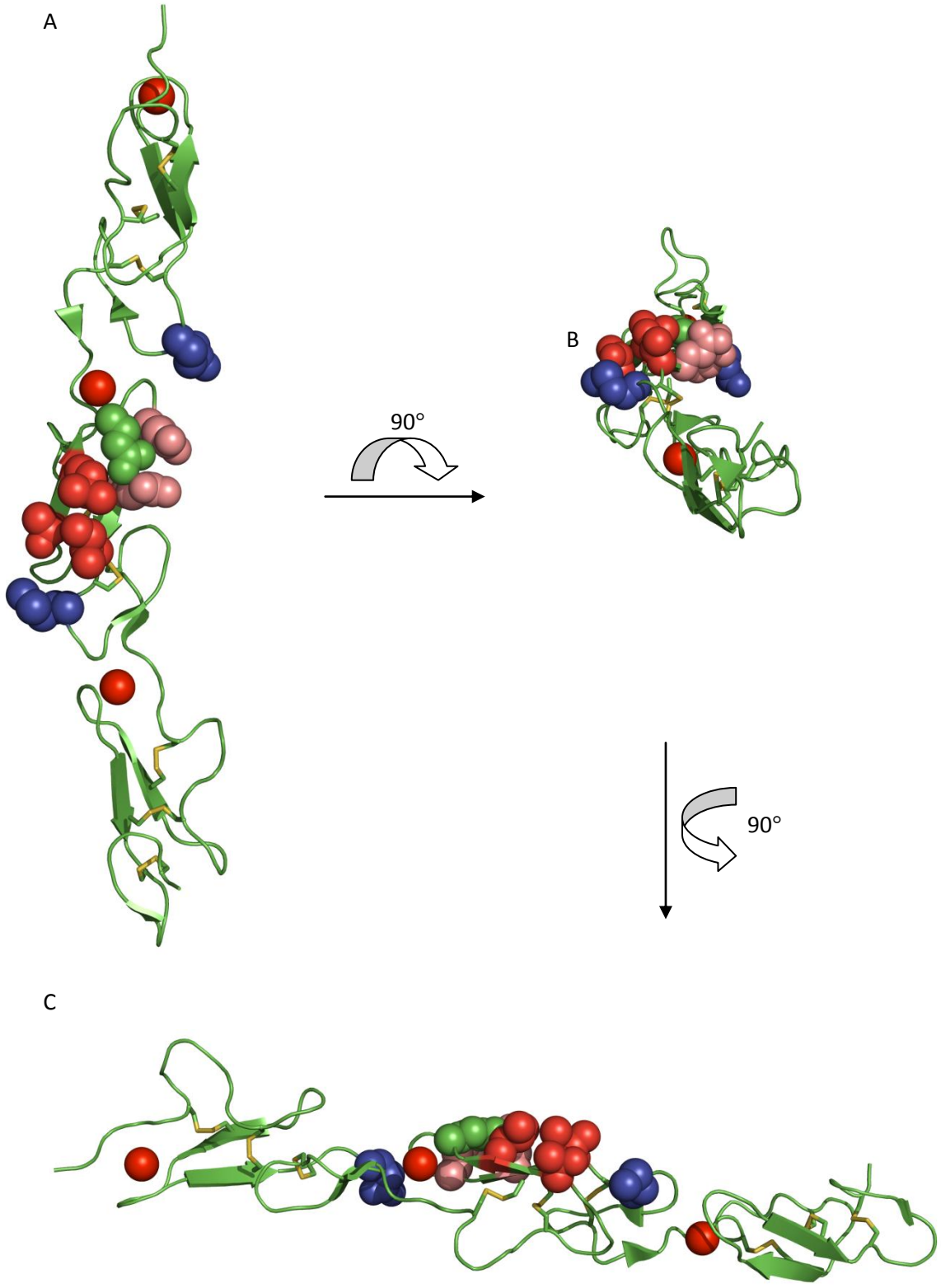


Figure 4-17 The residues in EGF12 required for binding to Jagged1. A) The hydrophobic side-chains from T466, L468 and I477 pack against each other (red). E473 and Q475 (pale red) and Q470 (green) are also involved in binding. B & C) These residues form a patch on the surface of EGF12 that suggests that due to the elongated nature of $hN1_{11\text{-}13}$ other domains may form additional contacts with Jagged1. Q442 and M479 are shown in blue, and do not appear to be involved in binding.

suggests that these residues might act to fine-tune ligand binding by forming additional contacts with the Notch ligands, and that the precise binding site might vary slightly for each ligand.

It is also interesting to note that the residue T466 that forms part of the ligand binding site also forms part of the consensus sequence that allows EGF12 to be modified with O-fucose glycans, which suggests that glycosylation of this domain may directly influence ligand binding, and this is investigated further in the next chapter.

Chapter 5

The role of glycosylation in modulating ligand binding

5.1 Introduction

A number of studies have investigated the effects of different sugar modifications to the Notch receptor on both ligand binding and receptor activation, in both *Drosophila* and mammalian experimental systems (Okajima and Irvine, 2002) (Rampal *et al.*, 2005b). These studies have used a number of *in vitro* and *in vivo* techniques to determine how these modifications may regulate Notch signalling. As discussed in Chapter 1, the role of the Fringe enzymes in regulating Notch signalling has been studied in particular detail.

The three Fringe enzymes in mammals have different effects on Notch signalling, probably as a result of the enzymes modifying different regions of the Notch receptor. The results of these studies are summarised in Section 1.7 and Table 1-2. Despite these numerous and sometimes contradictory studies, there is little information about which domains within the Notch receptors contribute to the changes in ligand binding and receptor activation. Some information exists about the specificity of the enzymes for particular substrates however: MFng has been shown to extend the fucose moiety in EGF12 of Notch1 (Shao *et al.*, 2003) and within the Abruptex region (EGF23-29) (Shimizu *et al.*, 2001), and LFng preferentially acts on the N-terminal region (N-terminus-EGF15) of Notch2.

It is clear that multiple sites within the various Notch receptors are modified, but it is not known to what extent the O-fucose sugar is extended at each site, and how this might contribute towards the changes in binding and signalling reported in Section 1.7. There are several universally conserved O-fucosylation sites within the Notch1 receptor, including in EGF12 in the ligand binding region, and EGF26 and EGF27 in the Abruptex region of Notch. Previous attempts to determine which domains contribute to the regulation of Notch signalling have typically substituted the serine or threonine residues that form part of the consensus sequences for O-fucosylation from these domains. Removing the O-fucosylation site in EGF12 of dNotch via a S→A substitution leads to an increase in signalling and binding by Serrate and Delta (Lei *et al.*, 2003) and renders the protein insensitive to the Fringe effect in an *in vivo* wing disc assay. A similar study that removed the equivalent O-

fucosylation site in mouse Notch1 found that a T→A substitution in EGF12 results in near-complete reduction in both Jagged1 and Delta1 signalling (Rampal *et al.*, 2005a). This same study also showed that the equivalent T→A substitution in EGF26 caused an increase in activation by both ligands in a manner that resembles certain classes of *Ax* mutations, and in EGF27 results in a reduction of Notch1 at the cell surface. However, EGF27 in Notch1 contains an unpaired cysteine residue in addition to the six normally associated with an EGF domain (see Section 1.3), so it is possible that this substitution could affect protein folding.

These studies have generally failed to address the effects of the amino acid substitutions themselves, and instead attribute the changes that arise to the loss of the sugar modifications at a particular location without considering the effect of the amino acid substitutions independently from the loss of glycosylation. As they have included the removal of the O-fucosylation site from EGF12 of hNotch1 via a T→A substitution (a substitution that was found to reduce binding of prokaryotically-expressed $hN1_{11\text{-}13}$ to Jagged1 in Chapter 4) it is possible that the changes seen in these studies may not arise purely as a result of the loss of glycosylation at this location.

This chapter aims to identify the effect that specific sugar modifications have on the binding of $hN1_{11\text{-}13}$ or $dN_{11\text{-}13}$ to various Notch ligands, in an attempt to correlate specific sugar modifications to the ligand-binding region of hNotch1 and dNotch with the more global effects on ligand binding reported in the previous studies, and outlined in Section 1.7. It will also investigate in more detail the effect of the amino acid substitutions used in previous studies on the binding of Notch to its ligands. Initially the same flow-cytometry assay was used as in Chapter 4, and a more quantitative SPR-based assay was subsequently developed to measure how these modifications affected binding to Jagged1. Subsequent to this the X-ray crystal structures of some of the sugar-modified proteins were solved in order to see the position of the sugars relative to ligand-binding site identified in Chapter 4. The aim of this is to elucidate how the sugar modifications within the ligand-binding region of the Notch receptor are able to modulate binding at a molecular level.

5.2 The effect on ligand binding of substituting the fucosylation site within EGF12

Previous studies, that have investigated the role of sugar modifications at specific locations within the Notch receptor, have generally substituted the serine or threonine residues that form part of the consensus sequences for glycosylation. However, before any conclusions can be made about the effect of the loss of a specific sugar modification on ligand binding or receptor activation, it is first necessary to consider the effect of the amino acid substitution itself. As shown in the previous chapter, the T466 residue in EGF12 of hNotch1 that forms part of the consensus sequence for the addition of fucose by Pofut1 is also involved in binding to Jagged1, as the T466A substitution leads to a decrease in binding to cells expressing mJagged1 or hJagged1 in a flow cytometry assay (see Section 4.3).

To further investigate the effect of substituting this residue, a second round of mutagenesis was performed. T466 was substituted with valine (T466V) and serine (T466S) and tested for binding in the same assays, to see if the reduction in binding to Jagged1 caused by the T466A substitution was due to the loss of the methyl group or the loss of the hydroxyl group from the threonine side chain. The analogous substitution (S502A) was also made in $dN_{11\text{-}13}$, in order to see if the results seen in the previous studies on the effect of glycosylation in EGF12 of *Drosophila* Notch were solely due to the loss of the sugar modification at this site. The effect of this substitution in dNotch on binding to Serrate was assayed by flow cytometry.

5.2.1 Assaying the effect on ligand binding of substituting T466 in $hN1_{11\text{-}13}$

The three different substitutions at residue T466 have very different effects on binding of $hN1_{11\text{-}13}$ to B16 mJagged1 cells. As already demonstrated in the previous chapter, the T466A substitution led to a near-complete elimination of binding to Jagged1. The T466S substitution had a similar effect to T466A on binding to B16 mJagged1 cells. In contrast the T466V substitution led to a small increase in binding similar compared to $hN1_{11\text{-}13}$ WT (Figure 5-1). This suggests that the presence of the methyl group at this position is essential for unmodified $hN1_{11\text{-}13}$ to bind to mJagged1, and supports the

conclusions of the previous chapter that showed that a hydrophobic platform is essential for the binding to Notch to its ligands. It also shows that in the previous study, the T466A substitution used to investigate the effect or removing the O-fucosylation site in EGF12 of Notch1 could affect binding independently of glycosylation, and that the T466V substitution may be more appropriate to use in future studies of this kind (Rampal *et al.*, 2005a).

Although neither the T466A nor the T466S substitutions affected binding to DLL4, there was a very slight increase in binding observed for the T466V substitution. The effect of these substitutions on binding to both ligands was subsequently studied in a BIAcore binding assay for a more quantitative analysis (see Section 5.4).

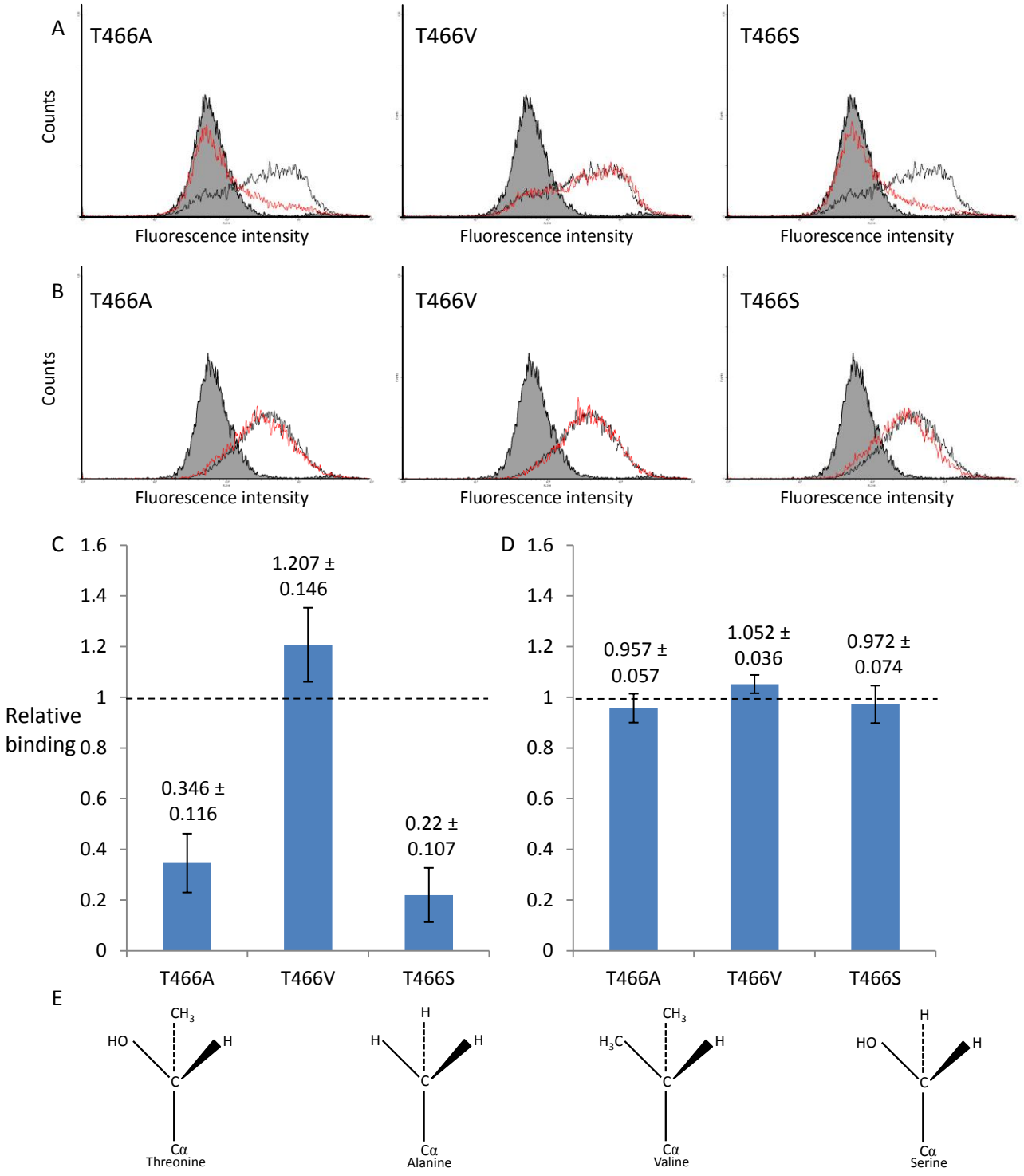


Figure 5-1 The effect of substituting the T466 residue on binding to mJagged1 and mDLL4 cells. Binding to fibrillin1 cbEGF12-14 is shown in grey, WT in black and each mutant in red. A) The T466A and T466S substitutions lead to an almost complete reduction in binding to B16 mJagged1 cells, whereas the T466V substitution causes a slight increase in binding. B) T466A and T466S bind to B16 mDLL4 cells similarly to $hN1_{11\text{-}13}$ WT, T466V shows lightly elevated binding. C-D) Quantitative analysis of the effect of each of these substitutions on binding to B16 cells expressing Jagged1 (C) and DLL4 (D) ($n \geq 3$ for each mutant), with mean and 95% confidence limits indicated. E) Amino acid side chains from threonine, alanine, valine and serine.

5.2.2 Assaying the effect of substituting S502 in dN_{11-13} on binding to Serrate

The O-fucosylation site in EGF12 was removed using the S→A substitution, and binding to Serrate was tested using the same flow cytomtry assay as in the previous chapter. The S502A substitution had no measurable effect on the binding of dN_{11-13} (Figure 5-2), which is not surprising given the relatively conservative nature of this substitution (Figure 5-1 C). This suggests that the S502A substitution used to investigate the effect of removing the O-fucosylation site in EGF12 of dNotch is unlikely to affect binding, and that the results seen in this earlier study are likely to reflect the effects of the loss of glycosylation at this site (Lei *et al.*, 2003).

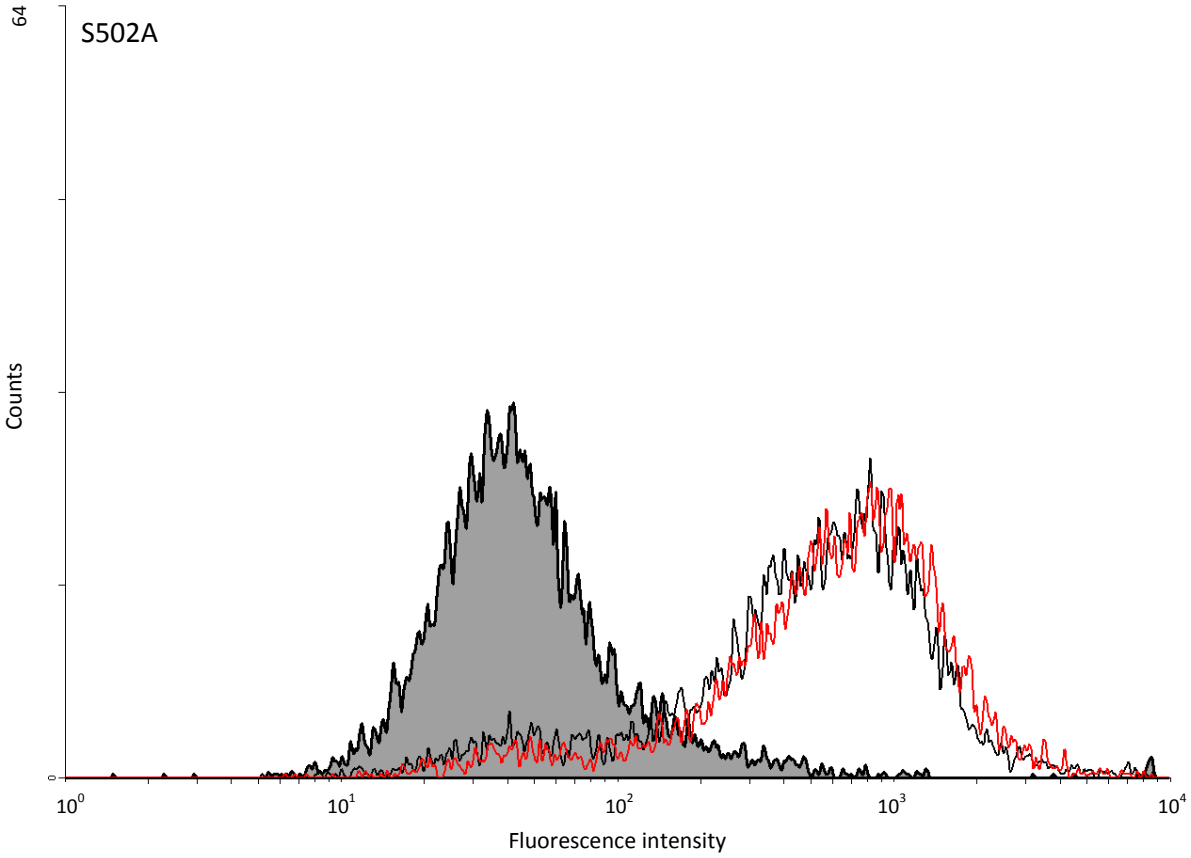


Figure 5-2 The effect of substituting the S502 residue in dN_{11-13} on binding to Serrate. Binding to S2 cells transiently transfected with Serrate-GFP was measured using the same assay as in the previous chapter. Binding to fibrillin1 cbEGF12-14 is shown in grey, WT in black and each mutant in red. The binding profile for the mutant protein is shown in red. The S502A substitution has no measurable effect on binding in this assay.

5.3 The effect of individual sugar modifications on ligand binding

Previous studies have always had problems identifying which residues within the Notch protein are modified with glycans, the extent to which each glycan is extended, and how homogeneous the material being used in the study is. To overcome both of these problems, prokaryotically-expressed and refolded proteins were specifically glycosylated *in vitro* and purified by HPLC, before being tested for binding to a selection of Notch ligands. This meant that changes in binding could be attributed to specific sugar modifications at specific sites within the ligand binding region of the Notch receptor from both humans and *Drosophila*.

All sugar modifications were added to proteins and the products analysed by HPLC and ESI-MS by Dr Hideyuki Takeuchi, in Prof Robert Haltiwanger's laboratory at Stony Brook University, New York. This analysis confirmed that each of the sugar-modified Notch fragments tested for binding was fully modified and homogeneous. All unmodified material used in these binding assays was also purified in the same way, in order to ensure that the glycosylation process was not somehow further purifying the unmodified material and removing protein that might be misfolded.

5.3.1 Assaying the effect of sugar modifications on the mammalian interaction

The $hN1_{11\text{-}13}$ minimal binding fragment was used as the substrate for glycosylation, and as the positive control protein for all of the assays that tested effect that individual sugar modifications had on binding. This construct contains three separate sites for O-linked glycosylation: O-glucosylation sites at S458 and S496, and an O-fucosylation site at T466 (Figure 5-3). It was possible to sequentially attach the tetrasaccharide modification via O-fucose, GlcNAc-fucose and galactose-GlcNAc-fucose intermediates (see Section 1.7) to the threonine residue in EGF12, and both the glucose monosaccharide and xylose-glucose disaccharide modifications to each of the O-glucosylation sites. The effect that each of the modifications had on binding was tested using the flow cytometry assays described in Chapter 4 using a minimum of three repeats.

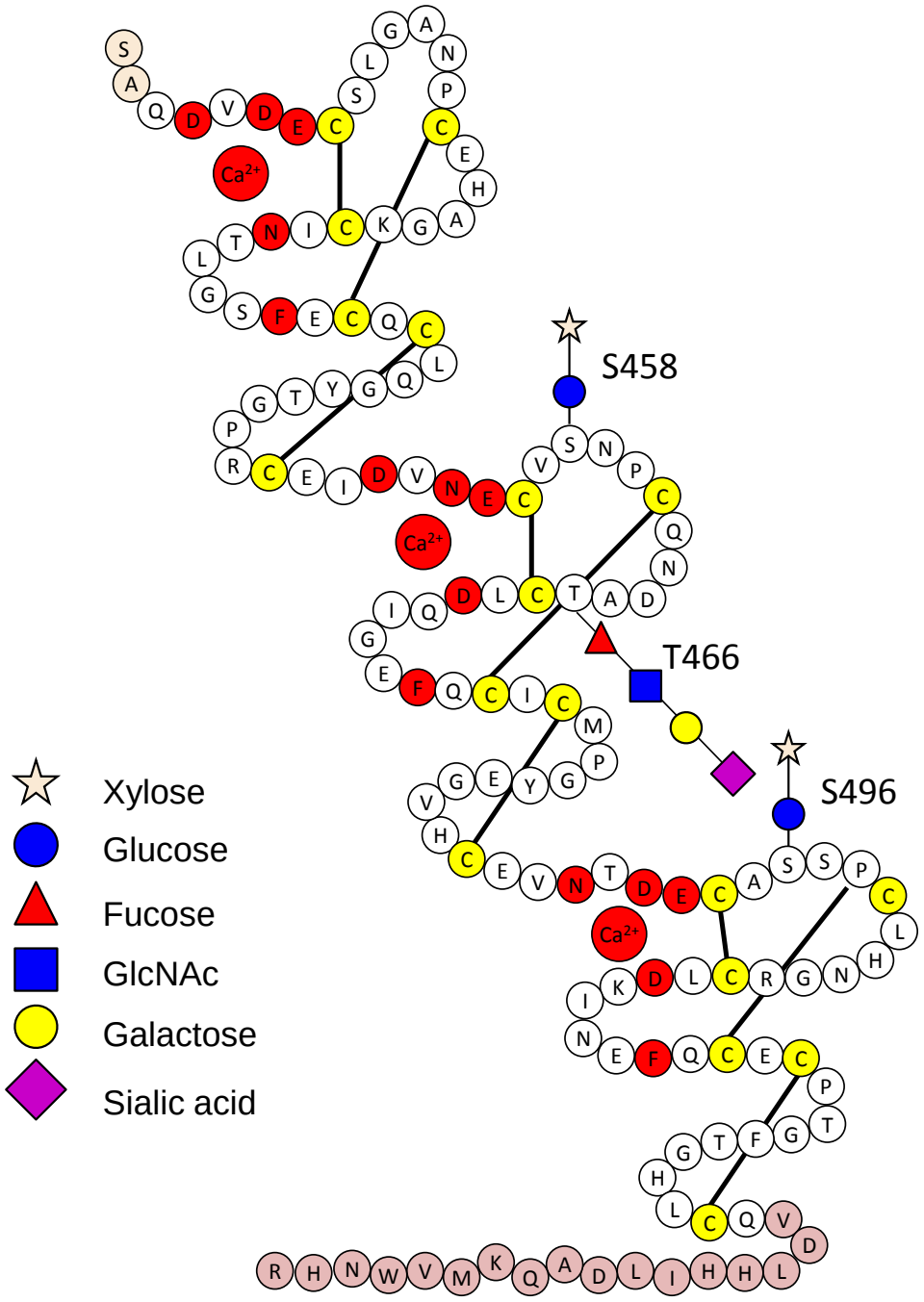


Figure 5-3 Glycosylation sites and sugar modifications made to hN1$_{11-13}$. There are a total of three predicted glycosylation sites within hN1$_{11-13}$ – a single O-fucosylation site in EGF12 (T466) and an O-glucosylation site in each of EGF12 and EGF13 (S458 and S496 respectively). The extensions added to each site are indicated. (Note – the xylose-glucose sugar modifications were not extended beyond the disaccharide).

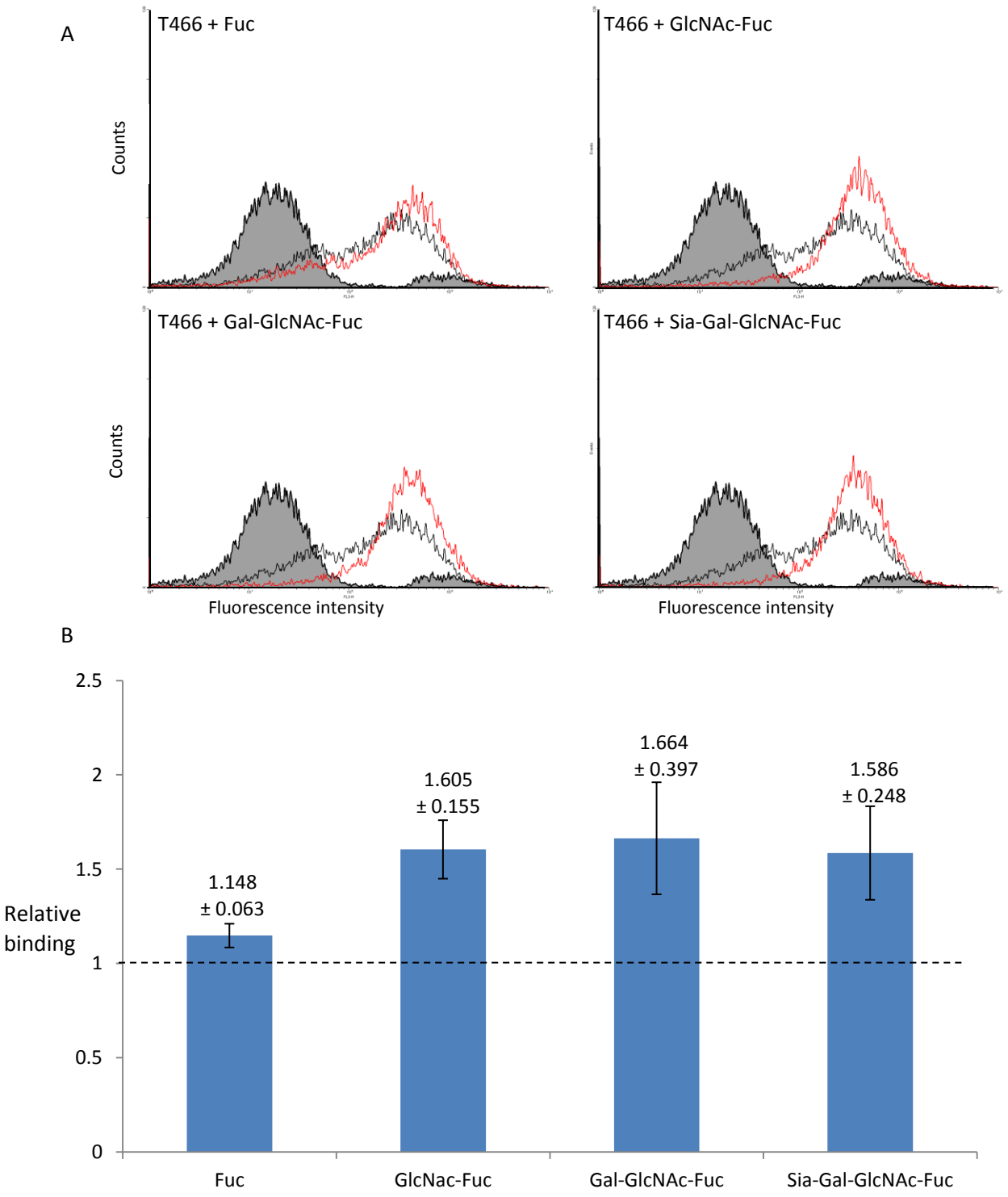


Figure 5-4 The effect of fucose modifications at T466 on binding to B16 mJagged1 cells. Binding to fibrillin1 cbEGF12-14 is shown in grey, unmodified $hN1_{11-13}$ in black and $hN1_{11-13}$ with each sugar modification in red. A) The addition of the O-fucitol monosaccharide leads to a small but reproducible increase in binding to mJagged1 cells. Extension with GlcNAc leads to a larger increase. Further elongation has no further effect on binding. B) Quantitative analysis of the effect of each of the sugar modifications on binding ($n \geq 3$ for each modification), with mean and 95% confidence limits indicated.

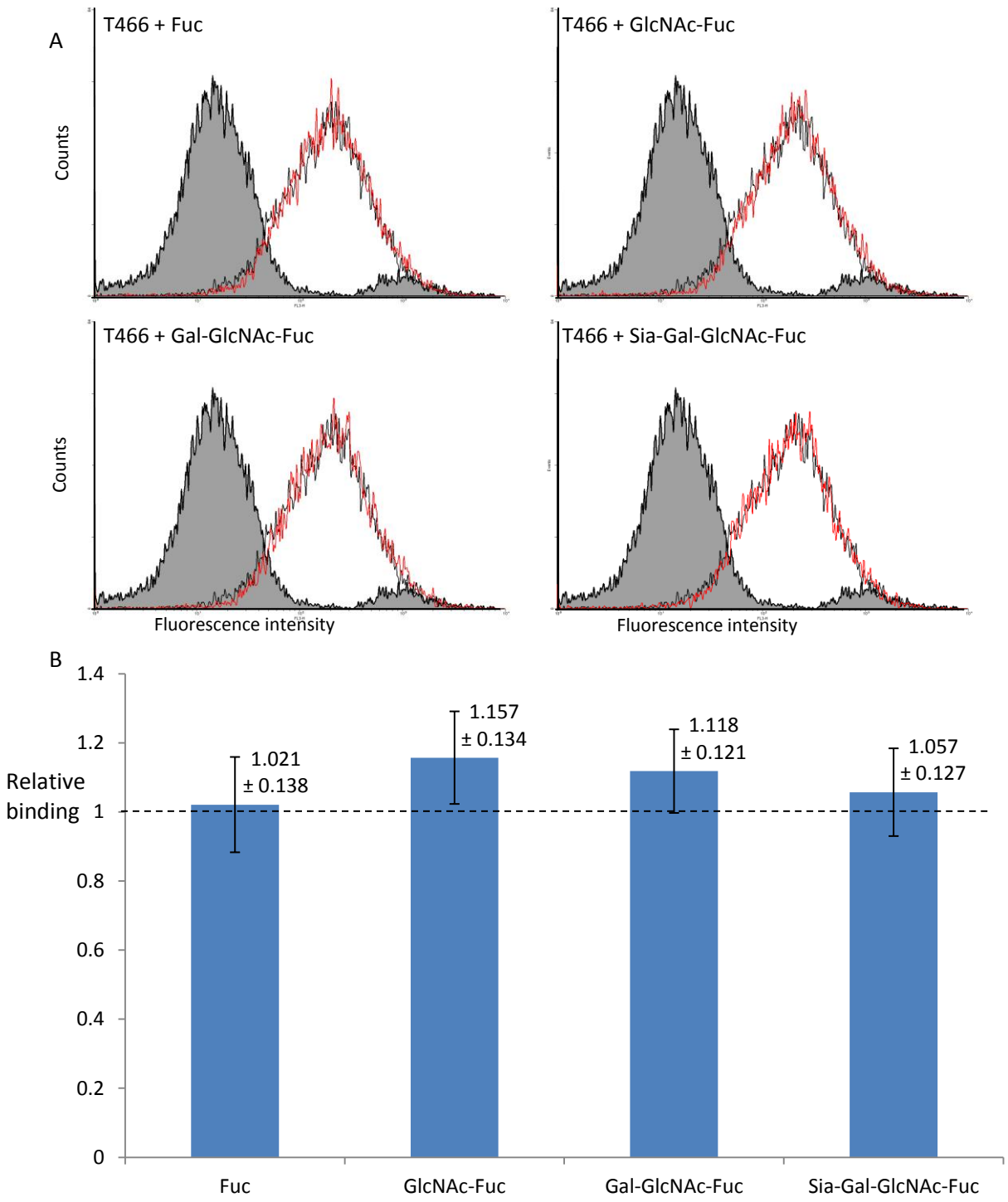


Figure 5-5 The effect of fucose modifications at T466 on binding to B16 mDLL4 cells. Binding to fibrillin1 cbEGF12-14 is shown in grey, unmodified $hN1_{11-13}$ in black and $hN1_{11-13}$ with each sugar modification in red. A) The addition of the O-fucitol monosaccharide had no apparent effect on binding. Extension with GlcNAc leads to a very small increase in binding, and further elongation has no further effect on binding. B) Quantitative analysis of the effect of each of the sugar modifications on binding ($n \geq 3$ for each modification), with mean and 95% confidence limits indicated.

The addition of fucose to T466 led to a small but reproducible increase in binding to B16 mJagged1cells, indicated by the rightwards shift of the fluorescence profile compared to the unmodified protein. Extension of this sugar with GlcNAc resulted in a larger increase in binding, while further extension to the trisaccharide and tetrasaccharide had no further effects on binding in this assay (Figure 5-4 A-B). Binding to B16 cells expressing mDLL4 was tested alongside the B16 mJagged1 cells, and none of the O-fucose glycans had any measurable effect on binding (Figure 5-5 A-B).

In contrast to the changes in binding to mJagged1 that occur as a result of the addition of fucose glycans to T466 in EGF12, there was no difference in binding to B16 cells expressing either mJagged1 or mDLL4 when the O-glucosylation sites at S458 and S496 within EGF domains 12 and 13 were modified with either glucose, or the xylose-glucose disaccharide (Figure 5-6).

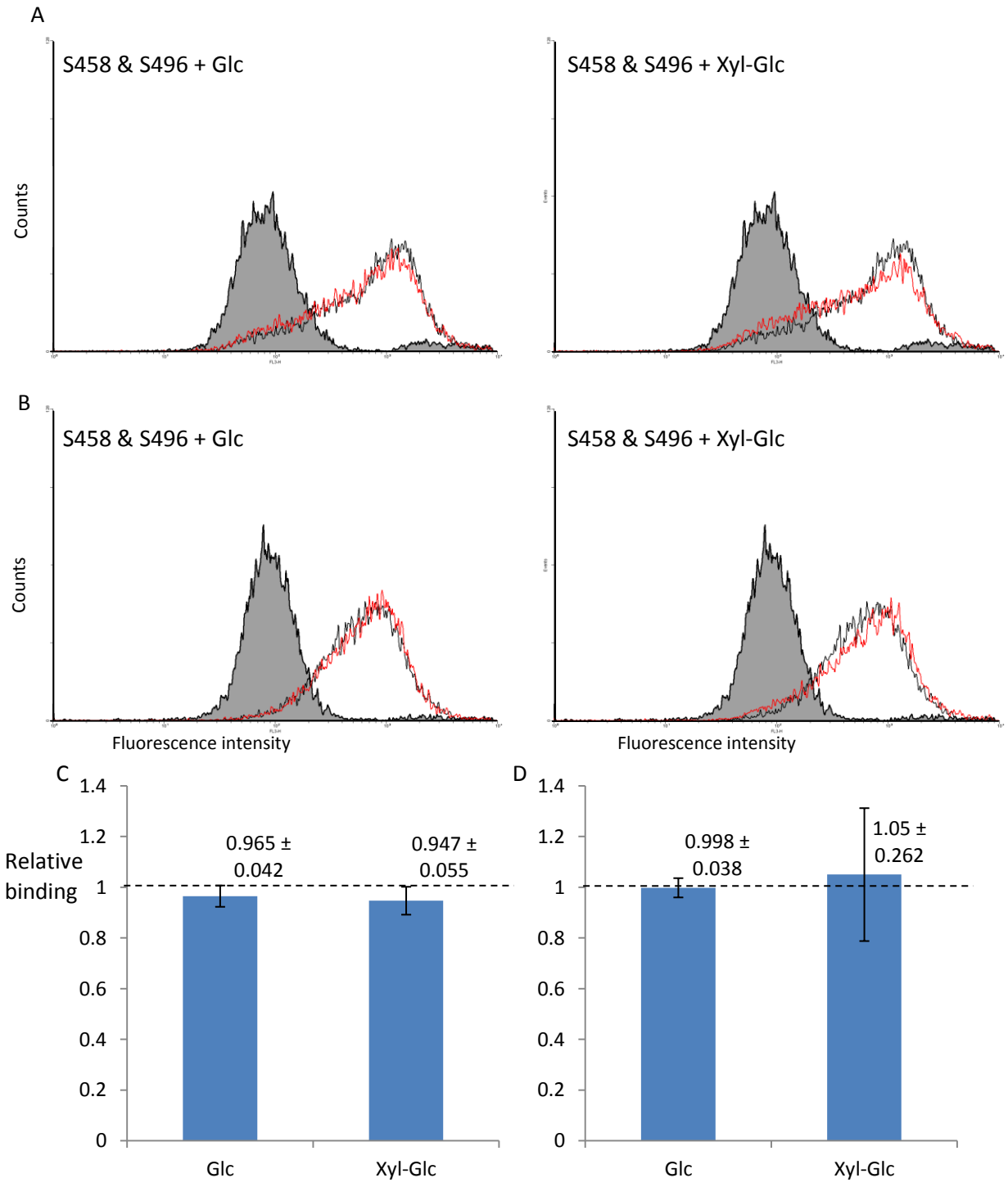


Figure 5-6 The effect of glucose modifications on binding to B16 mJagged1 and mDLL4 cells. Binding to fibrillin1 cbEGF12-14 is shown in grey, WT in black and $hN1_{11\text{-}13}$ with each sugar modification in red. Binding to neither B16 mJagged1 cells (A), nor B16 mDLL4 cells (B) was affected by the addition of glucose or xylose-glucose to the two O-glucosylation sites within $hN1_{11\text{-}13}$ (S458 and S496). C-D) Quantitative analysis of the effect of each of the sugar modifications on binding ($n \geq 3$ for each modification), with mean and 95% confidence limits indicated.

In addition to testing the effect on binding of each of these modifications individually, it was also possible to assay binding for $hN1_{11-13}$ modified at multiple O-glycosylation sites. Glucose and xylose-glucose were added to residues S458 and S496 for $hN1_{11-13}$ modified with fucose or GlcNAc-fucose at T466. For T466 modified with fucose or GlcNAc-fucose, neither the addition of glucose, nor its extension with xylose had any effect on binding to Jagged1 (Figure 5-7).

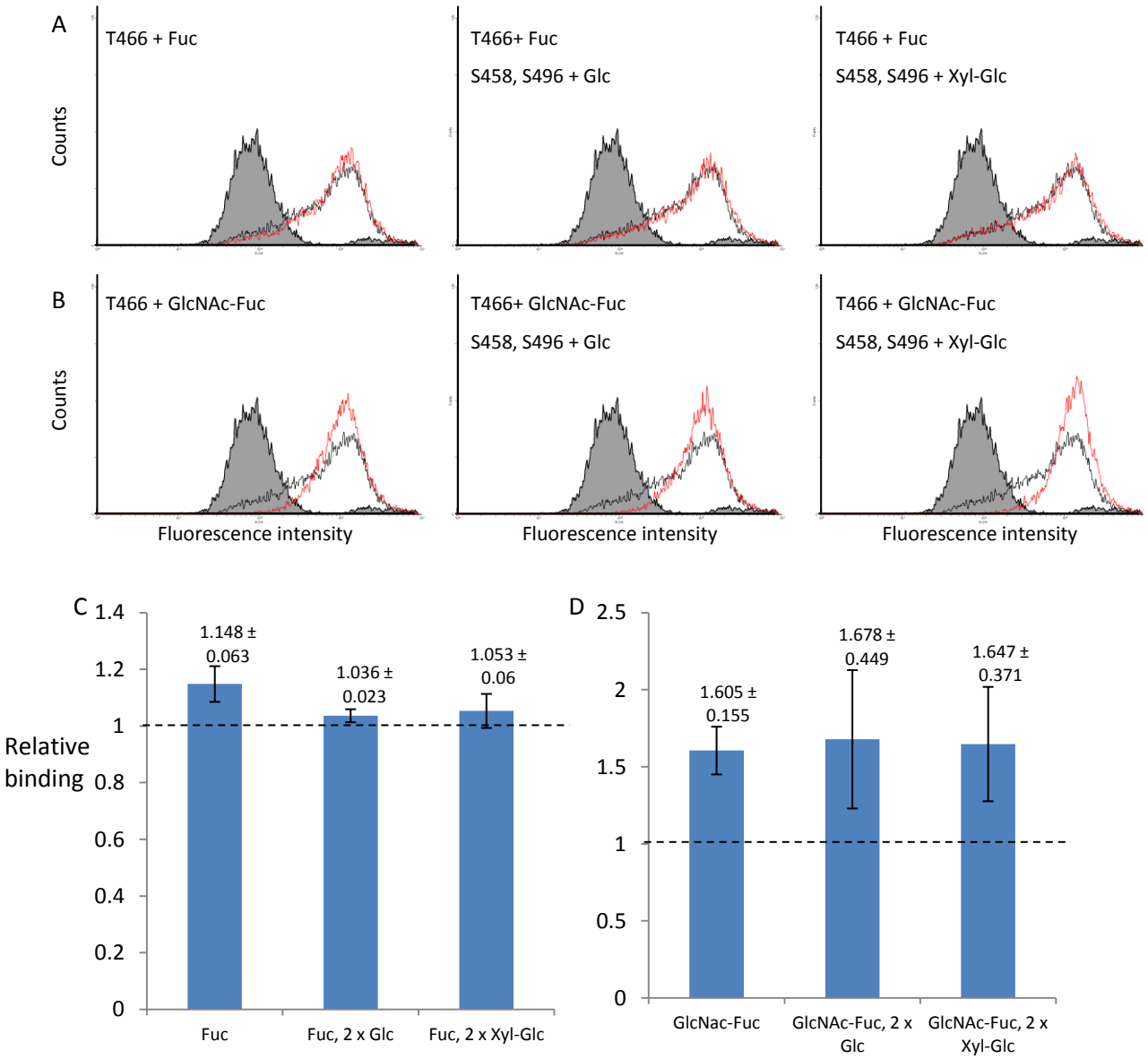


Figure 5-7 The effect of combinations of sugar modifications on binding to B16 mJagged1 cells. Binding to fibrillin1 cbEGF12-14 is shown in grey, unmodified $hN1_{11-13}$ in black and $hN1_{11-13}$ with each sugar modification in red. A-B) Adding glucose or xylose-glucose at S458 and S496 did not further alter binding of $hN1_{11-13}$ modified with fucose (A) or GlcNAc-fucose (D) at T466. C-D) Quantitative analysis of the effect of each of the sugar modifications on binding ($n \geq 3$ for each modification), with mean and 95% confidence limits indicated, for T466 modified with the monosaccharide (C) and disaccharide (D).

In order to confirm that the changes in binding to mJagged1 seen in the flow cytometry experiments above are representative of the human system, each of the sugar modifications was tested for binding against HEK293 hJagged1 cells (Figure 5-8). As in the previous chapter, it was necessary to gate a selection of these cells in order to see a single population (see Section 4.3.4), and the R1 population of cells was used to monitor the effects of the sugar modifications on binding to hJagged1. The addition of fucose to T466 had little effect in binding, whereas the addition of GlcNAc-fucose led to an increase in binding. When these modifications were tested in combination with the O-glucosylation modifications, there were no further changes in binding. It is possible that this assay is not able to detect the subtle changes in binding seen for the B16 mJagged1 cells because it is necessary to select a particular population of cells by using gating, but overall the trends are the same – that the addition of the GlcNAc-fucose disaccharide to T466 causes a large increase in binding to Jagged1.

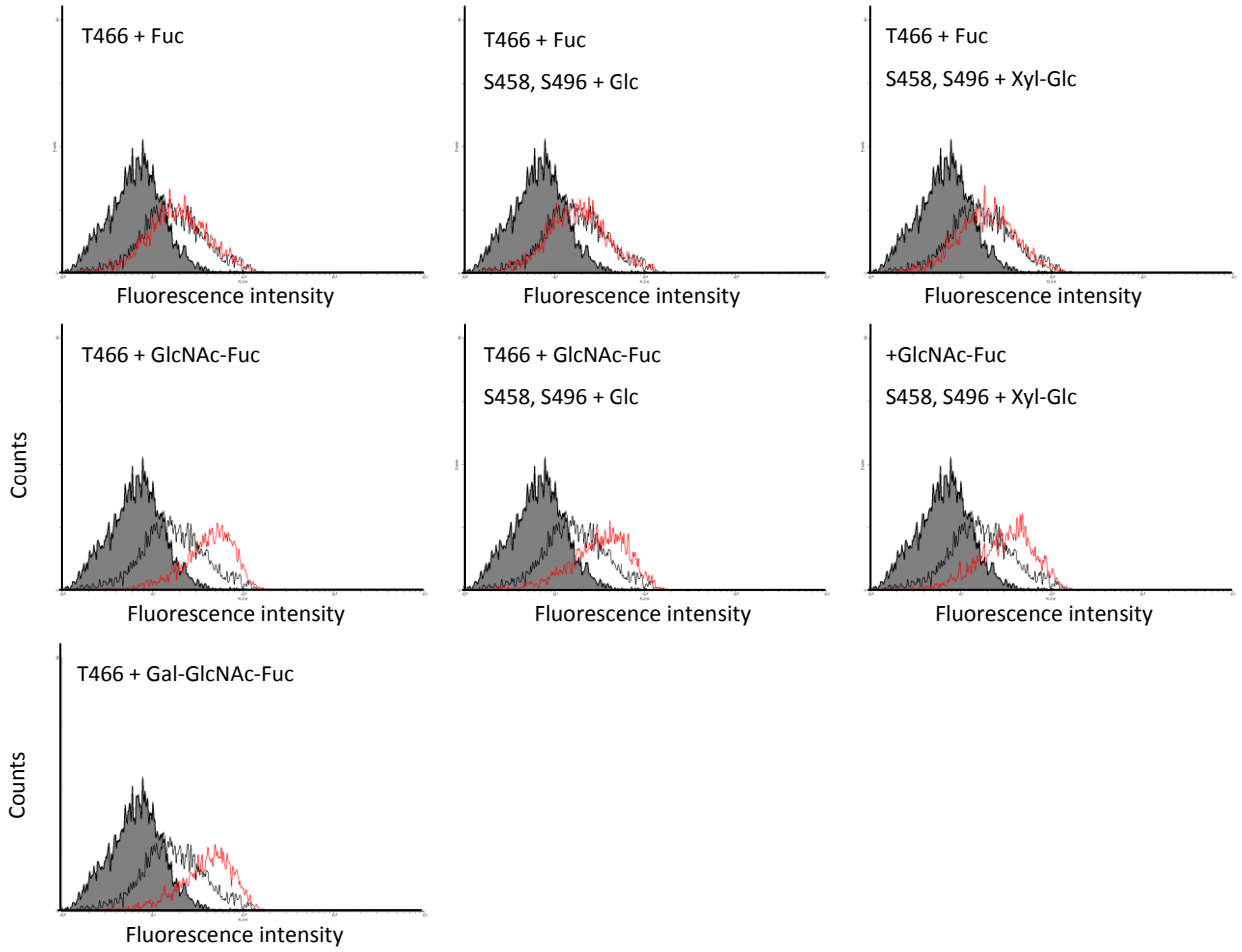


Figure 5-8 The effect of fucose modifications at T466 on binding to HEK293 hJagged1 cells. Binding to fibrillin1 cbEGF12-14 is shown in grey, unmodified $hN1_{11\text{-}13}$ in black and $hN1_{11\text{-}13}$ with each sugar modification in red. The R1 gate was applied to these data (see Section 4.3.4). The addition of fucose had a minimal effect on binding, whereas extension with GlcNAc led to a large increase in binding. The extension of the GlcNAc-fucose sugar with galactose had no further effect on binding. The addition of glucose or xylose-glucose to S458 and S496 had no further effects on binding.

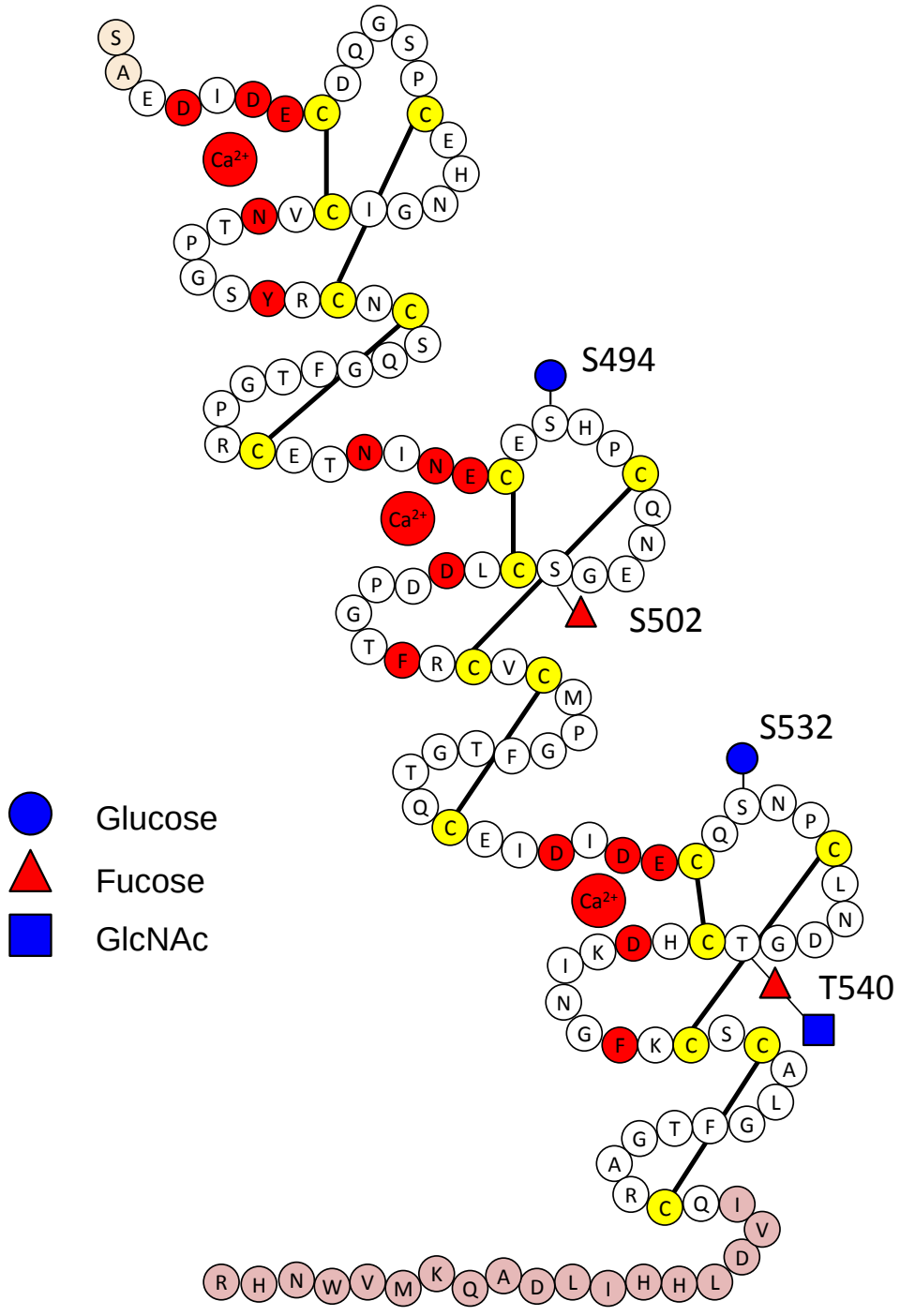


Figure 5-9 Glycosylation sites and sugar modifications made to dN$_{11-13}$. There are a total of four predicted glycosylation sites within dN1$_{11-13}$. Both EGF12 and EGF13 contain the consensus sequences for the addition of both O-fucose and O-glucose. Whilst it was possible to add fucose to each domain, it was only possible to extend this with GlcNAc in domain 13 (i.e. T540), and the fucose attached to S502 remained as a monosaccharide.

5.3.2 The effect of sugar modifications on the *Drosophila* Notch/Serrate interaction

The dN_{11-13} minimal binding fragment was used as the substrate for glycosylation, and as the reference against which to test the effect that individual sugar modifications had on binding. This construct contains four separate sites for O-linked glycosylation: O-glucosylation sites at S494 and S532, and O-fucosylation sites at S502 and T540 (Figure 5-9). It was possible to attach the monosaccharide to both O-fucosylation sites, but it was only possible to extend one of these sites with GlcNAc using Fringe. Both O-glucosylation sites were successfully modified with glucose. The effect of the modifications on binding was tested in the same flow cytometry assay using as described in Chapter 4.

Neither the addition of the O-fucose sugars to S502 or T540 in dN_{11-13}, nor the extension of one of these sugars with GlcNAc had any visible effect on binding to S2 Serrate-GFP cells (Figure 5-10). However, it was not possible to determine which O-fucose sugar had been extended with GlcNAc. Therefore the dN_{11-13} S502A protein that had been used in the earlier binding studies (see Section 5.2.2) was used as a substrate for glycosylation, as this protein lacks the O-fucosylation site in EGF12. It was possible to attach the GlcNAc-fucose disaccharide to T540 in EGF13, which suggests that in the earlier binding experiments, EGF12 was modified with the monosaccharide only.

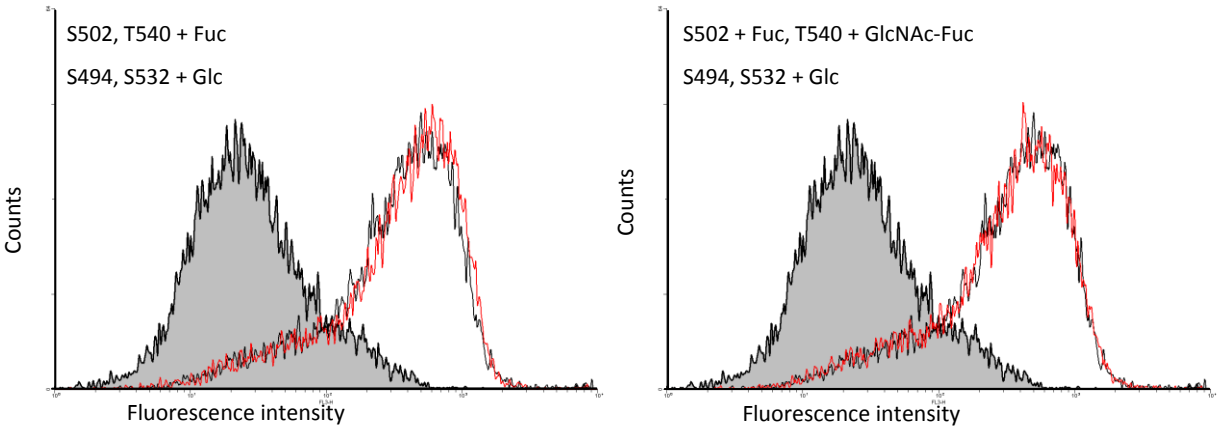


Figure 5-10 The effect of sugar modifications in dN_{11-13} on binding to S2 Serrate-GFP cells. Binding to fibrillin1 cbEGF12-14 is shown in grey, unmodified dN_{11-13} in black and dN_{11-13} with each sugar modification in red. The experiment was set up in the same way as in Chapter 4. None of the sugar modifications had any measurable effect on binding, though it was only possible to attach the O-fucose monosaccharide to S502.

5.4 Surface Plasmon Resonance

The flow cytometry-based binding experiment, that was used to map the ligand binding site in hNotch1, was able to identify how the addition of different sugars to $hN1_{11\text{-}13}$, and each of the T466 substitutions affected binding to Jagged1. The changes seen in this assay were interpreted as either an increase or decrease in binding. However, this assay is only semi-quantitative, and therefore in order to quantify the changes in binding caused by these various modifications, a surface plasmon resonance (SPR) assay was developed. Binding to a fragment of hJagged1 or hDLL4 was measured for proteins modified with the O-fucose monosaccharide and disaccharide, as well as each of the T466 substitutions, and compared to $hN1_{11\text{-}13}$ WT. The physical basis of the SPR phenomenon and the experimental setup for this experiment are outlined below.

5.4.1 The Surface Plasmon Resonance phenomenon

Light shone at the boundary between two different materials can either be refracted or reflected, depending on the angle of incidence of the light. At relatively small angles of incidence, light is refracted as it passes from one medium to another (Figure 5-11 A). As the angle of incidence is increased it reaches a critical angle, at which the light is no longer refracted but instead undergoes total internal reflection, and when plane-polarised light is used an evanescent wave resulting from the electromagnetic field component of the incident light can penetrate a short distance beyond the interface between the two media, parallel to the plane of polarisation of the incident light (Figure 5-11 B). If an inert metal foil (such as gold) is placed at the boundary between the two materials, this evanescent wave can interact with valence electrons within the metal, inducing a surface plasmon wave in the metal foil (Figure 11 C). At the appropriate wavelength of light and at an angle of incidence greater than the critical angle, the frequency of the evanescent wave can match the resonant frequency of the surface plasmons in the metal sheet, leading to the Surface Plasmon Resonance (SPR) effect (Figure 5-11 D). At this angle of incidence, the amount of light reflected is reduced, leading to a reduction in the signal seen at a detector. This angle of incidence is called θ_{SPR},

and depends on the refractive index between the two materials, which is in turn affected by changes in the local environment at the interface between the two materials.

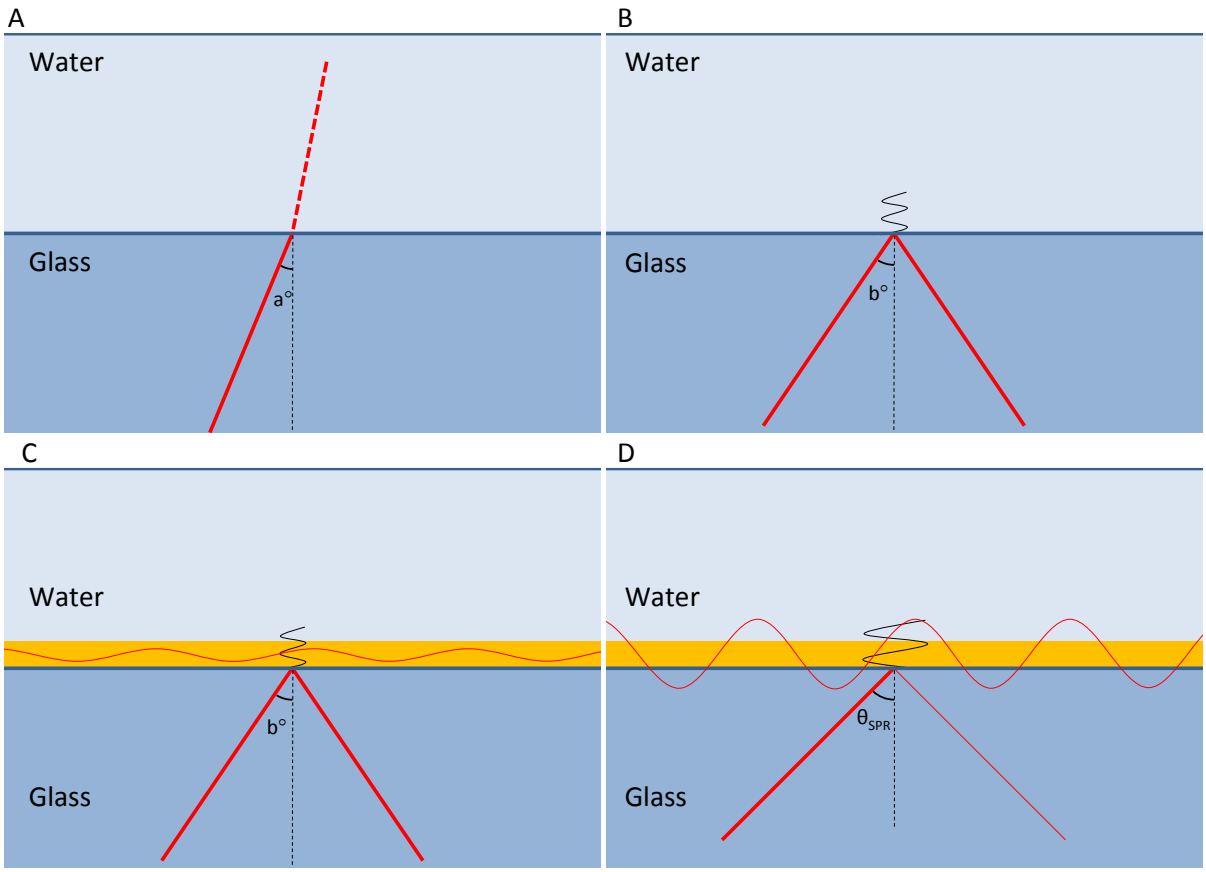


Figure 5-11 The Surface Plasmon Resonance phenomenon. The behaviour of light shone at the interface between two biological molecules is dependent on the angle of the incident light, and the refractive index between the two materials. A) At small angles of incidence (a°), the light is refracted. B) As the angle of incidence increases there reaches a point where the light is reflected (b° = $\theta_{crit)}$ rather than refracted. This induces an evanescent wave to emanate into the medium, which can induce a surface plasmon (C) when a metal foil is placed at the interface between the two materials. D) When the angle is increased beyond θ_{crit}, the frequency of the evanescent wave can match that of the resonant frequency of the surface plasmon (θ_{SPR}), causing the Surface Plasmon Resonance phenomenon. This leads to a reduction in the intensity of the reflected light at that angle.

5.4.2 The BIAcore system

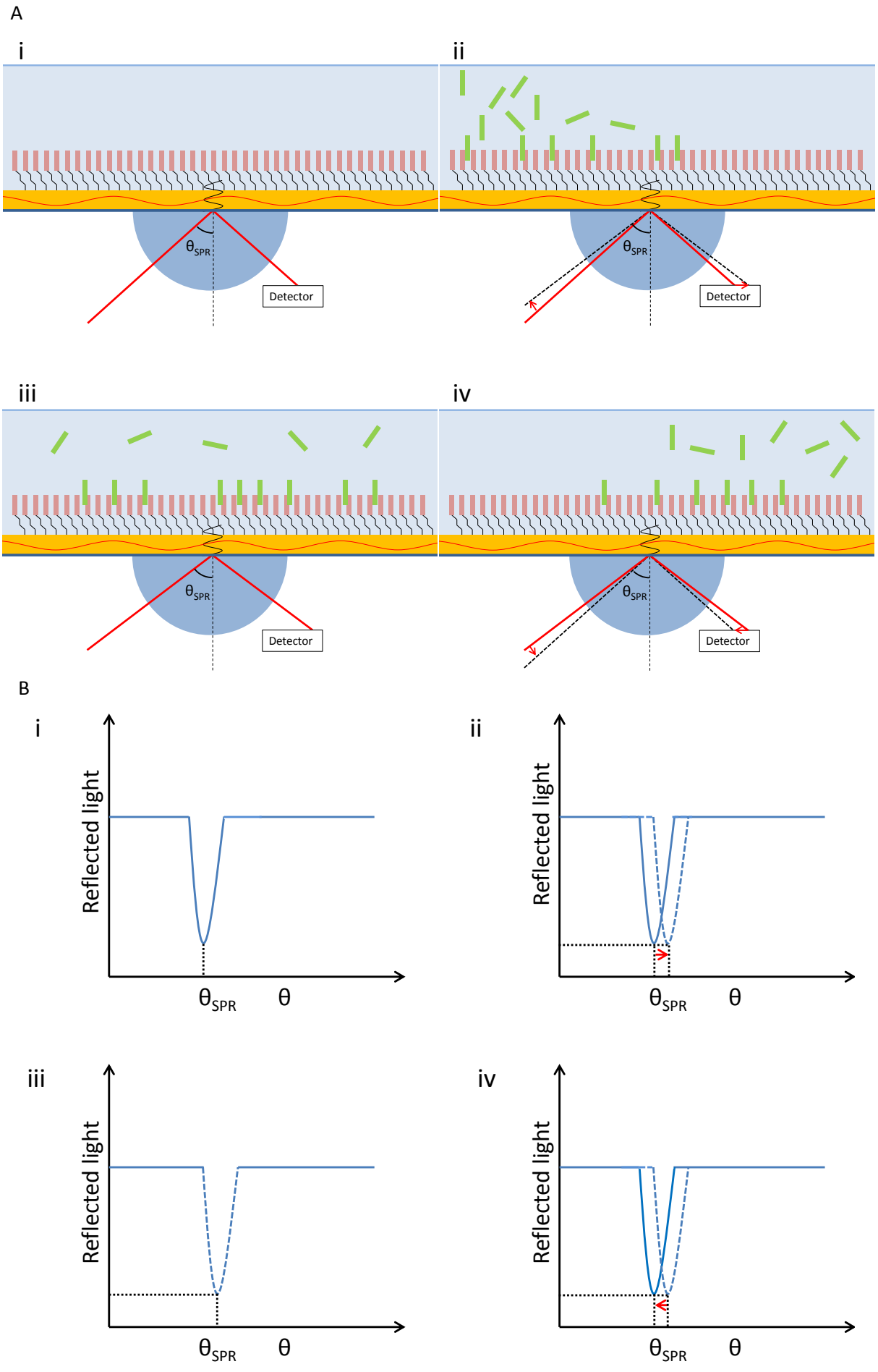
In a BIAcore system, the gold sheet is coated with a dextran matrix, and one of the binding partners can be covalently immobilised to this (Figure 5-12 A-i). The level of protein immobilised on the dextran matrix provides a set 'Response Unit' (RU) value, defined by θ_{SPR}, and defines the baseline for all binding experiments (Figure 5-12 B-i, C-i). The soluble ligand is then flowed over the immobilised protein, and its binding to the immobilised protein can be measured directly and in real-time using a BIAcore system.

Binding of the ligand to the immobilised protein causes the refractive index (and hence the angle required for SPR) at the interface between the buffer and the glass to increase (Figure 5-12 A-ii). This increases the angle required for θ_{SPR}, which means that the angle that corresponds to dip in the intensity of reflected light increases (Figure 5-12 B-ii). This change in angle is monitored at the detector as a change in RU: an increase in RU of 10^4 corresponds to a 1° increase in θ_{SPR}, which corresponds to 1 ng/mm^2 of protein binding to the surface of the chip (Figure 5-12 Cii).

Once the flow of ligand over the immobilised protein is halted, ligand bound to the protein immobilised on the chip dissociates from the dextran surface, and the refractive index decreases (Figure 5-12 A-iv). This corresponds to the θ_{SPR} and RU value returning to the pre-injection level (Figure 5-12 B,C-iv).

In order to calculate the relative affinities of the protein-protein interactions, it is possible to calculate the rate of association and dissociation, or allow the system to reach an equilibrium level of binding where the rate of association (k_{on}) is equal to the rate of dissociation (k_{off}). All of the SPR data recorded in order to determine how glycosylation or a T466 substitution affected binding to Jagged1 were based on equilibrium binding measurements at set concentrations – at equilibrium the rates of association (k_{on}) and dissociation (k_{off}) are equal.

$$[P] + [L] \underset{k_{off}}{\overset{k_{on}}{\rightleftharpoons}} [P.L]$$


A
i
ii
iii
iv
θSPR
Detector
B
Reflected light
θSPR
θ

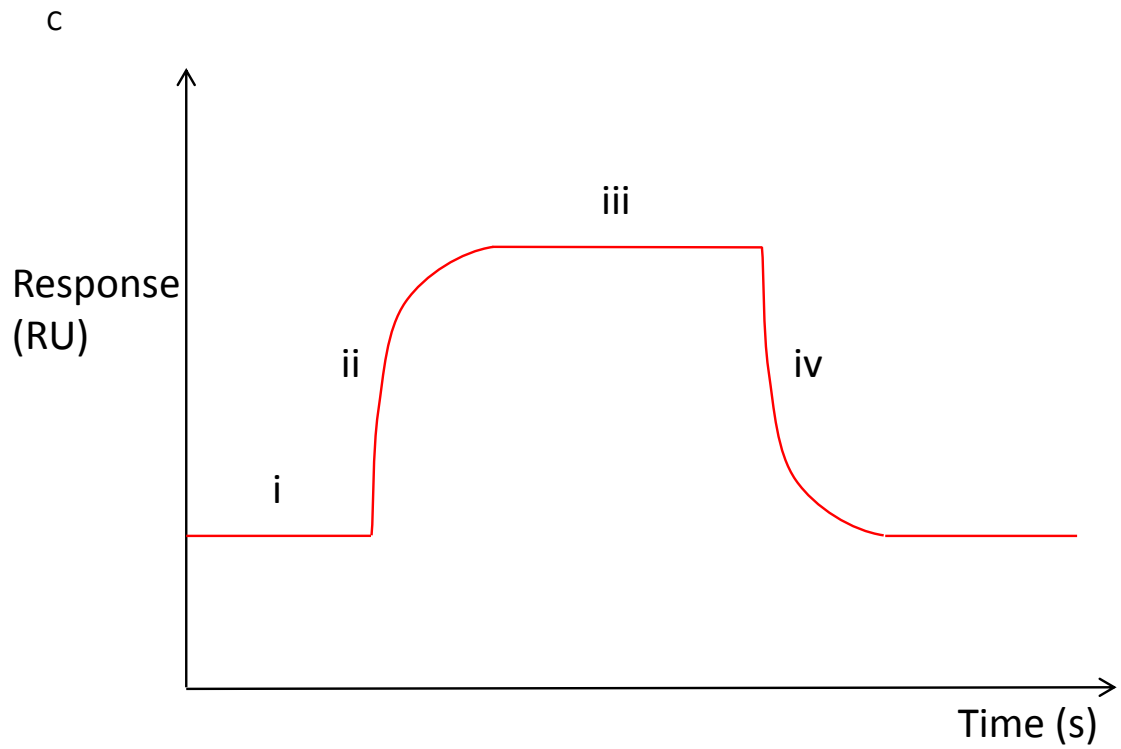


Figure 5-12 How Surface Plasmon Resonance can be used to measure binding in biological systems. The four stages of the interaction – i) equilibration, ii) association, iii) equilibrium and iv) dissociation are shown in three different ways. A) A representation of the ligand-protein interaction within the flow cell, with the immobilised protein (pink) covalently attached to the biological matrix (black lines), and the ligand flowing over the surface from left to right. B) How the changes in the refractive index at the interface between the two materials leads to a change in θ_{SPR}. Ligand binding to the immobilised protein causes an increase in the refractive index at the interface between the buffer and the glass, and hence θ_{SPR} to increase until equilibrium is reached, followed by the ligand dissociating and θ_{SPR} returning to its pre-injection value. C) Protein binding can be followed in real time by monitoring the change in θ_{SPR} over time, and converting the change in the angle to 'Response Units' (RU) over time, which can be displayed graphically.

5.4.3 The BIAcore binding assay

In order to investigate the changes in binding caused by substituting T466 for alanine, valine or serine, or adding sugars at this site, a quantitative binding assay was developed using a BIAcore T3000 system. Several attempts had previously been made to develop a binding assay using a minimal binding fragment from hJagged1 (DSL-EGF3) made using a prokaryotic expression system. It was found that the affinity of the interaction between this construct and $hN1_{11-13}$ was insufficiently high for this to be a viable approach, as $hN1_{11-13}$ protein concentrations in the 100 μM range were required to see any binding response above the experimental noise (data not shown). A longer fragment of hJagged1 that included the MNNL domain (see Chapter 3), was found to have a sufficiently high affinity for $hN1_{11-13}$ to be used in this assay. The equivalent construct from hDLL4 was used; the DLL4 protein was expressed and purified by Dr Chandramouli Chillakuri. Both the Jagged1 and DLL4 proteins were immobilised at a level of approximately 3000 RU in channels 2 and 4 respectively via amine coupling (see Section 2.15), whilst flow cell 1 was activated by NHS/EDC and inactivated by ethanolamine in order to provide a control surface for this experiment. The Notch proteins were tested for binding by injection onto the chip using the KINJECT injection method, and the chip was regenerated with a 15 μl injection of SPR buffer containing 3 mM EDTA in between each injection. Stock solutions of each of the proteins tested for binding were made by dissolving lyophilised protein in SPR buffer containing 1 mM $CaCl_2$ (see Section 2.15), and the concentration of each protein solution was measured in duplicate by Nanodrop.

5.4.4 Measuring the effect of the modifications at T466 on binding to hJagged1

Despite numerous attempts, it was not possible to perform a titration in order to calculate a K_D for the interaction between $hN1_{11-13}$ and hJagged1 MNNL-EGF3-Fc, as it was not possible to reach a saturated level of binding. Therefore in order to measure the effect of the various modifications at T466, equilibrium binding was measured for each of the proteins and compared to $hN1_{11-13}$ WT at set concentrations. This is a valid method for assessing the relative binding affinities for each of the proteins, as at the concentrations selected the response is still within the linear region of the binding

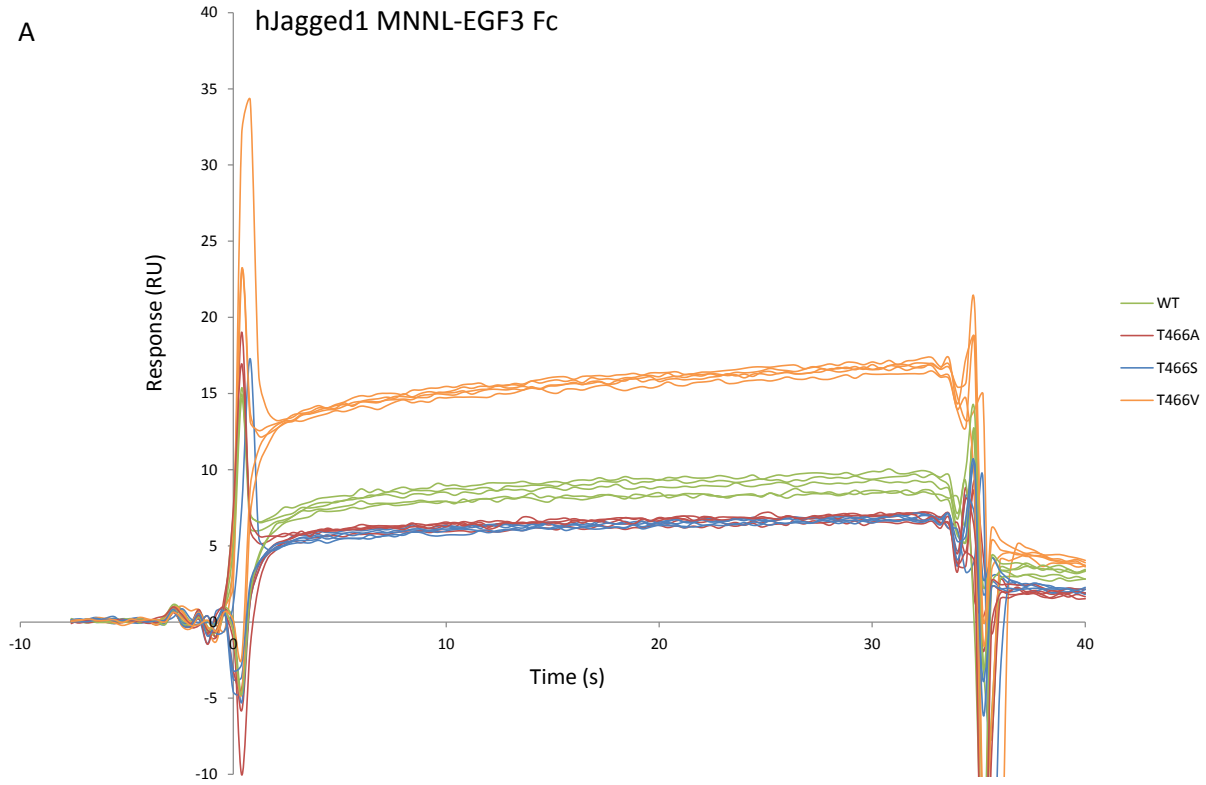
curve for each of these proteins. Each of the $hN1_{11-13}$ proteins were dissolved in SPR buffer to a final concentration of 10 μM, and binding was tested a total of five times for each protein.

The equilibrium binding interaction was measured for each protein. The response in the reference channel was subtracted from the response in the Jagged1 channel in order to remove the contribution from non-specific binding of $hN1_{11-13}$ to the surface of the chip, and the changes in refractive index that occur when a protein solution is injected over a flow cell. The remaining binding response was recorded and the equilibrium binding level was measured for each separate injection. A 10 μM protein solution was made independently five times for each of the proteins for injection over the chip, and the mean and standard deviation for each protein were calculated and compared to $hN1_{11-13}$ WT. After the binding experiments had been completed, a further injection of $hN1_{11-13}$ WT was performed in the presence of 10 mM EGTA in order to confirm the calcium-dependence of the interaction, and no binding was observed for any of these proteins (not shown).

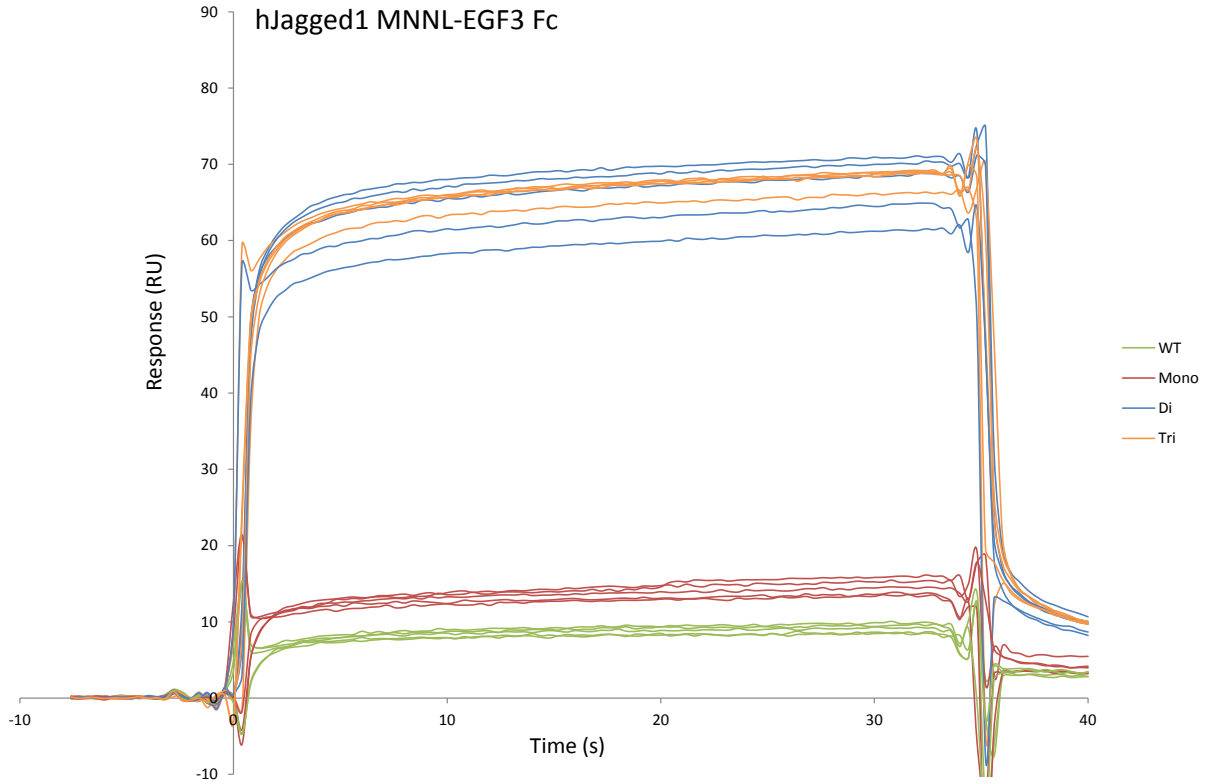
Both the T466A and T466S substitutions caused a 25% reduction in binding, while the T466V substitution caused a 100% increase in binding to hJagged1 MNNL-EGF3, compared to $hN1_{11-13}$ WT (Figure 5-13 A). This agrees well with the results of the flow cytometry experiments (see Section 5.2.1), although the T466V substutition had no apparent effect on binding to cells expressing Jagged1 in these experiments. This suggests that the changes in binding caused by amino acid substitutions in the previous chapter could be interpreted as genuine changes in the affinity of the Notch-ligand binding interaction.

The binding of the proteins containing the sugar modifications within EGF12 also showed a similar pattern in the SPR to the flow cytometry experiments using cells expressing Jagged1. The addition of the fucose monosaccharide (Mono) to EGF12 led to a small (50%) increase in binding to Jagged1 MNNL-EGF3, whereas the addition of the GlcNAc-fucose disaccharide (Di) led to a much larger (700%) increase in binding (Figure 5-12 B). Further elongation of this sugar with galactose had no further effects on binding (Tri).

A


hJagged1 MNNL-EGF3 Fc
Response (RU)
Time (s)
WT
T466A
T466S
T466V

B


hJagged1 MNNL-EGF3 Fc
Response (RU)
Time (s)
WT
Mono
Di
Tri

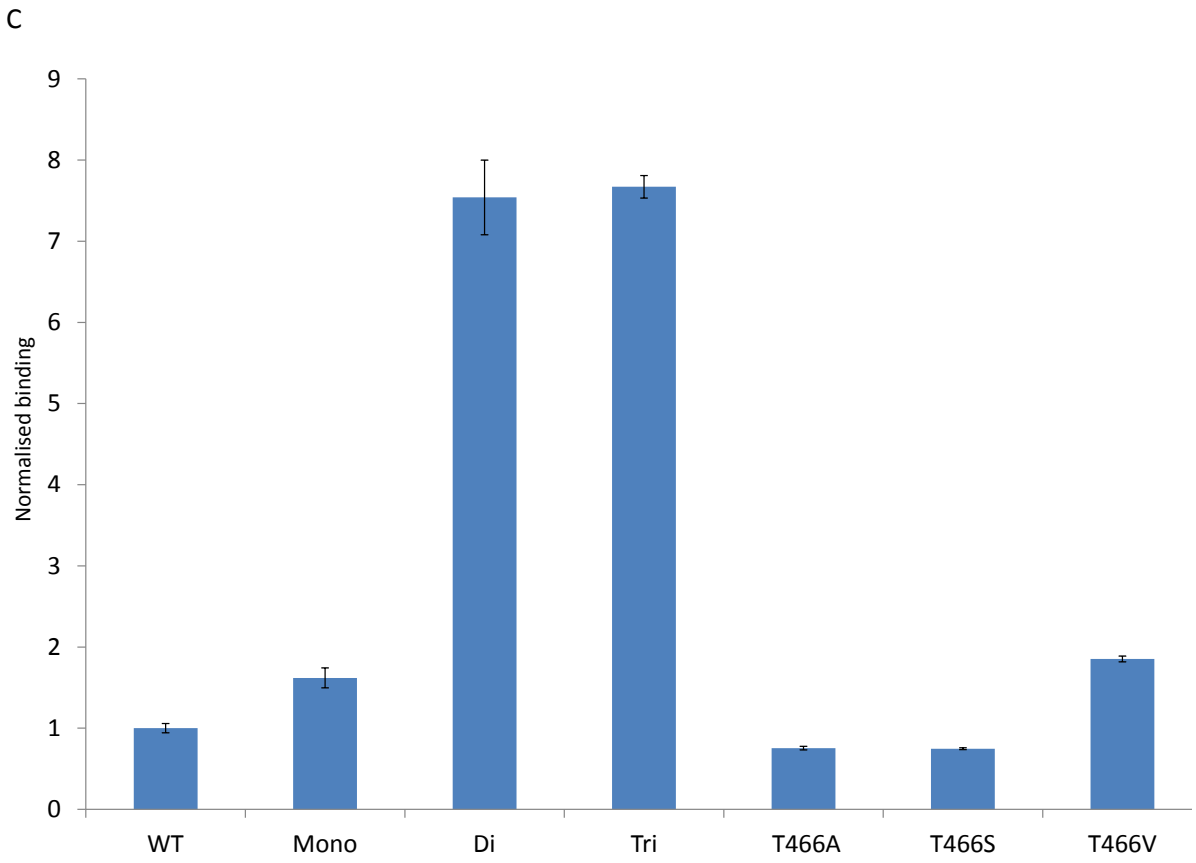


Figure 5-13 Equilibrium binding data to hJagged1 MNNL-EGF3-Fc for T466 substitutions, and sugar modifications. A) Binding was measured (n = 5) for $hN1_{11-13}$ with each of the T466 substitutions at a constant protein concentration of 10 μM. B) Binding was measured (n = 5) for $hN1_{11-13}$ modified with each of the O-fucose sugars at T466 at a constant protein concentration of 10 μM. C) Equilibrium binding was measured for each injection, and the response was normalised against unmodified $hN1_{11-13}$ WT. Mono = fucose, Di = GlcNAc-fucose, Tri = galactose-GlcNAc-fucose (see Section 1.7).

5.4.5 Measuring effect of the modifications at T466 on binding to hDLL4

During preliminary experiments, it was noticed that the response seen for the binding of unmodified $hN1_{11-13}$ to hDLL4 MNNL-EGF3 Fc was far higher than that seen for binding to hJagged1 MNNL-EGF3 Fc, despite the fact that both proteins had been immobilised in their respective flow cells at a similar level. The effect on binding of $hN1_{11-13}$ containing each of the T466 substitutions to hDLL4 was measured in a similar way to hJagged1. Each of the proteins were dissolved at 10 μM, and binding was measured as outlined above. Binding of the T466A protein was indistinguishable from WT. The T466S substitution caused a small increase in binding, and the T466V substitution caused a much

larger increase in binding (Figure 5-14 A). This differs from the earlier flow cytometry experiments, which suggested that none of these substitutions had any measurable on binding.

It was decided that rather than try and measure how equilibrium binding was affected by the sugar modifications at T466, that a K_D would be measured for $hN1_{11-13}$ modified with each of the sugars. A range of concentrations was tested for binding to DLL4 for each of the Notch proteins, in order to determine an upper concentration, above which there was no further increase in binding, and a lower concentration, below which there was no detectable binding. Based on these observations, a titration series was performed for each protein over a range of concentrations that lay between these two points – unmodified $hN1_{11-13}$ was tested for binding between 20 μM and 1.25 μM, $hN1_{11-13}$ + fucose was tested between 10 μM and 610 nM, and each of the other two proteins was tested between 4 μM and 250 nM. Each of these proteins bound well to hDLL4 over the range of concentrations tested, but it was not possible to fit a K_D to the data obtained for any of these proteins using this method. For the data collected for this assay, see Appendix B.

Whilst it was not possible to calculate K_D values for this interaction, it is possible to draw some conclusions about how glycosylation at this position affects binding to DLL4 based on the binding measurements performed at 10 μM (Figure 5-14 B). Unmodified $hN1_{11-13}$ binds well to DLL4, and appears to have a much higher affinity for this ligand than for Jagged1. The addition of the fucose monosaccharide increased binding, and the extension of this sugar with GlcNAc increase binding further still. It was not possible to detect and differences between the binding of $hN1_{11-13}$ modified with either the disaccharide, or the trisaccharide using this assay. The addition of the disaccharide or trisaccharide also ppears to decrease the rate at which protein dissociates from the surface of the chip. This is consistent for this interaction having a much higher affinity than either the unmodified material, or $hN1_{11-13}$ modified with O-fucose.

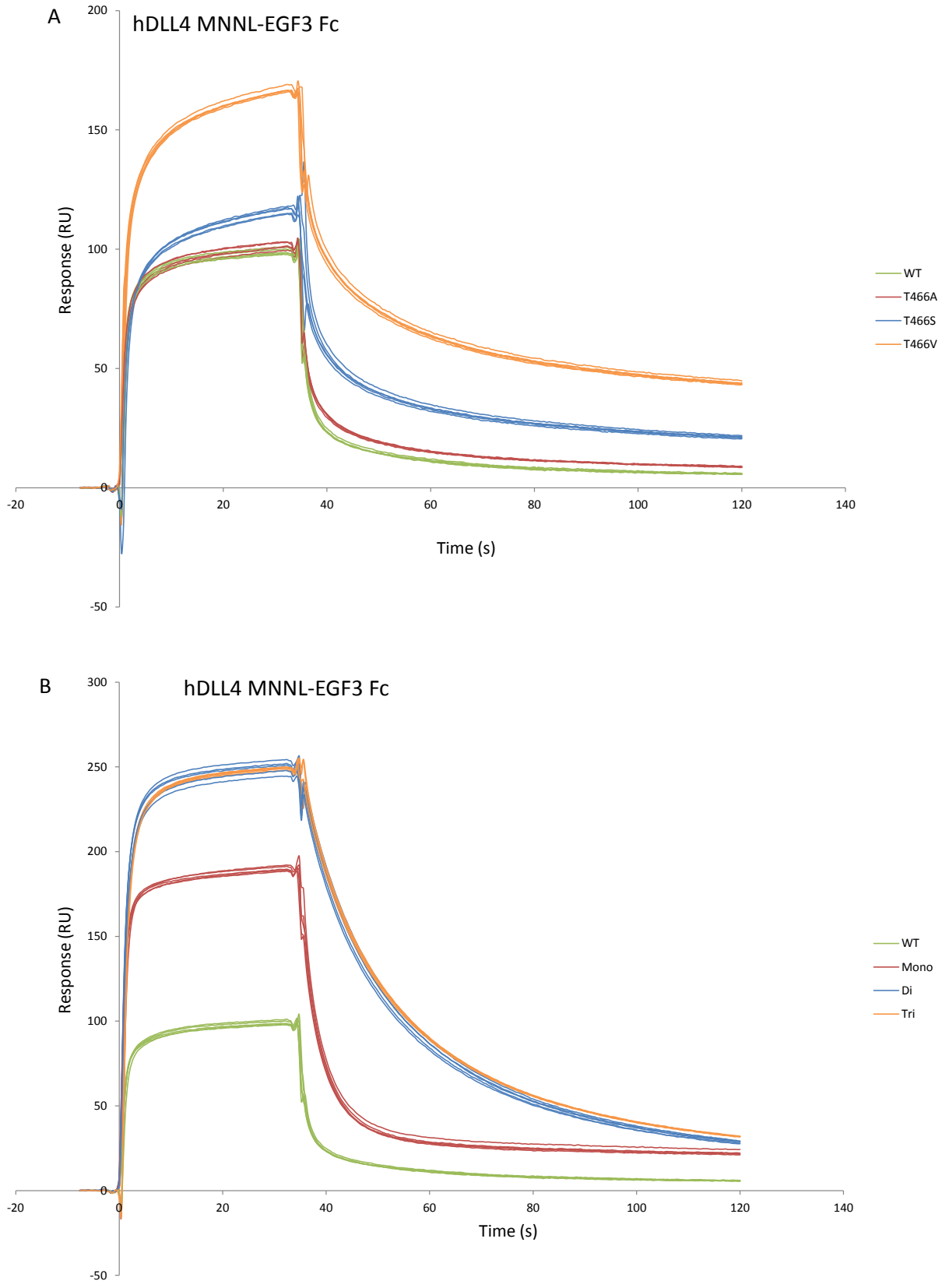


Figure 5-14 Binding to hDLL4 MNNL-EGF3 Fc of hN1$_{11-13}$ T466 substitutions and sugar modificaitons. A) Binding ws measured (n = 5) for hN1$_{11-13}$ with each of the T466 substitutions at a constant protein concentration of 10 µM. B) Binding was measured (n = 5) for hN1$_{11-13}$ modified with each of the O-fucose sugars at T466 at at constant protein concentration of 10 µM.

5.5 Structural effects of T466 substitutions

In order to investigate directly whether any of these substitutions had any effect on the structure of the central β-sheet of EGF12 that is implicated in ligand binding in the previous chapter, proteins containing each of the three T466 substitutions were set up in crystallisation trials.

5.5.1 Crystallisation of $hN1_{11-13}$ with T466 substitutions

Crystallisation of the purified hN_{11-13} proteins with substitutions at T466 was carried out by Dr Devon Sheppard and Prof. Susan Lea. Crystals were obtained by vapour diffusion, using the sitting drop method. Proteins containing each of the T466 substitutions were dissolved in 10 mM $BaCl_2$ to a final concentration of 16 mg/ml, and initially screened with the Stura FootPrint and MacroSol Screens (Molecular Dimensions) by mixing 0.2 μl of protein solution with mother liquor to a final concentration of either 50% or 70% protein solution for each crystallisation condition. Crystals for each protein appeared within a week at 293 K, at 100 mM ammonium acetate pH 4.5, 22.5% (w/v) PEG 10,000, with similar crystal morphology to that seen when $hN1_{11-13}$ was crystallised. Data were collected at the Diamond Synchrotron Light Source, and the structures were solved by molecular replacement using the published structure of $hN1_{11-13}$ WT – pdb 2VJ3 (Cordle *et al.*, 2008).

5.5.2 Substituting T466 does not significantly alter the structure of EGF12

When structures of each of the mutant proteins were compared with the WT protein, both the peptide backbone of EGF12, and the relative orientation of the three domains within the fragment were unchanged from WT for all three mutants (Figure 5-15). Aside from the T466 residue that was substituted, the relative positions and packing interactions made by the amino acid side-chains were also largely unchanged. This demonstrates that the changes in binding to Jagged1 seen in both the flow cytometry and BIAcore experiments were not due to any changes in intramolecular structure, but are instead due to local changes in the surface chemistry of the protein that arise from the substitution of the amino acid side-chains via mutagenesis.

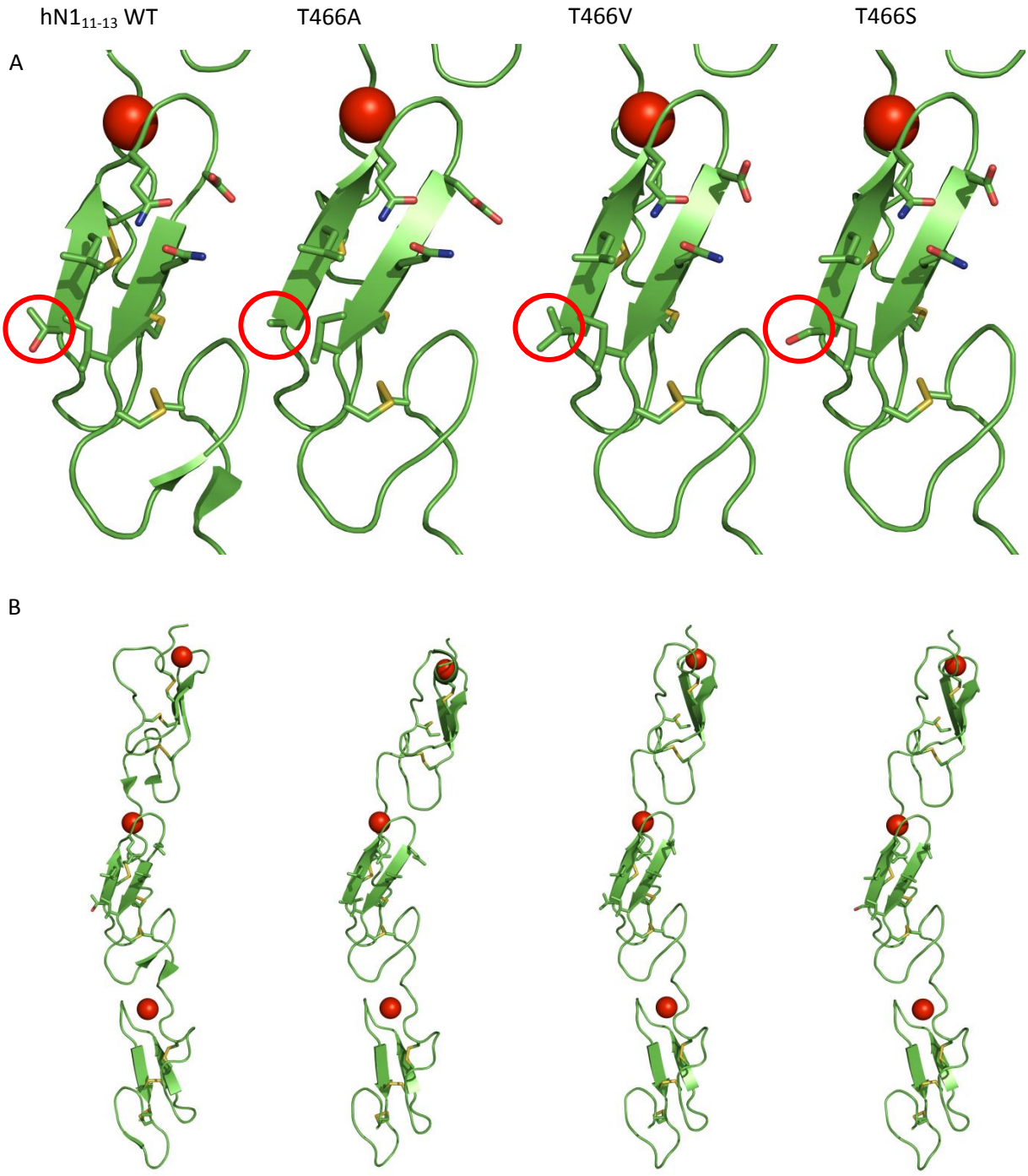


Figure 5-15 The structural effects of the substitutions at T466 in hN1$_{11-13}$. Crystal structures of the central β-hairpin within EGF12 (A), and the peptide backbone of hN1$_{11-13}$ (B) are shown side-by-side. There are no significant changes in the structure of EGF12, and the amino acid side-chains that are implicated in ligand binding in the previous chapter are unaffected by the substitutions (shown as sticks). In addition to this, the overall structure of hN1$_{11-13}$ is unaffected by these substitutions.

5.6 Structures of sugar-modified $hN1_{11\text{-}13}$

The only previous high resolution structural data for EGF12 of hNotch1 modified with sugars was recorded in the context of an isolated EGF12 domain, and in the absence of calcium (Hiruma-Shimizu *et al.*, 2010). This study compared the solution structure of the unmodified protein with the solution structures of the protein modified with fucose, and GlcNAc-fucose at T466, and showed that the addition of the sugars caused a conformational change in the protein (see Figure 1-11). This study concluded that the conformational changes that arise as a result of the addition of sugar modifications to T466 might represent a mechanism for how glycosylation of EGF12 can regulate Notch signalling.

5.6.1 The requirement for structural data for EGF12 in its native context

As the previous solution structure was obtained for an isolated cbEGF domain in the absence of calcium, it is not clear whether the changes that arise as a result of the addition of sugar modifications at T466 represent the changes that would occur when these modifications are added to EGF12 in its native context i.e. in the presence of calcium and flanked by EGF domains 11 and 13. X-ray crystallographic structural data for $hN1_{11\text{-}13}$ carrying the sugar modifications, where EGF12 is in its native context and in the presence of a Ca^{2+} (or Ba^{2+}) should indicate the orientation of the sugars relative to the ligand binding site identified in the previous chapter, and show how the sugars interact with the protein, and potentially affect intramolecular structure. $hN1_{11\text{-}13}$ modified with the fucose monosaccharide or GlcNAc-fucose disaccharide were selected for crystallisation.

5.6.2 Crystallisation of glycosylated $hN1_{11\text{-}13}$

Crystallisation trials were carried out as for the proteins with amino acid substitutions at T466. Crystals for each protein appeared under the same crystallisation conditions as above, and with similar morphology. Structures were solved to a resolution of 1.8 Å for $hN1_{11\text{-}13}$ modified with fucose, and at 1.6 Å for $hN1_{11\text{-}13}$ modified with GlcNAc-fucose.

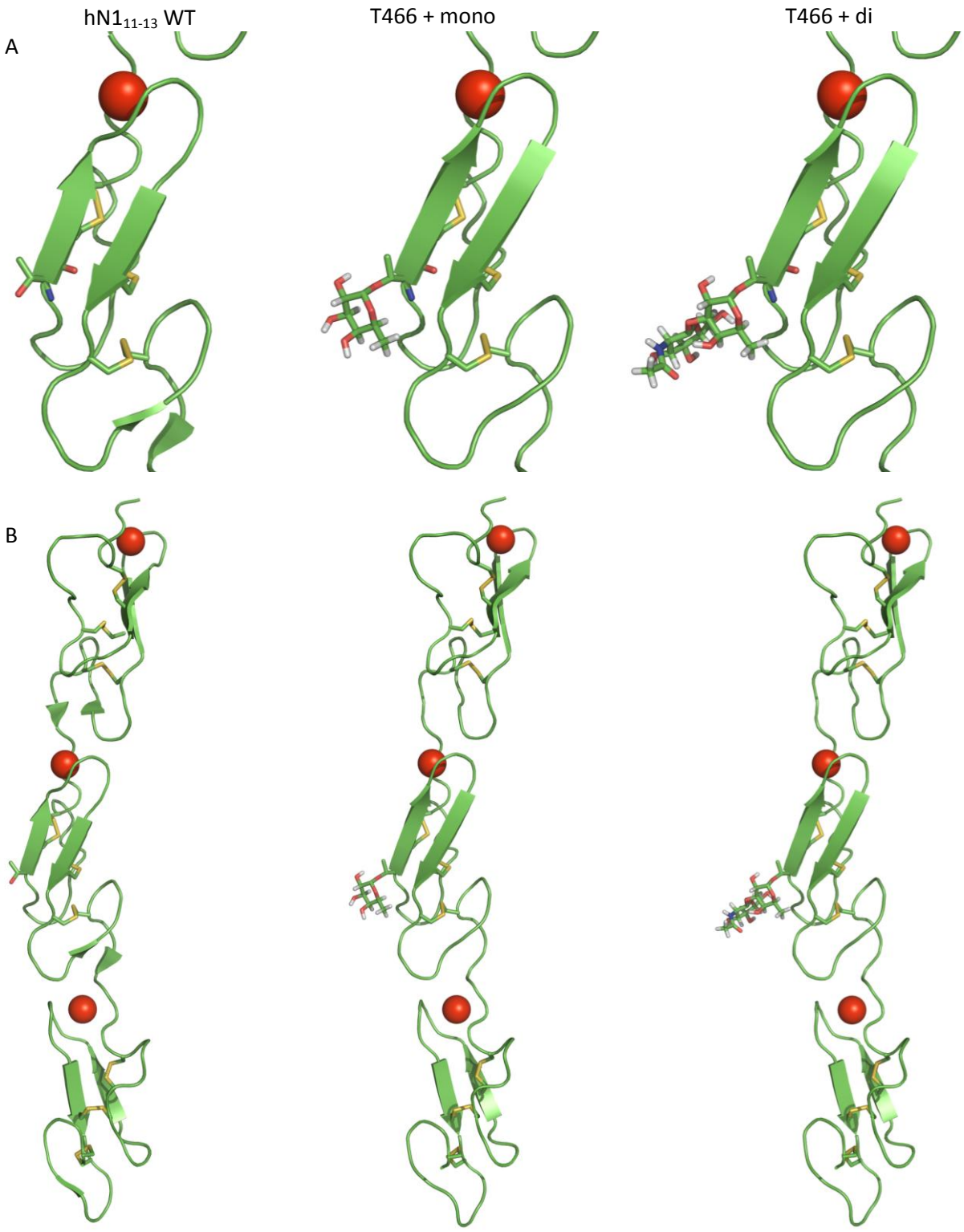


Figure 5-16 Structures of hN1$_{11-13}$ modified with a monosaccharide and disaccharide at T466, compared with the unmodified hN1$_{11-13}$. A) Neither the addition of the monosaccharide, nor the disaccharide, has any effect on the structure of EGF12. In particular, the central β-hairpin implicated in ligand binding in the previous chapter is unchanged. B) There is no change in the overall shape of hN1$_{11-13}$ as a result of the addition of these sugars. The fucose sugar points away from the central β-sheet in EGF12, and extension with GlcNAc extends further away from this face of the protein.

5.6.3 The effect of sugar-modifications on the structure of $hN1_{11-13}$

Each of the structures of $hN1_{11-13}$ modified with sugars at T466 was compared with the structure of the unmodified protein, in order to see whether the addition of these sugars induces a conformational change in the protein (Figure 5-16). In both cases the structure of EGF12 in the protein modified with a sugar at T466 was unchanged when compared to the structure of the unmodified protein, and neither the peptide backbone nor the orientation of the side chains within this domain were affected by the addition of the sugar at T466. The orientation of domains EGF11 and EGF13 with respect to EGF12 were also unchanged for the glycosylated proteins, and the inter-domain packing interactions were also unaffected.

In the structures of $hN1_{11-13}$ with either modification at T466, the fucose sugar projects away from the central β-sheet in EGF12 (Figure 5-16 B). The addition of GlcNAc to the fucose at the C3 position extends the modification in the same direction away from the EGF domain (Figure 5-16 C). Both of these sugars appear to be fairly rigid, as they are both clearly visible in the electron density for the structures of the modified material (Figure 5-17). It is likely that the orientation of the sugars relative to EGF12 is determined by the interactions that the sugars make with the protein. The C6 methyl group from the fucose sugar packs against the hydrophobic side-chains from I477 and M479. Elongation of the sugar with GlcNAc creates further sugar-protein interactions, as its C6 CH_2OH group packs against D464, and the N-Acetyl group packs against M479 and P480 (Figure 5-18 A). It is interesting that the orientation of these sugars and the interactions that they make with the protein closely resemble that of the solution structure of the isolated EGF12 domain modified with the disaccharide (Figure 5-18 B).

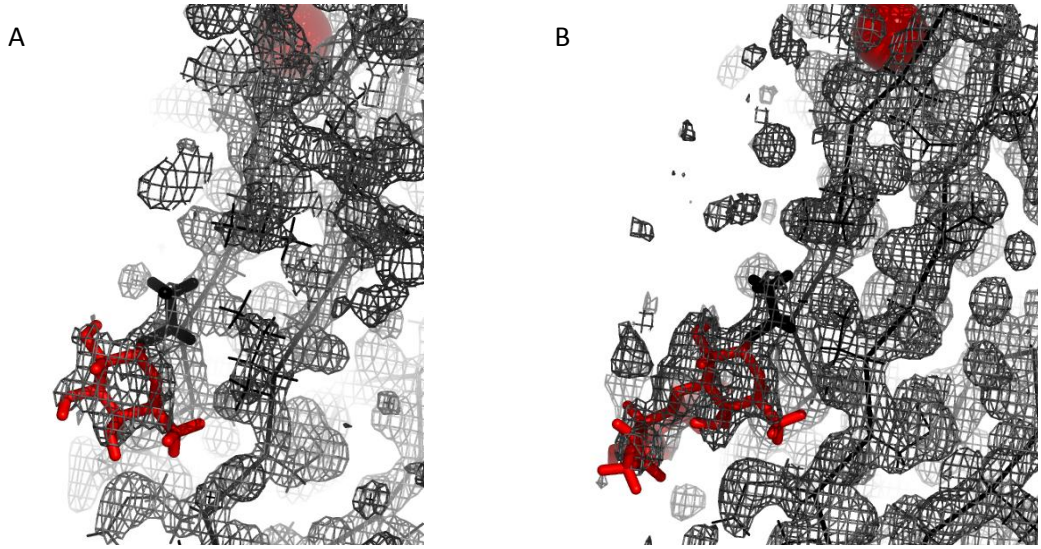


Figure 5-17 Electron density map for EGF12 of hN1$_{11-13}$ modified at T466. The position of the both the monosaccharide (A) and disaccharide (B) is clearly visible in the electron density maps for the structures of the glycosylated material, indicating that the sugars adopt rigid structures.

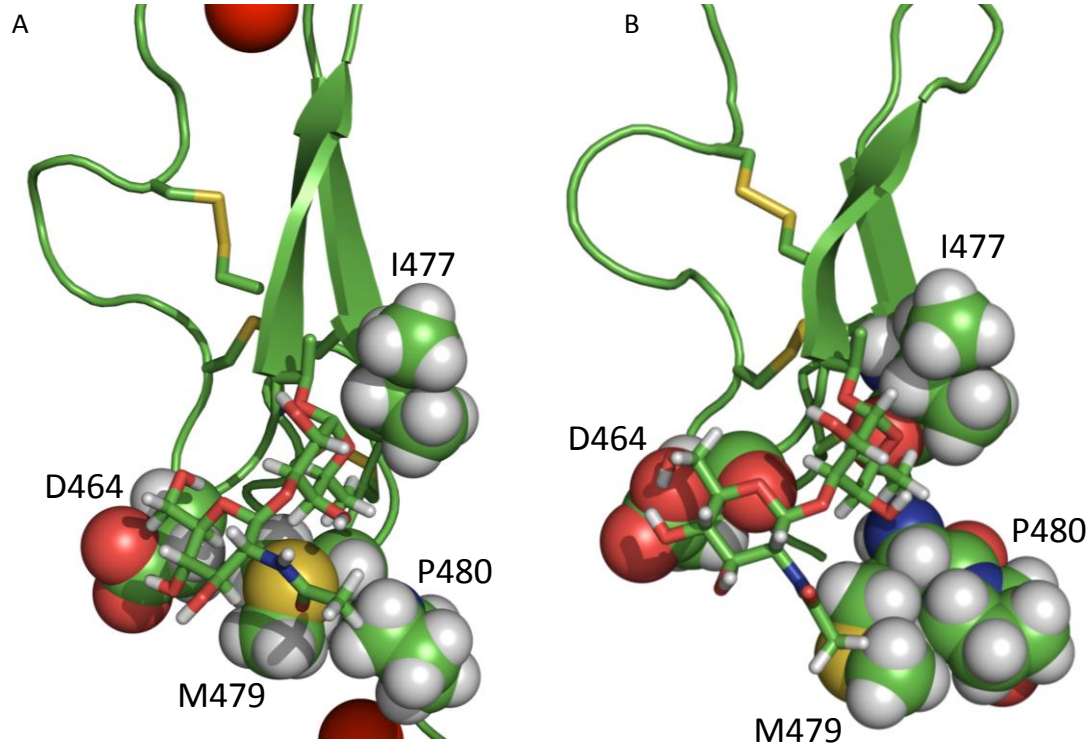


Figure 5-18 The packing of the disaccharide against residues in EGF12. The sugar modifications to EGF12 form extensive packing interactions with amino acid side chains within the protein. A) In the crystal structure of hN1$_{11-13}$ modified with the disaccharide the methyl group from the fucose sugar packs between the hydrophobic side-chains of I477 and M479, and the N-acetyl group from GlcNAc packs against M479 and P480. The hydroxyl groups from C5 and C6 from GlcNAc also contact D464. B) These interactions are also seen in the solution structure of the isolate domain modified with the disaccharide (pdb 2RQZ).

The conformational changes seen in the earlier structural study are not visible for the structures obtained for EGF12 within its native context. In this earlier study, the reported structure of the unmodified EGF12 domain is remarkably different to that of EGF12 modified with a disaccharide at T466 (Figure 5-19) (Hiruma-Shimizu *et al.*, 2010) and the solution structure of EGF12 with this modification is similar to that of EGF12 within $hN1_{11\text{-}13}$. This suggests that in the absence of calcium, the unmodified domain is not in a native-like fold, but that the addition of the disaccharide at T466 may stabilise the isolated domain and force it to adopt a conformation that is similar to the structure of this domain in its native context. This would explain the changes in the structure of EGF12 seen in this study, and suggests that the disaccharide might be able to stabilise the key ligand binding residues (L468 and I477) within EGF12 in the full-length molecule.

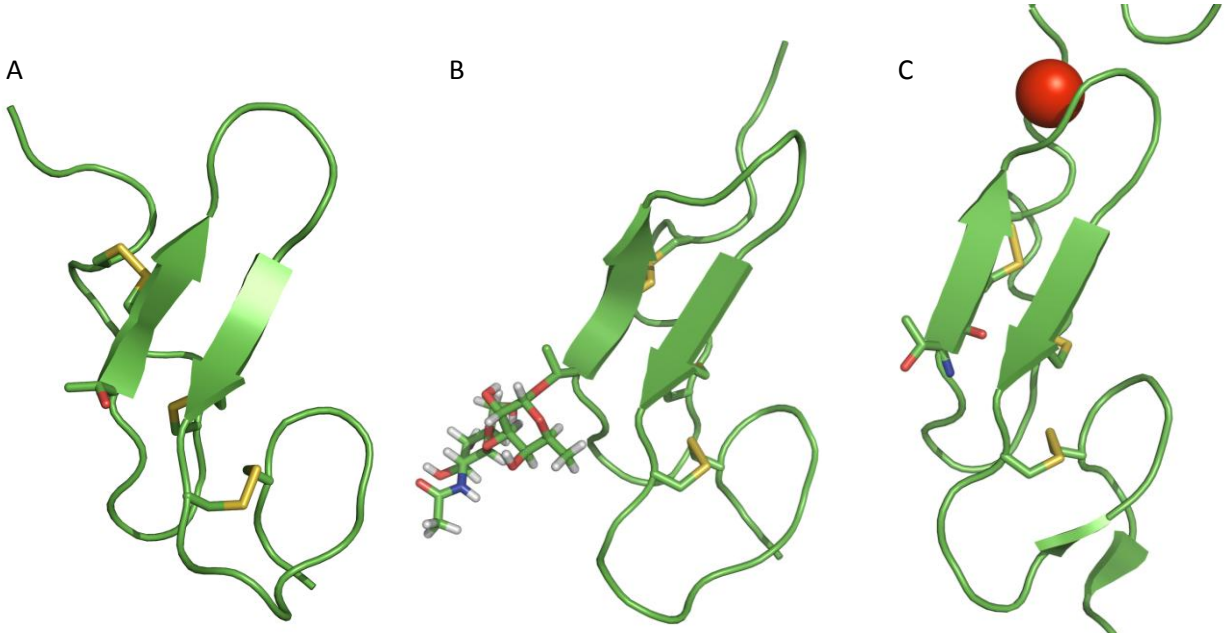


Figure 5-19 The solution structure of EGF12 + GlcNAc-fucose closely resembles the structure of EGF12 from $hN1_{11\text{-}13}$. The solution structure of the unmodified EGF12 domain (A) (pdb 2RR0) is remarkably different to that of the domain modified with the disaccharide (B) (pdb 2RQZ) and the crystal structure of EGF12 from $hN1_{11\text{-}13}$ (pdb 2VJ3) (C). This is because in its native context, EGF12 is stabilised by binding calcium in its N-terminus, and forms inter-domain packing interactions. The disaccharide is likely to stabilise the fold of the isolated domain in the absence of calcium.

5.6.4 The implications of the structures of modified $hN1_{11-13}$

The disaccharide modification to $hN1_{11-13}$ extends away from the ligand-binding site identified in the previous chapter, so it is not possible that the sugars modulate ligand binding by directly occluding the ligand binding site. Instead, the sugar extends the surface available for ligand binding (Figure 5-20 A-C), and it is likely that any ligand molecules contacting the residues in the central β-sheet in EGF12, would simultaneously contact the sugars on T466. This is in addition to the potential stabilisation of the restudies that form the core of the ligand binding site, caused by the protein-sugar contacts, as the CH_3 group from fucose and the N-acetyl group from GlcNAc could extend the hydrophobic surface that appears to be essential for ligand binding.

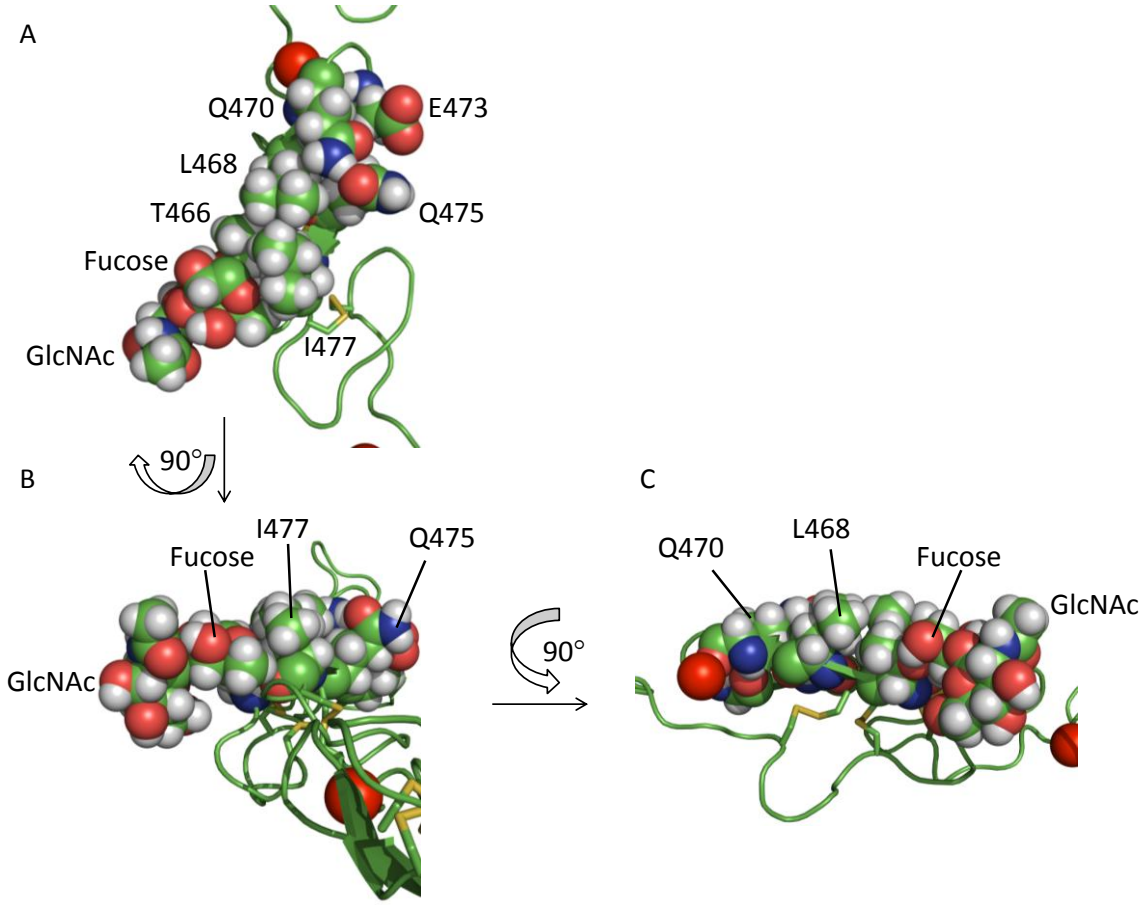


Figure 5-20 The extension of the ligand binding site by the disaccharide addition at T466. The addition of the disaccharide extends the ligand binding site, and increases the hydrophobic surface available for ligand binding. A-C) Rotations of the molecule to show the large flat hydrophobic surface available for ligand binding.

5.8 Conclusions

The aim of this chapter was to establish the effects that specific modifications to both hNotch1 and dNotch have on binding to the two Notch ligand families, within the context of the minimal binding fragment of each protein. These experiments used purified proteins that had been extensively characterised and were highly homogeneous. The effect of substituting the residue in EGF12 required for O-fucosylation (T466/S502) on binding has been established for prokaryotically expressed material that was refolded *in vitro*, showing that different substitutions can have different effects on binding. These findings are important for future functional studies that use mutants to study how glycosylation affects the function of the Notch receptor, as these substitutions are clearly able to alter binding, independently of any sugar modifications. The effect of *in vitro* glycosylation of $hN1_{11\text{-}13}$ and $dN_{11\text{-}13}$ with specific sugars has also established precisely how specific modifications within the ligand binding region of the Notch receptor are able to modulate ligand binding. In addition to this, it was possible to draw a direct comparison for the binding of $hN1_{11\text{-}13}$ to both hJagged1 and hDLL4 via SPR, which indicated that at the concentrations used in this assay $hN1_{11\text{-}13}$ may have a significant preference for binding to hDLL4. The structures of $hN1_{11\text{-}13}$ modified with sugars at T466 have also been obtained, which may rule out the possibility that the sugar modifications can directly occlude ligand binding.

Substituting the residues required for O-fucosylation in both $hN1_{11\text{-}13}$ and $dN_{11\text{-}13}$ was found to have varying effects on ligand binding. The T466A and T466S substitutions in hNotch1 decrease binding to Jagged1, whilst the T466V substitution binds at least as well as the WT protein when binding was assessed using the flow cytometry assay. These effects were confirmed in the SPR assay, which saw a 25% reduction in binding for the alanine and serine substitutions, and saw an increase in binding for the valine substitution. None of these modifications was found to affect binding to DLL4 in the flow cytometry assay. When binding was studied by SPR, it was found that none of the substitutions reduced binding, and the T466S and T466V substitutions were able to increase binding. This is

consistent with the results of the previous chapter, which showed that ligand biding requires a hydrophobic binding site in EGF12. The S502A substitution in dN_{11-13} was also found to have no effect on binding to Serrate, which is not surprising given the conservative nature of this substitution. Future studies that aim to establish how glycosylation of individual EGF domains can regulate Notch signalling by substituting the residue required for glycosylation should take into account the effect of the amino acid substitutions. For instance, The T→V substitution may be more appropriate than the T→A substitution, as this appeared to perturb binding to a lesser extent.

When the effects of the sugar modifications at T466 on binding were assessed by flow cytometry, the addition of the monosaccharide to $hN1_{11-13}$ was found to cause a small but reproducible increase in binding to Jagged1, and the addition of the disaccharide caused a much larger increase. Further extension of this sugar to the trisaccharide or tetrasaccharide was found to have no further effect on binding. This agrees well with the results of the SPR binding assay, which found that the addition of the fucose monosaccharide caused a 50% increase in binding to hJagged1 MNNL-EGF3 Fc, and the subsequent elongation with GlcNAc increased binding by 700% compared to the unmodified protein. Extending this sugar further with galactose to produce the trisaccharide showed no further effects on binding.

Whilst the data obtained in the SPR assay agreed well with the data obtained in the flow cytometry for Jagged1, the DLL4 data differed between the two assays. In the flow cytometry assay, none of these modifications was found to alter binding to DLL4, but when binding was measured in the SPR assay, the addition of the both the monosaccharide and disaccharide were found to increase binding to DLL4. The effect of the trisaccharide was indistinguishable from the disaccharide. In Section 5.4, it is apparent that the interaction between $hN1_{11-13}$ and DLL4 is substantially stronger than the interaction with Jagged1. This would mean that in the flow cytometry experiments that use B16 mDLL4 cells, unmodified $hN1_{11-13}$ binds to the DLL4 with a very high affinity, and therefore binding may already be at such a high level that any further increase caused by the addition of sugars to

$hN1_{11-13}$ will not be detected (Figure 5-21). It is possible that some of the apparent contradictions between previous studies into how glycosylation regulates Notch signalling (see Section 1.7.3 and Section 5.1) may have arisen for similar reasons; the relative levels of Notch or its ligands used in these studies may have masked changes in binding in certain cases.

The full extent of the increase in binding to DLL4 was not seen in the SPR experiments using 10 μM solutions of the proteins. Further experiments will need to be performed at lower concentrations in order to assess the full effect that this modification has on binding, and it would be desirable to do this by measuring the K_D for the interaction of both the unmodified, and disaccharide-modified $hN1_{11-13}$ protein with DLL4 in the future.

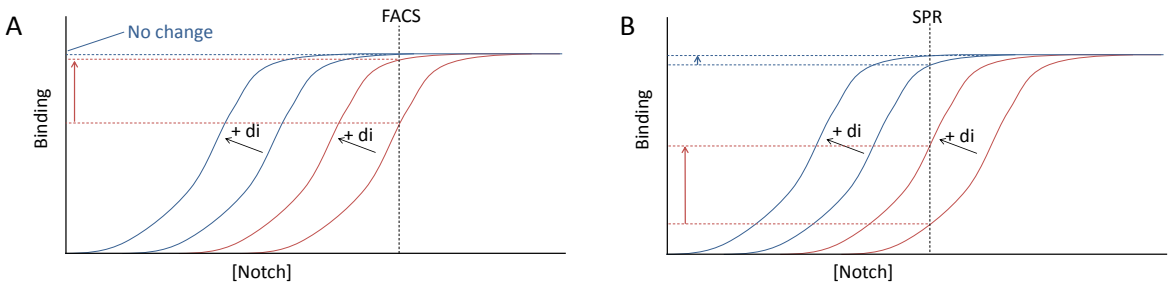


Figure 5-21 Illustration of a potential interpretation of the changes seen for Jagged1 and DLL4 binding to glycosylated vs unglycosylated $N1_{11-13}$. The effects of the addition of the GlcNAc-fucose sugar to $hN1_{11-13}$ on binding to Jagged1 (red) and DLL4 (blue) are shown. The addition of the disaccharide causes an increase in the affinity of the interaction with both ligands. A) In the flow cytometry experiments this increase is detected for Jagged1, but not for DLL4, due to the high affinity of the interaction with the unmodified protein. B) In SPR assays, the increased binding to both ligands is detected, but only a relatively small change in binding is observed for DLL4. Repeating these experiments at a much lower concentration of Notch protein will reveal the true extent of how this modification alters binding of $hN1_{11-13}$ to DLL4 (see Appendix B for additional SPR binding data).

The structure of the $hN1_{11-13}$ with the GlcNAc-fucose sugar attached indicates that the sugar extends linearly away from the ligand binding site, and forms extensive contacts with the protein that cause it to be rigid and adopt a well-defined structure. It is possible that these sugar-protein contacts may act to stabilise the EGF domain, but as there are no changes in the structure of $hN1_{11-13}$ when it is modified with GlcNAc-fucose at this position, the significance of this is not clear. This structure does

suggest however that the disaccharide is able to extend the ligand binding site within EGF12, in order to modulate ligand binding.

None of the sugar modifications attached to dN_{11-13} that were tested for binding to Serrate were found to have any effect, including the addition of GlcNAc-fucose to EGF13. However, it was not possible to extend the fucose sugar in EGF12 in sufficient quantities to test the effect of this modification on binding to Serrate.

Extension of O-fucose glycans with GlcNAc has previously been reported to reduce binding to Serrate (Haines and Irvine, 2003). A small amount of the disaccharide was detected at EGF12 of dN_{11-13} during the *in vitro* glycosylation process, and this modification has been observed in an isolated EGF12 domain, as well as in EGF12 within the full-length dNotch molecule (Prof. R. S. Haltiwanger, personal communication), so the extent to which EGF12 is modified with the disaccharide, and the significance of this modification in regulating Notch signalling *in vivo* is not clear. Given that the S502A substitution was found to increase the activation of dNotch by both Serrare and Delta, it is not clear whether the addition of the GlcNAc-fucose disaccharide at this position would alter binding to Serrate. However, given that the equivalent modification in hNotch1 alters binding to both classes of mammalian ligands studied here, this would appear to be likely.

Chapter 6

The effect of additional domains on ligand binding

6.1 Introduction

The ligand binding fragment spanning EGF domains 11-13 of hNotch1 has been shown to interact with both hJagged1 and DLL4 in the earlier chapters. In order to establish whether or not other domains within the Notch receptor modulate or are involved in ligand binding, a number of hNotch1 constructs of varying lengths were produced (Figure 6-1) and tested for binding using the same flow cytometry assay as in the previous chapters. A previous study has demonstrated that prokaryotically-expressed $hN1_{10-14}$ shows reduced binding to CHO cells expressing human Delta-like ligand 1 (hDLL1), compared to $hN1_{11-14}$, but that the loss of calcium binding from EGF11 can restore binding (Cordle *et al.*, 2008). These data indicate that EGF10 may somehow be involved in modulating the Notch-Delta interaction, but steric effects or misfolding could not be ruled out as the cause of this. The effect that this domain has on binding to Jagged1 has not yet been established, and the effect that additional domains beyond EGF10 have on binding to either ligand class is not clear. The aims of this chapter are to establish how EGF domains 9 and 10 affect binding to both Jagged1 and DLL4 using proteins produced using prokaryotic and eukaryotic expression systems, and to establish whether the addition of domains N-terminal to this region can further alter binding to either ligand class.

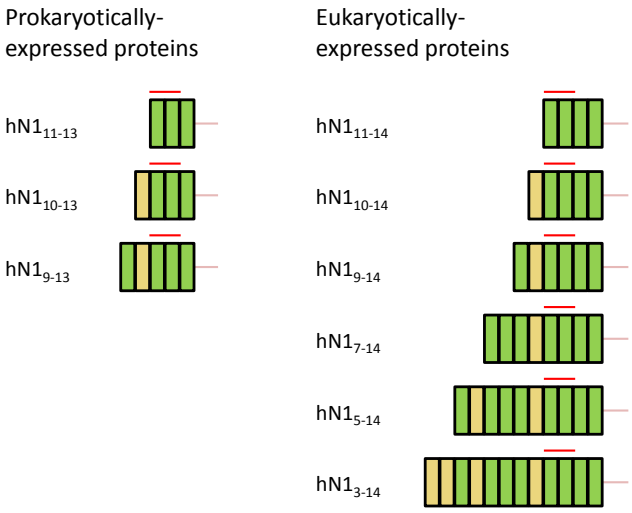


Figure 6-1 Diagram to indicate the domain architecture of the hNotch1 proteins used in the binding experiments in this chapter. A number of different truncated hNotch1 proteins were produced, using both a prokaryotic and eukaryotic expression system. EGF domains that contain the calcium binding consensus sequence are shown in green, non-calcium binding EGF domains are shown in tan. EGF domains 11 and 12 are indicated by the red bar.

6.2 Assaying the effects of longer prokaryotically-expressed hNotch1 constructs on binding

The effect that EGF domains 9 and 10 had on binding in the absence of any post-translational modifications was tested using the $hN1_{10-13}$ and $hN1_{9-13}$ constructs that had been produced using a prokaryotic expression system (see Chapter 3). Binding was tested using the same B16 cell lines as were used in the previous chapters, and compared with prokaryotically-expressed $hN1_{11-13}$. The level of protein loading for these experiments was confirmed to be even by Western Blot, to ensure that any changes in binding were not the result of unequal levels of protein being immobilised on the surface of the beads in the flow cytometry binding assay (Figure 6-2). A small degree of degradation was observed for $hN1_{9-13}$, which might decrease the overall level of protein available to participate in the binding interactions.

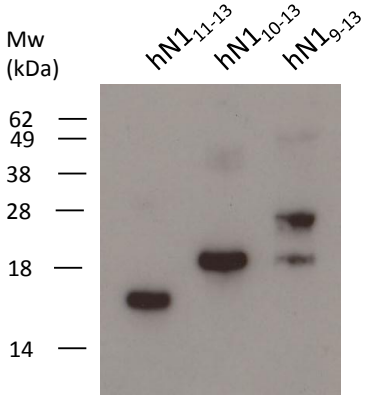


Figure 6-2 Western blot to show even loading of prokaryotically-expressed proteins used in these binding experiments. A small sample of beads from each of the samples was collected before the binding experiments were performed, and after heating with non-reducing Laemmli's buffer the proteins were run on a 16% SDS-PAGE gel and analysed by Western Blot using a streptavidin-peroxidase conjugate. The level of protein loaded for each sample appeared comparable, though there may be a small amount of degradation occurring for the $hN1_{9-13}$ construct.

6.2.1 Assaying binding of longer prokaryotically-expressed hNotch1 constructs to mJagged1

The $hN1_{10-13}$ construct bound to B16 mJagged1 cells less well overall than $hN1_{11-13}$. The addition of EGF9 reversed this: $hN1_{9-13}$ showed a slight enhancement in the overall level of binding to the B16 mJagged1 cells compared to $hN1_{11-13}$ (Figure 6-3). This suggests that EGF9 may have a role in stabilising EGF10. This overall increase in fluorescence seen for cells binding to $hN1_{9-13}$ was of a

smaller magnitude than seen for the increase caused by the addition of the GlcNAc-fucose disaccharide to $hN1_{11-13}$ in the previous chapter, but it is possible that this could also represent an increase in the affinity of the binding interaction. Further experiments using these prokaryotically-expressed proteins will be required to understand whether this is a genuine increase, or is an indirect change arising from this experimental system.

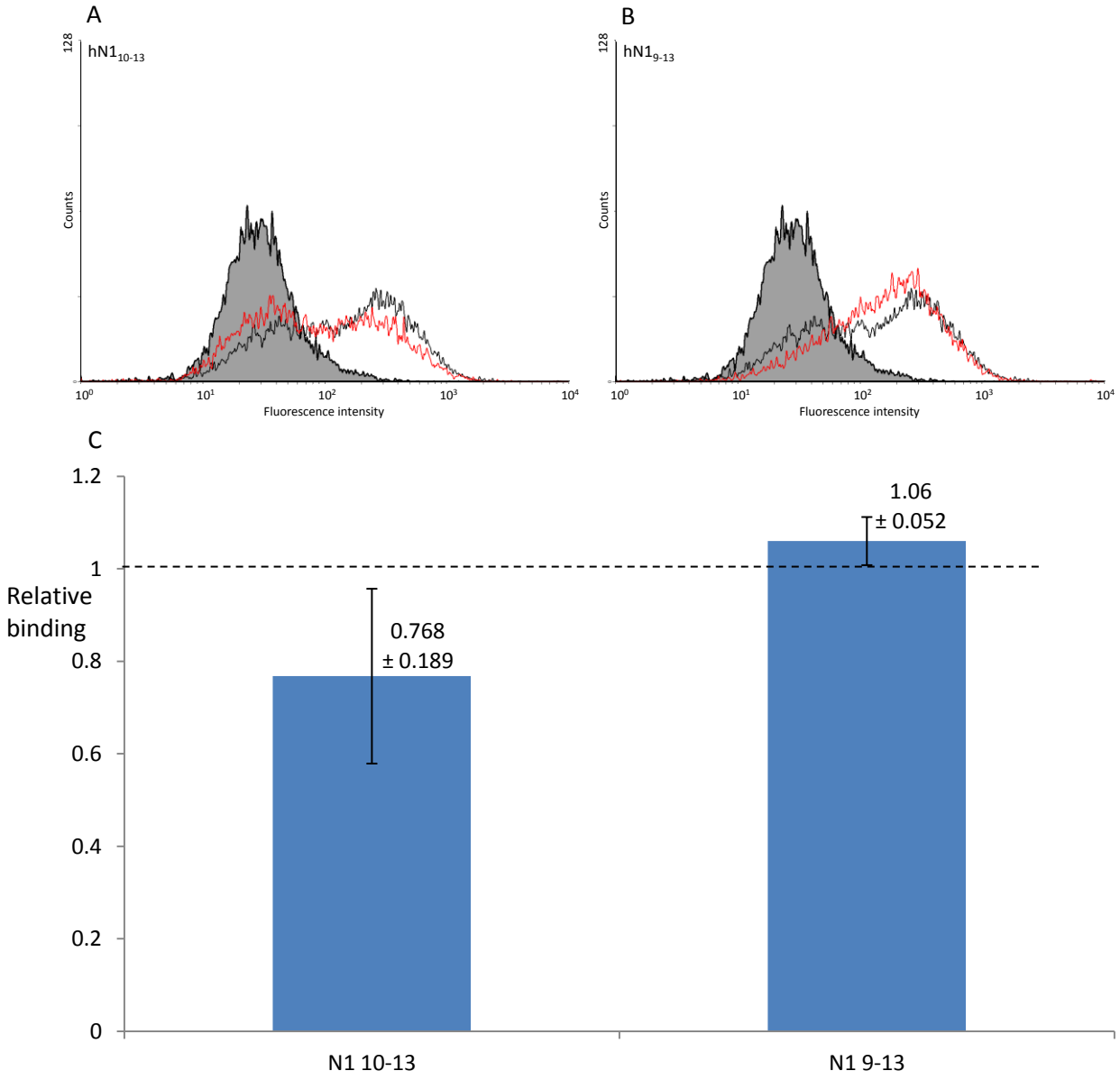


Figure 6-3 The effect of additional domains on binding to B16 mJagged1 cells using prokaryotically expressed proteins. Binding to fibrillin1 cbEGF12-14 is shown in grey, $hN1_{11-13}$ in black and each of the longer constructs in red. A) $hN1_{10-13}$ showed a reduced level of binding to B16 mJagged1 cells, compared to $hN1_{11-13}$. B) $hN1_{9-13}$ showed a slight increase in binding, compared $hN1_{11-13}$. These fluorescence profiles are representative of 3 repeats. C) Quantitative analysis of the effect of additional domains N-terminal to EGF11 on binding (n=3 for each construct), with mean and 95% confidence limits indicated.

6.2.2 Assaying binding of longer prokaryotically-expressed hNotch1 constructs to mDLL4

It has previously been reported that a construct containing EGF10 N-terminal to the ligand-binding region of hNotch1 significantly reduces binding to CHO cells expressing hDLL1, both in a flow cytometry binding assay and in SPR (Cordle *et al.*, 2008). In order to test whether this is a general trend for each of the mammalian Delta-like ligands, binding of the $hN1_{10-13}$ and $hN1_{9-13}$ to DLL4 was tested using B16 mDLL4 cells and compared to $hN1_{11-13}$.

The $hN1_{10-13}$ construct showed significantly reduced binding to B16 cells expressing mDLL4, compared to $hN1_{11-13}$. The addition of EGF9 had no further effect on binding, and $hN1_{9-13}$ bound to B16 mDLL4 cells similarly to $hN1_{10-13}$ (Figure 6-4).

This was unlike the results seen when binding was tested for the B16 mJagged1 cells, where EGF9 was found to cause a small enhancement in the overall level of binding. However, the reduction in binding to DLL4 seen for the constructs containing EGF10 is reminiscent of the results of the earlier study that tested binding to DLL1 (Cordle *et al.*, 2008). These data suggest that there may be a fundamental difference in how the Jagged and Delta ligand families bind to Notch, and that the various ligands may have different structures in the region involved in receptor binding.

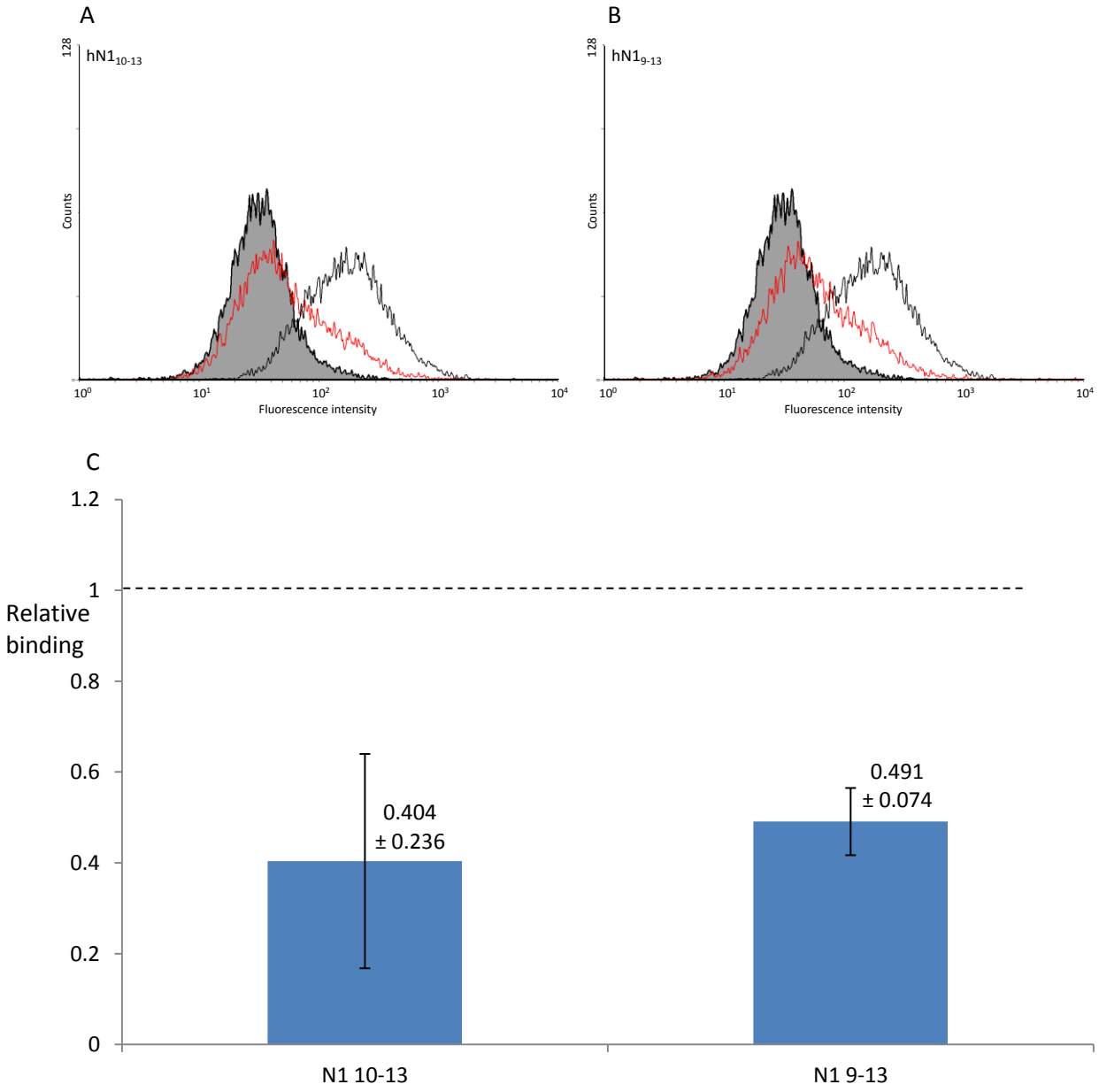


Figure 6-4 The effect of additional domains on binding to B16 mDLL4 cells using prokaryotically expressed proteins. Binding to fibrillin1 is shown in grey, $hN1_{11-13}$ in black and each longer construct in red. A) Binding was significantly reduced for $hN1_{10-13}$ compared to $hN1_{11-13}$. B) Binding of $hN1_{9-13}$ was significantly reduced for $hN1_{9-13}$ compared to $hN1_{11-13}$, and was similar to $hN1_{10-13}$. These fluorescence profiles are representative of 3 repeats. C) Quantitative analysis of the effect of additional domains N-terminal to EGF11 on binding (n=3 for each construct), with mean and 95% confidence limits indicated.

6.3 Assaying the effects of longer eukaryotically-expressed hNotch1 constructs on binding

In order to produce hNotch1 constructs that included domains N-terminal to EGF9, and rule out the possibility that the changes in binding seen in Section 6.2 might have been due to non-natively folded protein being produced in the *in-vitro* refolding system for the longer proteins, a series of constructs was produced in HEK 293T cells (see Section 3.7). Binding of each of these proteins to Jagged1 and DLL4 was measured by flow cytometry, and compared to $hN1_{11-14}$ that had been produced using the same eukaryotic expression system. The level of protein loading for these experiments was determined by Western Blot, to ensure that any changes in binding were had not occurred as a result of unequal levels of protein being used in the various binding assays (Figure 6-5). Small variations in the level of loading of the different hNotch1 proteins were observed, but were not likely to be sufficient to explain the changes in binding seen in this study.

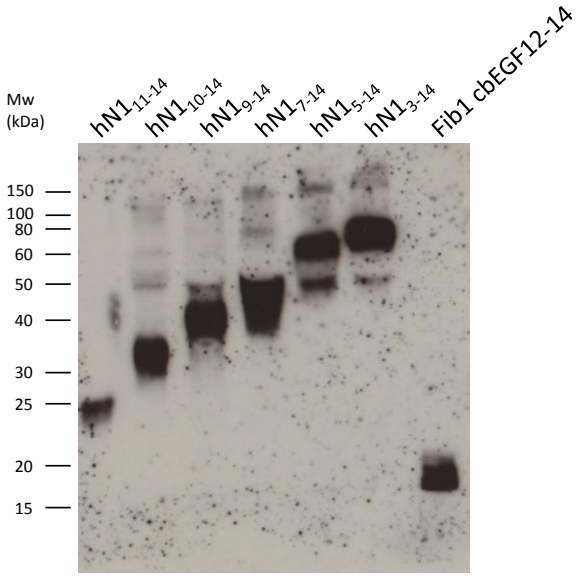


Figure 6-5 Western blot to show even loading of eukarotically-expressed proteins used in these binding experiments. A small sample of beads from each of the samples was collected before the binding experiments were performed, and after heating with non-reducing Laemmli's buffer the proteins were run on a 12% SDS-PAGE gel and analysed by Western Blot using a streptavidin-peroxidase conjugate. There was a small discrepancy between the loading of the proteins, but this is unlikely to affect the level of binding to the cells, and overall there appeared to be a high level of protein immobilised for each of these proteins.

The bands seen on the Western Blot for the eukaryotically-expressed proteins were broader than for the prokaryotic proteins. This may indicate that these proteins might be glycosylated with a variety of O-linked glycans, or might contain a proportion of misfolded protein.

Initially, eukaryotically-expressed $hN1_{11-14}$ was tested for binding to B16 mDLL4 (Figure 6-6) or mJagged1 cells (not shown), and compared to prokaryotically-expressed $hN1_{11-13}$, and both proteins were found to interact with cells in a similar way.

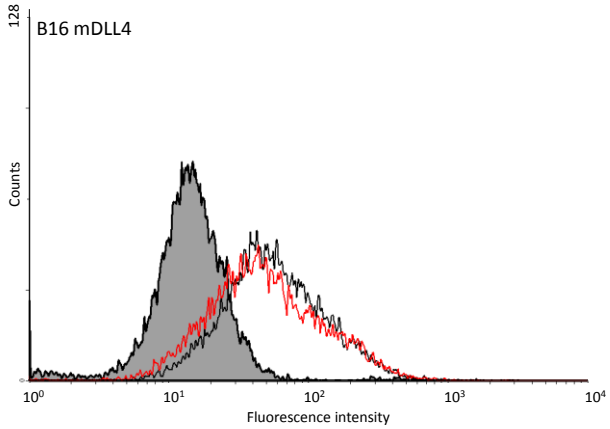


Figure 6-6 Comparing binding of prokaryotically-expressed $hN1_{11-13}$ with eukaryotically-expressed $hN1_{11-14}$, to B16 cells mDLL4. Binding to fibrillin1 cbEGF12-14 is shown in grey, prokaryotically-expressed $hN1_{11-13}$ in black and eukaryotically-expressed $hN1_{11-14}$ in red. Binding of eukaryotically-expressed $hN1_{11-14}$ was found to be indistinguishable from $hN1_{11-13}$.

6.3.1 Assaying binding of longer eukaryotically-expressed hNotch1 constructs to mJagged1

An $hN1_{9-14}$ construct was tested for binding using B16 cells expressing mJagged1 and compared to $hN1_{11-14}$. Overall there was a small but reproducible increase in binding for $hN1_{9-14}$ compared to $hN1_{11-14}$ (Figure 6-7 A). This observation agrees well with the experiments using the prokaryotically expressed proteins. In order to see whether additional domains in the N-terminal region of hNotch1 had any further effect on binding to Jagged1, $hN1_{7-14}$, $hN1_{5-14}$ and $hN1_{3-14}$ constructs were each tested for binding. Each of these proteins bound to the B16 mJagged1 cells in a similar manner to $hN1_{9-14}$ (Figure 6-7 B-D).

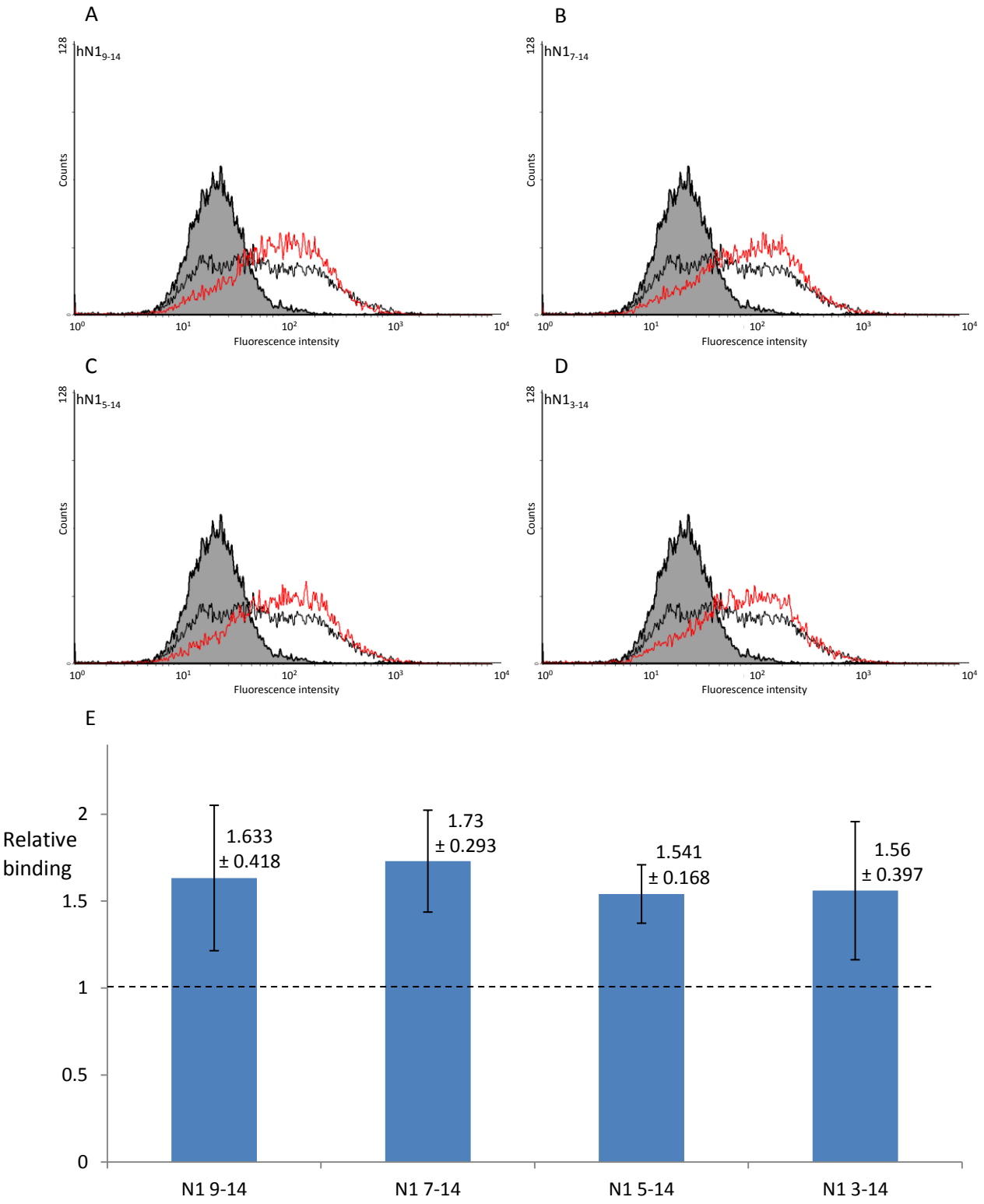


Figure 6-7 The effect of additional domains on binding to B16 mJagged1 cells using eukaryotically-expressed proteins. Binding to fibrillin1 cbEGF12-14 is shown in grey, eukaryotically expressed $hN1_{11-14}$ in black and each longer construct in red. A) $hN1_{9-14}$ showed a slight enhancement in binding compared to $hN1_{11-14}$. B-D) Further extension of the construct beyond EGF9 had no further changes in binding, as the fluorescence profiles for the longer proteins resembled the profile for $hN1_{9-14}$. These fluorescence profiles are representative of at least 2 repeats. E) Quantitative analysis of the effect of additional domains N-terminal to EGF11 on binding ($n \geq 2$ for each construct), relative to $hN1_{11-14}$. Mean and 95% confidence limits are indicated.

6.3.2 Assaying binding of longer eukaryotically-expressed hNotch1 constructs to mDLL4

The effect of EGF domains 9 and 10 on binding to DLL4 was tested, using the constructs $hN1_{10-14}$ and $hN1_{9-14}$, both of which had been produced using the HEK 293T eukaryotic expression system. $hN1_{10-14}$ used in this assay was a kind gift from Dr Chandramouli Chillakuri. As was the case for the equivalent prokaryotically-expressed proteins, the construct containing EGF10 N-terminal to the ligand binding region bound to the B16 mDLL4 cells less well than $hN1_{11-14}$. When $hN1_{9-14}$ was tested for binding in the same assay, it was found to bind to the B16 mDLL4 cells similarly to $hN1_{10-14}$ (Figure 6-8). The reduction in binding for the eukaryotically-expressed proteins was less pronounced than for the prokaryotically-expressed proteins (cf Figure 6-4 and 6-8).

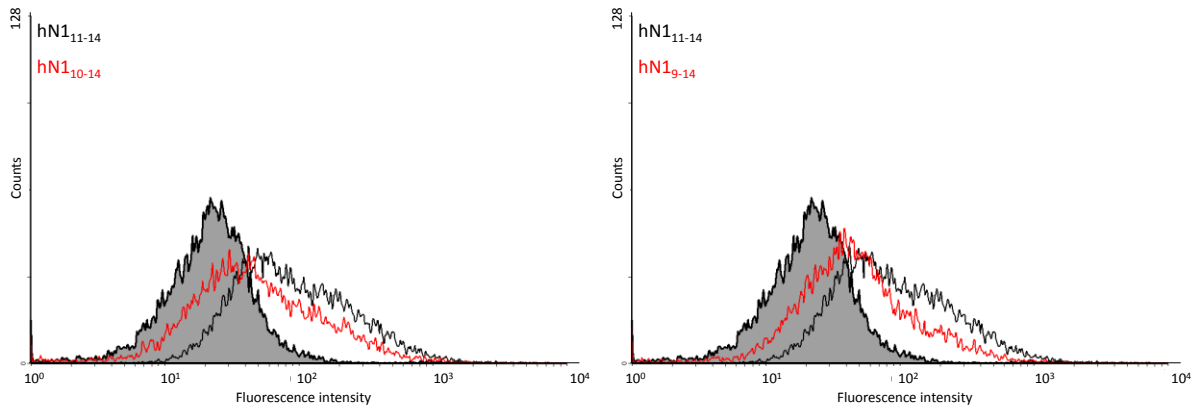


Figure 6-8 The effect of EGF domains 9 and 10 on binding to B16 mDLL4 cells using eukaryotically-expressed proteins. Binding to fibrillin1 cbEGF12-14 is shown in grey, eukaryotically-expressed $hN1_{11-14}$ in black, and each longer construct in red. Both $hN1_{10-14}$ and $hN1_{9-14}$ showed reduced binding compared to $hN1_{11-14}$. These fluorescence profiles are representative of at least 2 repeats.

Binding of the longer proteins ($hN1_{7-14}$, $hN1_{5-14}$ and $hN1_{3-14}$) was compared to $hN1_{9-14}$, in order to establish how the EGF domains in the N-terminal region of hNotch1 affected binding to DLL4. None of the constructs containing additional domains N-terminal to EGF9 was found to significantly alter binding to B16 cells expressing DLL4, as the confidence limits for these data overlap wit each other (Figure 6-9 B).

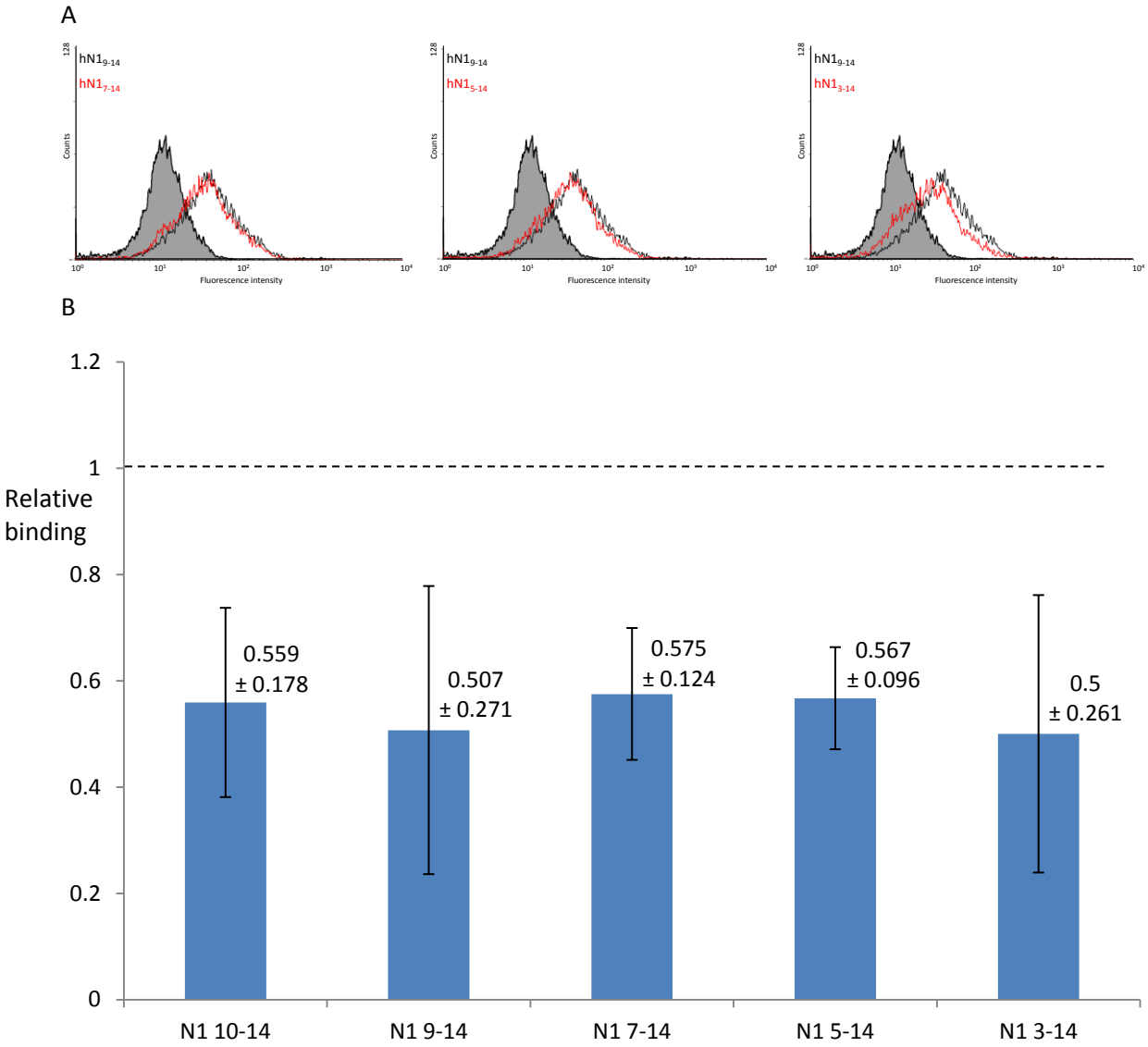


Figure 6-9 The effect of additional domains EGF7, 5 and 3 on binding to B16 mDLL4 cells using eukaryotically-expressed proteins. Binding to fibrillin1 cbEGF12-14 is shown in grey, eukaryotically-expressed $hN1_{9-14}$ in black, and each longer construct in red. A) No major changes in binding were detected for any of these proteins. These fluorescence profiles are representative of at least 2 repeats. B) Quantitative analysis of the effect of additional domains N-terminal to EGF11 on binding ($n \geq 2$ for each construct), relative to $hN1_{11-14}$. Mean and 95% confidence limits are indicated.

6.5 Blocking the interaction between $hN1_{11-13}$ and its ligands

A monoclonal mouse antibody had been produced (by the Oxford CRUK therapeutic antibody consortium) using prokaryotically-expressed $hN1_{11-13}$ as an antigen. This antibody was found to specifically block the interaction of hNotch1 with its ligands (mAb 39E). The binding epitope of this antibody has been mapped to a similar region within EGF12 that was implicated in ligand binding in the previous chapter (Whiteman *et al.*, 2013). The epitope of this antibody encompasses residues L468, Q470, E473, Q475 and I477, and does not include residues Q442, T466 or M479 (Figure 6-10). The T466 residue was not found to form part of the epitope for this antibody, but it was possible that the antibody might be able to discriminate between $hN1_{11-13}$ modified with the different sugars at this position, given the proximity of the O-fucose glycans to the known epitope in the structures obtained in Chapter 5 (Figure 6-10). The ability of this antibody to bind to glycosylated $hN1_{11-13}$ was initially tested using a simple dot-blot assay, after which the antibody's ability to block binding of $hN1_{11-13}$ modified with various sugars was tested in a flow-cytometry assay.

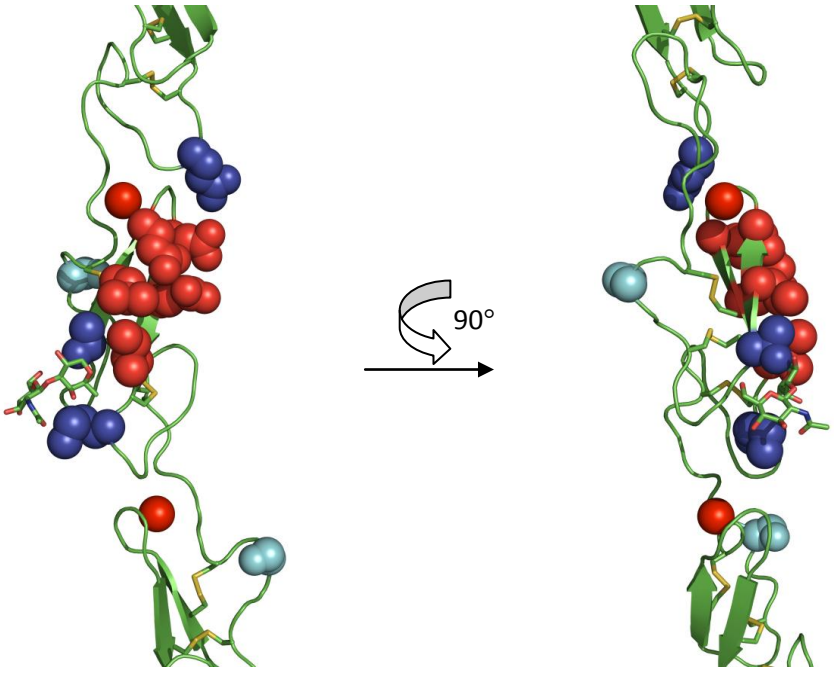


Figure 6-10 The epitope of the blocking antibody, as defined by dot-blot and flow cytometry against the mutants generated in Chapter 4. Residues that form part of the epitope are shown in red (L468, Q470, E473, Q475 and I477), residues that do not form part of the epitope are shown in blue (Q442, T466 and M479). Residues that are modified with O-glucose are shown in light blue (S458 and S496). The position of the GlcNAc-fucose disaccharide relative to this epitope is indicated.

6.5.1 Defining how the 39E mAb binds to glycosylated $hN1_{11-13}$

A dot blot was performed using the 39E antibody in order to see whether any of the O-fucosylation or O-glucosylation modifications affected its ability to recognise $hN1_{11-13}$. The blot was performed by pipetting approximately 10 ng of biotinylated $hN1_{11-13}$ that had been modified with a particular sugar (or sugars) directly onto a nitrocellulose membrane. Equivalent levels of protein loading onto the membrane were confirmed by using a streptavidin-peroxidase conjugate to detect biotin attached to the C-terminal BirA tag in a separate blot.

The antibody was able to bind to $hN1_{11-13}$ with each of the T466 substitutions from Chapter 5 (Figure 6-11 A, spots 3-5), confirming that T466 does not directly form part of the antibody's epitope. It is also able to detect the proteins modified with either O-glucose glycans at S458 and S496 (Figure 6-8 A, spots 9 and 10). This is to be expected as the residues to which these proteins are attached are not in the proximity of the antibody's epitope (Figure 6-10). However, none of the proteins modified with O-fucose sugars at T466 were able to bind to the antibody (Figure 6-11 A, spots 7, 8, 11-15) in the dot blot.

In order to confirm that the antibody did not recognise O-fucosylated $hN1_{11-13}$, the proteins modified with the O-fucose monosaccharide and GlcNAc-fucose disaccharide were tested for antibody binding in a flow cytometry assay. After the biotinylated protein had been immobilised on the beads overnight, and the beads had been washed and resuspended in HBSS/10% FCS, the antibody was mixed with the beads and incubated for an hour on ice before the beads were mixed with the cells.

The antibody completely blocks binding of unmodified $hN1_{11-13}$ to B16 mJagged1 cells, indicating that it is able to bind to this protein. This is shown by the fluorescence profile of unmodified $hN1_{11-13}$ in the presence of the antibody completely overlapping the fluorescence profile seen for the negative control protein fibrillin1 cbEGF12-14. However, the fluorescence profiles for $hN1_{11-13}$ modified with either of the O-fucose sugars binding to the B16 mJagged1 cells overlapped well for the profiles obtained in the presence of the antibody (Figure 6-11 B).

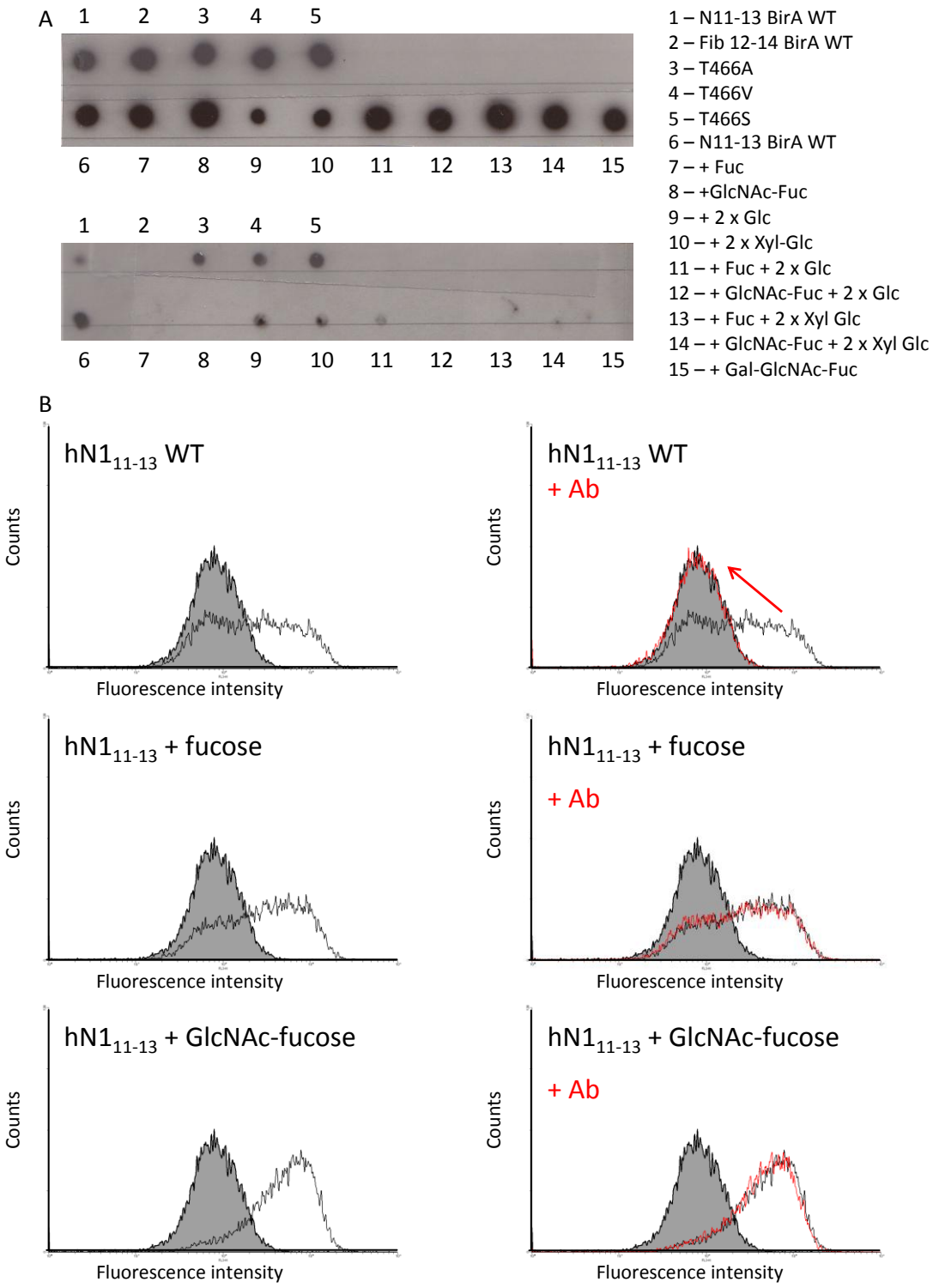


Figure 6-11 The effect of different O-glycosylation modifications to hN1$_{11-13}$ on the binding of a blocking antibody. A) A dot blot initially performed using the biotinylated proteins tested for binding earlier in this chapter. (Top) Streptavidin-HRP was used to measure protein loading. (Bottom) The blocking antibody recognised all of the amino acid substitutions at T466 (samples 3-5), but failed to recognise protein modified at T466 with either fucose or GlcNAc-fucose (samples 7, 8, 11-15). B) The same antibody blocked the interaction between hN1$_{11-13}$ and B16 Jagged1 cells, but failed to block the interaction between hN1$_{11-13}$ modified with fucose or GlcNAc-fucose at T466.

This indicates that the antibody is unable to block the interaction between these proteins and Jagged1, and is consistent with the results of the dot blot, that the antibody does not bind with high affinity to proteins modified with O-fucose glycans at this location. It is possible that the proximity of the C6 methyl group from the fucose sugar to the previously-defined epitope could alter the surface of the protein sufficient to eliminate binding.

6.5.2 Defining how the 39E mAb block binding of the longer prokaryotically-expressed hNotch1 constructs to Jagged1

The ability of the antibody to block binding of the extended prokaryotically-expressed hNotch1 constructs was tested, to investigate whether the antibody was able to block binding of the unmodified proteins despite the enhanced binding seen for the B16 mJagged1 cells binding to beads coated with $hN1_{9\text{-}13}$. The antibody was found to completely block the binding of prokaryotically-expressed $hN1_{10\text{-}13}$ and $hN1_{9\text{-}13}$ to B16 mJagged1 cells (Figure 6-12).

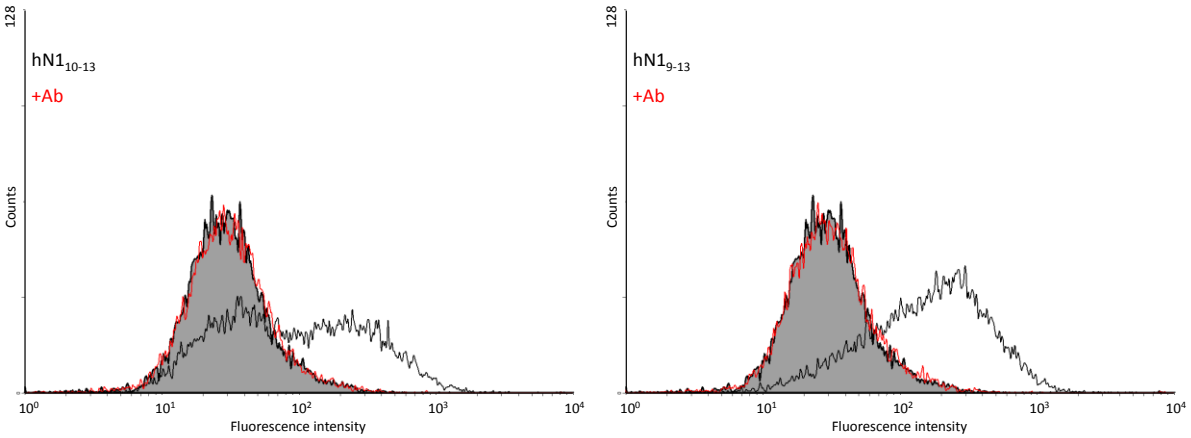


Figure 6-12 Blocking the interaction between extended prokaryotically-expressed hNotch1 proteins and mJagged1. Binding to fibrillin1 cbEGF12-14 is shown in grey, the hNotch1 construct in the absence of the antibody in black, and in the presence of the antibody in red. The antibody was able to completely block the interaction between each of these proteins and B16 mJagged1 cells.

6.5.3 Defining how the 39E mAb block binding of the longer eukaryotically-expressed hNotch1 constructs to Jagged1

The ability of the 39E mAb to block the interaction between the each of the eukaryotically-expressed hNotch1 proteins and B16 cells expressing mJagged1 was tested by flow cytometry. In contrast to the experiments using prokaryotically-expressed proteins, each of the eukaryotically-expressed hNotch1 constructs only showed a small reduction in binding in the presence of the antibody (Figure 6-13). This suggests that the antibody is only able to bind to a fraction of the total protein, and therefore that a significant portion of the protein may be glycosylated at T466. The degree to which binding was reduced by the antibody also varied from protein to protein, suggesting that the extent to which T466 is glycosylated may be variable.

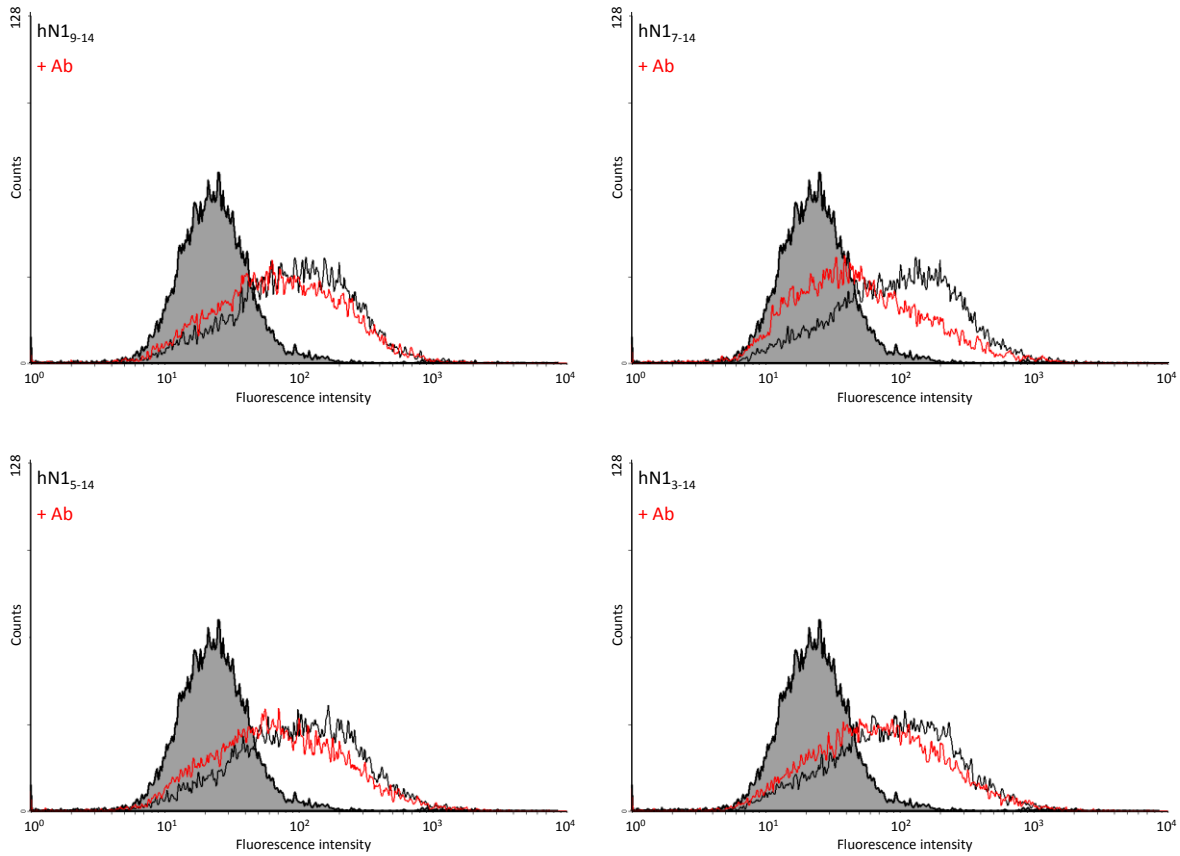


Figure 6-13 Blocking the interaction between eukaryotically-expressed hNotch1 proteins and mJagged1. Binding to fibrillin1 cbEGF12-14 is shown in grey, the hNotch1 construct in the absence of the antibody in black, and in the presence of the antibody in red. The antibody was found to cause a small reduction in binding of each of the eukaryotically expressed proteins to B16 mJagged1 cells, but the degree of inhibition varied from protein to protein.

6.5 Conclusions

The effect that additional domains N-terminal to the minimal ligand binding region of hNotch1 have on binding to DLL4 and Jagged1 has been established using proteins produced using both prokaryotic and eukaryotic expression systems. It is important to compare the binding results for each set of proteins, in order to ensure that factors such as glycosylation or protein misfolding can be taken into account when attributing the changes in binding to particular EGF domains. The trends in binding seen for each set of proteins correlate well with each other, with only minor differences: the addition of EGF domains 9 and 10 has opposite effects on binding to each of the two ligand classes used in this study.

Constructs containing EGF9 all showed an increase in the number of B16 mJagged1 cells that bound well to the beads coated with the respective hNotch1 proteins. Prokaryotically-expressed $hN1_{10-13}$ was found to bind to Jagged1 less well than $hN1_{11-13}$, but $hN1_{9-13}$ showed a small increase binding. This suggests that a small proportion of the prokaryotically-expressed $hN1_{10-13}$ may be partially misfolded or unstable, and when EGF9 is placed N-terminal to EGF10 the protein folds properly in the *in-vitro* refolding system, or stabilises EGF10 to allow it to bind to Jagged1. The $hN1_{9-14}$ construct shows a small increase in binding to the B16 mJagged1 cells compared to $hN1_{11-14}$, which resembles this increase seen for the prokaryotically-expressed proteins, supporting the observation that EGF9 can aid biding to Jagged1. None of the constructs containing additional EGF domains N-terminal to EGF9 showed any further changes in binding, as they all bound to the B16 mJagged1 cells similarly to $hN1_{9-14}$, which suggests that they may not be directly involved in ligand binding. It is possible that variable glycosylation between the various hNotch1 constructs may contribute to this apparent increase in binding, but since prokaryotically-expressed $hN1_{9-13}$ binds to B16 mJagged1 cells better than $hN1_{11-14}$, this indicates that EGF9 can aid binding of hNotch1 to Jagged1 independently of glycosylation.

In contrast, all of the constructs containing EGF10 show reduced binding to DLL4. Prokaryotically-expressed $hN1_{10-13}$ and $hN1_{9-13}$ both showed reduced binding to DLL4 compared to $hN1_{11-13}$, and the eukaryotically-expressed proteins containing EGF domains 10 and 9 both showed reduced binding compared to $hN1_{11-14}$. These findings agrees well with the previously published data, that showed that prokaryotically-expressed $hN1_{10-14}$ had substantially reduced binding to DLL1, compared to $hN1_{11-14}$ (Cordle *et al.*, 2008).

It is an interesting property of the 39E mAb that it only appears to bind to hNotch1 proteins that are not glycosylated at T466. As has been widely reported (Stahl *et al.*, 2008) there is a requirement for the mammalian Notch receptor to be glycosylated in order to functionally active, so it is not yet clear whether this antibody would be able to block Notch signalling. Nevertheless, its ability to discriminate between $hN1_{11-13}$ with or without O-fucose sugars in EGF12 could be used to probe the glycosylation state of eukaryotically-expressed hNotch1 proteins, and may help explain how glycosylation can regulate Notch signalling in the future.

Chapter 7

Discussion and future work

7.1 Objectives of this thesis

The aims of this thesis were to identify the location of the ligand binding site within the Notch receptor, and to determine the effects of different O-linked glycosylation modifications in this region on binding to different Notch ligands. In order to put this work into a broader context, a series of constructs of varying lengths were also created in order to try and understand whether any other domains of the Notch receptor are involved in ligand binding.

By creating a series of mutant Notch proteins, it was possible to identify a region within the central β-sheet of EGF12 that is required to initiate binding. The effect that individual sugar modifications in the minimal ligand binding region have on binding to both mammalian ligand families has been established. Other domains beyond the minimal ligand-binding region of Notch1 have been found to differentially affect binding to the two mammalian ligand families. This raises the possibility that the ligand binding site within the Notch receptor may extend over several domains.

7.2 The location of the ligand binding site within the Notch receptor

Residues L468 and I477 in hNotch1 appear to form an evolutionarily conserved hydrophobic binding platform that is essential for ligand binding. The position of this site casts doubt on the accuracy of previous attempts to model the interaction between the minimal interacting partners from the Notch receptor and its ligands (Cordle *et al.*, 2008). It also provides a direct mechanism for how glycosylation might modulate ligand binding, as the T466/S502 residue that forms part of the O-fucosylation consensus sequence within EGF12 is located directly adjacent to these residues.

The core residues involved in ligand binding are highly conserved amongst the Notch receptors from other species identified in Chapter 4. The surrounding residues on the β-hairpin show a degree of diversity amongst the other human Notch isoforms (Figure 4-1). It is possible that this sequence variation could provide a mechanism to fine-tune binding to the different Notch ligands. As demonstrated in Chapter 5, there is a large difference in the binding affinity of $hN1_{11\text{-}13}$ to Jagged1 and DLL4. This suggests that hNotch1 may have significantly different affinities for all four of the

ligands known to activate Notch signalling, and raises the possibility that sequence variability amongst the four Notch receptors in this region may alter how each receptor binds to a given ligand. The relative binding of Notch1-4 to each of the mammalian Notch ligands is likely to be the subject of future work, in order to obtain more information about the nature of the Notch-ligand binding interaction, and how sequence variability between the four mammalian Notch receptors might affect Notch signalling *in vivo*.

7.3 Regulation of Notch-ligand binding by O-glycosylation

The residue within EGF12 of hNotch1 that is fucosylated by Pofut (T466) lies adjacent to the L468 and I477 residues that were found to be essential for ligand binding. The addition of different O-fucose glycans to this residue was found to modulate binding to both mammalian ligand classes used in this study, and the extension of the O-fucose sugar attached to EGF12 with GlcNAc caused a much larger increase in binding to both ligands. This is the first time that it has been possible to monitor the effect of individual sugar modifications, at a specific site within a Notch receptor, on ligand binding. The new structural information for $hN1_{11\text{-}13}$ modified with sugars at this location shows the position of the sugars relative to the ligand binding site identified in Chapter 4, and suggests that the changes in binding to Jagged1 and DLL4 may be a direct result of the sugars extending the surface within EGF12 that is able to bind to the ligands. It also shows that for the domain in its native context, glycosylation has no effect on the structure of this region, and that the conformational changes observed previously (Hiruma-Shimizu *et al.*, 2010) probably arise as an artefact of this experiment being performed on an isolated domain in the absence of calcium. The addition of O-fucose to the equivalent residue in dNotch was found to have no effect on binding in the flow cytometry assay used, but it was not possible to extend the O-fucose sugar at this position beyond the monosaccharide in order to test the effect that the 'Fringe' modification at this site would have on binding.

The T466A substitution in hNotch1 has previously been found to decrease signalling by both Jagged1 and DLL1 (Rampal *et al.*, 2005a), and in a separate study, hNotch1 containing the T466S substitution was found to be fucosylated in EGF12, and is activated by DLL1 in a similar manner to WT, whereas the T466A substitution eliminated receptor activity (Shi *et al.*, 2007). Neither of these studies considered the effect that the amino acid substitution itself may have had on ligand binding, but it seems likely from the changes in binding seen in Chapters 4 and 5 that these effects are predominantly due to the loss of the O-fucosylation site from EGF12. Although the decrease in binding to Jagged1 caused by the T466A substitution is significant, the loss of O-fucosylation at this position would have a far greater impact on ligand binding. This suggests that O-fucosylation of EGF12 is essential for activation of Notch1 by either ligand family. In order to confirm this however, it may be appropriate to repeat the experiments that investigated the effects of removing the O-fucosylation site from EGF12 using the T466V substitution, as this was not found to reduce binding to either ligand. A similar study that investigated the role of glycosylation of EGF12 in dNotch found that the S502A substitution increased signalling by both Serrate and Delta (Lei *et al.*, 2003). The data in Chapter 5 show no evidence to suggest that the addition of sugars to the minimal ligand binding fragment of dNotch, or the S502A substitution, affect binding to Serrate, but it is important to note that it was not possible to extend the O-fucose sugar in EGF12 with GlcNAc. Assaying the effects of this modification on binding to Serrate and Delta would be required before it is possible to establish the precise effect of glycosylation of EGF12 in flies.

It is interesting to note that the 39E mAb is only able to recognise hNotch1 that is not glycosylated at T466, and is only able to partially disrupt the interaction between the eukaryotically-expressed proteins and the Notch ligands in a flow cytometry assay. This suggests that the proteins produced using HEK 293T cells may not be homogenously glycosylated, which highlights the main strength of the approach used in Chapter 5 to investigate the effects of specific sugar modifications on binding. It also suggests that a degree of caution must be used when interpreting data from previous studies that have tried to elucidate how various post-translational modifications to the Notch receptors are

able to regulate signalling (Okajima *et al.*, 2003) (Rampal *et al.*, 2005b), where the proteins used have not been thoroughly characterised.

Lunatic fringe has previously been found to increase the binding of soluble Jagged1 and DLL1 to cells expressing full length hNotch1, and increase the ability of DLL1 to activate Notch1 (Hicks *et al.*, 2000). Based on the binding data presented in Chapter 5, it is possible that the extension of the O-fucose sugar with GlcNAc in EGF12 within the context of the full length molecule may be at least partially responsible for the changes in binding seen in this early study.

What is clear is that the addition of glycans to EGF12 cannot be the sole mechanism for regulating Notch signalling via O-fucosylation in either the human or the *Drosophila* systems (see Section 1-7), and that it is likely that several other glycosylation sites in addition to EGF12 have important roles in regulating Notch signalling. In mammals, each of the three Fringe enzymes have been found to have different, and sometimes opposing, effects on ligand binding and receptor activation (see Table 1-2). They are known to extend O-fucose sugars with varying efficiency, depending on the amino acid sequences of different EGF domains (Rampal *et al.*, 2005c), and may therefore modify different or partially overlapping sets of EGF domains in the Notch receptor, and act independently or in combination to regulate Notch signalling in mammals.

7.4 Docking $hN1_{11\text{-}13}$ and hJagged1 DSL-EGF3

In order to investigate how the position of the ligand binding site within $hN1_{11\text{-}13}$ might enable the Notch receptor to bind to its ligands, a new attempt to model the interaction between $hN1_{11\text{-}13}$ and the DSL-EGF3 domains from hJagged1 was undertaken, based on the results from Chapter 4. As in the previous studies (Cordle *et al.*, 2008), the HADDOCK online docking server was used for this (Dominguez *et al.*, 2003). Residues L468 and I477 from $hN1_{11\text{-}13}$ (PDB 2VJ3), and F199 and F207 from hJagged1 DSL-EGF3 (PDB 2VJ2) were selected as the active residues to drive docking. The equivalent residues in Serrate (F249 and F257) were found to have the most marked effects on binding to Notch

in a cell aggregation assay in a previous study when substituted to alanine (Cordle *et al.*, 2008). The residues from the BirA peptide at the C-terminus of $hN1_{11-13}$ were not use in the docking simulations.

7.4.1 HADDOCK docking

The output of the HADDOCK docking simulation returned 112 structures in 13 clusters, out of a total of 200 water-refined models. The clusters were ranked according to their HADDOCK scores, which reflect the buried surface area, Van der Waals energy, electrostatic energy and desolvation energy for each cluster. The majority of the top 10 clusters showed that the molecules might interact in a parallel orientation, with only the third and fifth best clusters returning models that showed an anti-parallel orientation. The top cluster (HADDOCK score -56.3 +/- 19.7) and the third best cluster (HADDOCK score -43.9 +/- 24.7) are shown below for comparison (Figure 7-1). Caution must be exercised when drawing conclusions from these models, particularly because minimal binding fragments were used to drive docking. However, these models provide a basis to design new experiments to determine how the full-length molecules interact (Figure 7-2).

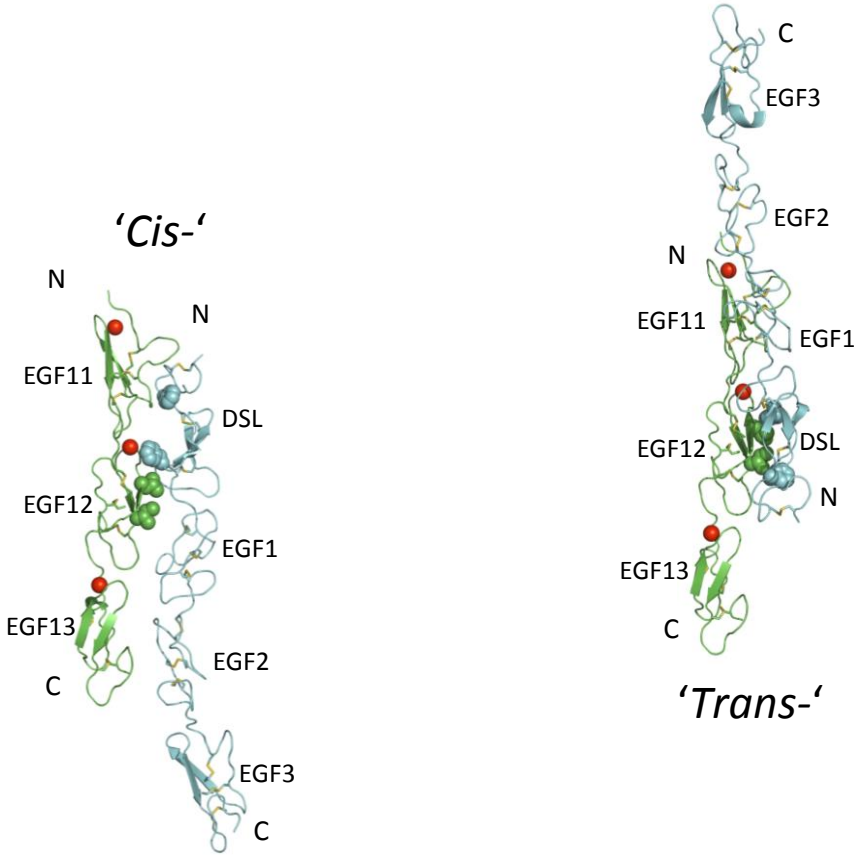


Figure 7-1 Results of the HADDOCK docking, suggesting that the molecules might be able to interact in one of two potential orientations. The structure of $hN1_{11-13}$ is indicated in green, and of Jagged1 DSL-EGF in blue. The residues used to drive docking are shown as spheres. The parallel orientation is labelled as '*cis*' and the anti-parallel orientation is labelled as '*trans*', though it is not clear whether these represent the modes of interaction for *cis*-inhibition and *trans*-activation.

7.4.2 Possible implications of the docking models

This docking model provides some potential targets for future mutagenesis experiments, in order expand the surface of Notch that might be involved in ligand binding. Based on the models obtained from the docking, residues N421, E424 and H425 might be appropriate candidates for future mutagenesis, as they all contact the ligand molecule in each of the models described above, lie on the same face of the structure of $hN1_{11-13}$ as the ligand binding site identified in Chapter 4, and are very highly conserved at these positions (Figure 7-2 A).

As was the case for the previous attempts to model the interaction between the minimal binding fragments of Notch and its ligands, the HADDOCK docking simulation indicated that the minimal binding fragments could interact in two distinct modes – parallel and antiparallel. Whilst this cannot be ruled out, it is already known that the formation of a *trans*-activating or *cis*-inhibiting Notch-ligand complex is mutually-exclusive (Sprinzak *et al.*, 2010), and that the same site in Serrate is required for both *trans*-activation and *cis*-inhibition (Cordle *et al.*, 2008). However, the mathematical modelling performed by Sprinzak *et al*. required different affinities for the two modes of interaction, so it is not yet clear whether *trans*-activation and *cis*-inhibition require the same local complex to be formed or not.

Were the molecules to interact in a parallel orientation, EGF10 of Notch would pack alongside a portion of the MNNL domain, and if they were to interact in an antiparallel orientation then EGF10 would pack alongside EGF3 (Figure 7-2 B). There is some evidence to suggest that EGF3 of *Drosophila* Delta is not required to activate Notch signalling, or for the Notch receptor to bind in a cell aggregation assay (Parks *et al.*, 2006), but it remains to be seen if this is the case for Jagged/Serrate ligand family, and in the human system. Either way, it would suggest that the portion of the Notch receptor involved in binding does not extend far beyond the minimal ligand binding fragment spanning domains 11-13.

A

```
EGF11
Homo sapiens          411 QDVDECSLGANPCEHAGKCINTLGSFECQCLQGYTGPRCE 450
Pan troglodytes       411 QDVDECSLGANPCEHAGKCINTLGSFECQCLQGYTGPRCE 450
Bos taurus            325 QDVDECSLGANPCEHAGKCINTLGSFECQCLQGYTGPRCE 364
Canis familiaris      398 QDVDECSLGANPCEHAGKCINTLGSFECQCLQGYTGPRCE 437
Mus musculus          411 QDVDECDLGANRCEHAGKCLNTLGSFECQCLQGYTGPGCE 450
Gallus gallus         407 QDVDECSLGANPCEHAGKCINTQGSFQCQCLQGYSGPRCE 446
Danio rerio           431 QDVDECSLGANPCEHAGKCINTKGSFQCKCLQGYVGARCE 470
Xenopus laevis        410 NDVDECSLGANPCEHGGRCTNTLGSFQCNCPQGYAGPRCE 449
D. melanogaster       448 EDIDECDQGS-PCEHNGICVNTPGSYRCNCSQGFTGPRCE 486
```

B

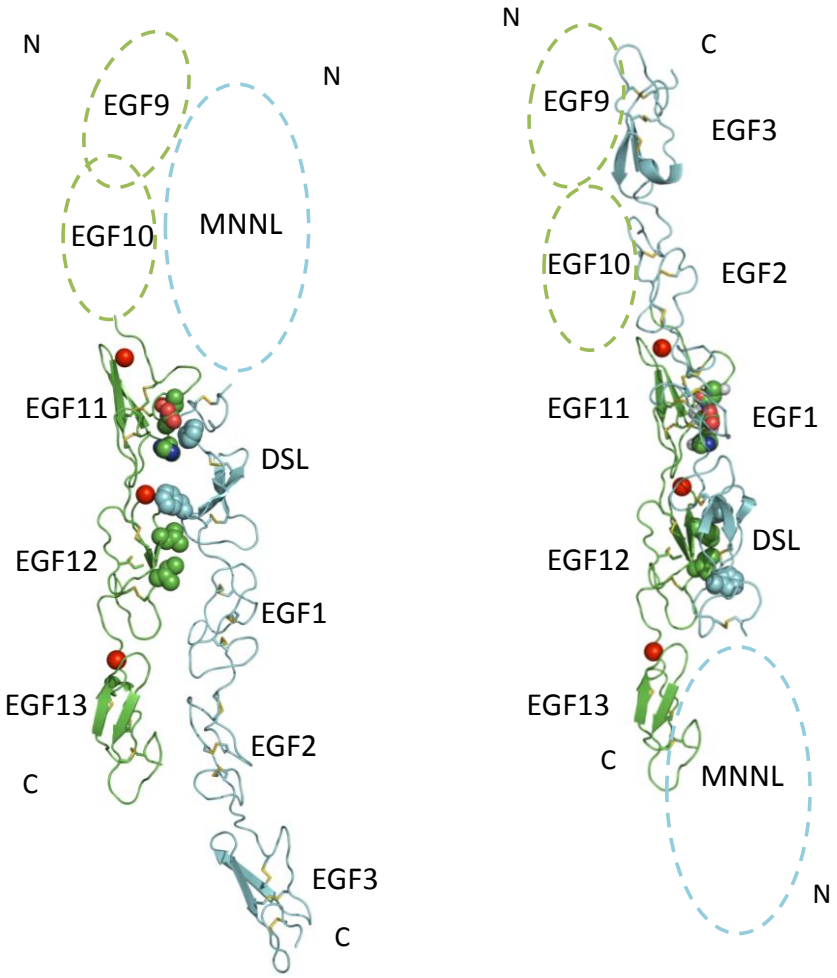


Figure 7-2 Potential residues to target for mutagenesis in the future, and possible modes of interaction for extended Notch constructs with the Jagged MNNL-EGF3 construct. A) An alignment of EGF11 from Notch1 is shown, with the residues that might be targets for future mutagenesis indicated with arrows. B) Depending on the orientation of the Notch-ligand binding interaction, the domains N-terminal to EGF11 may either interact with the MNNL domain, or EGF3. More work is needed to establish which orientation is more likely. The residues in EGF11 that might be potential future targets for mutagenesis are displayed in both models.

7.4.3 Towards the structure of a Notch-ligand complex

The information gathered in this thesis suggests a potential strategy for future experiments to determine the structural basis for how Notch binds to its ligands. The highest affinity interaction seen in this study was between DLL4 MNNL-EGF3 and $hN1_{11-13}$ modified with the GlcNAc-fucose disaccharide. It may be possible to design a strategy to co-crystallise a Notch/ligand complex, or perform an NMR shift-mapping experiment, using some of these proteins.

7.5 The effect of additional domains on ligand binding

In Chapter 6, a variety of longer Notch constructs containing domains N-terminal to the ligand-binding region of hNotch1 were produced using both prokaryotic and eukaryotic expression systems. The presence of these additional domains had opposite effects on the binding to the two different ligand families tested in this study; binding to cells expressing Jagged1 was increased for all constructs containing EGF9, and binding to cells expressing DLL4 was decreased for all constructs containing EGF10. The presence of additional domains beyond EGF9 appeared not to further affect on binding to either ligand class. The use of proteins that had been produced using prokaryotic and eukaryotic expression systems suggests that these changes occur independently from glycosylation.

EGF9 of Notch1 contains a very highly conserved O-fucosylation site, and a previous study has looked at the effect of removing this O-fucosylation site by using a T→A substitution (Rampal *et al.*, 2005a). This substitution was not to found to affect activation by either Jagged1 or DLL1 in a co-culture assay when full-length Notch1 was expressed in COS-7 cells. However, the extent to which this site was glycosylated by these cells in the WT protein in this study is not known, and it is possible that this domain is not widely modified in these cells, and therefore removing this glycosylation site would have no detectable effect on the level of receptor activation measured in this assay. It would be desirable to perform a systematic study on the effect of O-fucosylation at this site using prokaryotically-expressed proteins, in order to establish whether glycosylation of EGF9 alters binding to either class of Notch ligands.

7.6 Future work

The results of the experiments performed in this thesis have answered several questions regarding the mode of binding of Notch to its ligands. However, several questions remain, and more work is needed as part of the ongoing investigation into the molecular details behind how the Notch receptor is activated by its ligands. In particular, the following areas would be appropriate to build upon the results of this study:

- Further mutagenesis on both hJagged1 and hNotch1 in order to validate the models arising from the docking, eg N421, E424 and H425.
- Testing how the minimal binding fragments of the hNotch1-4 isoforms bind to each of the mammalian Notch ligands. In particular, the Notch2-Jagged1 interaction is thought to be physiologically important, as mutations in genes that encode these proteins are known to cause Alagille syndrome.
- Testing how $hN1_{11-13}$ modified with the various O-glucose and O-fucose sugars binds to the other mammalian Notch ligands, in addition to the ligands tested in this study.
- Testing the effect of the O-fucose modifications on the binding of dN_{11-13} to Delta.
- Attempt to modify longer prokaryotically-expressed hNotch1 proteins with O-fucose and O-glucose sugars, in particular O-fucosylation of EGF9. This should establish how specific sugar modifications beyond the minimal binding fragment can modulate ligand binding.
- Optimisation of the eukaryotic expression system for producing extended Notch constructs, in order to confirm the observations seen in Chapter 6. Assaying the binding of extended dNotch constructs to Delta and Serrate would also be of interest.

7.7 Summary

This study has identified the position of the ligand binding site within EGF12 of hNotch1 and dNotch, using flow cytometry-based binding assays. Binding to both the Jagged and Delta-like ligand families has been shown to be altered by the addition of O-fucose glycans, in particular the GlcNAc-fucose

modification to the threonine residue immediately adjacent to this site in hNotch1. O-fucose glycans were not found to affect binding in the fly system, but it was not possible to extend the O-fucose sugar in $dN_{11\text{-}13}$. The presence of additional domains N-terminal to EGF11 has small but reproducible opposite effects on binding to the two ligand classes, which could provide information about the relative orientations of the two proteins. This work also provides a potential new strategy for obtaining a crystal structure for the receptor-ligand complex.

References

ACAR, M., JAFAR-NEJAD, H., TAKEUCHI, H., RAJAN, A., IBRANI, D., RANA, N., PAN, H., HALTIWANGER, R. & BELLEN, H. 2008. Rumi is a CAP10 domain glycosyltransferase that modifies Notch and is required for Notch signaling. *Cell,* 132, 247-58.

AHIMOU, F., MOK, L. P., BARDOT, B. & WESLEY, C. 2004. The adhesion force of Notch with Delta and the rate of Notch signaling. *J Cell Biol,* 167, 1217-29.

AOKI, K., PERLMAN, M., LIM, J. M., CANTU, R., WELLS, L. & TIEMEYER, M. 2007. Dynamic developmental elaboration of N-linked glycan complexity in the Drosophila melanogaster embryo. *J Biol Chem,* 282, 9127-42.

ARICESCU, A. R., LU, W. & JONES, E. Y. 2006. A time- and cost-efficient system for high-level protein production in mammalian cells. *Acta Crystallogr D Biol Crystallogr,* 62, 1243-50.

ARNETT, K. L., HASS, M., MCARTHUR, D. G., ILAGAN, M. X., ASTER, J. C., KOPAN, R. & BLACKLOW, S. C. 2010. Structural and mechanistic insights into cooperative assembly of dimeric Notch transcription complexes. *Nat Struct Mol Biol,* 17, 1312-7.

BAILEY, A. M. & POSAKONY, J. W. 1995. Suppressor of hairless directly activates transcription of enhancer of split complex genes in response to Notch receptor activity. *Genes Dev,* 9, 2609-22.

BALADRÓN, V., RUIZ-HIDALGO, M. J., NUEDA, M. L., DÍAZ-GUERRA, M. J., GARCÍA-RAMÍREZ, J. J., BONVINI, E., GUBINA, E. & LABORDA, J. 2005. dlk acts as a negative regulator of Notch1 activation through interactions with specific EGF-like repeats. *Exp Cell Res,* 303, 343-59.

BECAM, I., FIUZA, U. M., ARIAS, A. M. & MILÁN, M. 2010. A role of receptor Notch in ligand cis-inhibition in Drosophila. *Curr Biol,* 20, 554-60.

BIRNBOIM, H. C. & DOLY, J. 1979. A rapid alkaline extraction procedure for screening recombinant plasmid DNA. *Nucleic Acids Res,* 7, 1513-23.

BLAUMUELLER, C., QI, H., ZAGOURAS, P. & ARTAVANIS-TSAKONAS, S. 1997. Intracellular cleavage of Notch leads to a heterodimeric receptor on the plasma membrane. *Cell,* 90, 281-91.

BOZKULAK, E. C. & WEINMASTER, G. 2009. Selective use of ADAM10 and ADAM17 in activation of Notch1 signaling. *Mol Cell Biol,* 29, 5679-95.

BULMAN, M. P., KUSUMI, K., FRAYLING, T. M., MCKEOWN, C., GARRETT, C., LANDER, E. S., KRUMLAUF, R., HATTERSLEY, A. T., ELLARD, S. & TURNPENNY, P. D. 2000. Mutations in the human delta homologue, DLL3, cause axial skeletal defects in spondylocostal dysostosis. *Nat Genet,* 24, 438-41.

CAGAN, R. L. & READY, D. F. 1989. Notch is required for successive cell decisions in the developing Drosophila retina. *Genes Dev,* 3, 1099-112.

CHEN, J., MOLONEY, D. & STANLEY, P. 2001. Fringe modulation of Jagged1-induced Notch signaling requires the action of beta 4galactosyltransferase-1. *Proc Natl Acad Sci U S A,* 98, 13716-21.

CHENEY, W. D. 1965. ACRO-OSTEOLYSIS. *Am J Roentgenol Radium Ther Nucl Med,* 94, 595-607.

CHITNIS, A., HENRIQUE, D., LEWIS, J., ISH-HOROWICZ, D. & KINTNER, C. 1995. Primary neurogenesis in Xenopus embryos regulated by a homologue of the Drosophila neurogenic gene Delta. *Nature,* 375, 761-6.

CHOI, S. H., WALES, T. E., NAM, Y., O'DONOVAN, D. J., SLIZ, P., ENGEN, J. R. & BLACKLOW, S. C. 2012. Conformational locking upon cooperative assembly of notch transcription complexes. *Structure,* 20, 340-9.

CORDLE, J., JOHNSON, S., TAY, J., ROVERSI, P., WILKIN, M., DE MADRID, B., SHIMIZU, H., JENSEN, S., WHITEMAN, P., JIN, B., REDFIELD, C., BARON, M., LEA, S. & HANDFORD, P. 2008a. A conserved face of the Jagged/Serrate DSL domain is involved in Notch trans-activation and cis-inhibition. *Nat Struct Mol Biol,* 15, 849-57.

CORDLE, J., REDFIELDZ, C., STACEY, M., VAN DER MERWE, P., WILLIS, A., CHAMPION, B., HAMBLETON, S. & HANDFORD, P. 2008b. Localization of the delta-like-1-binding site in human Notch-1 and its modulation by calcium affinity. *J Biol Chem,* 283, 11785-93.

CROSNIER, C., DRIANCOURT, C., RAYNAUD, N., DHORNE-POLLET, S., POLLET, N., BERNARD, O., HADCHOUEL, M. & MEUNIER-ROTIVAL, M. 1999. Mutations in JAGGED1 gene are predominantly sporadic in Alagille syndrome. *Gastroenterology,* 116, 1141-8.

DE CELIS, J. F., BARRIO, R., DEL ARCO, A. & GARCÍA-BELLIDO, A. 1993. Genetic and molecular characterization of a Notch mutation in its Delta- and Serrate-binding domain in Drosophila. *Proc Natl Acad Sci U S A,* 90, 4037-41.

DE CELIS, J. F. & BRAY, S. 1997. Feed-back mechanisms affecting Notch activation at the dorsoventral boundary in the Drosophila wing. *Development,* 124, 3241-51.

DE CELIS, J. F. & BRAY, S. J. 2000. The Abruptex domain of Notch regulates negative interactions between Notch, its ligands and Fringe. *Development,* 127, 1291-302.

DE CELIS, J. F. & GARCIA-BELLIDO, A. 1994. Modifications of the notch function by Abruptex mutations in Drosophila melanogaster. *Genetics,* 136, 183-94.

DE STROOPER, B., ANNAERT, W., CUPERS, P., SAFTIG, P., CRAESSAERTS, K., MUMM, J., SCHROETER, E., SCHRIJVERS, V., WOLFE, M., RAY, W., GOATE, A. & KOPAN, R. 1999. A presenilin-1-dependent gamma-secretase-like protease mediates release of Notch intracellular domain. *Nature,* 398, 518-22.

DEBLANDRE, G. A., LAI, E. C. & KINTNER, C. 2001. Xenopus neuralized is a ubiquitin ligase that interacts with XDelta1 and regulates Notch signaling. *Dev Cell,* 1, 795-806.

DEY, A. & SZOSZKIEWICZ, R. 2012. Complete noise analysis of a simple force spectroscopy AFM setup and its applications to study nanomechanics of mammalian Notch 1 protein. *Nanotechnology,* 23, 175101.

DINCHUK, J. E., FOCHT, R. J., KELLEY, J. A., HENDERSON, N. L., ZOLOTARJOVA, N. I., WYNN, R., NEFF, N. T., LINK, J., HUBER, R. M., BURN, T. C., RUPAR, M. J., CUNNINGHAM, M. R., SELLING, B. H., MA, J., STERN, A. A., HOLLIS, G. F., STEIN, R. B. & FRIEDMAN, P. A. 2002. Absence of post-translational aspartyl beta-hydroxylation of epidermal growth factor domains in mice leads to developmental defects and an increased incidence of intestinal neoplasia. *J Biol Chem,* 277, 12970-7.

DINCHUK, J. E., HENDERSON, N. L., BURN, T. C., HUBER, R., HO, S. P., LINK, J., O'NEIL, K. T., FOCHT, R. J., SCULLY, M. S., HOLLIS, J. M., HOLLIS, G. F. & FRIEDMAN, P. A. 2000. Aspartyl beta -hydroxylase (Asph) and an evolutionarily conserved isoform of Asph missing the catalytic domain share exons with junctin. *J Biol Chem,* 275, 39543-54.

DOE, C. Q. & GOODMAN, C. S. 1985. Early events in insect neurogenesis. II. The role of cell interactions and cell lineage in the determination of neuronal precursor cells. *Dev Biol,* 111, 206-19.

DOMENGA, V., FARDOUX, P., LACOMBE, P., MONET, M., MACIAZEK, J., KREBS, L. T., KLONJKOWSKI, B., BERROU, E., MERICSKAY, M., LI, Z., TOURNIER-LASSERVE, E., GRIDLEY, T. & JOUTEL, A. 2004. Notch3 is required for arterial identity and maturation of vascular smooth muscle cells. *Genes Dev,* 18, 2730-5.

DOMINGUEZ, C., BOELENS, R. & BONVIN, A. M. 2003. HADDOCK: a protein-protein docking approach based on biochemical or biophysical information. *J Am Chem Soc,* 125, 1731-7.

DOU, S., ZENG, X., CORTES, P., ERDJUMENT-BROMAGE, H., TEMPST, P., HONJO, T. & VALES, L. D. 1994. The recombination signal sequence-binding protein RBP-2N functions as a transcriptional repressor. *Mol Cell Biol,* 14, 3310-9.

DOWNING, A. K., KNOTT, V., WERNER, J. M., CARDY, C. M., CAMPBELL, I. D. & HANDFORD, P. A. 1996. Solution structure of a pair of calcium-binding epidermal growth factor-like domains: implications for the Marfan syndrome and other genetic disorders. *Cell,* 85, 597-605.

DUERING, M., KARPINSKA, A., ROSNER, S., HOPFNER, F., ZECHMEISTER, M., PETERS, N., KREMMER, E., HAFFNER, C., GIESE, A., DICHGANS, M. & OPHERK, C. 2011. Co-aggregate formation of CADASIL-mutant NOTCH3: a single-particle analysis. *Hum Mol Genet,* 20, 3256-65.

EIRAKU, M., HIRATA, Y., TAKESHIMA, H., HIRANO, T. & KENGAKU, M. 2002. Delta/notch-like epidermal growth factor (EGF)-related receptor, a novel EGF-like repeat-containing protein targeted to dendrites of developing and adult central nervous system neurons. *J Biol Chem,* 277, 25400-7.

ELDADAH, Z. A., HAMOSH, A., BIERY, N. J., MONTGOMERY, R. A., DUKE, M., ELKINS, R. & DIETZ, H. C. 2001. Familial Tetralogy of Fallot caused by mutation in the jagged1 gene. *Hum Mol Genet,* 10, 163-9.

ELLISEN, L. W., BIRD, J., WEST, D. C., SORENG, A. L., REYNOLDS, T. C., SMITH, S. D. & SKLAR, J. 1991. TAN-1, the human homolog of the Drosophila notch gene, is broken by chromosomal translocations in T lymphoblastic neoplasms. *Cell,* 66, 649-61.

FEHON, R. G., KOOH, P. J., REBAY, I., REGAN, C. L., XU, T., MUSKAVITCH, M. A. & ARTAVANIS-TSAKONAS, S. 1990. Molecular interactions between the protein products of the neurogenic loci Notch and Delta, two EGF-homologous genes in Drosophila. *Cell,* 61, 523-34.

FERNANDEZ-VALDIVIA, R., TAKEUCHI, H., SAMARGHANDI, A., LOPEZ, M., LEONARDI, J., HALTIWANGER, R. S. & JAFAR-NEJAD, H. 2011. Regulation of mammalian Notch signaling and embryonic development by the protein O-glucosyltransferase Rumi. *Development,* 138, 1925-34.

FERNLUND, P. & STENFLO, J. 1983. Beta-hydroxyaspartic acid in vitamin K-dependent proteins. *J Biol Chem,* 258, 12509-12.

FIUZA, U. M., KLEIN, T., MARTINEZ ARIAS, A. & HAYWARD, P. 2010. Mechanisms of ligand-mediated inhibition in Notch signaling activity in Drosophila. *Dev Dyn,* 239, 798-805.

FORTINI, M. & BILDER, D. 2009. Endocytic regulation of Notch signaling. *Curr Opin Genet Dev*.

FOSTER, G. G. 1975. Negative complementation at the notch locus of Drosophila melanogaster. *Genetics,* 81, 99-120.

FRIEDMANN, D. R., WILSON, J. J. & KOVALL, R. A. 2008. RAM-induced allostery facilitates assembly of a notch pathway active transcription complex. *J Biol Chem,* 283, 14781-91.

FRISE, E., KNOBLICH, J. A., YOUNGER-SHEPHERD, S., JAN, L. Y. & JAN, Y. N. 1996. The Drosophila Numb protein inhibits signaling of the Notch receptor during cell-cell interaction in sensory organ lineage. *Proc Natl Acad Sci U S A,* 93, 11925-32.

FRYER, C. J., LAMAR, E., TURBACHOVA, I., KINTNER, C. & JONES, K. A. 2002. Mastermind mediates chromatin-specific transcription and turnover of the Notch enhancer complex. *Genes Dev,* 16, 1397-411.

GARG, V., MUTH, A. N., RANSOM, J. F., SCHLUTERMAN, M. K., BARNES, R., KING, I. N., GROSSFELD, P. D. & SRIVASTAVA, D. 2005. Mutations in NOTCH1 cause aortic valve disease. *Nature,* 437, 270-4.

GASTEIGER, E., JUNG, E. & BAIROCH, A. 2001. SWISS-PROT: connecting biomolecular knowledge via a protein database. *Curr Issues Mol Biol,* 3, 47-55.

GEFFERS, I., SERTH, K., CHAPMAN, G., JAEKEL, R., SCHUSTER-GOSSLER, K., CORDES, R., SPARROW, D. B., KREMMER, E., DUNWOODIE, S. L., KLEIN, T. & GOSSLER, A. 2007. Divergent functions and distinct localization of the Notch ligands DLL1 and DLL3 in vivo. *J Cell Biol,* 178, 465-76.

GLITTENBERG, M., PITSOULI, C., GARVEY, C., DELIDAKIS, C. & BRAY, S. 2006. Role of conserved intracellular motifs in Serrate signalling, cis-inhibition and endocytosis. *EMBO J,* 25, 4697-706.

GORDON, W. R., VARDAR-ULU, D., HISTEN, G., SANCHEZ-IRIZARRY, C., ASTER, J. C. & BLACKLOW, S. C. 2007. Structural basis for autoinhibition of Notch. *Nat Struct Mol Biol,* 14, 295-300.

GREENWALD, I. 1998. LIN-12/Notch signaling: lessons from worms and flies. *Genes Dev,* 12, 1751-62.

GREENWALD, I. S., STERNBERG, P. W. & HORVITZ, H. R. 1983. The lin-12 locus specifies cell fates in Caenorhabditis elegans. *Cell,* 34, 435-44.

HAINES, N. & IRVINE, K. D. 2003. Glycosylation regulates Notch signalling. *Nat Rev Mol Cell Biol,* 4, 786-97.

HAINES, N. & IRVINE, K. D. 2005. Functional analysis of Drosophila beta1,4-N-acetylgalactosaminyltransferases. *Glycobiology,* 15, 335-46.

HALTIWANGER, R. S. & STANLEY, P. 2002. Modulation of receptor signaling by glycosylation: fringe is an O-fucose-beta1,3-N-acetylglucosaminyltransferase. *Biochim Biophys Acta,* 1573, 328-35.

HAMBLETON, S., VALEYEV, N. V., MURANYI, A., KNOTT, V., WERNER, J. M., MCMICHAEL, A. J., HANDFORD, P. A. & DOWNING, A. K. 2004. Structural and functional properties of the human notch-1 ligand binding region. *Structure,* 12, 2173-83.

HANDFORD, P. A., BARON, M., MAYHEW, M., WILLIS, A., BEESLEY, T., BROWNLEE, G. G. & CAMPBELL, I. D. 1990. The first EGF-like domain from human factor IX contains a high-affinity calcium binding site. *EMBO J,* 9, 475-80.

HANDFORD, P. A., MAYHEW, M., BARON, M., WINSHIP, P. R., CAMPBELL, I. D. & BROWNLEE, G. G. 1991. Key residues involved in calcium-binding motifs in EGF-like domains. *Nature,* 351, 164-7.

HARRIS, R. J., VAN HALBEEK, H., GLUSHKA, J., BASA, L. J., LING, V. T., SMITH, K. J. & SPELLMAN, M. W. 1993. Identification and structural analysis of the tetrasaccharide NeuAc alpha(2-->6)Gal beta(1-->4)GlcNAc beta(1-->3)Fuc alpha 1-->O-linked to serine 61 of human factor IX. *Biochemistry,* 32, 6539-47.

HARTLEY, D. A., XU, T. A. & ARTAVANIS-TSAKONAS, S. 1987. The embryonic expression of the Notch locus of Drosophila melanogaster and the implications of point mutations in the extracellular EGF-like domain of the predicted protein. *EMBO J,* 6, 3407-17.

HEITZLER, P. & SIMPSON, P. 1991. The choice of cell fate in the epidermis of Drosophila. *Cell,* 64, 1083-92.

HENDERSON, S. T., GAO, D., CHRISTENSEN, S. & KIMBLE, J. 1997. Functional domains of LAG-2, a putative signaling ligand for LIN-12 and GLP-1 receptors in Caenorhabditis elegans. *Mol Biol Cell,* 8, 1751-62.

HENLEY, D. B., MAY, P. C., DEAN, R. A. & SIEMERS, E. R. 2009. Development of semagacestat (LY450139), a functional gamma-secretase inhibitor, for the treatment of Alzheimer's disease. *Expert Opin Pharmacother,* 10, 1657-64.

HICKE, L. & DUNN, R. 2003. Regulation of membrane protein transport by ubiquitin and ubiquitin-binding proteins. *Annu Rev Cell Dev Biol,* 19, 141-72.

HICKS, C., JOHNSTON, S. H., DISIBIO, G., COLLAZO, A., VOGT, T. F. & WEINMASTER, G. 2000. Fringe differentially modulates Jagged1 and Delta1 signalling through Notch1 and Notch2. *Nat Cell Biol,* 2, 515-20.

HIRUMA-SHIMIZU, K., HOSOGUCHI, K., LIU, Y., FUJITANI, N., OHTA, T., HINOU, H., MATSUSHITA, T., SHIMIZU, H., FEIZI, T. & NISHIMURA, S. 2010. Chemical synthesis, folding, and structural insights into O-fucosylated epidermal growth factor-like repeat 12 of mouse Notch-1 receptor. *J Am Chem Soc,* 132, 14857-65.

HOFMANN, J. J., ZOVEIN, A. C., KOH, H., RADTKE, F., WEINMASTER, G. & IRUELA-ARISPE, M. L. 2010. Jagged1 in the portal vein mesenchyme regulates intrahepatic bile duct development: insights into Alagille syndrome. *Development,* 137, 4061-72.

HSIEH, J. J., ZHOU, S., CHEN, L., YOUNG, D. B. & HAYWARD, S. D. 1999. CIR, a corepressor linking the DNA binding factor CBF1 to the histone deacetylase complex. *Proc Natl Acad Sci U S A,* 96, 23-8.

IRVINE, K. D. & WIESCHAUS, E. 1994. fringe, a Boundary-specific signaling molecule, mediates interactions between dorsal and ventral cells during Drosophila wing development. *Cell,* 79, 595-606.

ITOH, M., KIM, C. H., PALARDY, G., ODA, T., JIANG, Y. J., MAUST, D., YEO, S. Y., LORICK, K., WRIGHT, G. J., ARIZA-MCNAUGHTON, L., WEISSMAN, A. M., LEWIS, J., CHANDRASEKHARAPPA, S. C. & CHITNIS, A. B. 2003. Mind bomb is a ubiquitin ligase that is essential for efficient activation of Notch signaling by Delta. *Dev Cell,* 4, 67-82.

JARRIAULT, S., BROU, C., LOGEAT, F., SCHROETER, E., KOPAN, R. & ISRAEL, A. 1995. Signalling downstream of activated mammalian Notch. *Nature,* 377, 355-8.

JENSEN, S., CORBETT, A., KNOTT, V., REDFIELD, C. & HANDFORD, P. 2005a. Ca2+-dependent interface formation in fibrillin-1. *J Biol Chem,* 280, 14076-84.

JENSEN, S. A., CORBETT, A. R., KNOTT, V., REDFIELD, C. & HANDFORD, P. A. 2005b. Ca2+-dependent interface formation in fibrillin-1. *J Biol Chem,* 280, 14076-84.

JOHANSEN, K. M., FEHON, R. G. & ARTAVANIS-TSAKONAS, S. 1989. The notch gene product is a glycoprotein expressed on the cell surface of both epidermal and neuronal precursor cells during Drosophila development. *J Cell Biol,* 109, 2427-40.

JOHNSON, S. E., ILAGAN, M. X., KOPAN, R. & BARRICK, D. 2010. Thermodynamic analysis of the CSL x Notch interaction: distribution of binding energy of the Notch RAM region to the CSL beta-trefoil domain and the mode of competition with the viral transactivator EBNA2. *J Biol Chem,* 285, 6681-92.

JOHNSTON, S. H., RAUSKOLB, C., WILSON, R., PRABHAKARAN, B., IRVINE, K. D. & VOGT, T. F. 1997. A family of mammalian Fringe genes implicated in boundary determination and the Notch pathway. *Development,* 124, 2245-54.

JOUTEL, A., ANDREUX, F., GAULIS, S., DOMENGA, V., CECILLON, M., BATTAIL, N., PIGA, N., CHAPON, F., GODFRAIN, C. & TOURNIER-LASSERVE, E. 2000. The ectodomain of the Notch3 receptor accumulates within the cerebrovasculature of CADASIL patients. *J Clin Invest,* 105, 597-605.

JOUTEL, A., CORPECHOT, C., DUCROS, A., VAHEDI, K., CHABRIAT, H., MOUTON, P., ALAMOWITCH, S., DOMENGA, V., CÉCILLION, M., MARECHAL, E., MACIAZEK, J., VAYSSIERE, C., CRUAUD, C., CABANIS, E. A., RUCHOUX, M. M., WEISSENBACH, J., BACH, J. F., BOUSSER, M. G. & TOURNIER-LASSERVE, E. 1996. Notch3 mutations in CADASIL, a hereditary adult-onset condition causing stroke and dementia. *Nature,* 383, 707-10.

JOUTEL, A., MONET, M., DOMENGA, V., RIANT, F. & TOURNIER-LASSERVE, E. 2004. Pathogenic mutations associated with cerebral autosomal dominant arteriopathy with subcortical infarcts and leukoencephalopathy differently affect Jagged1 binding and Notch3 activity via the RBP/JK signaling Pathway. *Am J Hum Genet,* 74, 338-47.

JOUTEL, A., MONET-LEPRÊTRE, M., GOSELE, C., BARON-MENGUY, C., HAMMES, A., SCHMIDT, S., LEMAIRE-CARRETTE, B., DOMENGA, V., SCHEDL, A., LACOMBE, P. & HUBNER, N. 2010. Cerebrovascular dysfunction and microcirculation rarefaction precede white matter lesions in a mouse genetic model of cerebral ischemic small vessel disease. *J Clin Invest,* 120, 433-45.

KAGEYAMA, R. & NAKANISHI, S. 1997. Helix-loop-helix factors in growth and differentiation of the vertebrate nervous system. *Curr Opin Genet Dev,* 7, 659-65.

KAMATH, B. M., BAUER, R. C., LOOMES, K. M., CHAO, G., GERFEN, J., HUTCHINSON, A., HARDIKAR, W., HIRSCHFIELD, G., JARA, P., KRANTZ, I. D., LAPUNZINA, P., LEONARD, L., LING, S., NG, V. L., HOANG, P. L., PICCOLI, D. A. & SPINNER, N. B. 2012. NOTCH2 mutations in Alagille syndrome. *J Med Genet,* 49, 138-44.

KAO, H. Y., ORDENTLICH, P., KOYANO-NAKAGAWA, N., TANG, Z., DOWNES, M., KINTNER, C. R., EVANS, R. M. & KADESCH, T. 1998. A histone deacetylase corepressor complex regulates the Notch signal transduction pathway. *Genes Dev,* 12, 2269-77.

KAO, Y. H., LEE, G. F., WANG, Y., STAROVASNIK, M. A., KELLEY, R. F., SPELLMAN, M. W. & LERNER, L. 1999. The effect of O-fucosylation on the first EGF-like domain from human blood coagulation factor VII. *Biochemistry,* 38, 7097-110.

KELLEY, M. R., KIDD, S., DEUTSCH, W. A. & YOUNG, M. W. 1987. Mutations altering the structure of epidermal growth factor-like coding sequences at the Drosophila Notch locus. *Cell,* 51, 539-48.

KELLY, D. F., LAKE, R. J., MIDDELKOOP, T. C., FAN, H. Y., ARTAVANIS-TSAKONAS, S. & WALZ, T. 2010. Molecular structure and dimeric organization of the Notch extracellular domain as revealed by electron microscopy. *PLoS One,* 5, e10532.

KIDD, S., BAYLIES, M. K., GASIC, G. P. & YOUNG, M. W. 1989. Structure and distribution of the Notch protein in developing Drosophila. *Genes Dev,* 3, 1113-29.

KIM, J., IRVINE, K. D. & CARROLL, S. B. 1995. Cell recognition, signal induction, and symmetrical gene activation at the dorsal-ventral boundary of the developing Drosophila wing. *Cell,* 82, 795-802.

KIMBLE, J. 1981. Alterations in cell lineage following laser ablation of cells in the somatic gonad of Caenorhabditis elegans. *Dev Biol,* 87, 286-300.

KLUEG, K. M. & MUSKAVITCH, M. A. 1999. Ligand-receptor interactions and trans-endocytosis of Delta, Serrate and Notch: members of the Notch signalling pathway in Drosophila. *J Cell Sci,* 112 (Pt 19), 3289-97.

KNOTT, V., DOWNING, A. K., CARDY, C. M. & HANDFORD, P. 1996. Calcium binding properties of an epidermal growth factor-like domain pair from human fibrillin-1. *J Mol Biol,* 255, 22-7.

KOMATSU, H., CHAO, M. Y., LARKINS-FORD, J., CORKINS, M. E., SOMERS, G. A., TUCEY, T., DIONNE, H. M., WHITE, J. Q., WANI, K., BOXEM, M. & HART, A. C. 2008. OSM-11 facilitates LIN-12 Notch signaling during Caenorhabditis elegans vulval development. *PLoS Biol,* 6, e196.

KOO, B. K., LIM, H. S., SONG, R., YOON, M. J., YOON, K. J., MOON, J. S., KIM, Y. W., KWON, M. C., YOO, K. W., KONG, M. P., LEE, J., CHITNIS, A. B., KIM, C. H. & KONG, Y. Y. 2005. Mind bomb 1 is essential for generating functional Notch ligands to activate Notch. *Development,* 132, 3459-70.

KOVALL, R. A. 2007. Structures of CSL, Notch and Mastermind proteins: piecing together an active transcription complex. *Curr Opin Struct Biol,* 17, 117-27.

KOVALL, R. A. 2008. More complicated than it looks: assembly of Notch pathway transcription complexes. *Oncogene,* 27, 5099-109.

KRANTZ, I. D., COLLITON, R. P., GENIN, A., RAND, E. B., LI, L., PICCOLI, D. A. & SPINNER, N. B. 1998. Spectrum and frequency of jagged1 (JAG1) mutations in Alagille syndrome patients and their families. *Am J Hum Genet,* 62, 1361-9.

KRIDEL, R., MEISSNER, B., ROGIC, S., BOYLE, M., TELENIUS, A., WOOLCOCK, B., GUNAWARDANA, J., JENKINS, C., COCHRANE, C., BEN-NERIAH, S., TAN, K., MORIN, R. D., OPAT, S., SEHN, L. H., CONNORS, J. M., MARRA, M. A., WENG, A. P., STEIDL, C. & GASCOYNE, R. D. 2012. Whole transcriptome sequencing reveals recurrent NOTCH1 mutations in mantle cell lymphoma. *Blood,* 119, 1963-71.

KRIDEL, R., MEISSNER, B., ROGIC, S., BOYLE, M., TELENIUS, A., WOOLCOCK, B., GUNAWARDANA, J., JENKINS, C., COCHRANE, C., BEN-NERIAH, S., TAN, K., OPAT, S., SEHN, L. H., CONNORS, J. M., WENG, A. P., STEIDL, C. & GASCOYNE, R. D. 2011. Whole transcriptome sequencing reveals recurrent NOTCH1 mutations in mantle cell lymphoma. *Blood*.

KUROOKA, H. & HONJO, T. 2000. Functional interaction between the mouse notch1 intracellular region and histone acetyltransferases PCAF and GCN5. *J Biol Chem,* 275, 17211-20.

LADI, E., NICHOLS, J. T., GE, W., MIYAMOTO, A., YAO, C., YANG, L. T., BOULTER, J., SUN, Y. E., KINTNER, C. & WEINMASTER, G. 2005. The divergent DSL ligand Dll3 does not activate Notch signaling but cell autonomously attenuates signaling induced by other DSL ligands. *J Cell Biol,* 170, 983-92.

LAEMMLI, U. K. 1970. Cleavage of structural proteins during the assembly of the head of bacteriophage T4. *Nature,* 227, 680-5.

LAI, E. C., DEBLANDRE, G. A., KINTNER, C. & RUBIN, G. M. 2001. Drosophila neuralized is a ubiquitin ligase that promotes the internalization and degradation of delta. *Dev Cell,* 1, 783-94.

LAKE, R. J., GRIMM, L. M., VERAKSA, A., BANOS, A. & ARTAVANIS-TSAKONAS, S. 2009. In vivo analysis of the Notch receptor S1 cleavage. *PLoS One,* 4, e6728.

LAVAISSIERE, L., JIA, S., NISHIYAMA, M., DE LA MONTE, S., STERN, A. M., WANDS, J. R. & FRIEDMAN, P. A. 1996. Overexpression of human aspartyl(asparaginyl)beta-hydroxylase in hepatocellular carcinoma and cholangiocarcinoma. *J Clin Invest,* 98, 1313-23.

LAWRENCE, N., KLEIN, T., BRENNAN, K. & MARTINEZ ARIAS, A. 2000. Structural requirements for notch signalling with delta and serrate during the development and patterning of the wing disc of Drosophila. *Development,* 127, 3185-95.

LECOURTOIS, M. & SCHWEISGUTH, F. 1995. The neurogenic suppressor of hairless DNA-binding protein mediates the transcriptional activation of the enhancer of split complex genes triggered by Notch signaling. *Genes Dev,* 9, 2598-608.

LEHMANN, R., DIETRICH, U., JIMINEZ, F. & CAMPOS-ORTEGA, J. A. 1981. Mutations of early neurogenesis in *Drosophila*. Wilhelm Roux's Archives.

LEHMANN, R., JIMINEZ, F., DIETRICH, U. & CAMPOS-ORTEGA, J. A. 1983. On the phenotype and development of mutants of early neurogenesis in *Drosophila melanogaster*. Roux's Arch. Dev. Biol.

LEI, L., XU, A., PANIN, V. & IRVINE, K. 2003. An O-fucose site in the ligand binding domain inhibits Notch activation. *Development,* 130, 6411-21.

LEONARDI, J., FERNANDEZ-VALDIVIA, R., LI, Y. D., SIMCOX, A. A. & JAFAR-NEJAD, H. 2011. Multiple O-glucosylation sites on Notch function as a buffer against temperature-dependent loss of signaling. *Development,* 138, 3569-78.

LI, K., LI, Y., WU, W., GORDON, W. R., CHANG, D. W., LU, M., SCOGGIN, S., FU, T., VIEN, L., HISTEN, G., ZHENG, J., MARTIN-HOLLISTER, R., DUENSING, T., SINGH, S., BLACKLOW, S. C., YAO, Z., ASTER, J. C. & ZHOU, B. B. 2008. Modulation of Notch signaling by antibodies specific for the extracellular negative regulatory region of NOTCH3. *J Biol Chem,* 283, 8046-54.

LI, L., KRANTZ, I. D., DENG, Y., GENIN, A., BANTA, A. B., COLLINS, C. C., QI, M., TRASK, B. J., KUO, W. L., COCHRAN, J., COSTA, T., PIERPONT, M. E., RAND, E. B., PICCOLI, D. A., HOOD, L. & SPINNER, N. B. 1997. Alagille syndrome is caused by mutations in human Jagged1, which encodes a ligand for Notch1. *Nat Genet,* 16, 243-51.

LI, T., WEN, H., BRAYTON, C., DAS, P., SMITHSON, L. A., FAUQ, A., FAN, X., CRAIN, B. J., PRICE, D. L., GOLDE, T. E., EBERHART, C. G. & WONG, P. C. 2007. Epidermal growth factor receptor and notch pathways participate in the tumor suppressor function of gamma-secretase. *J Biol Chem,* 282, 32264-73.

LOOMES, K. M., UNDERKOFFLER, L. A., MORABITO, J., GOTTLIEB, S., PICCOLI, D. A., SPINNER, N. B., BALDWIN, H. S. & OAKEY, R. J. 1999. The expression of Jagged1 in the developing mammalian heart correlates with cardiovascular disease in Alagille syndrome. *Hum Mol Genet,* 8, 2443-9.

LOWELL, S., JONES, P., LE ROUX, I., DUNNE, J. & WATT, F. M. 2000. Stimulation of human epidermal differentiation by delta-notch signalling at the boundaries of stem-cell clusters. *Curr Biol,* 10, 491-500.

LUO, Y. & HALTIWANGER, R. S. 2005. O-fucosylation of notch occurs in the endoplasmic reticulum. *J Biol Chem,* 280, 11289-94.

MAJUMDER, R., ROY, S. & THAKUR, A. R. 2012. Analysis of Delta-Notch interaction by molecular modeling and molecular dynamic simulation studies. *J Biomol Struct Dyn,* 30, 13-29.

MALECKI, M. J., SANCHEZ-IRIZARRY, C., MITCHELL, J. L., HISTEN, G., XU, M. L., ASTER, J. C. & BLACKLOW, S. C. 2006. Leukemia-associated mutations within the NOTCH1 heterodimerization domain fall into at least two distinct mechanistic classes. *Mol Cell Biol,* 26, 4642-51.

MAREK, K. W., VIJAY, I. K. & MARTH, J. D. 1999. A recessive deletion in the GlcNAc-1-phosphotransferase gene results in peri-implantation embryonic lethality. *Glycobiology,* 9, 1263-71.

MAYHEW, M., HANDFORD, P., BARON, M., TSE, A. G., CAMPBELL, I. D. & BROWNLEE, G. G. 1992. Ligand requirements for Ca2+ binding to EGF-like domains. *Protein Eng,* 5, 489-94.

MCGETTRICK, A. J., KNOTT, V., WILLIS, A. & HANDFORD, P. A. 2000. Molecular effects of calcium binding mutations in Marfan syndrome depend on domain context. *Hum Mol Genet,* 9, 1987-94.

MELOTY-KAPELLA, L., SHERGILL, B., KUON, J., BOTVINICK, E. & WEINMASTER, G. 2012. Notch ligand endocytosis generates mechanical pulling force dependent on dynamin, epsins, and actin. *Dev Cell,* 22, 1299-312.

MOHR, O. 1919. CHARACTER CHANGES CAUSED BY MUTATION OF AN ENTIRE REGION OF A CHROMOSOME IN DROSOPHILA. Genetics.

MOLONEY, D., PANIN, V., JOHNSTON, S., CHEN, J., SHAO, L., WILSON, R., WANG, Y., STANLEY, P., IRVINE, K., HALTIWANGER, R. & VOGT, T. 2000a. Fringe is a glycosyltransferase that modifies Notch. *Nature,* 406, 369-75.

MOLONEY, D. J., SHAIR, L. H., LU, F. M., XIA, J., LOCKE, R., MATTA, K. L. & HALTIWANGER, R. S. 2000b. Mammalian Notch1 is modified with two unusual forms of O-linked glycosylation found on epidermal growth factor-like modules. *J Biol Chem,* 275, 9604-11.

MONET, M., DOMENGA, V., LEMAIRE, B., SOUILHOL, C., LANGA, F., BABINET, C., GRIDLEY, T., TOURNIER-LASSERVE, E., COHEN-TANNOUDJI, M. & JOUTEL, A. 2007. The archetypal R90C CADASIL-NOTCH3 mutation retains NOTCH3 function in vivo. *Hum Mol Genet,* 16, 982-92.

MOON, Y. S., SMAS, C. M., LEE, K., VILLENA, J. A., KIM, K. H., YUN, E. J. & SUL, H. S. 2002. Mice lacking paternally expressed Pref-1/Dlk1 display growth retardation and accelerated adiposity. *Mol Cell Biol,* 22, 5585-92.

MORGAN, T. H. 1917. The Theory of the Gene. *The American Naturalist,* 51, 513-544.

MORRISSETTE, J. D., COLLITON, R. P. & SPINNER, N. B. 2001. Defective intracellular transport and processing of JAG1 missense mutations in Alagille syndrome. *Hum Mol Genet,* 10, 405-13.

MUNRO, S. & FREEMAN, M. 2000. The notch signalling regulator fringe acts in the Golgi apparatus and requires the glycosyltransferase signature motif DXD. *Curr Biol,* 10, 813-20.

NAM, Y., SLIZ, P., SONG, L., ASTER, J. C. & BLACKLOW, S. C. 2006. Structural basis for cooperativity in recruitment of MAML coactivators to Notch transcription complexes. *Cell,* 124, 973-83.

NAM, Y., WENG, A. P., ASTER, J. C. & BLACKLOW, S. C. 2003. Structural requirements for assembly of the CSL.intracellular Notch1.Mastermind-like 1 transcriptional activation complex. *J Biol Chem,* 278, 21232-9.

NICHOLS, J. T., MIYAMOTO, A., OLSEN, S. L., D'SOUZA, B., YAO, C. & WEINMASTER, G. 2007. DSL ligand endocytosis physically dissociates Notch1 heterodimers before activating proteolysis can occur. *J Cell Biol,* 176, 445-58.

NUEDA, M., BALADRÓN, V., SÁNCHEZ-SOLANA, B., BALLESTEROS, M. & LABORDA, J. 2007. The EGF-like protein dlk1 inhibits notch signaling and potentiates adipogenesis of mesenchymal cells. *J Mol Biol,* 367, 1281-93.

OBERG, C., LI, J., PAULEY, A., WOLF, E., GURNEY, M. & LENDAHL, U. 2001. The Notch intracellular domain is ubiquitinated and negatively regulated by the mammalian Sel-10 homolog. *J Biol Chem,* 276, 35847-53.

OKAJIMA, T. & IRVINE, K. D. 2002. Regulation of notch signaling by o-linked fucose. *Cell,* 111, 893-904.

OKAJIMA, T., REDDY, B., MATSUDA, T. & IRVINE, K. 2008. Contributions of chaperone and glycosyltransferase activities of O-fucosyltransferase 1 to Notch signaling. *BMC Biol,* 6, 1.

OKAJIMA, T., XU, A. & IRVINE, K. D. 2003. Modulation of notch-ligand binding by protein O-fucosyltransferase 1 and fringe. *J Biol Chem,* 278, 42340-5.

OKAJIMA, T., XU, A., LEI, L. & IRVINE, K. D. 2005. Chaperone activity of protein O-fucosyltransferase 1 promotes notch receptor folding. *Science,* 307, 1599-603.

OPHERK, C., DUERING, M., PETERS, N., KARPINSKA, A., ROSNER, S., SCHNEIDER, E., BADER, B., GIESE, A. & DICHGANS, M. 2009. CADASIL mutations enhance spontaneous multimerization of NOTCH3. *Hum Mol Genet,* 18, 2761-7.

PANIN, V., PAPAYANNOPOULOS, V., WILSON, R. & IRVINE, K. 1997a. Fringe modulates Notch-ligand interactions. *Nature,* 387, 908-12.

PANIN, V. M., PAPAYANNOPOULOS, V., WILSON, R. & IRVINE, K. D. 1997b. Fringe modulates Notch-ligand interactions. *Nature,* 387, 908-12.

PARKS, A. L., KLUEG, K. M., STOUT, J. R. & MUSKAVITCH, M. A. 2000. Ligand endocytosis drives receptor dissociation and activation in the Notch pathway. *Development,* 127, 1373-85.

PARKS, A. L., STOUT, J. R., SHEPARD, S. B., KLUEG, K. M., DOS SANTOS, A. A., PARODY, T. R., VASKOVA, M. & MUSKAVITCH, M. A. 2006. Structure-function analysis of delta trafficking, receptor binding and signaling in Drosophila. *Genetics,* 174, 1947-61.

PEI, Z. & BAKER, N. E. 2008. Competition between Delta and the Abruptex domain of Notch. *BMC Dev Biol,* 8, 4.

PETCHERSKI, A. G. & KIMBLE, J. 2000. Mastermind is a putative activator for Notch. *Curr Biol,* 10, R471-3.

PETERS, N., OPHERK, C., ZACHERLE, S., CAPELL, A., GEMPEL, P. & DICHGANS, M. 2004. CADASIL-associated Notch3 mutations have differential effects both on ligand binding and ligand-induced Notch3 receptor signaling through RBP-Jk. *Exp Cell Res,* 299, 454-64.

PINTAR, A., DE BIASIO, A., POPOVIC, M., IVANOVA, N. & PONGOR, S. 2007. The intracellular region of Notch ligands: does the tail make the difference? *Biol Direct,* 2, 19.

PORTIN, P. 1975. Allelic negative complementation at the Abruptex locus of Drosophila melanogaster. *Genetics,* 81, 121-33.

PORTIN, P. 2001. Numb suppresses the negative complementation at the Notch locus of Drosophila melanogaster, suggesting a putative mechanism for negative complementation. *Genet Res,* 78, 219-23.

POULSON, D. F. 1937. Chromosomal deficiencies and the embryonic development of *Drosophila melanogaster*. Proc. Natl. Acad. Sci. USA.

RAMPAL, R., ARBOLEDA-VELASQUEZ, J. F., NITA-LAZAR, A., KOSIK, K. S. & HALTIWANGER, R. S. 2005a. Highly conserved O-fucose sites have distinct effects on Notch1 function. *J Biol Chem,* 280, 32133-40.

RAMPAL, R., LI, A. S., MOLONEY, D. J., GEORGIOU, S. A., LUTHER, K. B., NITA-LAZAR, A. & HALTIWANGER, R. S. 2005b. Lunatic fringe, manic fringe, and radical fringe recognize similar specificity determinants in O-fucosylated epidermal growth factor-like repeats. *J Biol Chem,* 280, 42454-63.

RAMPAL, R., LI, A. S., MOLONEY, D. J., GEORGIOU, S. A., LUTHER, K. B., NITA-LAZAR, A. & HALTIWANGER, R. S. 2005c. Lunatic fringe, manic fringe, and radical fringe recognize similar specificity determinants in O-fucosylated epidermal growth factor-like repeats. *J Biol Chem,* 280, 42454-63.

RAO, Z., HANDFORD, P., MAYHEW, M., KNOTT, V., BROWNLEE, G. G. & STUART, D. 1995. The structure of a Ca(2+)-binding epidermal growth factor-like domain: its role in protein-protein interactions. *Cell,* 82, 131-41.

RAUSKOLB, C., CORREIA, T. & IRVINE, K. D. 1999. Fringe-dependent separation of dorsal and ventral cells in the Drosophila wing. *Nature,* 401, 476-80.

REBAY, I., FLEMING, R., FEHON, R., CHERBAS, L., CHERBAS, P. & ARTAVANIS-TSAKONAS, S. 1991. Specific EGF repeats of Notch mediate interactions with Delta and Serrate: implications for Notch as a multifunctional receptor. *Cell,* 67, 687-99.

REES, D. J., JONES, I. M., HANDFORD, P. A., WALTER, S. J., ESNOUF, M. P., SMITH, K. J. & BROWNLEE, G. G. 1988. The role of beta-hydroxyaspartate and adjacent carboxylate residues in the first EGF domain of human factor IX. *EMBO J,* 7, 2053-61.

REINHARDT, D. P., ONO, R. N. & SAKAI, L. Y. 1997. Calcium stabilizes fibrillin-1 against proteolytic degradation. *J Biol Chem,* 272, 1231-6.

REYNOLDS, T. C., SMITH, S. D. & SKLAR, J. 1987. Analysis of DNA surrounding the breakpoints of chromosomal translocations involving the beta T cell receptor gene in human lymphoblastic neoplasms. *Cell,* 50, 107-17.

RIPKA, J., ADAMANY, A. & STANLEY, P. 1986. Two Chinese hamster ovary glycosylation mutants affected in the conversion of GDP-mannose to GDP-fucose. *Arch Biochem Biophys,* 249, 533-45.

ROGERS, S., WELLS, R. & RECHSTEINER, M. 1986. Amino acid sequences common to rapidly degraded proteins: the PEST hypothesis. *Science,* 234, 364-8.

RÖPKE, A., KUJAT, A., GRÄBER, M., GIANNAKUDIS, J. & HANSMANN, I. 2003. Identification of 36 novel Jagged1 (JAG1) mutations in patients with Alagille syndrome. *Hum Mutat,* 21, 100.

SAKAIDANI, Y., FURUKAWA, K. & OKAJIMA, T. 2010. O-GlcNAc modification of the extracellular domain of Notch receptors. *Methods Enzymol,* 480, 355-73.

SAKAIDANI, Y., ICHIYANAGI, N., SAITO, C., NOMURA, T., ITO, M., NISHIO, Y., NADANO, D., MATSUDA, T., FURUKAWA, K. & OKAJIMA, T. 2012. O-linked-N-acetylglucosamine modification of mammalian Notch receptors by an atypical O-GlcNAc transferase Eogt1. *Biochem Biophys Res Commun,* 419, 14-9.

SAKAMOTO, K., CHAO, W. S., KATSUBE, K. & YAMAGUCHI, A. 2005. Distinct roles of EGF repeats for the Notch signaling system. *Exp Cell Res,* 302, 281-91.

SAKAMOTO, K., OHARA, O., TAKAGI, M., TAKEDA, S. & KATSUBE, K. 2002. Intracellular cell-autonomous association of Notch and its ligands: a novel mechanism of Notch signal modification. *Dev Biol,* 241, 313-26.

SASAMURA, T., SASAKI, N., MIYASHITA, F., NAKAO, S., ISHIKAWA, H. O., ITO, M., KITAGAWA, M., HARIGAYA, K., SPANA, E., BILDER, D., PERRIMON, N. & MATSUNO, K. 2003. neurotic, a novel maternal neurogenic gene, encodes an O-fucosyltransferase that is essential for Notch-Delta interactions. *Development,* 130, 4785-95.

SETHI, M. K., BUETTNER, F. F., ASHIKOV, A., KRYLOV, V. B., TAKEUCHI, H., NIFANTIEV, N. E., HALTIWANGER, R. S., GERARDY-SCHAHN, R. & BAKKER, H. 2012. Molecular cloning of a xylosyltransferase that transfers the second xylose to O-glucosylated epidermal growth factor repeats of notch. *J Biol Chem,* 287, 2739-48.

SETHI, M. K., BUETTNER, F. F., KRYLOV, V. B., TAKEUCHI, H., NIFANTIEV, N. E., HALTIWANGER, R. S., GERARDY-SCHAHN, R. & BAKKER, H. 2010. Identification of glycosyltransferase 8 family members as xylosyltransferases acting on O-glucosylated notch epidermal growth factor repeats. *J Biol Chem,* 285, 1582-6.

SHAO, L., MOLONEY, D. J. & HALTIWANGER, R. 2003. Fringe modifies O-fucose on mouse Notch1 at epidermal growth factor-like repeats within the ligand-binding site and the Abruptex region. *J Biol Chem,* 278, 7775-82.

SHELLENBARGER, D. L. & MOHLER, J. D. 1978. Temperature-sensitive periods and autonomy of pleiotropic effects of l(1)Nts1, a conditional notch lethal in Drosophila. *Dev Biol,* 62, 432-46.

SHERGILL, B., MELOTY-KAPELLA, L., MUSSE, A. A., WEINMASTER, G. & BOTVINICK, E. 2012. Optical tweezers studies on Notch: single-molecule interaction strength is independent of ligand endocytosis. *Dev Cell,* 22, 1313-20.

SHI, S., GE, C., LUO, Y., HOU, X., HALTIWANGER, R. S. & STANLEY, P. 2007. The threonine that carries fucose, but not fucose, is required for Cripto to facilitate Nodal signaling. *J Biol Chem,* 282, 20133-41.

SHI, S. & STANLEY, P. 2003. Protein O-fucosyltransferase 1 is an essential component of Notch signaling pathways. *Proc Natl Acad Sci U S A,* 100, 5234-9.

SHIMIZU, K., CHIBA, S., KUMANO, K., HOSOYA, N., TAKAHASHI, T., KANDA, Y., HAMADA, Y., YAZAKI, Y. & HIRAI, H. 1999. Mouse jagged1 physically interacts with notch2 and other notch receptors. Assessment by quantitative methods. *J Biol Chem,* 274, 32961-9.

SHIMIZU, K., CHIBA, S., SAITO, T., KUMANO, K., TAKAHASHI, T. & HIRAI, H. 2001. Manic fringe and lunatic fringe modify different sites of the Notch2 extracellular region, resulting in different signaling modulation. *J Biol Chem,* 276, 25753-8.

SIDOW, A., BULOTSKY, M. S., KERREBROCK, A. W., BRONSON, R. T., DALY, M. J., REEVE, M. P., HAWKINS, T. L., BIRREN, B. W., JAENISCH, R. & LANDER, E. S. 1997. Serrate2 is disrupted in the mouse limb-development mutant syndactylism. *Nature,* 389, 722-5.

SIMPSON, M. A., IRVING, M. D., ASILMAZ, E., GRAY, M. J., DAFOU, D., ELMSLIE, F. V., MANSOUR, S., HOLDER, S. E., BRAIN, C. E., BURTON, B. K., KIM, K. H., PAULI, R. M., AFTIMOS, S., STEWART, H., KIM, C. A., HOLDER-ESPINASSE, M., ROBERTSON, S. P., DRAKE, W. M. & TREMBATH, R. C. 2011. Mutations in NOTCH2 cause Hajdu-Cheney syndrome, a disorder of severe and progressive bone loss. *Nat Genet,* 43, 303-5.

SIMPSON, P. 1990. Notch and the choice of cell fate in Drosophila neuroepithelium. *Trends Genet,* 6, 343-5.

SPARROW, D. B., CHAPMAN, G., TURNPENNY, P. D. & DUNWOODIE, S. L. 2007. Disruption of the somitic molecular clock causes abnormal vertebral segmentation. *Birth Defects Res C Embryo Today,* 81, 93-110.

SPARROW, D. B., CHAPMAN, G., WOUTERS, M. A., WHITTOCK, N. V., ELLARD, S., FATKIN, D., TURNPENNY, P. D., KUSUMI, K., SILLENCE, D. & DUNWOODIE, S. L. 2006. Mutation of the LUNATIC FRINGE gene in humans causes spondylocostal dysostosis with a severe vertebral phenotype. *Am J Hum Genet,* 78, 28-37.

SPARROW, D. B., GUILLÉN-NAVARRO, E., FATKIN, D. & DUNWOODIE, S. L. 2008. Mutation of Hairy-and-Enhancer-of-Split-7 in humans causes spondylocostal dysostosis. *Hum Mol Genet,* 17, 3761-6.

SPINNER, N. B., COLLITON, R. P., CROSNIER, C., KRANTZ, I. D., HADCHOUEL, M. & MEUNIER-ROTIVAL, M. 2001. Jagged1 mutations in alagille syndrome. *Hum Mutat,* 17, 18-33.

SPRINZAK, D., LAKHANPAL, A., LEBON, L., SANTAT, L. A., FONTES, M. E., ANDERSON, G. A., GARCIA-OJALVO, J. & ELOWITZ, M. B. 2010. Cis-interactions between Notch and Delta generate mutually exclusive signalling states. *Nature,* 465, 86-90.

STAHL, M., UEMURA, K., GE, C., SHI, S., TASHIMA, Y. & STANLEY, P. 2008. Roles of Pofut1 and O-fucose in mammalian Notch signaling. *J Biol Chem,* 283, 13638-51.

STENFLO, J., HOLME, E., LINDSTEDT, S., CHANDRAMOULI, N., HUANG, L. H., TAM, J. P. & MERRIFIELD, R. B. 1989. Hydroxylation of aspartic acid in domains homologous to the epidermal growth factor precursor is catalyzed by a 2-oxoglutarate-dependent dioxygenase. *Proc Natl Acad Sci U S A,* 86, 444-7.

STENFLO, J., OHLIN, A. K., OWEN, W. G. & SCHNEIDER, W. J. 1988. beta-Hydroxyaspartic acid or beta-hydroxyasparagine in bovine low density lipoprotein receptor and in bovine thrombomodulin. *J Biol Chem,* 263, 21-4.

SUK, J. Y., JENSEN, S., MCGETTRICK, A., WILLIS, A. C., WHITEMAN, P., REDFIELD, C. & HANDFORD, P. A. 2004. Structural consequences of cysteine substitutions C1977Y and C1977R in calcium-binding epidermal growth factor-like domain 30 of human fibrillin-1. *J Biol Chem,* 279, 51258-65.

SUNNERHAGEN, M. S., PERSSON, E., DAHLQVIST, I., DRAKENBERG, T., STENFLO, J., MAYHEW, M., ROBIN, M., HANDFORD, P., TILLEY, J. W. & CAMPBELL, I. D. 1993. The effect of aspartate hydroxylation on calcium binding to epidermal growth factor-like modules in coagulation factors IX and X. *J Biol Chem,* 268, 23339-44.

SÁNCHEZ-SOLANA, B., NUEDA, M. L., RUVIRA, M. D., RUIZ-HIDALGO, M. J., MONSALVE, E. M., RIVERO, S., GARCÍA-RAMÍREZ, J. J., DÍAZ-GUERRA, M. J., BALADRÓN, V. & LABORDA, J. 2011. The EGF-like proteins DLK1 and DLK2 function as inhibitory non-canonical ligands of NOTCH1 receptor that modulate each other's activities. *Biochim Biophys Acta,* 1813, 1153-64.

TAKEUCHI, H., FERNÁNDEZ-VALDIVIA, R. C., CASWELL, D. S., NITA-LAZAR, A., RANA, N. A., GARNER, T. P., WELDEGHIORGHIS, T. K., MACNAUGHTAN, M. A., JAFAR-NEJAD, H. & HALTIWANGER, R. S. 2011. Rumi functions as both a protein O-glucosyltransferase and a protein O-xylosyltransferase. *Proc Natl Acad Sci U S A,* 108, 16600-5.

TAMURA, K., TANIGUCHI, Y., MINOGUCHI, S., SAKAI, T., TUN, T., FURUKAWA, T. & HONJO, T. 1995. Physical interaction between a novel domain of the receptor Notch and the transcription factor RBP-J kappa/Su(H). *Curr Biol,* 5, 1416-23.

TECHNAU, G. & CAMPOS-ORTEGA, J. A. 1986. Lineage analysis of transplanted individual cells in embryos of *Drosophila melanogaster*. Roux's Arch. Dev. Biol.

TIAN, X., HANSEN, D., SCHEDL, T. & SKEATH, J. B. 2004. Epsin potentiates Notch pathway activity in Drosophila and C. elegans. *Development,* 131, 5807-15.

TIKKA, S., MYKKÄNEN, K., RUCHOUX, M. M., BERGHOLM, R., JUNNA, M., PÖYHÖNEN, M., YKI-JÄRVINEN, H., JOUTEL, A., VIITANEN, M., BAUMANN, M. & KALIMO, H. 2009. Congruence between NOTCH3 mutations and GOM in 131 CADASIL patients. *Brain,* 132, 933-9.

TOMLINSON, A. & READY, D. F. 1987. Neuronal differentiation in Drosophila ommatidium. *Dev Biol,* 120, 366-76.

TOWBIN, H., STAEHELIN, T. & GORDON, J. 1979. Electrophoretic transfer of proteins from polyacrylamide gels to nitrocellulose sheets: procedure and some applications. *Proc Natl Acad Sci U S A,* 76, 4350-4.

UEMURA, T., SHEPHERD, S., ACKERMAN, L., JAN, L. Y. & JAN, Y. N. 1989. numb, a gene required in determination of cell fate during sensory organ formation in Drosophila embryos. *Cell,* 58, 349-60.

VAN TETERING, G., VAN DIEST, P., VERLAAN, I., VAN DER WALL, E., KOPAN, R. & VOOIJS, M. 2009. Metalloprotease ADAM10 is required for Notch1 site 2 cleavage. *J Biol Chem,* 284, 31018-27.

VARDAR, D., NORTH, C. L., SANCHEZ-IRIZARRY, C., ASTER, J. C. & BLACKLOW, S. C. 2003. Nuclear magnetic resonance structure of a prototype Lin12-Notch repeat module from human Notch1. *Biochemistry,* 42, 7061-7.

VOOIJS, M., SCHROETER, E. H., PAN, Y., BLANDFORD, M. & KOPAN, R. 2004. Ectodomain shedding and intramembrane cleavage of mammalian Notch proteins is not regulated through oligomerization. *J Biol Chem,* 279, 50864-73.

WALLBERG, A. E., PEDERSEN, K., LENDAHL, U. & ROEDER, R. G. 2002. p300 and PCAF act cooperatively to mediate transcriptional activation from chromatin templates by notch intracellular domains in vitro. *Mol Cell Biol,* 22, 7812-9.

WANG, W. & STRUHL, G. 2004. Drosophila Epsin mediates a select endocytic pathway that DSL ligands must enter to activate Notch. *Development,* 131, 5367-80.

WANG, Y., SHAO, L., SHI, S., HARRIS, R. J., SPELLMAN, M. W., STANLEY, P. & HALTIWANGER, R. S. 2001. Modification of epidermal growth factor-like repeats with O-fucose. Molecular cloning and expression of a novel GDP-fucose protein O-fucosyltransferase. *J Biol Chem,* 276, 40338-45.

WARTHEN, D. M., MOORE, E. C., KAMATH, B. M., MORRISSETTE, J. J., SANCHEZ, P., PICCOLI, D. A., KRANTZ, I. D. & SPINNER, N. B. 2006. Jagged1 (JAG1) mutations in Alagille syndrome: increasing the mutation detection rate. *Hum Mutat,* 27, 436-43.

WEINMASTER, G. & FISCHER, J. A. 2011. Notch ligand ubiquitylation: what is it good for? *Dev Cell,* 21, 134-44.

WELSHONS, W. J. 1965. Analysis of a gene in *Drosophila*. Science.

WELSHONS, W. J. 1971. Genetic basis for two types of recessive lethality at the notch locus of Drosophila. *Genetics,* 68, 259-68.

WENG, A. P., FERRANDO, A. A., LEE, W., MORRIS, J. P., SILVERMAN, L. B., SANCHEZ-IRIZARRY, C., BLACKLOW, S. C., LOOK, A. T. & ASTER, J. C. 2004. Activating mutations of NOTCH1 in human T cell acute lymphoblastic leukemia. *Science,* 306, 269-71.

WENG, A. P., NAM, Y., WOLFE, M. S., PEAR, W. S., GRIFFIN, J. D., BLACKLOW, S. C. & ASTER, J. C. 2003. Growth suppression of pre-T acute lymphoblastic leukemia cells by inhibition of notch signaling. *Mol Cell Biol,* 23, 655-64.

WERNER, J. M., KNOTT, V., HANDFORD, P. A., CAMPBELL, I. D. & DOWNING, A. K. 2000. Backbone dynamics of a cbEGF domain pair in the presence of calcium. *J Mol Biol,* 296, 1065-78.

WESTHOFF, B., COLALUCA, I. N., D'ARIO, G., DONZELLI, M., TOSONI, D., VOLORIO, S., PELOSI, G., SPAGGIARI, L., MAZZAROL, G., VIALE, G., PECE, S. & DI FIORE, P. P. 2009. Alterations of the Notch pathway in lung cancer. *Proc Natl Acad Sci U S A,* 106, 22293-8.

WHARTON, K. A., JOHANSEN, K. M., XU, T. & ARTAVANIS-TSAKONAS, S. 1985. Nucleotide sequence from the neurogenic locus notch implies a gene product that shares homology with proteins containing EGF-like repeats. *Cell,* 43, 567-81.

WHEELER, S. R., STAGG, S. B. & CREWS, S. T. 2008. Multiple Notch signaling events control Drosophila CNS midline neurogenesis, gliogenesis and neuronal identity. *Development,* 135, 3071-9.

WHITEMAN, P., HERNANDEZ DE MADRID, B., TAYLOR, P., LI, D., HESLOP, R., VITICHEEP, N., TAN, J. Z., SHIMIZU, H., CALLAGHAN, J., MASIERO, M., LI, J. L., BANHAM, A. H., HARRIS, A. L., LEA, S. M., REDFIELD, C., BARON, M. & HANDFORD, P. A. 2013. Molecular basis for Jagged-1/Serrate recognition by Notch. *J Biol Chem*.

WHITTOCK, N. V., SPARROW, D. B., WOUTERS, M. A., SILLENCE, D., ELLARD, S., DUNWOODIE, S. L. & TURNPENNY, P. D. 2004. Mutated MESP2 causes spondylocostal dysostosis in humans. *Am J Hum Genet,* 74, 1249-54.

WRIGHT, T. R. 1970. The genetics of embryogenesis in *Drosophila*. Adv. Genet.

XU, A., HAINES, N., DLUGOSZ, M., RANA, N., TAKEUCHI, H., HALTIWANGER, R. & IRVINE, K. 2007. In vitro reconstitution of the modulation of Drosophila Notch-ligand binding by Fringe. *J Biol Chem,* 282, 35153-62.

XU, T., REBAY, I., FLEMING, R. J., SCOTTGALE, T. N. & ARTAVANIS-TSAKONAS, S. 1990. The Notch locus and the genetic circuitry involved in early Drosophila neurogenesis. *Genes Dev,* 4, 464-75.

YAN, M., CALLAHAN, C. A., BEYER, J. C., ALLAMNENI, K. P., ZHANG, G., RIDGWAY, J. B., NIESSEN, K. & PLOWMAN, G. D. 2010. Chronic DLL4 blockade induces vascular neoplasms. *Nature,* 463, E6-7.

YANG, L. T., NICHOLS, J. T., YAO, C., MANILAY, J. O., ROBEY, E. A. & WEINMASTER, G. 2005. Fringe glycosyltransferases differentially modulate Notch1 proteolysis induced by Delta1 and Jagged1. *Mol Biol Cell,* 16, 927-42.

YOCHEM, J. & GREENWALD, I. 1989. glp-1 and lin-12, genes implicated in distinct cell-cell interactions in C. elegans, encode similar transmembrane proteins. *Cell,* 58, 553-63.

YOCHEM, J., WESTON, K. & GREENWALD, I. 1988. The Caenorhabditis elegans lin-12 gene encodes a transmembrane protein with overall similarity to Drosophila Notch. *Nature,* 335, 547-50.

Appendix A – primers

Primers for mutagenesis of $hN1_{11-13}$:

T466A
Forward: GAC GCC GCC TGC CTG GAC
Reverse: GTT CTG GCA CGG GTT CGA AG

T466S (QC)
Forward: CAG AAC GAC GCC TCC TGC CTG GAC CAG ATT GGG
Reverse: CCC AAT CTG GTC CAG GCA GGA GGC GTC GTT CTG

T466V
Forward: GAC GCC GTC TGC CTG GAC
Reverse: GTT CTG GCA CGG GTT CGA AG

Q470A
Forward: CTG GAC GCG ATT GGG GAG
Reverse: CAG AAC GAC GCC ACC TGC

E473A
Forward: GAT TGG GGC GTT CCA GTG CAT C
Reverse: TGG TCC AGG CAG GTG GCG TC

Q475A
Forward: GAG TTC GCG TGC ATC TGC ATG C
Reverse: CCC AAT CTG GTC CAG GCA GGT G

I477A
Forward: CAG TGC GCC TGC ATG CCC G
Reverse: GAA CTC CCC AAT CTG GTC CAG G

Primers for mutagenesis of dN_{11-13}

S502A (QC)
Forward: GCC AGA ACG AGG GAG CTT GCC TGG ATG ATC CG
Reverse: CGG ATC ATC CAG GCA AGC TCC CTC GTT CTG GC

L504A (QC)
Forward: GAA CGA GGG ATC TTG CGC GGA TGA TCC GGG AAC G
Reverse: CGT TCC CGG ATC ATC CGC GCA AGA TCC CTC GTT C

D506A (QC)
Forward: GGA TCT TGC CTG GAT GCT CCG GGA ACG TTC CG
Reverse: CGG AAC GTT CCC GGA GCA TTC AGG CAA GAT CC

Primers for producing $hN1_{9\text{-}13}$ (with enterokinase-cleavable 6 x His tag):

Forward: TAG TAG GGA TCC GAT GAC GAT GAC AAA TCA GCA AAC ATT GAT GAC TGT GCC AGC
Reverse: GAT GAT GTC GAC CTG GCA CAG ATG CCC AGT GAA GC

Primers for producing pUAST Serrate-GFP:

1. Serrate Sfi1 F: TAGTAGGGCCCGCGTGGCCGATGG
2. Serrate-GFP F: CTTGCCACCACTGTGATGGTTATGGTGAGCAAGGGCGAGG
3. GFP-Serrate F: GCATGGATGAACTATACAAATAGTAGCCGTGATCTCACCAACC
4. pUAST Xho1 R: TAGTAGCTCGAGCGCGGCCGCAA
5. GFP-Serrate R: GGTTGGTGAGATCACGGCTACTATTTGTATAGTTCATCCATGC
6. Serrate-GFP R: CCTCGCCCTTGCTCACCATAACCATCACAGTGGTGGCAAG

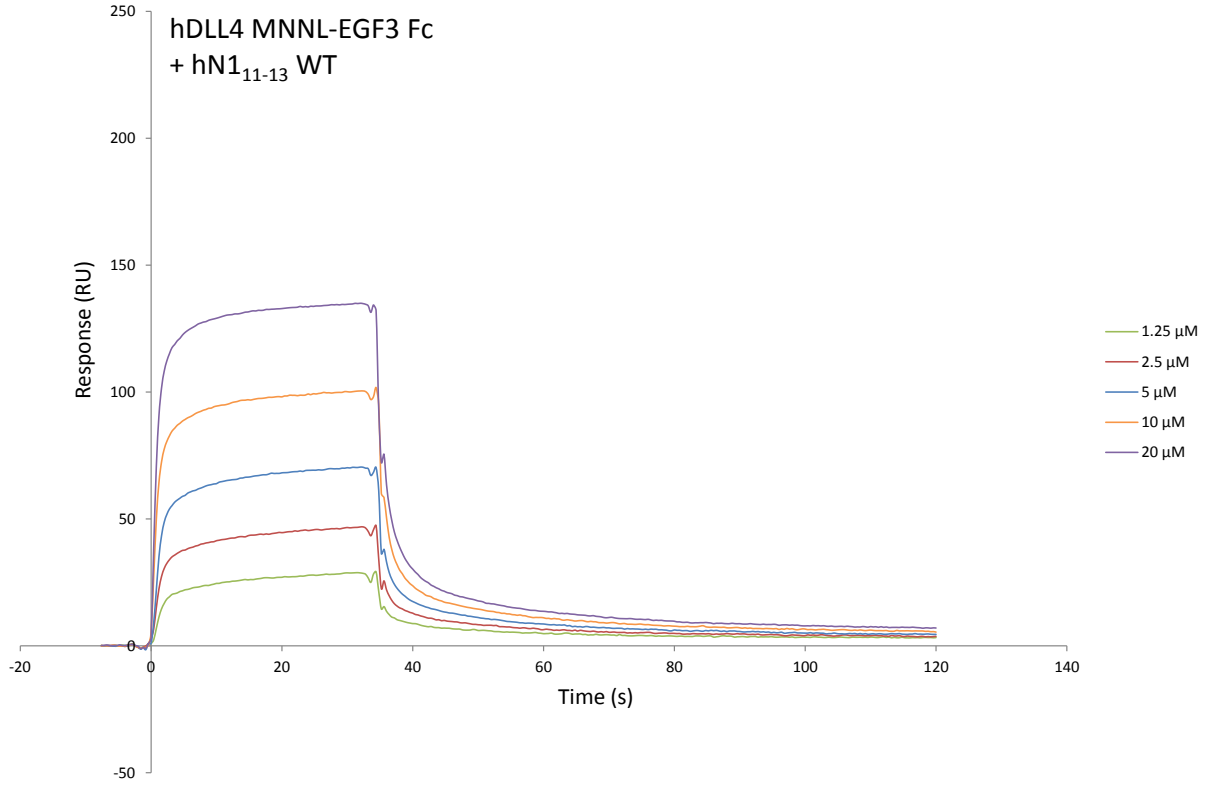
Primers for producing hNotch1-avitag proteins:

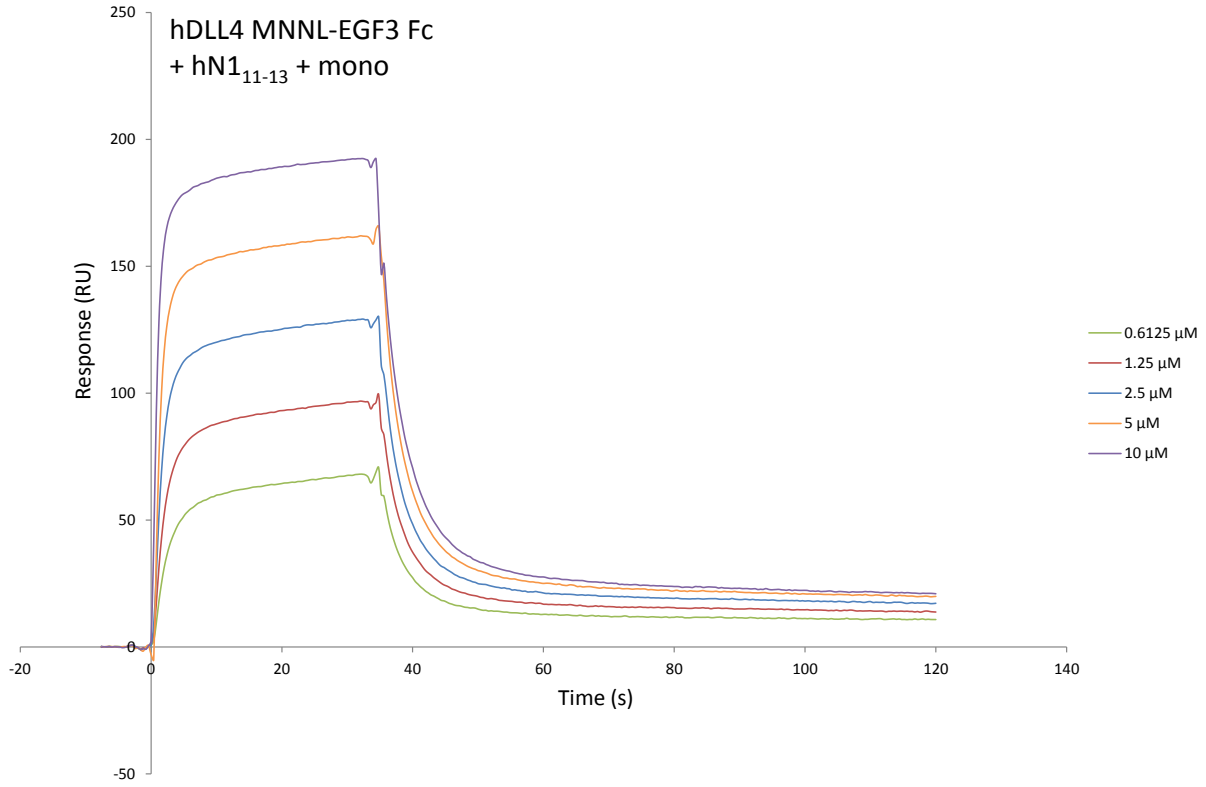
Forward:
C GGA GGT TCC GGT GGT CTG AAT GAT ATC TTT GAA GCT CAG AAG ATT GAA TGG CAT GAA GGA AAG CAC CAC CAT CAC CAT CAC TAA TGA C

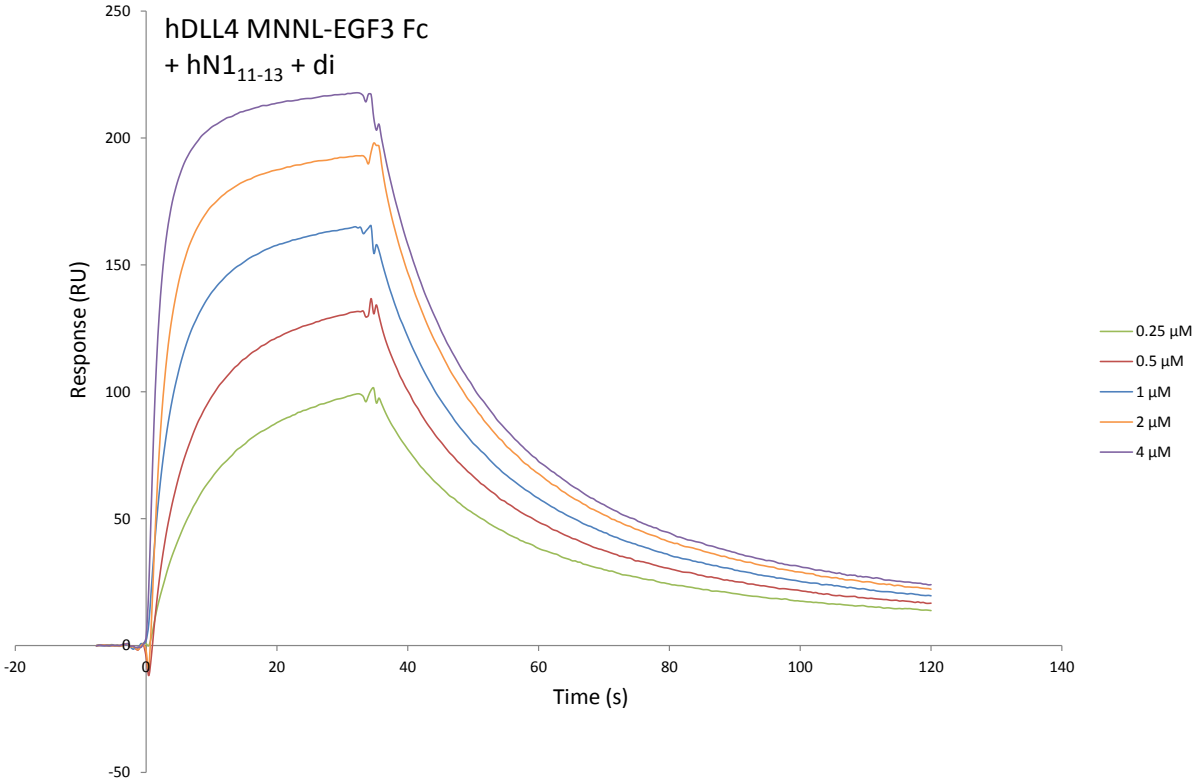
Reverse:
TC GAG TCA TTA GTG ATG GTG ATG GTG GTG CTT TCC TTC ATG CCA TTC AAT CTT CTG AGC TTC AAA GAT ATC ATT CAG ACC ACC GGA ACC TCC GGT AC

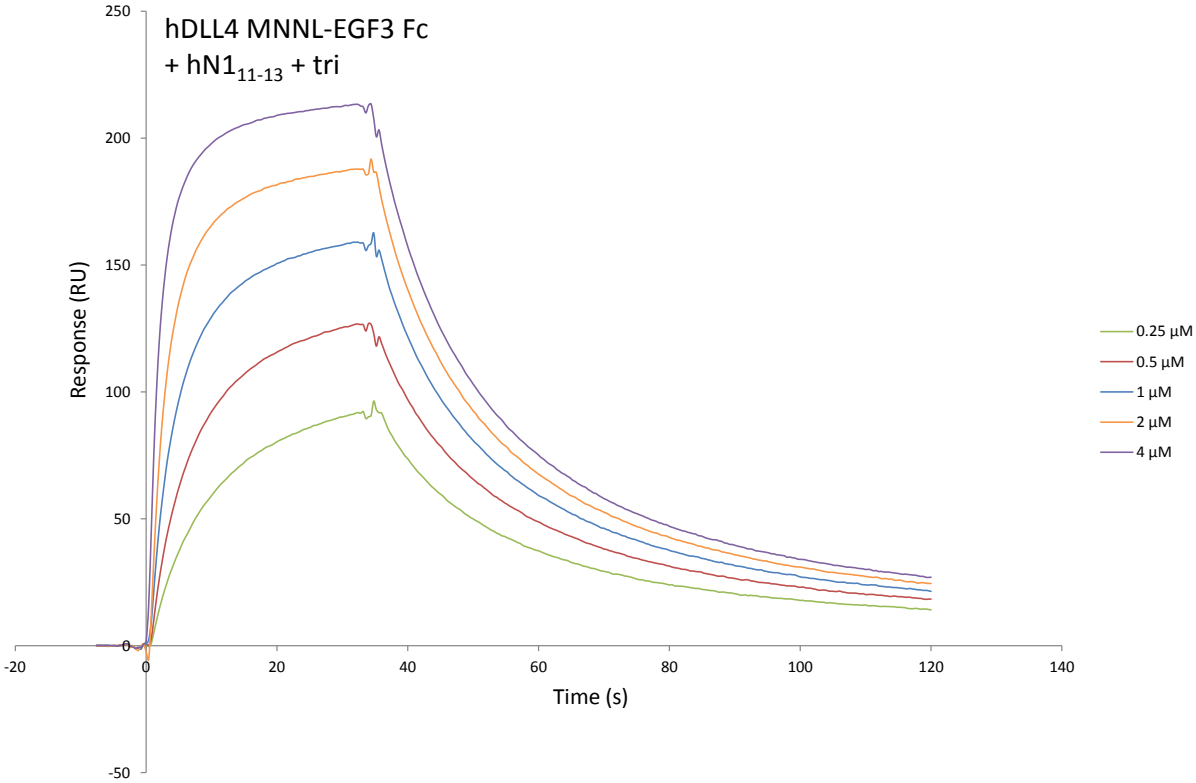
n.b. All primers are displayed 5’ to 3’

Appendix B – supplementary SPR data






hDLL4 MNNL-EGF3 Fc
+ hN1$_{11-13}$ + di
Response (RU)
Time (s)
0.25 µM
0.5 µM
1 µM
2 µM
4 µM


hDLL4 MNNL-EGF3 Fc
+ hN1$_{11-13}$ + tri
Response (RU)
Time (s)
0.25 µM
0.5 µM
1 µM
2 µM
4 µM

Appendix C – published work

THE JOURNAL OF BIOLOGICAL CHEMISTRY VOL. 288, NO. 10, pp. 7305–7312, March 8, 2013
© 2013 by The American Society for Biochemistry and Molecular Biology, Inc. Published in the U.S.A.

Molecular Basis for Jagged-1/Serrate Ligand Recognition by the Notch Receptor*

Received for publication, October 19, 2012, and in revised form, December 14, 2012 Published, JBC Papers in Press, January 21, 2013, DOI 10.1074/jbc.M112.428854

Pat Whiteman[‡1], Beatriz Hernandez de Madrid[§1], Paul Taylor[‡1], Demin Li[¶], Rebecca Heslop[‡], Nattnee Viticheep[‡], Joyce Zi Tan[‖], Hideyuki Shimizu[§], Juliana Callaghan[‡], Massimo Masiero[¶], Ji Liang Li[**], Alison H. Banham[¶], Adrian L. Harris[**], Susan M. Lea[‖], Christina Redfield[‡], Martin Baron[§], and Penny A. Handford[‡2]**

*From the [‡]Department of Biochemistry, University of Oxford, South Parks Road, Oxford OX1 3QU, the [§]Faculty of Life Sciences, University of Manchester, Manchester M13 9PT, the [‖]Sir William Dunn School of Pathology, University of Oxford, South Parks Road, Oxford OX1 3RE, the [¶]Nuffield Department of Clinical Laboratory Sciences, Oxford National Institute for Health Research (NIHR) Biomedical Research Centre, John Radcliffe Hospital, University of Oxford, Headington, Oxford OX3 9DU, and the **Molecular Oncology Laboratories, Oxford University Department of Oncology, Weatherall Institute of Molecular Medicine, John Radcliffe Hospital, University of Oxford, Oxford OX3 9DS, United Kingdom*

Background: The site of Jagged/Serrate ligand recognition by Notch is unknown.
Results: Two critical residues involved in an intramolecular hydrophobic interaction across the central β-sheet of EGF_{12} form a ligand-binding platform.
Conclusion: The ligand-binding region is adjacent to a Fringe-sensitive residue involved in modulating Notch activity.
Significance: The results have implications for understanding receptor/ligand recognition, Notch regulation by *O*-glycosylation, and the development of paralogue-specific antibodies.

We have mapped a Jagged/Serrate-binding site to specific residues within the 12th EGF domain of human and *Drosophila* Notch. Two critical residues, involved in a hydrophobic interaction, provide a ligand-binding platform and are adjacent to a Fringe-sensitive residue that modulates Notch activity. Our data suggest that small variations within the binding site fine-tune ligand specificity, which may explain the observed sequence heterogeneity in mammalian Notch paralogues, and should allow the development of paralogue-specific ligand-blocking antibodies. As a proof of principle, we have generated a Notch-1-specific monoclonal antibody that blocks binding, thus paving the way for antibody tools for research and therapeutic applications.

The Notch receptor mediates a critical short range signal that is deployed in many developmental and adult contexts to refine cell fate choices (1). Genetic diseases affecting Notch pathway components give rise to a wide range of congenital and adult-onset disorders, and Notch dysregulation has been found to contribute to many types of human cancer (2). The Notch receptor is a single pass trans-membrane protein that, during its biosynthetic pathway, may be cleaved by a furin-like convertase (S1) in the trans-Golgi to generate a noncovalently associated heterodimer at the cell surface (3, 4). Canonical Notch signaling is initiated when a cell surface-expressed Delta/Serrate/LAG-2 (DSL)[3] ligand binds in trans to the Notch receptor expressed on an opposing cell surface (5). Various studies have localized the binding determinants to EGF_{11-12} of the receptor and the DSL and EGF_{1-2} of the ligands (6, 7). Endocytosis of the Notch ligand complex by the ligand-expressing cell leads to a second proteolytic cleavage event at S2, which removes the extracellular moiety of the heterodimer (8). This leaves the membrane-tethered stalk, which is then cleaved by γ-secretase at S3 (see Fig. 1*a*) (9, 10). Following this proteolysis event, an intracellular fragment of Notch is released (11, 12). This translocates to the nucleus and assembles into a transcriptional activation complex, which includes a DNA-binding protein of the CBF-1/Suppressor of Hairless/LAG-1 (CSL) family and its co-activator Mastermind. This new assembly relieves repression and activates Notch target genes such as Hairy/Enhancer of split (*Hes*) (13).

We have previously shown that the 12th EGF (EGF_{12}) domain of Notch is directly implicated in ligand binding (14), To investigate this region further, we have made a series of single amino acid substitutions in human and *Drosophila* Notch designed to probe ligand recognition, while retaining Notch calcium binding, which is already known to be critical for this interaction (15).Using flow cytometry and cell aggregation assays, we have identified a globally conserved hydrophobic binding site that is adjacent to the residue that forms part of the *O*-fucosylation consensus sequence (C^2-X_4-(S/T)-C^3) in EGF_{12}, where C^2 and C^3 represent the second and third conserved cysteines (16). This residue is reported to be subjected to further modification by the Fringe enzymes (17), resulting in changes to Notch activity (18). We discuss the functional significance of sequence variability within this region and show

* This work was supported by The Wellcome Trust Grants 087928 (to P. A. H., S. M. L., and M. B.) and 079440 (to C. R.), Cancer Research UK Programme Grant A10702 (to A. H. B., A. L. H., P. H., and S. M. L.), and Biotechnology and Biological Sciences Research Council studentship (to P. T.).
⌘ *Author's Choice*—Final version full access.
[1] These authors contributed equally to this work.
[2] To whom correspondence should be addressed. Tel.: 44 1865 613260; Fax: 44 1865 613201; Email: penny.handford@bioch.ox.ac.uk.

[3] The abbreviations used are: DSL, Delta/Serrate/LAG-2; J-1, Jagged-1; N-1, Notch-1; hN-1, human Notch-1; dN, *Drosophila* Notch; hNotch, human Notch.

Downloaded from www.jbc.org by guest, on April 21, 2013

that it can be exploited to raise paralogue-specific antibodies that block ligand binding.

EXPERIMENTAL PROCEDURES

Protein Production—hN-1_{11-13} was bacterially expressed and refolded *in vitro* as described previously and contains a 17-amino acid biotin ligase (Bir A) tag at the C terminus, which was shown to increase the efficiency of refolding (19). Calcium binding by hN-1_{11-13} wild type and mutants was measured by one-dimensional and two-dimensional NOE NMR spectroscopy, as described previously (20, 21).

Flow Cytometry of J-1/N-1 Interaction—Prokaryotically expressed and biotinylated hN-1_{11-13} wild-type and mutant constructs were coupled to purple fluorescent avidin-coated beads (Spherotech), as described previously (14). A negative control of calcium-binding EGF_{12-14} from human fibrillin-1, an unrelated protein with a similar domain organization, was used in all experiments. Coupled beads were washed with 100 μl of HBSS/BSA (Hanks' buffered saline solution without phenol red, 1% BSA), resuspended in 50 μl of HBSS, 10% fetal calf serum (FCS) and kept on ice before being incubated with the cells. Stably transfected B16 mouse melanoma cells expressing full-length mouse Jagged-1 (J-1) were grown in T75 flasks to 80–90% confluency before being detached with 5 ml of PBS, 10 mM EDTA at 37 °C for 5 min. Pelleted cells from each flask were washed three times and resuspended in 1 ml of ice-cold HBSS, 10% FCS. After 1 h, 50 μl of the beads were added to 50 μl of cells and incubated on ice for 1 h prior to being resuspended in 500 μl of ice-cold HBSS for flow cytometry analysis. hN-1-binding antibodies (see below) were screened for their ability to block binding of hN-1_{11-13} to HEK293 cells expressing full-length human J-1 by the addition of 10 μl of hybridoma supernatant to the coupled beads prior to incubation with cells. Flow cytometry was performed using a FACSCalibur machine (BD Biosciences). 10,000 cells were counted, and fluorescence intensity was monitored in FL3 at >670 nm, with excitation at 488 nm.

Drosophila Cell Aggregation Assay—For Serrate expression, the 4.2-kb cDNA sequence from pBKS+SerFL (22) was amplified by PCR to eliminate the stop codon, fused in-frame to a V5-His tag at its C terminus, and inserted into the pMT expression vector (23) to generate pMT Ser-V5. Schneider S2 cells (Invitrogen) were transfected with pMT-Ser-V5 as described previously (15). Expression was induced with 1 mM $CuSO_4$ at 48 h after transfection. After a further 16 h, cells were mixed with Notch-expressing cells. For Notch expression, S2 cells were transfected with pCaSper-HS Notch (19). Expression was induced after 48 h by heat shock at 37 °C for 40 min and, after a further 4 h at 25 °C, they were mixed with wild-type Ser-V5 cells in 1.5-ml Eppendorf tubes on a rotating platform at room temperature for 30 min. The cell suspension was then transferred to coverslips coated in 0.1% poly-L-Lysine (Sigma), fixed with 2% formaldehyde, PBS for 40 min, and permeabilized with 0.2% Triton X-100, PBS for 15 min. Cells were blocked for 1 h in 0.2% Triton X-100, PBS, 5% skimmed milk powder (Sigma-Aldrich) and immunostained for 90 min with rabbit anti-V5 (Bethyl Laboratories, 1:1000) and anti-Notch C17.9C6 (Developmental Studies Hybridoma Bank, Iowa City, IA, 1:500). Secondary antibodies were α-mouse-FITC (Jackson ImmunoResearch Laboratories, 1:100) and α-rabbit Cy3 (Jackson ImmunoResearch Laboratories, 1:150). Slides were imaged at ×63 with a Zeiss M2 fluorescence microscope and cooled digital camera (Orca-ER Hamamatsu), and processed using Openlab (Improvision) and Photoshop (Adobe) on an Apple Macintosh computer. Images displayed were obtained by deconvolution using the three nearest neighbors from optical sections obtained with a Z spacing of 0.5 μm. Aggregation was scored for the percentage of Notch-expressing cells adhering to at least one Serrate-expressing cell, and the mean percentage of aggregation was obtained from at least three independent transfections. Statistical significance was assessed using Student's *t* test.

Drosophila Notch Signaling—Full-length *Drosophila* Notch (dN) and L504A constructs were subcloned into pMT vectors (Invitrogen). S2 cells in 12-well dishes were transfected with pMT plasmids, Notch Response Element (NRE):Firefly (gift from S. Bray), and actin:*Renilla* (gift from G. Merdes). After 24 h, cells were resuspended and seeded into white 96-well plates (Nunc 136101), and $CuSO_4$ was added after a further 24 h to induce expression. Cells were reseeded into white 96-well plates on top of fixed Delta-expressing S2 cells (S2-Mt-Dl; *Drosophila* Genomics Resource Center (DGRC)). 24 h after induction, luciferase activity was assayed with Dual-Glo Luciferase (Promega) and quantified by luminometer (Berthold Technologies), and the Firefly/*Renilla* ratio was calculated for triplicate samples. Experiments were repeated a minimum of three times.

mAb Generation and Validation—Mouse monoclonal antibodies (N1-96A, isotype IgG2a and N1-39E, isotype IgG1) were raised, using MF1 mice and NS0 cells as the fusion partner (24). The antigen was bacterially expressed recombinant hN-1_{11-13} as described above, using TiterMax Gold as adjuvant. Fifteen hybridoma cell lines, generated from three fusions, were positive for antibody reactivity against hN-1_{11-13} by ELISA assay against the immunogen. Two hybridoma lines (N1-39E and N1-96A) were found to be positive for the detection of cell surface N-1 by FACS analysis of transient HEK293T transfectants. For epitope mapping, wild-type and mutant hN-1_{11-13} constructs were prepared at 20 ng/μl, and 1 μl of each was spotted onto nitrocellulose. The proteins were detected with the noninhibitory antibody N1-96A (1:200) and the blocking antibody N1-39E (1:400) followed by anti-mouse HRP conjugate (1:2000) and visualized by chemiluminescence (Amersham Biosciences ECL Plus Western blotting detection system).

Flow Cytometry and Immunocytochemistry to Test Paralogue Specificity—Full-length human Notch-1, -2, -3, and -4 transiently transfected HEK293T cells were generated. Cells were washed three times with FACS Wash Buffer (2% FBS in PBS + 0.01% NaN3) and then incubated on ice for 20 min with primary antibody, *i.e.* undiluted hybridoma supernatant. After two washes with FACS Wash Buffer, cells were incubated for 20 min at 4 °C (protected from light) with secondary conjugated antibody, *i.e.* allophycocyanin-conjugated anti-mouse Ig (H+L) (Invitrogen, A10539) at 1:50 dilution. Cells were washed with FACS Wash Buffer and resuspended in 500 μl of 1% formaldehyde in PBS before analysis using a FACSCalibur flow cytome-

Downloaded from www.jbc.org by guest, on April 21, 2013

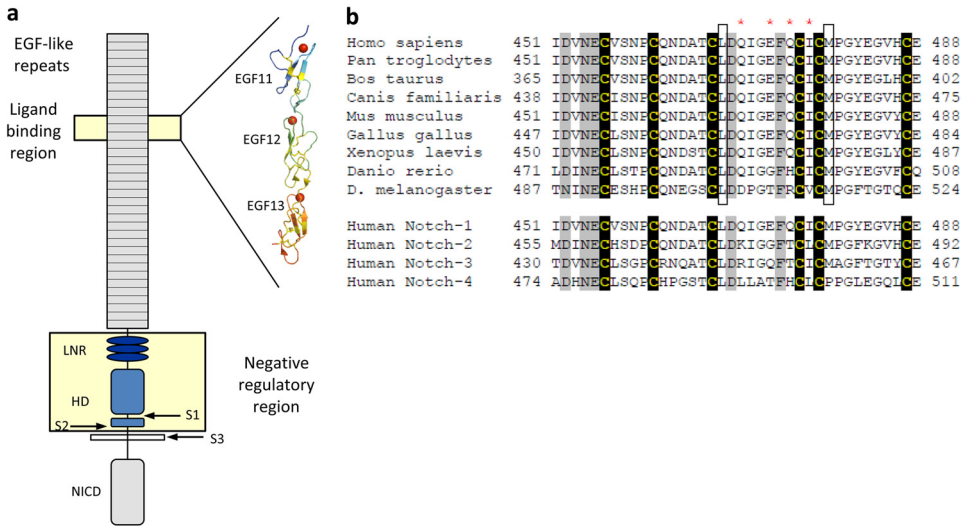


FIGURE 1. **Defining the J-1-binding site in hN-1.** *a*, domain organization of hN-1 showing structure of the hN-1_{11-13} ligand-binding region (Protein Data Bank (PDB) 2VJ3). *LNR,* Lin12-Notch Repeat modules; *HD,* Heterodimerization Domain; *NICD,* Notch Intracellular Domain. *Red spheres* indicate calcium ions. *b*, sequence homology of Notch EGF_{12} region from different species and the four human paralogues; cysteines are shown in *black*, calcium-binding consensus residues are in *gray*, two universally conserved residues that are candidates for ligand binding are *boxed*, and additional residues within the EGF_{12} β-hairpin targeted for mutagenesis are indicated by a *red asterisk*. *D. melanogaster*, *Drosophila melanogaster*.

ter (BD Biosciences) and FlowJo software (Tree Star). Cytospin cell preparations were incubated with primary antibody for 30 min at room temperature, Notch-1 (A6 mAb, Abcam, dilution 1:200), Notch-2 (goat polyclonal antibody, Abcam, dilution 1:200), Notch-3 (rabbit polyclonal antibody, Abcam, dilution 1:200), Notch-4 (rabbit polyclonal antibody, Abcam, dilution 1:200), or undiluted hybridoma supernatants. After washing in PBS, slides were incubated with secondary antibody, HRP-conjugated goat-anti-mouse antibody (Dako, 1:50 dilution), for murine monoclonal antibodies (mAbs) or with HRP-conjugated goat-anti-rabbit antibody for rabbit polyclonal antibodies (Dako, 1:12.5 dilution) for 30 min at room temperature. Goat antibodies were detected using a mouse-anti-goat monoclonal antibody between primary and secondary antibodies at a 1:12.5 dilution. After washing, color reaction was developed using diaminobenzidine substrate (Dako). Slides were washed and counterstained in hematoxylin before mounting in Aquatex mounting agent (BDH/VWR International).

RESULTS AND DISCUSSION

Site-directed Mutagenesis of Human N-1_{11-13}—Mutations in hN-1 were made in the context of the soluble hN-1_{11-13} construct (Fig. 1*a*), which we have previously demonstrated to be ligand binding-competent (19). To assay these hN-1_{11-13} mutants, we have used flow cytometry to study binding to full-length J-1 expressed on the surface of B16 cells. Initially, two mutants containing alanine substitutions were constructed on the basis of sequence conservation across Notch from multiple species (Fig. 1*b*). Of these, one was similar to wild type (WT) in its ability to bind J-1 (M479A), but the other, L468A, was completely unable to bind J-1 (Fig. 2). Mapping Leu-468 to the structure of hN-1_{11-13} shows that it lies within the central β-hairpin of EGF_{12}. The Notch-binding region previously identified in the J-1 DSL domain makes it unlikely that Leu-468 is the only residue to contribute to the ligand-binding interface (19); we therefore made a second round of alanine substitutions at residues that were seen to lie close to this region and to have surface-exposed side chains not involved in calcium coordination (Fig. 1*b*). This allowed us to identify one further mutant, I477A, which abrogated binding similarly to L468A, two other mutants, E473A and Q475A, which showed a more modest reduction in binding, and one mutant, Q470A ,which bound at least as well as WT hN-1_{11-13} (Fig. 2*a*). Loss of binding to L468A and I477A was not due to misfolding or indirect effects on calcium binding (in contrast to a previously studied D469G substitution) because two-dimensional NOESY analysis showed that a marker for calcium binding to EGF_{12} (Tyr-444) gave a similar change in chemical shift upon the addition of Ca^{2+} to that observed in the WT (Fig. 2*b*) (14). The crystal structure of hN-1_{11-13} (PDB 2VJ3) has previously shown that Leu-468 and Ile-477 side chains form a hydrophobic interaction across the central β-hairpin of EGF_{12} (19); our data suggest that this structural feature may serve as a stable platform for ligand interactions (Fig. 2*c*).

Site-directed Mutagenesis of Full-length Drosophila Notch—To extend this analysis to full-length Notch, we then substituted the equivalent amino acids in the evolutionarily distant dN and tested these mutants for interaction with *Drosophila* Serrate using cell aggregation assays. Results were very similar to those seen with the hN-1_{11-13}/J-1 interaction, with dN L504A showing the strongest reduction of binding, and as expected, a concomitant reduction in ligand-induced signaling (Fig. 3). An exception was dN V513A, which reduced but did not abrogate binding as had the equivalent hN-1_{11-13} I477A. This most likely reflects the more conservative nature of a valine to alanine change than that of the more bulky isoleucine to alanine. Collectively, our data suggest that the location of the ligand-binding site for the Jagged/Serrate family ligands is conserved across human and *Drosophila* Notch (Table 1) despite the observed sequence divergence within this region (Fig. 1*b*).

Downloaded from www.jbc.org by guest, on April 21, 2013

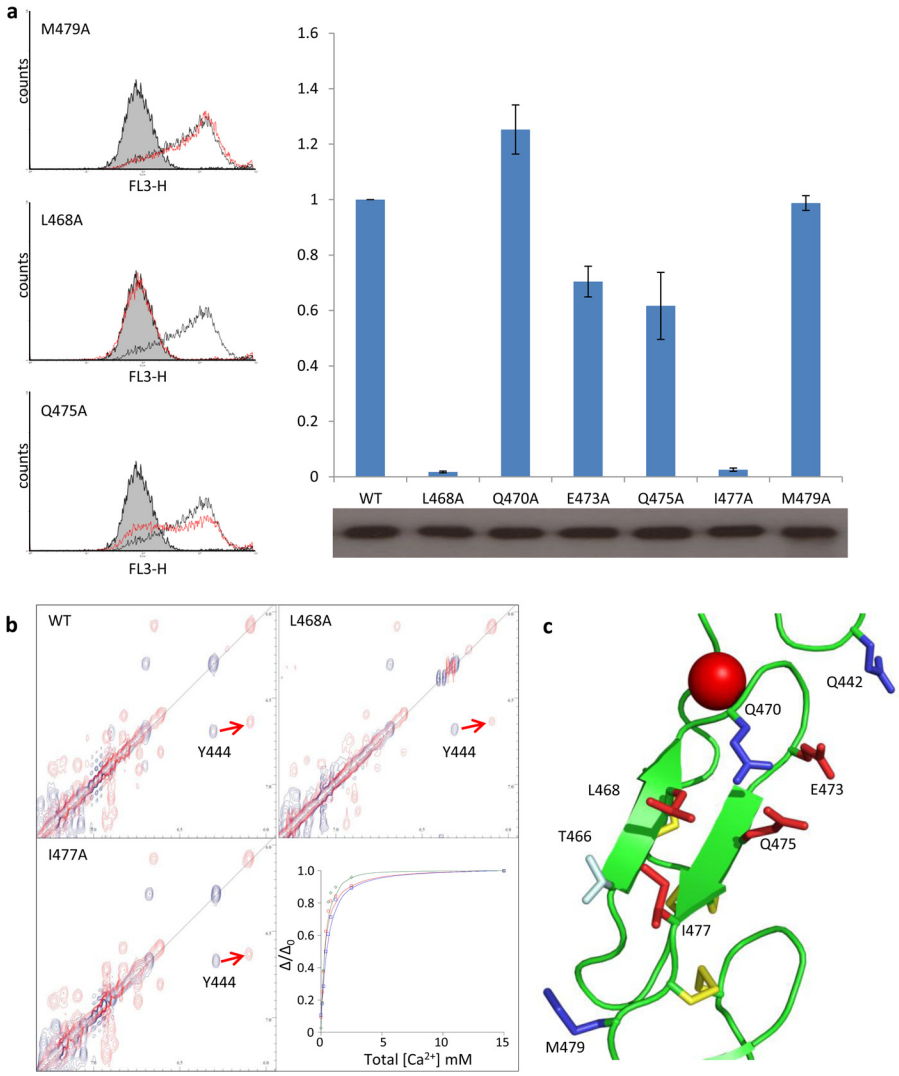


FIGURE 2. **Characterization and interaction studies of hN-1 variants.** *a*, flow cytometry analysis of the interaction between J-1 and biotinylated wild-type (WT) and mutant N-1_{11-13} constructs. *Left-hand panel*, flow cytometry of B16 cells expressing J-1 after interaction with biotinylated hN-1 mutants(*red line*) bound to avidin-coated fluorescent beads (see "Experimental Procedures"); in each case, a negative control (fibrillin calcium-binding EGF_{12-14}, *gray shading*) and positive control (WT hN-1_{11-13}, *black line*) are shown. Three representative mutant constructs are shown; M479A is indistinguishable from WT, L468A overlays negative control, and Q475A shows intermediate binding. *Right-hand panel*, quantification of flow cytometry data for all EGF_{12} mutants expressed relative to WT control (WT = 1) (*bars* indicate mean, *error bars* indicate S.D., $n \geq 3$) and Western blot of hN-1_{11-13} samples to show experiments controlled for protein loading. *b*, NMR analysis shows that WT and mutant constructs have native-like calcium binding properties indicative of correct folding. Aromatic regions of ^{1}H-^{1}H two-dimensional NOESY spectra at pH 7.5 of hN-1_{11-13} WT, L468A, and I477A are shown. A marker for calcium binding in EGF_{12} (Tyr-444) is highlighted in the absence (*blue*) and presence (*red*) of Ca^{2+} (15 mM), and the shift is indicated by a *red arrow*. Quantification of data indicates relative chemical shift change on addition of Ca^{2+}. *Red*, WT; *blue*, L468A; *green*, I477A. The structure of hN-1 EGF_{12} (PDB 2VJ3) is shown; residues implicated in binding by flow cytometry (*red*), non-binding residues (*blue*), position of residue Thr-466 that is implicated in regulation by *O*-fucosylation, and Fringe extension are indicated.

These mutational data now implicate a different face of Notch in ligand binding from our earlier studies based on NMR data derived from mapping intensity changes in the spectrum of hN-1_{11-13} upon titration of an hJ-$1_{DSL\text{-}EGF3}$ fragment (19) (the more informative chemical shift mapping was not possible due to a combination of the poor solubility of hJ-$1_{DSL\text{-}EGF3}$ and the kinetics/affinity of the interaction). The most perturbed residues in this assay were hN-1 Val-453 and Gly-472, which contribute to the EGF_{12} calcium binding by donation of a backbone carbonyl ligand and to an EGF_{11-12} packing interaction, respectively. The spatial distance and orientation of Val-453 and Gly-472, when compared with the Leu-468 and Ile-477 hydrophobic patch identified as being important for ligand binding in this study, preclude both sites making direct contacts to the ligand. To try and resolve this contradiction, we mutated the Val-453 equivalent residue, Ile-489, in dN. This had no effect on ligand binding (data not shown), implying that the intensity changes observed previously (19) reflect an indirect effect on the residues stabilizing calcium binding to EGF_{12} by ligand binding within the central β-hairpin (because β-hairpin stability and calcium binding affinity are closely coupled).

This conservation of ligand-binding site between human and evolutionary distant *Drosophila* Notch proteins, despite a relatively high level of sequence diversity (Fig. 1*b*) and differences in the specific ligands assayed, suggests that this region of Notch will be involved in ligand binding in all species. It is also interesting to note that the threonine/serine residue (Thr-466 in hN-1_{11-13}/Ser-502 in dN), implicated in the regula-

Downloaded from www.jbc.org by guest, on April 21, 2013

tion of Notch activity by *O*-fucosylation and subsequent Fringe extension, lies adjacent to the ligand-binding patch revealed in EGF_{12} (Fig. 2*c*), suggesting that direct effects on ligand recognition may explain the functional effects of this modification (25, 26).

Sequence Variation in Notch Paralogues—Inspection of the amino acid sequences of residues in the vicinity of our newly defined Notch ligand-binding site across mammalian Notch paralogues (human Notch 1–4 shown) reveals sequence variation (Fig. 1*b*), as we have observed between hN-1 and *Drosophila* Notch. Our binding data for human N-1 show that alanine substitution of residues in close proximity to the core binding site can subtly enhance or reduce ligand binding (Fig. 2*a*). One explanation for the sequence variation seen in such a functionally important site therefore is to allow fine tuning of the affinity, specificity, and regulation of different Notch-ligand combinations (there are five ligands and four Notch receptors in mammals). This is consistent with data from various assays that have demonstrated that hNotch paralogues 1–3 can all interact with both J-1 and Dll-1 (7, 14, 27–29). All paralogues maintain the leucine-isoleucine, or leucine-leucine, pairings predicted on the basis of structural homology with hN-1 to form the ligand-binding platform. It is also interesting to note that *Xenopus* Notch (Xotch) (which has an identical β-hairpin sequence between C^3 and C^5 in EGF_{12} to hN-1 (Fig. 1*b*)) has been observed to bind to *Drosophila* ligands Serrate and Delta (6). A potential consequence of the observed variability in the binding site is to allow generation of paralogue-specific antibodies that block ligand binding.

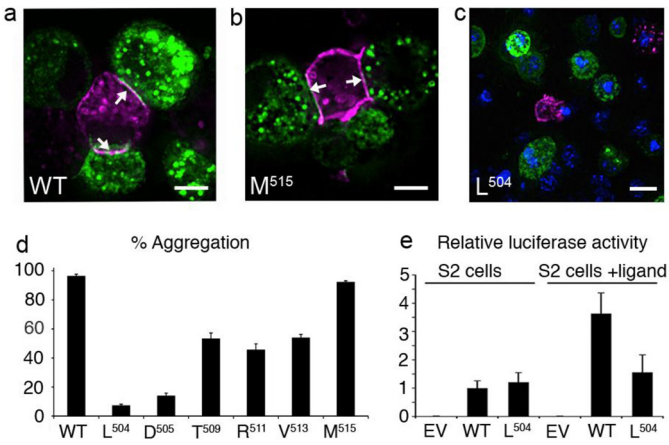


FIGURE 3. **Defining the ligand-binding site in dN.** *a–c*, cell aggregation assay of the interaction of full-length Serrate with WT and alanine substitution mutants of full-length dN expressed in S2 cells. Panels show merged immunofluorescence images of Serrate (*purple*), Notch (*green*), and DAPI (*blue*). Aggregated cells form junctions with clustered Serrate and Notch indicated by *arrows*, which are clearly evident for WT Notch (*a*) and the M515A mutant (*b*) but not for the L504A construct (*c*). The latter is shown at lower magnification to depict a field of nonaggregating cells. *Scale bars* are: 5 μm (*a* and *b*) and 10 μm (*c*). *d*, cell aggregation assay scored as the percentage of Notch-expressing cells adhered to at least one Serrate-expressing cell for WT dN, the control D505A substitution, and for substitutions located around the main β-sheet of EGF_{12}. *Error bars* in *d* indicate S.D., $n \geq 3$. *e*, Notch luciferase-reporter signaling assay. Mean normalized Notch signaling is shown relative to WT Notch expressed in S2 cells co-cultured with nonexpressing S2 cells. Signaling through wild-type Notch is increased by ligand-expressing (Delta) co-cultured S2 cells, but signaling through L504A mutant is not changed by exposure to ligand. *EV*, empty vector-transfected luciferase reporter controls. *Error bars* in *e* indicate S.D., $n = 6$.

Production of Paralogue-specific Antibodies—To test our hypothesis, we have used our soluble $hN\text{-}1_{11-13}$ containing the ligand-binding site to generate a panel of mAbs. Of these, one mAb (N1-39E) is seen to block receptor/ligand complex formation between $hN\text{-}1_{11-13}$ and cell surface expressed J-1 in our flow cytometry assay, whereas another mAb N1-96A has no effect on the interaction (Fig. 4*a*). Epitope mapping localizes the binding site of both N1-39E and N1-96A to EGF_{12} and/or the C-terminal region of EGF_{11} because they both recognize hN-1 mutants defective in calcium binding to EGF_{11} and EGF_{13}, but do not recognize a mutant defective in calcium binding to EGF_{12} (Fig. 4*b*). Subsequent testing against our panel of hN-1 EGF_{12} mutants demonstrates that the epitope of N1-39E, but not N1-96A, encompasses residues 468–477 of hN-1, which includes Leu-468 and Ile-477, directly implicated above in ligand binding, and Gln-470, Glu-473, and Gln-475 (Fig. 4*c*). The N1-39E epitope thus lies within the EGF_{12} Notch ligand-recognition site, explaining the molecular mechanism underlying its blockade of the hN-1/J-1 interaction. To test whether or not N1-39E is paralogue-specific, as suggested by the residues that form its epitope (Figs. 1*b* and 4*c*), we assayed whether or not it could recognize HEK 293 cells transfected individually with the different hNotch paralogues (N-1, N-2, N-3, and N-4). Flow cytometry analysis demonstrated that N1-39E specifically recognized only HEK293 cells expressing N-1 (expression of hNotch by each transfected cell line was confirmed by immunocytochemistry (Fig. 4*d*)). Recent work has demonstrated that selective interference of Notch paralogue activity by antibody binding can inhibit tumor growth in mouse xenograft models with reduced intestinal toxicity (30). Such reagents are likely to be valuable in the treatment of

TABLE 1

Site-directed mutagenesis of residues in hN-1 and *Drosophila* Notch and their respective effects in flow cytometry, ligand binding, and cell aggregation assays

ND, not determined.

hN-1 residue and substitution	EGF domain	Effect on ligand binding observed in flow cytometry analysis	Equivalent substitution in *Drosophila* Notch	Effect on Notch/Serrate cell aggregation
Q442A[a]	11	Binds as WT	Q478A	Close to WT level
L468A	12	No binding	L504A	Strongly reduced
D469G[b]	12	No binding	D505A	Strongly reduced
Q470A	12	Binds as WT	ND	ND
E473A	12	Moderate binding	T509A	Moderately reduced
Q475A	12	Moderate binding	R511A	Moderately reduced
I477A	12	No binding	V513A	Moderately reduced
M479A	12	Binds as WT	M515A	Binds as WT

[a] Gln-442 in EGF_{11} is in close proximity to the region of ligand binding in EGF_{12}.
[b] Conserved calcium-binding residue. Loss of ligand binding is due to loss in structural integrity, rather than direct involvement in N-1/ligand interaction.

Downloaded from www.jbc.org by guest, on April 21, 2013

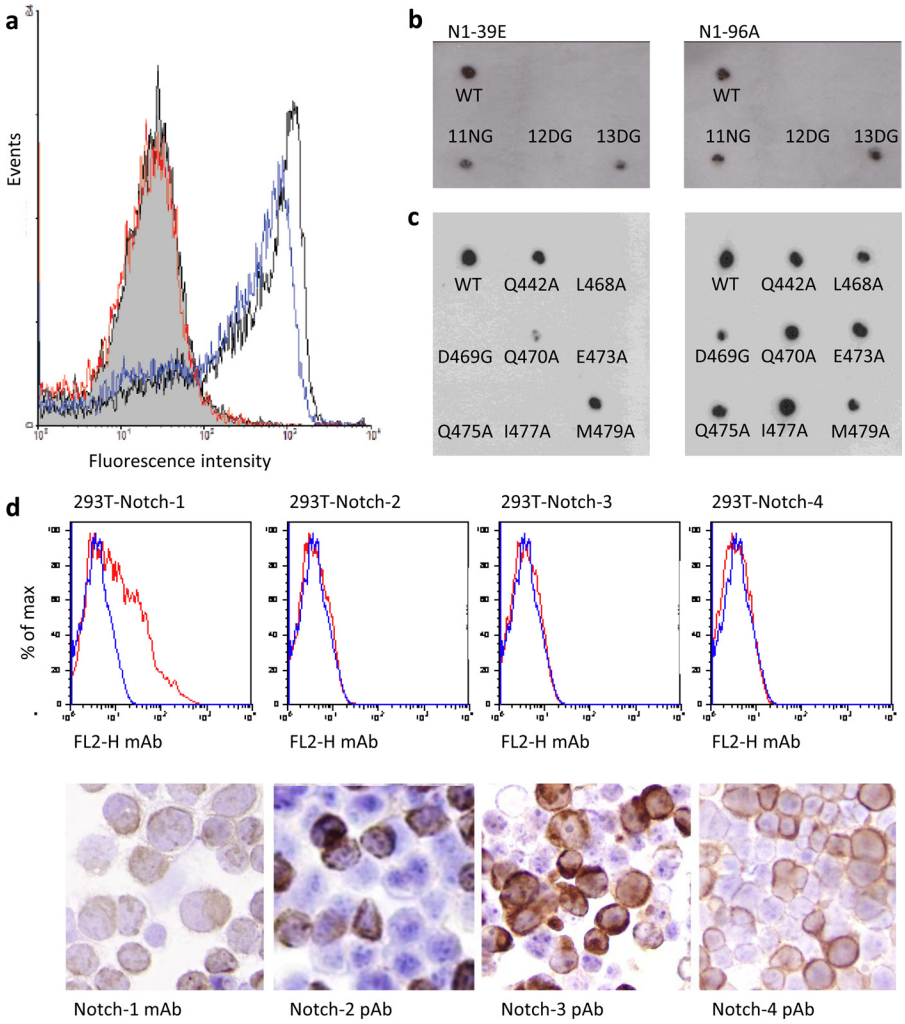


FIGURE 4. **Characterization of a ligand-blocking mAb to hN-1, which recognizes J-1-binding site.** *a*, flow cytometry assay to show mAb N1-39E (*red*), but not N1-96A (*blue*), blocks the binding of hN-1_{11-13} to HEK cells expressing hJ-1. *b* and *c*, epitope mapping by dot-blotting of WT and mutant hN-1_{11-14} proteins (11NG, 12DG, 13DG) that contain a calcium-binding mutation in EGF_{11}, EGF_{12}, or EGF_{13} localizes the epitope of mAb N1-39E and N1-96A to EGF_{12} or the C terminus of EGF_{11}. Dot-blotting of a panel of hN-1 EGF_{12} mutants demonstrates that L468A, Q470A, E473A, Q475A, and I477A are not recognized by N1-39E, and thus form part of its epitope. *d*, flow cytometry and immunocytochemistry (cytospin) analysis demonstrates that N1-39E is paralogue-specific. The *red line* indicates binding of mAb N1-39E; only 293T cells expressing hN-1 show a positive result, indicated by a rightward shift. Cytospin analysis (using monoclonal (*mAb*) or polyclonal (*pAb*) paralogue-specific antibodies) shows that each transfected cell line tested expresses a specific human Notch paralogue.

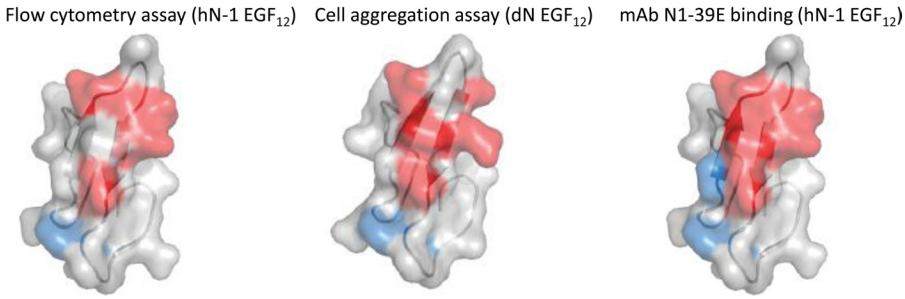


FIGURE 5. **Amino acid residues within β-hairpin implicated in ligand recognition and antibody binding in human and *Drosophila* Notch.** EGF_{12} of hN-1 is shown as a graphic and overlaid with a *semitransparent surface*. Positions that perturb activity in an assay are colored in *red*, those with no effect are colored in *blue*, and those not probed are colored in *gray*.

breast, melanoma, and T-cell acute lymphoblastic leukemia cancers, which are associated with aberrant Notch signaling, as well as important research tools (31). To date, potential therapeutic antibodies have targeted the negative regulatory region of Notch and have shown activity against Notch-1, -2, and -3 (30, 32, 33); antibodies to the extracellular domain of hN-1 encompassing EGF_{1-13} and EGF_{11-15} have also been reported (33, 34). We have now demonstrated a strategy for producing paralogue-specific antibodies to a region known to be critical for ligand binding. It should be noted that monoclonal antibodies raised to the ligand-binding region of Notch, and which block binding, may or may not reduce signaling (34, 35). This is

Downloaded from www.jbc.org by guest, on April 21, 2013

most likely due to the different affinities of the antibodies, their ability to recognize post-translationally modified forms of the receptor, or the cells used in the signaling assay expressing more than one paralogue on the cell surface. Nevertheless, given appropriate scale-up and screening of the molecular properties of such antibodies, this approach should yield reagents important for future research and therapeutics.

Our data demonstrate that the position and hydrophobic nature of the binding site for Jagged/Serrate ligands is conserved on the Notch EGF_{12} molecular surface throughout evolution (Fig. 5). Despite such global conservation, individual differences within the EGF_{12} site occur, suggesting that fine-tuning of the receptor/ligand interaction is possible, which may be subject to further regulation by *O*-glycosylation. As a consequence of the sequence variation observed, we demonstrate that it is possible to make targeted paralogue-specific, ligand-blocking mAbs (Fig. 5), which may be important for future research and therapeutics.

Acknowledgments—We thank Fiona Taylor for protein characterization, Carol Bentley, Jenny Greig, Tasneem Hassanali, and Jenna Yates for technical assistance in generating and characterizing Notch mAbs, and Devon Sheppard for assistance with figures. We also thank Sarah Bray and Gunter Merdes for luciferase reporter constructs.

REFERENCES

1. Artavanis-Tsakonas, S., Rand, M. D., and Lake, R. J (1999) Notch signaling: cell fate control and signal integration in development. *Science* **284,** 770–776
2. Hansson, E. M., Lendahl, U., and Chapman, G. (2004) Notch signaling in development and disease. *Semin. Cancer Biol.* **14,** 320–328
3. Blaumueller, C. M., Qi, H., Zagouras, P., and Artavanis-Tsakonas, S. (1997) Intracellular cleavage of Notch leads to a heterodimeric receptor on the plasma membrane. *Cell* **90,** 281–291
4. Sanchez-Irizarry, C., Carpenter, A. C., Weng, A. P., Pear, W. S., Aster, J. C., and Blacklow, S. C. (2004) Notch subunit heterodimerization and prevention of ligand-independent proteolytic activation depend, respectively, on a novel domain and the LNR repeats. *Mol. Cell. Biol.* **24,** 9265–9273
5. Fleming, R. J. (1998) Structural conservation of Notch receptors and ligands. *Semin. Cell Dev. Biol.* **9,** 599–607
6. Rebay, I., Fleming, R. J., Fehon, R. G., Cherbas, L., Cherbas, P., and Artavanis-Tsakonas, S. (1991) Specific EGF repeats of Notch mediate interactions with Delta and Serrate: implications for Notch as a multifunctional receptor. *Cell* **67,** 687–699
7. Shimizu, K., Chiba, S., Kumano, K., Hosoya, N., Takahashi, T., Kanda, Y., Hamada, Y., Yazaki, Y., and Hirai, H. (1999) Mouse Jagged1 physically interacts with Notch2 and other Notch receptors: assessment by quantitative methods. *J. Biol. Chem.* **274,** 32961–32969
8. Brou, C., Logeat, F., Gupta, N., Bessia, C., LeBail, O., Doedens, J. R., Cumano, A., Roux, P., Black, R. A., and Israël, A. (2000) A novel proteolytic cleavage involved in Notch signaling: the role of the disintegrin-metalloprotease TACE. *Mol. Cell* **5,** 207–216
9. Nichols, J. T., Miyamoto, A., Olsen, S. L., D'Souza, B., Yao, C., and Weinmaster, G. (2007) DSL ligand endocytosis physically dissociates Notch1 heterodimers before activating proteolysis can occur. *J. Cell Biol.* **176,** 445–458
10. Parks, A. L., Klueg, K. M., Stout, J. R., and Muskavitch, M. A. (2000) Ligand endocytosis drives receptor dissociation and activation in the Notch pathway. *Development* **127,** 1373–1385
11. Mumm, J.S., Schroeter, E. H., Saxena, M. T., Griesemer, A., Tian, X., Pan, D. J., Ray, W. J., and Kopan, R. (2000) A ligand-induced extracellular cleavage regulates γ-secretase-like proteolytic activation of Notch1. *Mol. Cell* **5,** 197–206
12. Schroeter, E. H., Kisslinger, J. A., and Kopan, R. (1998) Notch-1 signalling requires ligand-induced proteolytic release of intracellular domain. *Nature* **393,** 382–386
13. Jarriault, S., Brou, C., Logeat, F., Schroeter, E. H., Kopan, R., and Israel, A. (1995) Signalling downstream of activated mammalian Notch. *Nature* **377,** 355–358
14. Cordle, J., Redfield, C., Stacey, M., van der Merwe, P. A., Willis, A. C., Champion, B. R., Hambleton, S., and Handford, P. A. (2008) Localization of the Delta-like-1-binding site in human Notch-1 and its modulation by calcium affinity. *J. Biol. Chem.* **283,** 11785–11793
15. Fehon, R. G., Kooh, P. J., Rebay, I., Regan, C. L., Xu, T., Muskavitch, M. A., and Artavanis-Tsakonas, S. (1990) Molecular interactions between the protein products of the neurogenic loci *Notch* and *Delta*, two EGF-homologous genes in *Drosophila*. *Cell* **61,** 523–534
16. Harris, R. J., van Halbeek, H., Glushka, J., Basa, L. J., Ling, V. T., Smith, K. J., and Spellman, M. W. (1993) Identification and structural analysis of the tetrasaccharide NeuAc α(2→6)Gal β(1→4)GlcNAc β(1→3)Fuc α 1→*O*-linked to serine 61 of human factor IX. *Biochemistry* **32,** 6539–6547
17. Panin, V. M., Shao, L., Lei, L., Moloney, D. J., Irvine, K. D., and Haltiwanger, R. S. (2002) Notch ligands are substrates for protein *O*-fucosyltransferase-1 and Fringe. *J. Biol. Chem.* **277,** 29945–29952
18. Hicks, C., Johnston, S. H., diSibio, G., Collazo, A., Vogt, T. F., and Weinmaster, G. (2000) Fringe differentially modulates Jagged1 and Delta1 signalling through Notch1 and Notch2. *Nat. Cell Biol.* **2,** 515–520
19. Cordle, J., Johnson, S., Tay, J. Z., Roversi, P., Wilkin, M. B., de Madrid, B. H., Shimizu, H., Jensen, S., Whiteman, P., Jin, B., Redfield, C., Baron, M., Lea, S. M., and Handford, P. A. (2008) A conserved face of the Jagged/Serrate DSL domain is involved in Notch trans-activation and cis-inhibition. *Nat. Struct. Mol. Biol.* **15,** 849–857
20. Handford, P. A., Baron, M., Mayhew, M., Willis, A., Beesley, T., Brownlee, G. G., and Campbell, I. D. (1990) The first EGF-like domain from human factor IX contains a high-affinity calcium binding site. *EMBO J.* **9,** 475–480
21. Suk, J. Y., Jensen, S., McGettrick, A., Willis, A. C., Whiteman, P., Redfield, C., and Handford, P. A. (2004) Structural consequences of cysteine substitutions C1977Y and C1977R in calcium-binding epidermal growth factor-like domain 30 of human fibrillin-1. *J. Biol. Chem.* **279,** 51258–51265
22. Fleming, R. J., Scottgale, T. N., Diederich, R. J., and Artavanis-Tsakonas, S. (1990) The gene Serrate encodes a putative EGF-like transmembrane protein essential for proper ectodermal development in *Drosophila melanogaster*. *Genes Dev.* **4,** 2188–2201
23. Bunch, T. A., Grinblat, Y., and Goldstein, L. S. (1988) Characterization and use of the *Drosophila* metallothionein promoter in cultured *Drosophila melanogaster* cells. *Nucleic Acids Res.* **16,** 1043–1061
24. Mason, D., Cordell, J., and Pulford, K.. (1983) Production of monoclonal antibodies for immunocytochemical use. in *Techniques in Immunocytochemistry*, Vol 2 (Bullock, G. R., and Petrusz, P., eds) pp. 175–216. London Academic Press Ltd., London, UK
25. Panin, V. M., Papayannopoulos, V., Wilson, R., and Irvine, K. D. (1997) Fringe modulates Notch-ligand interactions. *Nature* **387,** 908–912
26. Moloney, D. J., Panin, V. M., Johnston, S. H., Chen, J., Shao, L., Wilson, R., Wang, Y., Stanley, P., Irvine, K. D., Haltiwanger, R. S., and Vogt, T. F. (2000) Fringe is a glycosyltransferase that modifies Notch. *Nature* **406,** 369–375
27. Hofmann, J. J., Zovein, A. C., Koh, H., Radtke, F., Weinmaster, G., and Iruela-Arispe, M. L. (2010) Jagged1 in the portal vein mesenchyme regulates intrahepatic bile duct development: insights into Alagille syndrome. *Development* **137,** 4061–4072
28. Shimizu, K., Chiba, S., Saito, T., Kumano, K., Takahashi, T., and Hirai, H. (2001) Manic fringe and lunatic fringe modify different sites of the Notch2 extracellular region, resulting in different signaling modulation. *J. Biol. Chem.* **276,** 25753–25758
29. Peters, N., Opherk, C., Zacherle, S., Capell, A., Gempel, P., and Dichgans, M. (2004) CADASIL-associated Notch3 mutations have differential effects both on ligand binding and ligand-induced Notch3 receptor signaling through RBP-Jk. *Exp. Cell Res.* **299,** 454–464
30. Wu, Y., Cain-Hom, C., Choy, L., Hagenbeek, T. J., de Leon, G. P., Chen, Y., Finkle, D., Venook, R., Wu, X., Ridgway, J., Schahin-Reed, D., Dow, G. J., Shelton, A., Stawicki, S., Watts, R. J., Zhang, J., Choy, R., Howard, P.,

Downloaded from www.jbc.org by guest, on April 21, 2013

Kadyk, L., Yan, M., Zha, J., Callahan, C. A., Hymowitz, S. G., and Siebel, C. W. (2010) Therapeutic antibody targeting of individual Notch receptors. *Nature* **464,** 1052–1057

31. Weng, A. P., Ferrando, A. A., Lee, W., Morris, J. P., 4th, Silverman, L. B., Sanchez-Irizarry, C., Blacklow, S. C., Look, A. T., and Aster, J. C. (2004) Activating mutations of NOTCH1 in human T cell acute lymphoblastic leukemia. *Science* **306,** 269–271
32. Li, K., Li, Y., Wu, W., Gordon, W. R., Chang, D. W., Lu, M., Scoggin, S., Fu, T., Vien, L., Histen, G., Zheng, J., Martin-Hollister, R., Duensing, T., Singh, S., Blacklow, S. C., Yao, Z., Aster, J. C., and Zhou, B. B. (2008) Modulation of Notch signaling by antibodies specific for the extracellular negative regulatory region of NOTCH3. *J. Biol. Chem.* **283,** 8046–8054
33. Aste-Amézaga, M., Zhang, N., Lineberger, J. E., Arnold, B. A., Toner, T. J., Gu, M., Huang, L., Vitelli, S., Vo, K. T., Haytko, P., Zhao, J. Z., Baleydier, F., L'Heureux, S., Wang, H., Gordon, W. R., Thoryk, E., Andrawes, M. B., Tiyanont, K., Stegmaier, K., Roti, G., Ross, K. N., Franlin, L. L., Wang, H., Wang, F., Chastain, M., Bett, A. J., Audoly, L. P., Aster, J. C., Blacklow, S. C., and Huber, H. E. (2010) Characterization of Notch1 antibodies that inhibit signaling of both normal and mutated Notch1 receptors. *PLoS One* **5,** e9094
34. Sharma, A., Paranjape, A. N., Rangarajan, A., and Dighe, R. R. (2012) A monoclonal antibody against human Notch1 ligand binding domain depletes subpopulation of breast cancer stem-like cells. *Mol. Cancer Ther.* **11,** 77–86
35. Falk, R., Falk, A., Dyson, M. R., Melidoni, A. N., Parthiban, K., Young, J. L., Roake, W., McCafferty, J. (2012) Generation of anti-Notch antibodies and their application in blocking Notch signalling in neural stem cells. *Methods* **58,** 69–78

Downloaded from www.jbc.org by guest, on April 21, 2013